BIOPROCESSING OPTIMIZATION TO MANUFACTURE THYMUS-DERIVED REGULATORY T CELLS FOR THERAPY

by

Katherine Nicole MacDonald

B.Eng., McGill University, 2016

A THESIS SUBMITTED IN PARTIAL FULFILLMENT OF

THE REQUIREMENTS FOR THE DEGREE OF

DOCTOR OF PHILOSOPHY

in

THE FACULTY OF GRADUATE AND POSTDOCTORAL STUDIES

(Biomedical Engineering)

THE UNIVERSITY OF BRITISH COLUMBIA

(Vancouver)

March 2022

The following individuals certify that they have read, and recommend to the Faculty of Graduate and Postdoctoral Studies for acceptance, the dissertation entitled:

BIOPROCESSING OPTIMIZATION TO MANUFACTURE THYMUS-DERIVED REGULATORY T CELLS FOR THERAPY

submitted by Katherine Nicole MacDonald in partial fulfillment of the requirements for

the degree of Doctor of Philosophy

in Biomedical Engineering

Examining Committee:

James Piret, Chemical and Biological Engineering, UBC
Supervisor

Megan Levings, Surgery, UBC
Co-supervisor

Pascal Lavoie, Pediatrics, UBC
University Examiner

Vikramaditya Yadav, Chemical and Biological Engineering, UBC
University Examiner

Additional Supervisory Committee Members:

Peter Zandstra, Biomedical Engineering, UBC
Supervisory Committee Member

Brad Nelson, Medical Genetics, UBC
Supervisory Committee Member

Abstract

Regulatory T cell therapy has shown promise in treating autoimmune disorders, transplant rejection and graft-versus-host disease in early clinical trials. However, efficient manufacturing of clinical grade cells is still a significant hurdle that must be overcome before these therapies can see widespread use. Previous work showed that large numbers of pure, naïve Tregs can be isolated from pediatric thymus. This research aims to investigate the variables governing Treg expansion with serum-free media and non-cell-based activation reagents to develop manufacturing protocols to produce therapeutic doses of thymus-derived Tregs. First, we tested activation reagents, cell culture media, restimulation timing, and cryopreservation to develop good manufacturing practice compatible protocols to expand and cryopreserve Tregs. Cryopreservation tests revealed a critical effect of timing: only cells cryopreserved 1-3 days, but not > 3 days, after restimulation maintained high viability and FOXP3 expression upon thawing. We next investigated how changing cell density and feed frequency influenced Treg expansion, viability, and phenotype in a 3-week expansion protocol and found that Treg viability and expansion were correlated with the cell density at restimulation. Tregs restimulated at low cell densities ($1x10^5$ cells/cm^2) initially had high growth rates, viability, and FOXP3 expression, but at later culture times these parameters were reduced compared to slower growing Tregs restimulated at higher cell densities ($5x10^5$ cells/cm^2). High density expansion was associated with lower nutrient concentrations and higher accumulations of lactate, but this could be alleviated by decreasing the interval between feeds. We tested platforms to scale up Treg manufacturing and observed that Tregs expanded in gas permeable cell expansion bags were of higher quality than those expanded in agitated suspension culture or the G-Rex. Finally, we tested labelling expanded Tregs with a ^{19}F-perfluorocarbon (PFC) nanoemulsion to enable *in*

vivo tracking using MRI. While Tregs could be labelled with the ^{19}F-PFC and detected *in vivo* in immunocompromised mice, labelling during expansion reduced cell viability, particularly after cryopreservation. Together, this research developed protocols and process understanding necessary to efficiently produce clinical grade Tregs, laying the groundwork for the first clinical trial of thymic Treg cell therapy in Canada.

Lay Summary

A type of immune cell called regulatory T cells (Tregs) has the potential to be used as a therapy to prevent rejection or tissue damage following organ or stem cell transplantation. A challenge with using Tregs as a therapy is that Tregs are rare, so we need methods to isolate them and increase their numbers in the lab. We have developed methods to isolate these cells from the thymus, an organ above the heart that is removed during pediatric heart surgery. In this thesis, I developed methods to grow thymus-derived Tregs that are compatible with clinical standards and identified aspects of the process that must be controlled to generate high quality cells. I also tested a method to label cells that would allow them to be tracked after administration to a patient. Developing these methods to efficiently produce thymus-derived Tregs is a critical step towards their use as a therapy.

Preface

Individual sections of **Chapter 1** have been published:

- MacDonald KN, Piret JM, Levings MK. Methods to manufacture regulatory T cells for cell therapy. *Clinical and Experimental Immunology*. 2019; 197(1): 52-63. [1]
- Wardell CM, MacDonald KN, Levings MK, Cook L. Cross talk between human regulatory T cells and antigen-presenting cells: Lessons for clinical applications. *European Journal of Immunology*. 2020. [2]

I performed literature review and wrote the majority of the text represented in my thesis. I edited the final manuscripts with the co-authors.

Chapter 3 has been published:

- MacDonald KN, Ivison S, Hippen KL, Hoeppli RE, Hall M, Zheng G, Dijke E, Al-Aklabi M, Freed D, Rebeyka I, Gandhi S, West L, Piret JM, Blazar BR, Levings MK. Cryopreservation timing is a critical process parameter in a thymic regulatory T-cell therapy manufacturing protocol. *Cytotherapy*. 2019; 21(12): 1216-1233. [3]

I conceived of, designed and conducted all experiments, analyzed data for all experiments except for the following: REH, MH, and GZ assisted with Treg isolations; Treg expansions with KT64/86 cells in Figure 3.6 and Figure 3.7 were conducted by KLH at the University of Minnesota; TSDR methylation analysis was conducted by Jana Gilles, a technician in the Levings Lab; MH assisted with experiments in Figure 3.13 under my supervision. I wrote the manuscript, which was edited by all co-authors.

Chapter 4 is in revision for peer-reviewed publication:

- MacDonald KN, Hall M, Ivison S, Gandhi S, Klein Geltink RI, Piret JM, Levings MK. Consequences of adjusting cell density and feed frequency on serum-free expansion of thymic regulatory T cells.

I conceived of, designed and conducted all experiments, analyzed data for all experiments except for the following: MH assisted with experiments in Figure 4.1 and Figure 4.2 under my supervision; amino acid analysis was performed by Chris Sherwood, a technician in the Piret Lab. I wrote the manuscript, which was edited by all co-authors.

The work in **Chapter 5** has yet to be published.

I conceived of, designed and conducted all experiments, analyzed data for all experiments except for the following: Dr. Sabine Ivison and Dr. Romy Hoeppli assisted with the experiments in Figure 5.2 and Figure 5.3; amino acid analysis was performed by Chris Sherwood, a technician in the Piret Lab.

The work in **Chapter 6** has yet to be published.

Expansion of cells for experiments in Figure 6.1 and Figure 6.2 were performed by me or Michael Hall under my supervision. Cell injection into immunocompromised mice and MRI imaging were performed and analyzed by Dr. Corby Fink and Olivia Sehl in the Dekaban and Foster Labs at the Robarts Research Institute (Western University). I conceived of, designed and conducted all experiments to assess the impact of ^{19}F-PFC labelling during expansion.

All research was approved by the University of British Columbia (UBC) Research Ethics Board under the protocols “Thymus Tregs” (H17-01490) and “BCCHRI phlebotomy protocol” (H18-

02553). Blood was obtained from healthy volunteers by Canadian Blood Services. Thymus samples were collected at BC Children's Hospital and University of Alberta Stollery Children's Hospital. Thymuses collected at the University of Alberta were approved by the University of Alberta Human Research Ethics Board under protocol Pro00001408. Approval for animal work in Chapter 6 was obtained from the Western University Animal Care Committee.

Table of Contents

Abstract ..... **iii**

Lay Summary ..... **v**

Preface ..... **vi**

Table of Contents ..... **ix**

List of Tables ..... **xiv**

List of Figures ..... **xv**

List of Abbreviations ..... **xviii**

Acknowledgements ..... **xx**

Dedication ..... **xxi**

Chapter 1: Introduction **1**

1.1 $CD4^+$ T cells and the adaptive immune response 1

1.2 Regulatory T cells 2

1.2.1 Treg development in the thymus and periphery 3

1.2.2 Treg mechanisms of suppression 7

1.3 Regulatory T cells as an adoptive cell therapy 9

1.3.1 Treg cell therapy in stem cell transplantation 11

1.3.2 Treg cell therapy in solid organ transplantation 13

1.3.3 Treg cell therapy in autoimmunity 14

1.3.4 Hurdles to Treg cell therapy 16

1.4 Sources of Tregs 17

1.4.1 Autologous versus allogeneic Tregs 19

1.4.2 Polyclonal vs. antigen specific 21

1.5 Regulatory T cell therapy manufacturing 22
1.5.1 Strategies to isolate Tregs 22
1.5.2 Strategies to expand polyclonal Tregs 23
1.5.2.1 Large-scale expansion platforms 29
1.5.3 Cryopreservation of Tregs 30
1.5.4 Next generation Treg cell therapies 31
1.5.4.1 Modulating Treg function or stability with culture conditions 31
1.5.4.2 Modulating Treg function or stability with genome editing 33
1.6 Monitoring infused Tregs *in vivo* 34
1.6.1 Direct vs. indirect cell labelling 36
1.7 Research objectives 37
Chapter 2: Materials and Methods 39
2.1 Cell isolation 39
2.2 Cell expansion 40
2.3 Cryopreservation of expanded cells 43
2.4 Flow cytometry and cytokine analysis 44
2.5 DNA isolation and Treg-specific demethylation region (TSDR) analysis 44
2.6 In vitro suppression assays. 45
2.7 Apoptosis assay 45
2.8 Media analysis 46
2.9 Calculation of specific growth rates, specific glucose uptake rates, and specific lactate production rates 47
2.10 Cell labelling with ^{19}F-perfluorocarbon 48

2.11 ^{19}F-PFC labelled cell injection into immunocompromised mice 48

2.12 Statistical analyses 49

Chapter 3: Cryopreservation timing is a critical process parameter in a thymic regulatory T-cell therapy manufacturing protocol 50

3.1 Introduction 50

3.2 Results 51

3.2.1 Development of clinical-grade thymic Treg isolation protocol 51

3.2.2 Comparison of activation reagents for thymic Treg expansion 53

3.2.3 Effect of activation reagents on thymic Treg function 56

3.2.4 Effect of cell culture media on thymic Treg expansion 58

3.2.5 Comparison of thymic Treg expansion with Treg Xpander versus GMP-compatible aAPCs 64

3.2.6 Cryopreservation 1-3 days post-restimulation preserves Treg viability, phenotype and function 66

3.2.7 Increased expansion when Tregs are restimulated after returning to resting size 68

3.2.8 Thymic Treg cryopreservation timing is a more critical process parameter than restimulation day 71

3.3 Discussion 80

Chapter 4: Consequences of adjusting cell density and feed frequency on serum-free expansion of thymic regulatory T cells 84

4.1 Introduction 84

4.2 Results 85

4.2.1 Cell density at restimulation correlates with subsequent variation in Treg expansion and viability 85
4.2.2 Cell density influences Treg viability and phenotype 88
4.2.3 Comparing Treg cultures from $1x10^5$ to $20x10^5$ cells/cm^2 93
4.2.4 Excessively dense culture conditions inhibit Treg proliferation and increase in cell size 99
4.2.5 Density dependent effects on costimulatory and co-inhibitory proteins do not influence Treg expansion 102
4.2.6 Transient exposure to low oxygen concentration does not affect Treg expansion 103
4.2.7 Medium limitations affect Treg proliferation and FOXP3 expression 107
4.2.8 Supplementing antioxidants did not improve Treg expansion 113
4.3 Discussion 116
Chapter 5: Comparing platforms for large-scale thymic Treg manufacturing 121
5.1 Introduction 121
5.2 Results 123
5.2.1 Isolating Tregs from an entire thymus 123
5.2.2 Comparing platforms for large-scale Treg expansion 126
5.2.3 Cryopreserving Tregs using rate-controlled freezers 131
5.2.4 Estimate of Treg cell yield from large-scale manufacturing 133
5.3 Discussion 134
Chapter 6: Tracking Tregs *in vivo* using ^{19}F-perfluorocarbon cell labelling and MRI 138
6.1 Introduction 138
6.2 Results 140

6.2.1 Tregs can be efficiently labelled with ^{19}F-PFC 140
6.2.2 Infused Tregs accumulate in lymph nodes and spleen 140
6.2.3 Testing ^{19}F-PFC labelling during expansion 143
6.2.4 Recovery and viability of ^{19}F-PFC labelled Tregs after cryopreservation 147
6.3 Discussion 149
Chapter 7: Conclusion 151
7.1 Summary 151
7.2 Limitations 153
7.3 Future directions 155
7.4 Overall significance 158
Bibliography 160
Appendices 186
Appendix A Antibodies and labelling dyes 186
Appendix B Cell Handling in large-scale Treg expansions 188

List of Tables

Table 1.1: Published clinical manufacturing protocols for polyclonal Tregs. 24

Table 3.1: Effects of media on fold expansion, viability and phenotype of thymic Tregs. 63

Table 5.1: Theoretical yield of Tregs from large-scale manufacturing. 134

Table A.1: Antibodies and labelling dyes used in this thesis. 186

Table B.1: Cell handling in first large-scale Treg expansion. 188

Table B.2: Cell handling in second large-scale Treg expansion. 189

List of Figures

Figure 1.1: Overview of regulatory T cell (Treg) manufacturing protocols. 23

Figure 1.2: Research aims addressed by this thesis. 38

Figure 3.1: Isolation of thymic Treg using a two-step magnetic-bead-based selection process. .. 52

Figure 3.2: Comparison of cell-free activation reagents for thymic Treg expansion. 55

Figure 3.3: Function of thymic Tregs expanded with cell-free activation reagents. 57

Figure 3.4: Effect of cell culture media on thymic Treg expansion. 59

Figure 3.5: Effect of cell culture media on thymic Treg expansion with Dynabeads Treg Xpander or CD3/CD28/CD2 T Cell Activator. 61

Figure 3.6: Thymic Treg expansion with KT64/86 aAPCs..... 65

Figure 3.7: Phenotype of thymic Tregs expanded using KT64/86 aAPCs or Dynabeads Treg Xpander. 66

Figure 3.8: Cryopreservation of thymic Tregs following a second restimulation at day 14..... 67

Figure 3.9: Effect of restimulation time on thymic Treg expansion. 70

Figure 3.10: Cryopreservation of thymic Tregs following restimulation on day 9. 73

Figure 3.11: Cryopreservation of thymic Tregs, naïve peripheral blood Tregs and naïve peripheral blood Tconv following restimulation at day 9. 74

Figure 3.12: Function of cryopreserved thymic Tregs, naïve peripheral blood Tregs and naïve peripheral blood Tconv. 76

Figure 3.13: Effect of restimulation on day 9-14. 79

Figure 3.14: FOXP3 expression of thymic Tregs over the course of expansion. 79

Figure 4.1: Variability in Treg viability and expansion correlated with cell density at restimulation. 86

Figure 4.2: Changing the bead ratio or rapamycin did not improve Treg expansion or viability. 87
Figure 4.3: Varying cell density affects Treg viability and phenotype.....90
Figure 4.4: Expansion of Tregs at $1x10^5$ cells/cm^2 or $5x10^5$ cells/cm^2 with varying medium heights. 92
Figure 4.5: Comparing Treg expansion at $1x10^5$ to $20x10^5$ cells/cm^2. 95
Figure 4.6: Expansion of Tregs adjusted to different cell densities at restimulation.....97
Figure 4.7: Restimulation at high densities inhibits cell proliferation and increase in cell size. 100
Figure 4.8: Restimulation at high cell densities inhibits proliferation and increase in cell size. 101
Figure 4.9: Tregs expanded at different cell densities differentially express costimulatory and co-inhibitory proteins. 103
Figure 4.10: Low oxygen concentrations at high cell densities did not affect Treg expansion. .105
Figure 4.11: Oxygen staining of Tregs treated with sodium azide and phenotype of Tregs restimulated under low oxygen. 106
Figure 4.12: Additional feeding improved expansion, viability and phenotype for Tregs restimulated at $5x10^5$ cells/cm^2.....110
Figure 4.13: Nutrient/metabolite levels and phenotype of Tregs restimulated at different cell densities with different feeding strategies. 111
Figure 4.14: Supplementing antioxidants did not improve Treg expansion. 115
Figure 5.1: Comparison of thymus processing with tissue chopper or gentleMACS with varying media volumes. 124
Figure 5.2: Isolation of thymic Tregs with either a small-scale or large-scale magnet. 125
Figure 5.3: Expansion of thymic Tregs with large-scale expansion platforms. 127
Figure 5.4: Analysis of conditioned medium from large-scale Treg expansions. 128

Figure 5.5: Concentration of essential amino acids in conditioned medium from large-scale Treg expansions. 129

Figure 5.6: Amino acid concentrations in conditioned medium from large-scale Treg expansions. 130

Figure 5.7: Cryopreservation of expanded Tregs using rate-controlled freezers. 132

Figure 6.1: Tregs can be efficiently labelled with ^{19}F-PFC. 140

Figure 6.2: Tregs accumulate in lymph nodes and spleen of immunocompromised mice. 142

Figure 6.3: ^{19}F-PFC labelling during expansion induced apoptosis, reduced expression of Treg phenotypic markers. 145

Figure 6.4: Function of Tregs labelled with ^{19}F-PFC during expansion. 146

Figure 6.5: Recovery, viability, and phenotype of Tregs labelled with ^{19}F-PFC prior to cryopreservation 148

List of Abbreviations

7AAD	7-aminoactinomycin D
aAPC	artificial APC
AIRE	autoimmune regulator
allo	allogeneic
ALS	amyotrophic lateral sclerosis
APC	antigen presenting cell
BLI	bioluminescence imaging
CAR	chimeric antigen receptor
CD	cluster of differentiation
CFSE	carboxyfluorescein succinimidyl ester
CNS	conserved non-coding sequence
CPD	cell proliferation dye
CS10	Cryostor CS10
CTLA-4	cytotoxic T lymphocyte-associated antigen 4
CT	computed tomography
DC	dendritic cell
DI	division index
DMSO	dimethyl sulfoxide
DN	double negative
DP	double positive
FBS	fetal bovine serum
FOXP3	forkhead box protein 3
FVD	fixable viability dye
GARP	glycoprotein A repetitions predominant
GVHD	graft-versus-host disease
GVL	graft-versus-leukemia
HLA	human leukocyte antigen
HPLC	high performance liquid chromatography
HSCT	hematopoietic stem cell transplantation
IFN	interferon
IL	interleukin
iPSC	induced pluripotent stem cells
IT	intrathecally
iTreg	induced Treg
IV	intravenously
IU	international units
LAG3	lymphocyte activation gene-3
LAP	latency-associated peptide
MFI	mean fluorescence intensity
MHC	major histocompatibility complex
MRI	magnetic resonance imaging
MS	multiple sclerosis
mTOR	mammalian target of rapamycin

NK	natural killer
P/S	penicillin/streptomycin
PBMC	peripheral blood mononuclear cell
PBS	phosphate-buffered saline
PET	positron emission tomography
PMA	phorbol myristate acetate
pTreg	peripherally-derived Tregs
RAG	recombination-activating gene
rh	recombinant human
SD	standard deviation
SLE	systemic lupus erythematosus
SP	single positive
SPECT	single photon-emission computed tomography
SOT	solid organ transplantation
Tconv	conventional T cells
TCR	T cell receptor
TGF	transforming growth factor
Th	T helper
Tr1	type 1 regulatory T cells
Treg	regulatory T cells
TSDR	Treg-specific demethylated region
tTreg	thymically-derived Tregs
UCB	umbilical cord blood
xenoGVHD	xenogenous GVHD

Acknowledgements

Thank you to my supervisors Jamie and Megan for your support and encouragement, your mentorship, and your patience as I navigated this complex project. I learned so much from working in both labs and am grateful for all of the opportunities that I received.

Thank you to everyone in the Levings and Piret Labs for your help and friendship over the last 6 years. Alina, Shreyas, and Rene, thank you for all of the coffee breaks, beers, potlucks, bike rides, and hikes, as well as for your encouragement and your constructive feedback. Thank you to Romy for your patient mentorship as I entered this new field. Thank you to Michael for being my second pair of hands and for all of your help in doing some of these big, ambitious experiments. Thank you to Manjurul for being so willing to help with everything. Thank you to Sabine for all your encouragement, emotional support, and humour, and for pushing me to ask questions and think creatively in tackling these projects. And thank you to everyone else in both labs for all of your help in and out of the lab.

I would also like to acknowledge my committee members, our collaborators in the West Lab at University of Alberta and the Dekaban and Foster Labs at Western University, Dr. Ramon Klein Geltink for many helpful discussions, all of the patients who donated tissue and their families, the cardiac surgery team at BCCH, as well as UBC, BCCHR, and CIHR for funding.

Thank you to my friends, family, and fuzzies for all of your support. Thanks to my parents, Chrissy, and Courtney for your continuous encouragement. Finally, to Joey, thank you for everything. You have been a constant source of love and support since Douglas Hall.

To Joey, Chrissy, and Courtney,

For your unwavering love and support, and for learning more than you ever expected to know about regulatory T cells.

Chapter 1: Introduction

1.1 $CD4^+$ T cells and the adaptive immune response

$CD4^+$ T cells develop from lymphocyte progenitors that migrate from the bone marrow to the thymus, where they mature [4]. During T cell development, cells begin to express cell surface proteins including the T cell receptor (TCR), allowing them to recognize peptides presented by major histocompatibility complex (MHC) proteins and CD4 co-receptors. $CD4^+$ T cells recognize antigens presented by MHC class II, primarily expressed on the surface of antigen presenting cells (APCs) such as dendritic cells (DCs), macrophages and B cells [5].

Three signals are involved in the activation and differentiation of $CD4^+$ T cells. Signal 1 is provided by the interaction of the TCR with an MHC-peptide complex on the surface of an APC. Signaling through the TCR activates pathways involved in T cell differentiation and proliferation, and stimulates expression of functional molecules [6]. Signal 2 is provided by ligands on APCs that interact with costimulatory receptors on the surface of T cells. Typically, this involves CD28 on T cells interacting with the ligands CD80 and CD86 on APCs. Signals 1 and 2 are both essential for T cell activation. Without the co-stimulatory signal 2, the T cell will be anergic and not respond to antigen activation [7]. Additional signals (signal 3) are provided by cytokines that the T cell encounters during and/or after activation. These signals direct the differentiation of $CD4^+$ T cells into different Th subsets including Th1, Th2, Th17, T follicular helper cells (Tfh), or regulatory T cells (Tregs), which express lineage-defining transcription factors and unique combinations of chemokine and adhesion receptors to enable homing to specific sites of inflammation [8, 9].

1.2 Regulatory T cells

Tregs are a subset of $CD4^+$ T cells that suppress immune responses to maintain immune homeostasis; the absence of Tregs is associated with autoimmunity [10]. $CD4^+FOXP3^+$ Tregs can develop either in the thymus from cells with high affinity to self-peptides [6, 11] or in the periphery when $CD4^+$ T cells are activated under tolerogenic conditions [12]. Other types of regulatory T cells including type 1 regulatory T cells (Tr1) cells and $CD8^+FOXP3^+$ cells have also been described [13-15] but are not the focus of this thesis. Both thymus-derived and peripheral Tregs are identified by high expression of the transcription factor FOXP3 and by demethylation of the Treg specific demethylation region (TSDR), located within in first intron of the *FOXP3* gene locus [16-18]. Demethylation of this region allows efficient transcriptional activation and maintenance of the high FOXP3 expression in Tregs needed for suppressive function [19-21]. Since activated, non-regulatory $CD4^+$ T cells can also express FOXP3, measurement of the TSDR methylation status is an important way to distinguish Tregs from effector T cells [16]. $CD4^+FOXP3^+$ Tregs are also characterized by constitutive expression of CD25 (IL-2Rα, the high affinity subunit of the IL-2 receptor) and low expression of CD127 (IL-7Rα) [22]. Many Tregs additionally express the transcription factor Helios. $Helios^+$ Tregs appear to be more stable than $Helios^-$ Tregs, as loss of Helios expression in Tregs during expansion has been correlated with increased TSDR methylation and reduced suppressive capacity [23, 24].

In this thesis, tTreg and pTreg will be used to refer to Tregs that develop in the thymus or periphery, respectively. Tregs that are specifically isolated from the thymus will be referred to as ‘thymus-derived Tregs’ or ‘thymic Tregs’, those isolated from peripheral blood will be referred to as ‘blood Tregs’, and those isolated from umbilical cord blood (UCB) will be referred to as

'cord blood Tregs' or 'UCB Tregs'. Blood Tregs contain a mixture of tTreg and pTreg unless specifically isolated as $CD4^+CD25^{high}CD127^-CD45RA^+$ naïve Tregs.

1.2.1 Treg development in the thymus and periphery

T cells develop in the thymus from hematopoietic progenitors that migrate from the bone marrow and, based on studies in mice, enter at the cortico-medullary junction [25]. T cells pass through progressive stages of differentiation as they migrate through the thymus, with each stage marked by expression of specific surface proteins and/or interactions with antigen presenting cells (reviewed by [26]). Notch signaling induces T cell lineage commitment [27, 28], then these progenitors progress through a series of double-negative (DN; $CD4^-CD8^-$) thymocyte stages as they migrate through the cortex. In mice, these stages are identified by expression of CD25 and CD44 (DN1 – $CD25^-CD44^+$; DN2 – $CD25^+CD44^+$; DN3 – $CD25^+CD44^-$; DN4 – $CD25^-CD44^-$) [4]. Similar stages in humans are characterized as $CD34^+CD38^-CD1a^-$, $CD34^+CD38^+CD1a^-$, $CD34^+CD38^+CD1a^+$, and immature $CD4^+$ single positive [29, 30]. T cell development has been more extensively studied in mice than humans but there are similarities in many of the key steps between the species [31].

TCR rearrangement begins during the DN stages [4, 29, 32]. The TCR consists of α and β chains, which undergo somatic recombination driven by recombination activating gene (RAG) proteins to produce a functional TCR [33]. Rearrangement of the TCRβ begins first, then the rearranged TCRβ pairs with a pre-TCRα to form a pre-TCR which is expressed and associates with the CD3ζ complex. Signaling through the pre-TCR promotes survival; cells that do not receive productive signaling through the pre-TCR undergo 'death by neglect' [26]. This signaling also induces full recombination of the TCR and signaling through Lck, which

associates with CD4 and CD8 co-receptors to induce their expression, leading to double positive (DP; $CD4^+CD8^+$) thymocytes. In humans, recombined TCRβ chains have been detected starting from late DN and immature single positive stages, with recombined TCRα chains detected starting from early DP stages [26, 29, 32].

DP thymocytes interact with thymic epithelial cells (TECs) and thymic DCs to undergo positive and negative selection [34]. Cortical TECs and DCs present self-peptide in the context of MHC to engage with the newly formed TCRs on thymocytes. Interactions between self-peptide MHC complexes on these cells and TCRs on the differentiating thymocytes lead to different consequences for the thymocytes depending on the affinity of the interaction. High affinity interactions induce apoptosis (negative selection), low affinity interactions promote survival and differentiation to single positive (SP; $CD4^+CD8^-$ or $CD4^-CD8^+$) thymocytes (positive selection), and insufficient TCR signaling leads to 'death by neglect' [4, 34].

With positive selection, DP thymocytes migrate to the medulla where they become $CD4^+$ or $CD8^+$ single positive (SP) thymocytes. Additional negative selection of self-reactive thymocytes occurs in the medulla, where thymocytes encounter additional antigen displayed by medullary TECs (mTECs), whose expression of the transcription factor AIRE allows for presentation of tissue-restricted antigens [35], or medullary DCs, which can either acquire self-antigens in the periphery or from mTECs [34]. Finally, mature T cells leave the thymus through the cortico-medullary junction and enter circulation in the peripheral blood [36].

Studies in mice indicate that Tregs develop from thymocytes with TCRs specific for self-antigen that receive high affinity TCR stimulation below the threshold for negative selection [11, 37, 38]. Two developmental pathways have been proposed for tTregs. In the first, better studied pathway, TCR stimulation causes upregulation of CD25, which is followed by IL-2 induced

expression of FOXP3 [39-41]. A second pathway was identified in mice in which $CD25^{+}Foxp3^{+}$ Tregs develop through a $CD25^{-}Foxp3^{lo}$ intermediate [42, 43]. These $Foxp3^{lo}$ Treg precursors had a distinct TCR repertoire from $CD25^{+}Foxp3^{-}$ Treg precursors and different functionality *in vivo*. A $FOXP3^{lo}$ intermediate linked to differentiated tTregs has also been identified in human thymus [32]. While most $FOXP3^{+}$ cells in human thymus are $CD4^{+}$ SP thymocytes, the results of several studies suggest that Treg commitment may occur earlier, at the DP stage. $FOXP3^{+}$ DP thymocytes that have undergone positive selection and appear to be committed to the Treg lineage [44-46] have been identified, with TSDR demethylation even detected at the DP stage [47]. Results from studies of the co-culture of DP cells with TECs and multiple linear regression analysis indicate that this $FOXP3^{+}$ DP thymocyte population differentiates further to $CD4^{+}$ and $CD8^{+}$ SP $FOXP3^{+}$ cells and suggest that it gives rise to the majority of the tTreg population, although $CD4^{+}$ SP thymocytes can also differentiate to tTregs with appropriate differentiation cues [39, 46, 48].

pTregs can differentiate in the periphery when $CD4^{+}$ T cells are activated in the presence of suppressive molecules such as TGFβ [49]. FOXP3 expression is induced by TGFβ-induced phosphorylation of SMAD2/3, which binds the conserved non-coding sequence 1 (CNS1) in the *FOXP3* gene to activate transcription [21, 50, 51]. This is enhanced by molecules such as retinoic acid, a vitamin A metabolite produced by mucosal DCs [52, 53]. pTregs are highly prevalent in the gut, where they regulate tolerance towards commensal bacteria and food-borne antigens [49, 54], and in the placenta, where they play a key role in maternal-fetal tolerance [55].

Treg maintenance and homeostasis in the periphery requires continuous, low level TCR stimulation and IL-2 signaling [56, 57]. Ablating the TCR in mouse Tregs did not affect Foxp3 expression but resulted in loss of the effector Treg pool, largely due to the inability of these cells

to proliferate [57, 58]. IL-2 signaling activates STAT5 and TET demethylases which stabilize FOXP3 expression by binding CNS2 of the *FOXP3* gene (containing the TSDR) and preventing its methylation [21, 59-62]. IL-2 is also involved in controlling the size of the Treg pool [63, 64] and regulating the expression of anti-apoptotic proteins such as MCL1 [65].

Upon activation by APCs, Tregs can further differentiate into subsets with specialised functions and phenotypes. These include Th1-, Th2-, or Th17-like Tregs, driven by the respective Th-polarizing cytokines IFN-γ/IL-12, IL-5 (possibly also IL-4), and IL-6/TGF-β, produced by APCs [66-68]. Th-like Tregs share many phenotypic similarities to their Th1, Th2, or Th17 effector cell counterparts, including expression of the same lineage defining transcription factors (T-BET, GATA3/IRF4, and RORC2 respectively) and chemokine receptors (CXCR3, CCR4/CCR8, and CCR6 respectively), which enable them to home to the corresponding sites of inflammation [68, 69]. Another important Treg subset comprises T follicular regulatory (Tfr) cells, which modulate T follicular helper (Tfh) cells and B cell germinal centre responses, thus shaping antibody repertoires (reviewed in [70]). Like their T follicular helper cell counterparts, T follicular regulatory cells express the transcription factor BCL6 and chemokine receptor CXCR5, enabling migration towards CXCL13 released from DCs in B cell areas of germinal centres. Although not yet directly demonstrated, it is likely specialisation into Th-like and Tfr subsets occurs for both tTregs and pTregs upon encountering antigen in lymph nodes or in the tissues. Although these Th-like Treg subsets are required to control their corresponding Th cells *in vivo* in mouse models [71-76], *in vitro* experiments with human cells have not yet identified differential mechanisms of suppression [77, 78]. Thus, their ability to preferentially control different types of Th cells is most likely related to their ability to migrate to the same sites of action rather than major differences in function.

1.2.2 Treg mechanisms of suppression

Tregs suppress other immune cells by a variety of mechanisms, including cell-contact mechanisms, metabolic competition, and production of immunosuppressive molecules [79-81]. Tregs must be activated in an antigen-specific manner but once activated, can suppress in an antigen-independent manner.

One of the main ways that Tregs suppress immune responses is through interactions with APCs. Tregs form a strong immune synapse with APCs, which can block Tconv access to the APC, preventing activation [82-84]. During these interactions, Tregs can reshape the cytoskeleton of DCs [85] and remove MHC class II from the cell surface by trogocytosis [86]. Furthermore, interaction between LFA-1 on Tregs and ICAM-1 on APCs blocks upregulation of CD80 and CD86 by APCs, suppressing their ability to activate Tconv [87]. FOXP3 induces the expression of a number of suppressive molecules including CTLA-4 [21]. CTLA-4 binds CD80 and CD86, the same ligands as CD28, on APCs with higher affinity [88], allowing it to outcompete conventional T cells (Tconv) to bind these ligands. Tregs can internalize CTLA-4, thereby removing CD80 or CD86 from the surface of APCs [89-91]. CTLA-4 signaling from Tregs can induce additional effects on DCs including expression of indoleamine 2,3-dioxygenase (IDO) [92], which converts tryptophan to kynurenines, a metabolite that is toxic to T cells [93-95].

Tregs can suppress Tconv through metabolic effects including consumption of IL-2, production of adenosine, and altering the redox balance of the local environment. Tregs express high levels of CD25, the high affinity chain of the IL-2 receptor. High expression of CD25 may cause Tregs to consume large amounts of IL-2, reducing the availability of the cytokine for Tconv cells [64, 96]. IL-2 deprivation may also limit the expansion of natural killer (NK) cells,

as Treg-depleted mice have been shown to have increased numbers of and cytokine production by NK cells, which was reversed with the addition of an IL-2 neutralizing antibody [97]. Tregs promote the conversion of ATP to adenosine through expression of CD39 and CD73, ectoenzymes that catalyze the conversion of ATP to ADP and AMP, or AMP to adenosine, respectively [98]. Adenosine induces signaling through A2A receptors, which suppresses target cells through mechanisms including reduced proliferation and cytokine production by activated T cells [99, 100] and reduced CD86 upregulation by DCs [101]. Whereas CD39 is expressed at high levels by both mouse and human Tregs [100-102], CD73 is expressed at high levels on the surface of mouse Tregs but low levels on the surface of human Tregs [99, 100, 102]. Human Tregs were shown to have higher levels of CD73 expression when stained intracellularly [100] or after prolonged expansion *in vitro* [103], so it is possible that CD73 is still active on human Tregs even if not normally expressed at high levels extracellularly, or that the conversion of AMP to adenosine is aided by other CD73-expressing cells [98]. Tregs can also alter the local redox environment by limiting the accumulation of extracellular cysteine from DCs, which is needed for proliferation of T cells [104, 105].

Tregs also exert suppressive effects through the expression of suppressive cytokines such as TGF-β and IL-10 [81] or expression of granzymes [106]. Tregs can express both active TGFβ and inactive TGFβ, bound to LAP, and express GARP, the receptor for latent TGFβ [107, 108]. TGFβ is important for maintaining intestinal tolerance and for infectious tolerance (described further below), as TGFβ induces the differentiation of pTregs [109]. IL-10 is also involved in intestinal homeostasis [110], although its effects may be more important *in vitro* than *in vivo* [111]. Additionally, Tregs can express IL-35 [112], which reduces inflammation in a variety of

mouse models including inflammatory bowel disease [113, 114], and granzyme A and B, which induce programmed cell death [106].

Different suppressive mechanisms are likely involved depending on the location, effector cell types involved, and stage of the immune response. The concept of infectious tolerance is also important in Treg-mediated suppression [115]. In addition to directly supressing immune cells and responses, the suppressive environment created by Tregs promotes the induction of new regulatory cells. Immunosuppressive cytokines including TGFβ and IL-10 promote the differentiation of pTregs and Tr1 cells, respectively [14, 49] and Treg interactions with APCs can influence APCs to adopt a more tolerogenic phenotype. This has been observed *in vitro* with monocytes co-cultured with Tregs downregulating the expression of costimulatory ligands and inflammatory cytokines, skewing towards an immunosuppressive phenotype [116]. This concept will likely be important for long-term effectiveness of Treg cell therapies, particularly if the infused cells do not survive long-term.

1.3 Regulatory T cells as an adoptive cell therapy

Transplantation of solid organs or hematopoietic stem cells can be life-saving therapies for patients with late-stage diseases or hematological malignancies; however, transplantation success is still limited by organ rejection or graft-versus-host disease (GVHD). For successful transplantation, tolerance must be developed between the immune system and the transplanted cells or organ to limit immune rejection. Currently, transplant recipients are given immunosuppressive drugs to prevent immune rejection; however, this leaves patients vulnerable to side effects including cancer and infections.

We are interested in using adoptive transfer of Tregs to prevent GVHD following hematopoietic stem cell transplantation (HSCT) or organ rejection following solid organ transplantation (SOT). Immune tolerance is determined by the ratio of regulatory to effector cells, so administration of Tregs should shift the balance in favour of immune suppression. Treg cell therapy could also be applied in the context of autoimmunity, where defects in regulatory T cell number or function may prevent their control of self-reactive T cells [117].

Treg cell therapy has been tested in a variety of preclinical models in GVHD, solid organ transplantation, and autoimmune diseases. Administering Tregs delayed the progression of GVHD in mice undergoing bone marrow transplantation [118-120] without inhibiting the graft-versus-leukemia effect from co-injected Tconv [121]. In the context of SOT, animal models have shown that Treg cell therapy can prevent acute and chronic rejection of allografts [122] but that antigen specificity is important for therapy success. Direct antigen presentation by donor-derived APCs from the allograft or indirect presentation of donor antigen by host APCs appear to be important for protection against acute and chronic rejection, respectively [122, 123].

Non-obese diabetic (NOD) mice spontaneously develop autoimmune diabetes, largely mediated through T cell attack of insulin-producing beta cells. Transfer of antigen-specific BDC2.5 Tregs to NOD mice suppressed the development of diabetes from transferred BDC2.5 T cells [124]. Adoptively transferred Tregs could also delay the diabetes progression in mice with new onset of disease [124]. Treg cell therapy can similarly delay the progression of disease in autoimmune models of lupus [125] and experimental autoimmune encephalomyelitis (a common experimental model for multiple sclerosis (MS)) [126].

Preclinical studies of Treg cell therapy have also been conducted in non-human primates using kidney and heart transplantation models (reviewed in [127]). The increased relevancy of

these models to human immunity has allowed for testing of the effect of immunosuppression regimens and enhancing agents such as IL-2 or rapamycin. In one such study, cynomolgus monkeys that had undergone renal transplantation received multiple infusions of donor alloantigen-specific Tregs with low-dose rapamycin. Infusion of Tregs with rapamycin prolonged graft survival compared to animals that received Tregs alone, although none of the grafts survived long-term (median survival time of 48.5 days vs. 32 days) [128]. Results from these studies should provide valuable guidance in translating results from preclinical studies in mice to human trials.

1.3.1 Treg cell therapy in stem cell transplantation

Tregs were first administered as a cell therapy in humans over 10 years ago to two patients with GVHD [129]. The therapy allowed immunosuppression to be reduced in a patient with chronic GVHD but only provided transient improvement of symptoms for a patient with acute GVHD. Nonetheless, this clinical report indicated that expansion and infusion of Tregs at a clinical dose was possible and could be tolerated by patients.

Following this clinical report, a larger study was performed in which freshly isolated Tregs were administered as a prophylaxis for GVHD to acute leukemia patients undergoing allogeneic HLA-haploidentical HSCT [130, 131]. In that trial, 43 patients were administered Treg and Tconv derived from the HSCT donor 4 and 1 days prior to the stem cell infusion, respectively. In the phase I/II study, patients had a lower relapse rate than historical controls without an increased risk of GVHD, suggesting that infusion of Tregs lowered the risk of GVHD from administering Tconv with the HSCT without impairing the graft-versus-leukemia (GVL) effect. Treg suppression of GVHD without impairing GVL could be related to different migration patterns of

the Treg and Tconv. In follow-up animal studies, this group showed that the infused Tregs had lower expression of CXCR4, the bone marrow homing receptor, than the accompanying Tconv. So while Tconv that migrated to the bone marrow mediated GVL in a humanized mouse model, the Tregs primarily remained in the periphery, where they suppressed the development of GVHD [132]. A follow-up phase II trial is underway, with results of 50 patients reported to date indicating that there was a 75% moderate/severe chronic GVHD/relapse-free survival rate at a median follow-up of 29 months [133].

The first report of cell therapy with allogeneic Tregs (not from a transplant donor) came from a study of patients receiving umbilical cord blood (UCB) transplants, who received Tregs isolated and expanded from an additional separate cord blood unit, administered 15 days after the first transplant. The UCB units were all at least 4/6 HLA matched to the recipient but no inter-cord matching was performed. Patients who received UCB Tregs had similar survival to historical controls but lower incidence of grade II-IV acute GVHD (43% vs. 61%) [134]. A follow-up report indicated that these patients had an increase in opportunistic infections compared to historical controls during the first 30 days following transplant but these did not affect overall non-relapse mortality [135]. Another phase I/II study from the same group (with an altered Treg manufacturing protocol) showed Treg cell therapy to have a tolerable safety profile and to reduce the incidence of acute grade II-IV acute GVHD to 9% compared to 45% for contemporary controls ($p=0.05$) [136]. This group has since completed a first-in-human clinical trial testing infusion of TGFβ-induced Tregs (iTregs) as a prophylaxis for GVHD [137].

Overall, the results from these studies indicate that administration of Tregs is well-tolerated by HSCT patients and that Treg cell therapy has the potential to reduce the incidence or severity of GVHD without impairing the graft-versus-leukemia effect if administered around the

time of stem cell infusion [130, 131, 133, 134, 136, 138]. However, there is still limited evidence for improvement in patients with established GVHD [129, 139].

1.3.2 Treg cell therapy in solid organ transplantation

Tregs were first tested as a cell therapy for solid organ transplantation in kidney and liver transplantation. The first clinical reports came from two studies with 3 [140] and 9 [141] patients, who received infusion of autologous Tregs >6 months or 60 days after kidney transplantation, respectively. In each of these studies no serious adverse events were reported, but the studies were not sufficiently powered to show efficacy.

The largest study of Treg cell therapy in SOT completed to date was the ONE Study in which 7 centres tested 6 different cell therapy products with control arms that received the same immunosuppression regimen across all sites. Four of the cell therapy products were Tregs, with two polyclonal Treg and two donor antigen-specific Treg products. The rate of biopsy-confirmed acute rejection was similar overall between the control and cell therapy arms of the ONE Study [142], and individual reports from two of the centres that infused polyclonal Tregs indicated that patients in both the control and cell therapy arms had 100% graft survival at three- or four-years post-transplant [143, 144]. The cell therapy arm had a lower incidence of infection, likely from absence of basiliximab (anti-CD25) induction therapy, which was administered to the control but not the cell therapy groups [142]. Additionally, 40% of the cell therapy recipients could be weaned from mycophenolate mofetil (MMF) and maintained on tacrolimus monotherapy. Overall, these results indicated that Treg cell therapy is well tolerated in patients undergoing SOT and that administration of Tregs may allow for tapering of immunosuppression.

Results have also been reported from a phase I study in liver transplantation (NCT02166177) [145]. Whereas patients in the ONE Study received Tregs 5-7 days post-transplant, many of the patients in NCT02166177 received Tregs around or > 1-year post-transplant. Treg infusion was safe for most patients (there was one report of infusion-related toxicity) and patients who received the higher dose tested had a trend toward decreased donor-specific T cell responses. There are many other trials of Treg cell therapy underway or with results still to be reported in kidney (NCT02711826, NCT03867617 [146] and NCT03284242) and liver transplantation (NCT03654040, NCT02474199 and NCT02188719), as well as more recent trials underway in pediatric heart transplantation (NCT04924491) and islet transplantation (NCT04820270 and NCT03444064). The first clinical trials of chimeric antigen receptor (CAR) Treg therapy are also underway in kidney and liver transplantation (NCT04817774 and NCT05234190), using a CAR specific for HLA-A2 to recognize HLA-A2 on the donor organ in HLA-A2 mismatched transplants.

1.3.3 Treg cell therapy in autoimmunity

Treg cell therapy has been tested in autoimmunity in the context of type 1 diabetes, ALS, and MS. Additionally, one patient with SLE has been treated. Clinical trials of Treg cell therapy to treat type 1 diabetes have been performed in both children [147-149] and adults [150, 151]. In children, 8 of the 12 patients treated were in remission 1 year after Treg infusion compared to just 2 of 10 patients in the control group [148]. Patients who received Treg infusion tended to have better beta cell function, lower insulin doses and higher fasting C-peptide levels than control patients [149]. In adults, Treg infusion was safe and the Treg phenotype was generally stable after infusion, but the study did not detect an improvement in metabolic function from

Treg infusion [150]. A follow-up study was performed in which Treg infusion was accompanied with administration of low dose IL-2. Low dose IL-2 caused a transient increase in the frequency of Tregs in peripheral blood, but also increased the frequency of NK and $CD8^+$ T cells and did not cause a noticeable improvement in metabolic function [151]. Two major differences between these studies were the age of patients and time from diagnosis. Whereas patients in the pediatric study were enrolled within 2 months of diagnosis, patients in the adult studies were enrolled 3-24 months after diagnosis [150, 151]. Being further from diagnosis, the adult patients likely had less functional beta cell mass remaining and more advanced disease than the pediatric patients, contributing to the decreased efficacy of the therapy.

Another study examined the effect of Treg cell therapy in patients with relapsing-remitting MS [152]. 13 patients were treated with autologous Tregs – 10 received infusions of expanded Tregs intravenously (IV) and 3 received freshly isolated Tregs intrathecally (IT). No serious adverse events were reported; however, 5 of 10 patients treated IV had relapses and 5 of 10 patients had an increase in the mass of T2 lesions in the central nervous system. Interestingly, the 3 patients treated IT had no adverse events and stable disease throughout the study. Overall, Treg administration was safe in MS patients and this study suggests that local administration of Tregs may be more effective than IV infusion.

There have been case reports from small studies of Treg cell therapy in amyotrophic lateral sclerosis (ALS) and systemic lupus erythematosus (SLE). Three patients with ALS were treated with repeated infusions of autologous Tregs and IL-2 [153]. These patients received 4 Treg infusions each 2 weeks apart, then another 4 infusions spaced 4 weeks apart at a later time. The rate of decline due to disease slowed during the first round of infusions, accelerated between the two rounds of Treg infusion, then slowed again during the second round of infusions for all

patients. This group is now performing a larger trial to compare Treg cell therapy to a placebo in ALS patients (NCT04055623). One patient with SLE was treated with infusion of autologous Tregs [154]. The patient's disease score remained stable after infusion of Tregs, though there was an increase in the frequency of activated Tregs detected in the skin. Additional studies are currently underway in patients with pemphigus (NCT03239470), Guillain-Barré Syndrome (NCT03773328), Crohn's disease (NCT03185000), ulcerative colitis (NCT04691232), Alzheimer's disease (NCT03865017), and COVID-19 induced acute respiratory distress syndrome (NCT04468971).

1.3.4 Hurdles to Treg cell therapy

The results from clinical trials completed to date demonstrate the safety and feasibility of generating Treg cell therapy products for use in transplantation and autoimmunity. However, important hurdles remain that limit their widespread use. Results from animal studies and the early clinical trials suggest that a high proportion of Tregs to Tconv (around 1:1-1:2 ratio) is required for effective suppression [155]. However, the frequency of Tregs in the peripheral blood is low (<1% of white blood cells) [156], so *in vitro* expansion is required to generate enough cells for a full dose. A second challenge is to isolate sufficiently pure Tregs. Tregs have been isolated for clinical studies to date based on positive selection of $CD25^+$ cells with or without depletion of $CD8^+$ cells [131, 134, 136, 157] but, isolation of Tregs from the peripheral blood based on these markers results a mixed population of cells: naïve Tregs, memory Tregs and activated Tconv, which express CD25 upon activation. Finally, $CD25^+$ Tregs isolated from peripheral blood include a mixture of tTreg and pTreg. pTreg are inherently less stable than tTreg and may lose their Treg-specific characteristics when exposed to inflammatory cytokines

[158]. This is of concern, as inflammatory cytokines are unavoidable in transplantation and autoimmunity. The next sections describe methods that have been used to manufacture Tregs for clinical trials and how new methods could be used to overcome these hurdles in Treg manufacturing.

1.4 Sources of Tregs

Whereas Tregs are present throughout the body, peripheral and umbilical cord blood are the most practical sources of these cells. Peripheral blood is the most common source of Tregs, as it can be used to manufacture autologous products, although due to the prevalence of directed cord blood banking UCB may become a more common source of autologous cells in the future [159]. Third-party UCB units can also be used as an allogeneic source of Tregs for therapy, with an advantage being that these products are enriched with naïve Tregs that have a greater expansion potential than memory cells [160-162]. However, since a single cord blood unit contains a relatively small number of Tregs (~5-7.5 x 10^6) [163], these naïve Tregs must undergo multiple rounds of expansion in vitro (e.g. 27,000-fold reported by Brunstein et al. [136]) to generate enough cells for a clinical dose.

We have explored the feasibility of an alternate source of naïve Tregs: pediatric thymuses. These organs are routinely removed during pediatric cardiac surgeries and are well-suited for cell therapy applications [158]. A major advantage of using the thymus as a source of Tregs is the abundance of these cells: on average 1-2% of thymocytes are $CD4^+CD25^+$ Tregs, translating to ~500 x 10^6 cells, 100X more than in a single UCB unit and exceeding the number in the peripheral blood of an adult [158]. Another major advantage is the absence of activated conventional T cells, meaning that CD25 exclusively marks Tregs within the CD4 positive

population, reducing the risk of co-purification of conventional T cells. Accordingly, thymic Tregs are more suppressive than Tregs isolated in a similar manner from the blood and maintain their suppressive function upon exposure to inflammatory conditions [158]. As with UCB from an undirected bank, the application of thymus-derived Tregs would be as an allogeneic (partly HLA-matched) cell therapy, except in the case of heart transplantation where these cells could be isolated from an autologous thymus removed during the transplant procedure. The first phase I/II clinical trial using thymus-derived Tregs is currently underway for this context in pediatric heart transplantation (NCT04924491).

There is also growing interest in the unique properties of Tregs that reside in nonlymphoid tissues (e.g. muscle, skin, lungs, intestine, joints) [164]. Although it would be difficult to access these cells for clinical applications, increased understanding of human tissue-resident Treg biology should provide opportunities to identify desirable characteristics that could then be engineered into peripherally-sourced Tregs.

Finally, there are also efforts underway to generate Tregs by differentiation from induced pluripotent stem cells (iPSC), $CD4^+CD25^-$ conventional T cells, and/or by over-expression of FOXP3. In mouse iPSC, retroviral transduction of Foxp3 and co-culture on Notch ligand-expressing stromal cells provides a platform to generate immunoregulatory cells [165, 166]. Significant advances in this technology are being made for conventional T cells [167] and it is likely that protocols to generate iPSC-derived human Tregs are in development. *In vitro* induced Tregs generated by culturing $CD4^+CD25^-$ conventional T cells with IL-2, rapamycin and TGF-β are now being tested, with results of the first clinical trials recently reported (NCT01634217) [168]. Ectopic expression of FOXP3 can also be used to re-program conventional T cells into

Tregs [169, 170]. The first application of the latter approach will likely be in the context of gene therapy for IPEX, the systemic autoimmune disease caused by FOXP3 mutations [171, 172].

1.4.1 Autologous versus allogeneic Tregs

A key decision in the design of cellular therapy products is whether to use autologous or allogeneic cells. In the context of solid organ transplantation and autoimmunity, all clinical trials to date have used autologous Tregs derived from the patient peripheral blood. In hematopoietic stem cell transplantation, either autologous or allogeneic Tregs have been tested. Autologous cells have been derived from the stem cell donor whereas allogeneic cells came from UCB units that shared at least four HLA alleles with the recipient [134, 136, 173]. Although autologous products have the best chance of being accepted by the recipient immune system, they present manufacturing challenges. Since the products must be manufactured for each patient, the manufacturing processes for autologous cells must be sufficiently robust to be reproducible despite the large variability between donors. This can be challenging since the underlying pathologies may affect the immune cell numbers, growth potential and/or function. Indeed, there are several reports of Treg products failing to meet the target dose or release criteria [134, 136, 143-145, 150]. Finally, autologous manufacturing costs are high due to the independent cell production and validation required for each patient. Indeed, the concept of using allogeneic cell therapy products is gaining increasing interest, in particular to benefit from the economies of scale obtained when one lot of cells can treat many patients [174, 175]. These cells could be manufactured from less variable starting populations, undergo more comprehensive quality control to reduce the risks to patients, and be available for use in conditions with rapid onset such as acute GVHD.

There is evidence from mouse models and early clinical trials to support the use of allogeneic Treg therapy. In mice undergoing bone marrow transplantation, allogeneic Tregs were shown to be as potent as donor-derived Tregs at preventing allograft rejection [176]. In humans, allogeneic UCB-derived Tregs have been shown to be safe and to reduce the incidence of acute and chronic GVHD in patients undergoing umbilical cord blood transplantation [134, 136]. However, to date, allogeneic cell therapy products have only been tested in immunosuppressed and immunocompromised individuals. In immune competent individuals, a major limitation of these products may be their limited survival time in the patient, due to rejection [177]. Accordingly, in non-human primates, allogeneic Tregs were no longer detectable by flow cytometry in blood 3-6 days post-injection [177] and in a clinical trial of UCB-derived Tregs, infused Tregs could not be detected in blood 14 days after administration [134, 136]. By comparison, autologous Tregs have been detected in circulation for up to one-year post transfer using mass spectrometry. However, similar to findings with allogeneic cells, using a flow cytometry-based read out, the percentage of Tregs in circulation peaked 7-14 days post transfer [140, 150, 154] and fell near the detection limit within 3 months. Thus, more work is required to understand why the majority of infused Tregs seem to disappear from the circulation in these different contexts.

The tolerance for Treg HLA mismatching also remains an outstanding question. In anti-viral T cell therapy investigations, third-party virus-specific T cells matched for as little as a single HLA allele reduced viral loads when tested for the treatment of drug-refractory infections following hematopoietic stem cell transplantation [178]. Thus, it is possible that adoptively transferred Tregs will not have to be fully HLA-matched to the recipient to be effective. Furthermore, Tregs may not require long term survival if they can induce infectious tolerance by

conferring suppressive capacity onto other cell populations [115]. Indeed, in a murine study of graft versus host disease, Tregs exerted their suppressive effect early after transplantation and improved survival even if they were depleted 2 days after adoptive transfer [179].

A consideration is that allogeneic Treg products could pose a risk of alloimmune sensitization, particularly in non-immunosuppressed patients, or even GVHD. Notably, allogeneic virus-specific T cells have been administered as a therapy following allogeneic hematopoietic stem cell transplantation without resulting in significant GVHD [178]. Furthermore, since Tregs should suppress immune responses, the theoretical risk of alloimmune sensitization is likely lower than for allogeneic conventional T cells. To make allogeneic Tregs more likely to be accepted by the patient's immune system, genetic modification strategies could be used to eliminate and/or edit their HLA molecules. The field of HLA editing is being driven by work in the regenerative medicine/stem cell field where strategies such as knocking out Beta-2 Microglobulin (to eliminate Class I) and/or CIIT2 (class II transactivator for Class II) are being actively pursued [180-182]. Since such modifications could lead to NK cell-mediated non-self recognition, strategies to enforce expression of non-classical HLA molecules (to avoid elimination by NK cells) are also being developed [174, 182].

1.4.2 Polyclonal vs. antigen specific

Another key decision in the design of a Treg therapy is whether to use polyclonal or antigen-specific cells. Polyclonal Tregs are less complicated to manufacture but will likely have to be administered in greater numbers as only a small fraction of the cells would be specific for the disease-relevant antigens [155]. Antigen-specific Tregs would have increased cell-specific potency and decreased off-target suppression. Putnam et al. have shown that a donor alloantigen-

reactive Treg product can be generated by culturing sorted Tregs with donor B cells, followed by a polyclonal stimulation to increase cell numbers [183]. Alloantigen-reactive Tregs have been or are being tested in clinical trials of solid organ transplantation (NCT02188719, NCT02711826, NCT02244801) and GVHD (NCT01795573). An alternative approach to generate antigen-specific Tregs is to use genetic engineering to enforce expression of a CAR or TCR specific for an antigen of interest. These concepts are discussed in a later section.

1.5 Regulatory T cell therapy manufacturing

1.5.1 Strategies to isolate Tregs

Tregs are present at a low frequency in the peripheral blood, cord blood or thymus, so must be purified prior to expansion or infusion. Regardless of their source, CD25 is the main surface marker to identify Tregs and it is used as a positive selection parameter in all reported studies. In addition to CD25 there is considerable variation in the methods used to isolate clinical grade Tregs. For example, groups using magnetic selection to isolate Tregs from peripheral blood deplete $CD8^+$ cells [139, 141, 144, 145, 153, 157, 184], whereas groups isolating Tregs from UCB do not [134, 136, 173, 185]. Groups with access to flow cytometric sorting capability typically include additional markers such as positive selection for CD45RA or negative selection for CD127 [129, 140, 147, 150-152, 154, 186]. Inclusion of CD45RA or CD127 in the selection strategy increases the purity of the resulting cells compared to those isolated using magnetic selection since these markers remove most of the $CD25^+$ activated T cells that are primarily $CD45RO^+CD45RA^-$ and $CD127^+$ [187, 188]. To date, the technology to enable good manufacturing practice (GMP) grade flow cytometric cell sorting capacity has been limited, but with the development of closed system GMP sorters such as the Miltenyi MACSQuant Tyto and

the Sony FX500 Exchangeable Fluidics Cell Sorter, selection of Tregs using multiple markers will likely become more feasible.

1.5.2 Strategies to expand polyclonal Tregs

Freshly isolated Tregs have been used in clinical trials [130, 131, 133, 189]; however, due to the low frequency of Tregs in the periphery (<1% of white blood cells) [156], usually Tregs need to be expanded *in vitro* to generate a clinically relevant dose of cells **(Figure 1.1)**. There are numerous different reagents and approaches used to achieve this goal: **Table 1.1** summarizes the published clinical manufacturing protocols for polyclonal Treg expansion.

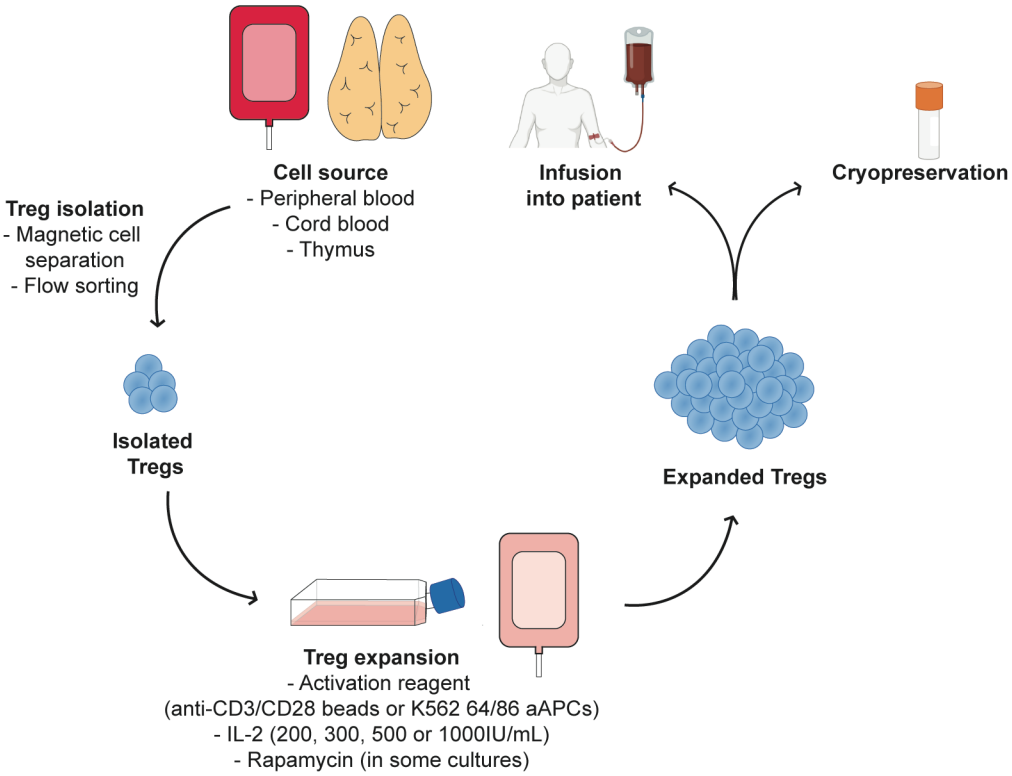

Figure 1.1: Overview of regulatory T cell (Treg) manufacturing protocols.
Tregs are isolated from peripheral blood, cord blood or thymus tissue by magnetic cell separation or flow cytometric sorting. Isolated Tregs are then expanded using anti-CD3/CD28 or artificial antigen-presenting cells (K562 64/86 aAPCs), interleukin (IL)-2 and in some cases rapamycin. After expansion, Tregs are harvested and directly administered to the patient or cryopreserved for future administration.

Table 1.1: Published clinical manufacturing protocols for polyclonal Tregs.

Study/ trial	Treg source	Isolation method	Expansion medium	Activation reagent	IL-2	Rapa-mycin	Restimu-lation	Length of expansion	Culture vessels	Fold expansion	Purity following expansion
Trzonkowski et al., 2009 **[129]**	Donor-derived peripheral blood	Flow-sorting $CD3^+CD4^+$ $CD25^{hi}$ $CD127^-$	RPMI 1640 +10% autologous plasma	anti-CD3/CD28 beads (Invitrogen)	1000 U/mL added on day 0	N/A	Day 7, day 14	Up to 3 weeks	Tissue culture plates/ flasks	Not specified	90% $FOXP3^+$
Brunstein et al., 2011**[134]**	Third-party umbilical cord blood	CliniMACS $CD25^+$	X-Vivo 15 +10% human AB serum	anti-CD3/CD28 beads (provided by academic collaborator)	300 U/mL added on day 3	N/A	N/A	18 days	Tissue culture plates/ flasks	Median 211 (range 13-1796)	Median 64% (range 31-96%) $CD4^+$ $CD127^-$ $FOXP3^+$
Marek-Trzonkowska et al., 2012 **[147]**	Autologous peripheral blood	Flow-sorting $CD3^+CD4^+$ $CD25^{hi}$ $CD127^-$	CellGro +10% autologous human serum	anti-CD3/CD28 beads (Invitrogen)	1000 U/mL added on day 0	N/A	Day 7	7-14 days	Tissue culture plates/ flasks	Not specified	Median 93% (range 90-97%) $FOXP3^+$
Brunstein et al., 2015 **[136]**	Third-party umbilical cord blood	CliniMACS $CD25^+$	X-Vivo 15 +10% human AB serum	K562 64/86 aAPCs + anti-CD3 mAb	300 U/mL added on day 3	N/A	Day 12	18 days	Not specified	Median 13,000 (range 1,352-27,183)	Median 87% (range 78-95%) $CD4^+$ $CD127^-$ $FOXP3^+$
Bluestone et al., 2015 **[150]** Dall'Era et al., 2018**[154]** Dong et al., 2021 **[151], Balcerek et al., 2021 [190]**	Autologous peripheral blood	Flow-sorting $CD4^+CD25^{hi}$ $CD127^{lo/-}$	X-Vivo 15 +10% human AB serum	anti-CD3/CD28 beads (Life Technologies)	300 U/mL added on day 2	N/A	Day 9	14 days	Tissue culture plates/flasks	Median 434.8 (range 29.8-2232)	Median 93.9% $FOXP3^+$ (range 20.9-98.6%) [190]

Study/ trial	Treg source	Isolation method	Expansion medium	Activation reagent	IL-2	Rapa-mycin	Restimu-lation	Length of expansion	Culture vessels	Fold expansion	Purity following expansion
Theil et al., 2015 **[139]**	Donor-derived peripheral blood	CliniMACS $CD8^-$, then $CD25^+$	X-Vivo 15 +10% human AB serum or TexMACS +5% human AB serum	anti-CD3/CD28 beads (Invitrogen) or ExpAct Treg Kit (Miltenyi Biotec)	300 U/mL added on day 2 or 1000 U/mL added on day 0	100 ng/mL for day 0-7	Day 7 or 8	7-12 days	Tissue culture flasks or cell differentiation bags	Median 4.5 (range 2.5-17.7)	Median 84.1% $CD4^+$ $CD25^{hi}$ $CD127^{lo}$ $FOXP3^+$ (range 77.7-91.8%)
Canavan et al., 2016 **[186]** (TRIBUTE)*	Autologous peripheral blood	Flow-sorting $CD4^+CD25^{hi}$ $CD127^{lo}$ $CD45RA^+$	X-Vivo 15 +5% human AB serum	anti-CD3/CD28 beads (Invitrogen)	1000 U/mL added on day 0	100 nM	Day 10-12	22-24 days	Not specified	Median 175 (range 66-531)	Not specified
Kellner et al., 2018 **[173, 185]**	Third party umbilical cord blood	MACS $CD25^+$	X-Vivo 15 +10% human AB serum +2mM L-glutamine	anti-CD3/CD28 beads (Invitrogen)	1000 U/mL added on day 0	N/A	N/A	14 days	Tissue culture plates/flasks	Median 71 (range 42-80)	Median 90% (range 86-93%) $CD4^+CD25^+$ $CD127^{lo}$
Chandran et al., 2017 **[140]** (TASK)	Autologous peripheral blood	Flow-sorting $CD4^+CD25^+$ $CD127^{lo/-}$	X-Vivo 15 +10% human serum	anti-CD3/CD28 beads (Invitrogen)	300 U/mL added on day 2	N/A	Day 9	14 days	Tissue culture plates/flasks	Not specified	Median 95.5% (range 93-96.7%) $FOXP3^+$
Thonhoff et al, 2018 **[153, 191]***	Autologous peripheral blood	CliniMACS $CD8^-CD19^-$, then $CD25^+$	TexMACS	ExpAct Treg Kit (Miltenyi Biotec)	500 U/mL added on day 6	100 nM	Day 14	25 days	Not specified	Median 75 (range 25-200)	97±1.4% $FOXP3^+$
Mathew et al., 2018 (TRACT) **[141]**	Autologous peripheral blood	CliniMACS $CD8^-$, then $CD25^+$	TexMACS +5% human serum +1 µg/mL TGF-β	ExpAct Treg Kit (Miltenyi Biotec)	1000 U/mL added on day 0	100 ng/mL for day 0-9	Day 7	21 days	G-Rex100	Not specified	>80% $FOXP3^+$
Sánchez-Fueyo et al, 2020 **[145, 157]** (ThRIL)*	Autologous peripheral blood	CliniMACS $CD8^-$, then $CD25^+$	TexMACS +5% human AB serum	ExpAct Treg Kit (Miltenyi Biotec)	500 U/mL added on day 4	100 nM	Day 12, day 24	24 or 36 days	Cell expansion bags	Median 67 (range 21-486)	Median 78% (range 61-92%) $CD4^+CD25^+$ $FOXP3^+$

Study/ trial	Treg source	Isolation method	Expansion medium	Activation reagent	IL-2	Rapa-mycin	Restimu-lation	Length of expansion	Culture vessels	Fold expansion	Purity following expansion
Harden et al, 2021 **[143, 184]** (The ONE study)*	Autologous peripheral blood	CliniMACS $CD8^-$, then $CD25^+$	TexMACS +5% human AB serum	ExpAct Treg Kit (Miltenyi Biotec)	500 U/mL added on day 4	100 nM	Day 12, day 24	36 days	Cell expansion bags	Not specified	Median 76.7% (range 74.7-88.2%) $CD4^+CD25^+$ $FOXP3^+$ [184]
Roemhild et al, 2020 **[144, 192, 193]** (The ONE study)*	Autologous peripheral blood	CliniMACS $CD8^-$, then $CD25^+$	X-Vivo 15 +10% human serum	anti-CD3/CD28 beads (Miltenyi Biotec)	500 U/mL	100 nM	Every 4-6 days	23 days	Not specified	Not specified	Median 91.9% (range 80.8%-99.6%) $CD4^+CD25^+$ $FOXP3^+$
Chwojnicki et al., 2021 **[152]**	Autologous peripheral blood	Flow-sorting $CD3^+CD4^+$ $CD25^{hi}$ $CD127^-$	X-Vivo20 +10% autologous human serum	anti-CD3/CD28 beads (Miltenyi Biotec)	1000 U/mL added on day 0	N/A	Day 7-9 (added each day to restore 1:1 ratio)	10-14 days	Not specified	Not specified	Median 91% (range 90-97%) $FOXP3^+$

*Details of expansion protocol and data taken from the referenced publication describing pre-clinical protocol development

TCR and costimulatory signals for Treg activation can be provided *in vitro* through antibodies bound to beads, soluble antibody reagents or artificial antigen presenting cells (aAPCs). The most commonly used activation reagent is magnetic beads with covalently attached antibodies specific for CD3 and CD28. A limitation of this approach is that the magnetic beads must be removed prior to infusion and overall it is unclear if this is the optimal way to stimulate Tregs. Another approach is to expand Tregs with artificial antigen presenting cells transduced with co-stimulatory molecules and an Fc receptor which can be used to present antibodies on the cell membrane. For example, K562 cells expressing CD86 and CD64 are considerably better than CD3 and CD28-coated beads at expanding UCB Tregs [136, 194, 195]. In these cells, expression of CD64, a high affinity Fc receptor, allows the cells to be 'loaded' with a monoclonal antibody that targets the CD3 receptor. Once these cells have been loaded, they can provide primary signals for activation through the anti-CD3 mAb bound to CD64 and costimulatory signals through CD86. These cells are lethally irradiated prior to use so disappear from culture over time, avoiding the need for a removal step at the end of the process. Although these cells are very effective at stimulating Treg expansions [194, 196], their use adds complexity to the cell manufacturing process with extensive cell testing and batch validation requirements.

Additional activation reagents are available in soluble forms to ease their removal prior to the administration of Tregs to a patient, although the use of these reagents in clinical protocols has not yet been reported. T cell TransAct (Miltenyi) is a polymer nanomatrix conjugated with antibodies to CD3 and CD28. This reagent is soluble, so excess reagent can be removed through centrifugation. Likewise, STEMCELL Technologies has developed T cell activators composed of soluble tetrameric antibody complexes that bind CD3 and CD28 or CD3, CD28 and CD2 (to

provide additional co-stimulation). STEMCELL Technologies does not yet have a GMP-grade format of these reagents available; however, this can be expected in the near future.

Reported Treg expansion protocols **(Table 1.1)** have used a variety of culture media including RPMI 1640 (Thermo Fisher), CellGro (CellGenix), X-Vivo 15 (Lonza) and TexMACS (Miltenyi Biotec), all available in GMP-compliant versions. One drawback of these media is that they are commonly supplemented with 5 or 10% human serum. Serum provides critical factors for Treg growth but is costly and can add significant regulatory hurdles due to its variability and the risk of possible adverse events [197, 198]. The use of serum free media, such as OpTmizer (Thermo Fisher) or ImmunoCult-XF (STEMCELL Technologies), or serum replacement supplements, would alleviate these concerns [199].

High levels of IL-2 are used in most Treg expansion protocols; however, the IL-2 concentration actually required for optimal Treg expansion is unclear. Original reports of Treg expansion used IL-2 at concentrations similar to those used for conventional T cells, e.g. ~100 international units (IU)/mL [200], but many groups now add this cytokine at concentrations up to 1000IU/mL [129, 141, 147, 152, 173, 186]. Notably, protocols differ not only in the concentration of IL-2 added, but also in the addition timing, with some groups adding IL-2 from the start and others only three or four days post stimulation [134, 136, 145, 157, 184]. Some groups also use the immunosuppressive drug rapamycin in Treg expansion protocols [139, 141, 144, 145, 153, 157, 184, 186] because it can limit the growth of effector T cells [201, 202]. There is evidence that rapamycin may increase the suppressive function of Tregs [184, 203], so culturing Tregs with rapamycin may result in a purer, more potent product. Although rapamycin improves purity, it also limits Treg proliferation, so it is most commonly used by groups who do not employ flow cytometric sorting as part of their protocol, such that maintaining sufficient

Treg purity is a greater challenge and more important than maximal expansion. Addition of the rapamycin derivative Everolimus has also been shown to yield a purer, more suppressive product and is now being tested in Treg expansion protocols [203].

1.5.2.1 Large-scale expansion platforms

In the research environment, Tregs are typically cultured in polystyrene multi-well plates or tissue-culture flasks. While plates and flasks have been used in clinical protocols [129, 134, 139, 140, 147, 150], these vessels are not well-suited to GMP production or scale-up. Many flasks are required to produce large doses and the use of open systems increases contamination risks. Closed systems such as gas permeable cell expansion bags are increasingly being used to reduce the risk of product contamination and to facilitate larger scale manufacturing. Alternative cell culture devices such as the G-Rex (Wilson Wolf) or rocking motion bioreactors are also being tested.

Gas permeable cell expansion bags allow cells to be cultured in a closed system. These bags are typically made of flexible polymers such as polyolefins or fluoropolymers [204], which have low evaporation rates and are permeable to allow incubator oxygen and carbon dioxide exchange through the sides of the bag. Sampling and medium additions can be performed using tube welding devices to maintain a closed system that minimize contamination risks; however, handling by operators is still required for sampling and feeding steps and these bags lack built-in analytics.

Rocking motion bioreactors use cell expansion bags which are placed on a heated platform that rocks to facilitate culture mixing and gas transfer. The cell expansion bags have ports for gas delivery, sampling and feeding, similar to a gas permeable bag. Some bags are additionally

equipped with lines for fresh medium delivery/conditioned medium removal to enable perfusion and/or probes to monitor pH and dissolved oxygen over the course of culture. These systems typically include software to provide automation and facilitate recording of manipulations; however, the minimum starting volumes and lack of scale-down systems make process development for these systems difficult. Rocking motion bioreactors have been used to manufacture other T cell products [205, 206], but their use has yet to be reported for a clinical Treg manufacturing protocol.

The G-Rex ("Gas permeable Rapid expansion") is a cell culture platform that has a gas-permeable silicone membrane at its base that facilitates gas exchange, allowing cells to be grown in a larger volume of media to reduce the frequency of medium additions compared to conventional cultures [207]. The G-Rex requires less handling than conventional tissue culture flasks or gas permeable cell expansion bags given this large volume of media, but is harder to sample and monitor. The G-Rex was recently used by Mathew et al. to generate Tregs for a clinical trial in kidney transplantation [141].

1.5.3 Cryopreservation of Tregs

Another key decision in designing a cellular therapy product is whether to use fresh or cryopreserved cells. Cryopreservation offers many advantages including long-term storage, time of infusion flexibility and more time to perform release testing. However, the quality of Treg products may be decreased after cryopreservation. For *ex vivo* cells there have been mixed reports as to whether cryopreservation reduces the proportion of $CD25^{high}CD127^{-}$ and $FOXP3^{+}$ cells among peripheral blood mononuclear cells (PBMCs): some groups observed a reduced Treg frequency whereas others did not [208-212]. It has also been shown that the expression of CD25

and FOXP3, as well as the suppressive capacity of Tregs can be impaired immediately after thawing [213, 214]; however, their normal characteristics can be restored upon re-activation [213, 214]. In part due to the uncertainly surrounding possible effects of cryopreservation, only a few clinical trials have infused cryopreserved Tregs [145, 157, 184]. As for other aspects of the Treg manufacturing process, the development of methods for high quality Treg cryopreservation should leverage the progress being made in manufacturing conventional T cells for cancer immunotherapy [215].

1.5.4 Next generation Treg cell therapies

1.5.4.1 Modulating Treg function or stability with culture conditions

Many groups have sought to find ways to modify culture conditions to modulate Treg function by enhancing their migration, persistence, and/or stability. Because there is evidence that Treg effectiveness depends in part on migration to both lymph nodes and sites of inflammation [216-219], the ability to preserve and/or change homing receptor expression during manufacturing would be desirable. We have recently shown that culture conditions can be modified to induce stable expression of homing receptors such as CXCR3 and α4β7 [77], which are important for Treg homing to sites of Th1 inflammation and intestinal inflammation, respectively. For example, adding IL-12 and IFNγ during the culture increased the expression of T-BET and CXCR3, enabling Tregs to migrate to CXCL10 [77]. These cells maintained high CXCR3 expression in the absence of IL-12 and IFN-γ, even post infusion into mice. Importantly, these they also retained expression of CD62L and CCR7 and hence their expected ability to migrate to lymphoid tissue.

As discussed previously, a major disadvantage of allogeneic cell therapy products could be their decreased persistence *in vivo*. Parmar et al. have shown that fucosylation, which adds fucose to the cell surface to form a sialyl-Lewis X moiety on the P-selectin ligand, increased the persistence of UCB Tregs in a xenogeneic GVHD model, likely through increased binding to E-selectin [220]. This concept is now being tested in a Phase I/II clinical trial (NCT02423915) to determine whether fucosylated Tregs are safe and effective at preventing or reducing GVHD in humans.

Modified culture conditions, such as non-standard temperatures, oxygen availability or metabolite concentrations, can also be used to enhance Treg stability. Marek-Trzonkowska et al. found that culturing Tregs at 33°C, compared to 37°C, yields a product with higher expression of CD25 and FOXP3, higher frequency of demethylated TSDR and higher suppressive capacity [221]. This group has since switched to using 33°C for manufacturing clinical grade cells [221]. Mixed results have been reported for the effect of oxygen on Treg stability and function in culture. Some groups have observed increased proliferation [222] or suppressive capacity [223] of Tregs under hypoxic conditions, while others have observed that hypoxic conditions favour the differentiation of Th17 cells rather than Tregs [224]. Low levels of amino acids such as glutamine and tryptophan, or the presence of tryptophan metabolites such as kynurenine, have been shown to promote the development of iTregs [225, 226]. Short-chain fatty acids such as butyrate, produced by microorganisms in the gut, have also been shown to promote the differentiation of Tregs [227-229]. These data suggest that amino acid or fatty acid levels could be tailored to favour the survival of Tregs over conventional T cells, but this concept has yet to be applied to clinical protocols.

1.5.4.2 Modulating Treg function or stability with genome editing

Treg function could also be modulated through genome editing such as to create antigen-specific Tregs and/or to enhance the expression of Treg-specific genes. The higher potency of TCR-engineered Tregs has been known for a decade, with some of the first evidence coming from the transplantation of Tregs transduced with a donor allospecific TCR which induced long-term survival of partially MHC-mismatched heart grafts in mice [230, 231]. This concept is now also being applied in the context of autoimmunity, where a limited number of defined peptide-MHC complexes makes it feasible to consider selecting a few TCRs that could be used to engineer Tregs that could be used in a relatively large proportion of affected subjects [232].

An alternative approach to TCRs is to engineer Tregs to express chimeric antigen receptors (CARs) for antigens of interest. CARs are synthetic proteins created by combining extracellular antigen binding domains with intracellular signaling domains [233, 234]. Early studies in mice demonstrated the efficacy of this approach by targeting myelin oligodendrocyte glycoprotein to treat experimental autoimmune encephalomyelitis [235] and carcinoembryonic antigen to treat colitis [236]. It has since been demonstrated that human Tregs can be transduced to express a CAR specific for HLA-A2 and that these cells are more protective than are polyclonal cells in models of xenogeneic GVHD [237] and humanized skin transplant [238, 239].

Recent advances in genome editing technology such as CRISPR/Cas9 offer an opportunity to precisely edit the genome or manipulate gene expression during the manufacturing process. Chen et al. have shown that CRISPR/Cas9 can be used to knock out genes in Tregs without affecting the expression of FOXP3 or Helios [240]. Furthermore, they showed that nuclease-deficient Cas9 can be used to induce expression of Treg-specific genes such as GARP [240]. Additionally, other groups have used this technique in CAR T cell manufacturing to direct a

CD19-specific CAR to the T-cell receptor α constant locus [241] or to enhance the efficacy of CAR T cells by disrupting the *Pdcd1* gene [242]. It is likely that CRIPSR/Cas9 could similarly be used to promote expression of genes to enhance Treg function or stability (e.g. FOXP3, CTLA-4) or the production of anti-inflammatory cytokines (e.g. IL-10).

1.6 Monitoring infused Tregs *in vivo*

Preclinical models suggest that Tregs must be able to migrate to both lymph nodes and to the site of the graft or inflammation for Treg cell therapies to be effective [217, 219]. However, little is known about the migration of Tregs in humans following infusion. More extensive cell monitoring after infusion will be critical for gathering information about the persistence and migration patterns of infused cells, to detect both migration to the site of transplant or inflammation and to sites where cells may have off-target effects. For example, it has been shown for CAR T cell therapy that long-term persistence of CAR T cells is linked to better outcomes [243]. It will be important to establish whether the same is true in Tregs, as it will inform the design of therapies and manufacturing protocols.

To date, Treg monitoring post-infusion in clinical trials has primarily been limited to analyzing peripheral blood by flow cytometry or mass spectrometry. More specifically, Tregs have been monitored by measuring the frequency of Tregs in peripheral blood by flow cytometry (with no way of distinguishing infused Tregs from endogenous Tregs), using flow cytometry to detect infused Tregs based on unique HLA type [134, 135], or using mass spectrometry to detect infused Tregs labelled with deuterium [140, 150, 151, 154]. These analyses offer a rough idea of the persistence of infused Tregs in the blood, but provide no information about cell persistence or migration to tissues.

Infused Tregs have been monitored in tissues in two clinical studies to date. A case study of Treg cell therapy for SLE showed an accumulation of Tregs in a skin biopsy taken 12 weeks following adoptive transfer [154]. In contrast, the percentage of Tregs in the peripheral blood was unchanged over this 12 week period and the percentage of deuterium enrichment for these adoptively transferred Tregs in the peripheral blood had fallen to near the limit of detection by week 12. In another study, Tregs were isolated from the peripheral blood of patients with autoimmune hepatitis, labelled with ^{111}indium *ex vivo*, then re-administered to the patient and monitored for up to 72 hours using single-photon emission computed tomography (SPECT) and computed tomography (CT) scanning, with the goal of monitoring Treg trafficking and tissue localization. The adoptively transferred Tregs were detected in the liver, bone marrow, and spleen of subjects in this study, with minimal off-target localization in other tissues [244]. While both of these studies were small (1 and 4 patients respectively), these observations indicate that more detailed analysis of Treg distribution will likely be required to properly measure the persistence of administered Tregs than monitoring peripheral blood alone.

Imaging techniques such as bioluminescence imaging (BLI), magnetic resonance imaging (MRI), or nuclear imaging by positron emission tomography (PET) or SPECT can be used to gain a more complete picture of cell distribution throughout the body. BLI is becoming a standard technique in preclinical models for cancer therapy and has been used by groups such as ours to monitor Treg migration to the site of a graft or inflammation *in vivo* [23, 77]. However, BLI offers minimal anatomical information, and cannot be easily translated to humans [245, 246]. As such, many groups are working on developing methods to track adoptively transferred cells using MRI or nuclear imaging, with the vision of translating those methods to humans to track cells in clinical trials.

1.6.1 Direct vs. indirect cell labelling

Cells must first be labelled to enable monitoring using non-invasive imaging methods (reviewed by [246]). Cells may be labelled directly with contrast agents or indirectly by genetically engineering cells to express receptors that allow them to uptake reporters at the time of imaging [245].

For direct cell labelling approaches, cells are labelled *ex vivo* using contrast agents (e.g. iron oxide, gadolinium, [^{19}F]-fluorine). Depending on the contrast agent, the label may be taken up through normal cellular processes (e.g. phagocytosis or internalizing receptors) or assisted by transfection agents [245, 246]. A limitation of direct cell labelling is that cells are labelled with a fixed amount of contrast agent, so the signal typically decays with time and as cells proliferate. However, direct cell labelling may be a better option for cell therapies that do not already involve genetic modification as it may be more easily incorporated into cell manufacturing protocols.

For indirect cell labelling approaches, cells are genetically engineered to express a reporter gene that allows them to uptake a contrast agent at the time of imaging (reviewed in [245]). The reporter is permanently integrated into cells, so repeat imaging can be performed by administering additional contrast agent. Reporter genes include enzymes, cell surface proteins, or transporter proteins that catalyze the reaction of, bind, or enable the transport of an administered substrate [245, 246]. For example, indirect cell labelling was used to track mouse and human Tregs modified to express the human sodium iodide symporter (hNIS) by NanoSPECT/CT after administration of Technetium-99m pertechnetate (99mTcO4$^-$) [247, 248]. Indirect cell labelling is generally better suited for cell therapy products that already involve genetic modification as adding genetic modification to a manufacturing process adds significant regulatory burden.

1.7 Research objectives

Pediatric thymus-derived Tregs are well suited for cell therapy applications as they are abundant, can be easily isolated on the basis of CD25 expression and maintain their suppressive function even under inflammatory conditions [158]. However, *in vitro* expansion is still required to generate a full therapeutic dose of cells. The need for efficient manufacturing of clinical-grade Tregs is an obstacle to the widespread use for Treg-based therapies. Methods for *in vitro* Treg expansion have thus far been derived from protocols intended for conventional T cells, with limited to Treg-specific optimization, especially under serum-free and aAPC-free conditions.

The overall goal of this thesis is to develop methods to manufacture thymic Tregs for use as a cell therapy product. To this end, each chapter addresses a specific research objective:

- **Chapter 3:** To develop manufacturing protocols for isolation, expansion and cryopreservation of thymic Tregs that are appropriate for a Phase I clinical trial [3];
- **Chapter 4:** To investigate critical process parameters for longer-term expansion of thymic Tregs;
- **Chapter 5:** To scale-up the thymic Treg manufacturing protocols;
- **Chapter 6:** To investigate methods to track Tregs *in vivo* using ^{19}F-perfluorocarbon direct cell labelling and MRI.

The aims of this thesis are summarized in **Figure 1.2**.

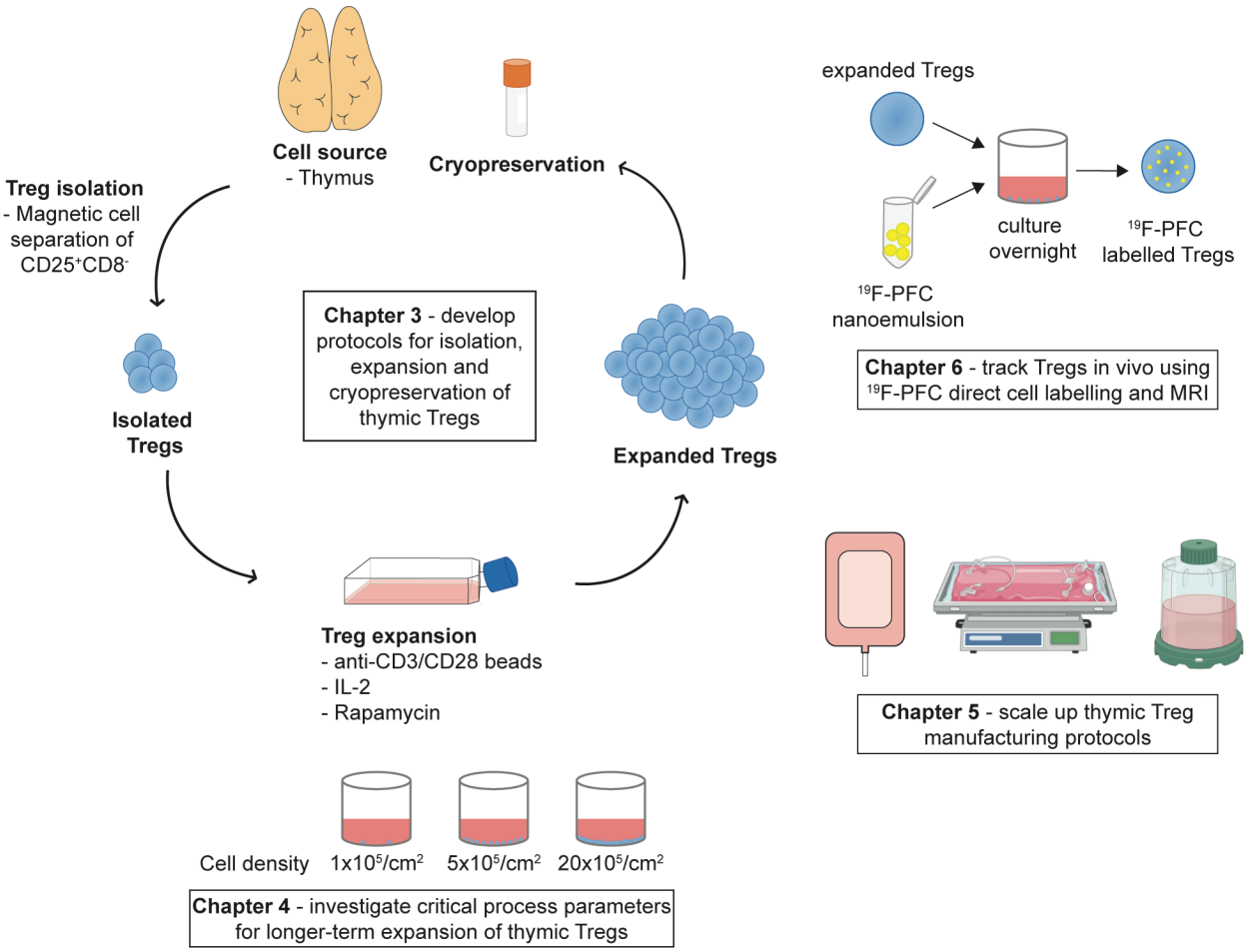

Figure 1.2: Research aims addressed by this thesis.
In chapter 3, protocols are developed to isolate, expand, and cryopreserve thymic Tregs that could be used in an early phase clinical trial. Chapter 4 investigates the consequences of adjusting cell density on longer-term expansion of thymic Tregs. Chapter 5 describes the scale-up of thymic Treg manufacturing protocols. In chapter 6, ^{19}F-perfluorocarbon (PFC) labelling is investigated as a technique to track Tregs in vivo using MRI.

Chapter 2: Materials and Methods

2.1 Cell isolation

Isolation of Tregs and Tconv from thymus: Thymus tissue was collected during infant cardiac surgery at British Columbia Children's Hospital or University of Alberta Stollery Children's Hospital. Tissue was dissociated in RPMI medium (Thermo Fisher Scientific) with 10% heat-inactivated fetal bovine serum (FBS) (VWR), 1% GlutaMAX (Thermo Fisher Scientific) and 1% penicillin/streptomycin (P/S) (Thermo Fisher Scientific) or ImmunoCult-XF T cell Expansion Medium (ImmunoCult-XF) (STEMCELL Technologies) with 1% P/S by manual dissociation using scissors, razor blades or McIlwain tissue chopper (Campden Instruments Ltd.) or by using the gentleMACS Dissociator (Miltenyi Biotec). $CD25^{+}CD8^{-}$ thymic Tregs were isolated by CD25 positive selection using Releasable RapidSpheres, followed by CD8 depletion according to manufacturer's instructions (STEMCELL Technologies). $CD25^{-}CD8^{-}$ thymic Tconv were isolated from the $CD25^{-}$ fraction by CD8 depletion followed by CD3 positive selection using EasySep Human CD3 Positive Selection Kit (STEMCELL Technologies).

Isolated thymic Tregs and Tconv were cryopreserved in CryoStor 10 (CS10) (STEMCELL Technologies) or FBS with 10% dimethyl sulfoxide (DMSO) prior to expansion. In data not shown, viability and recovery did not differ between these two types of freezing media. Cells expanded to generate data for Figure 3.6 and Figure 3.7 were cryopreserved in human serum (HS) (Wisent Bioproducts) with 10% DMSO.

Large-scale isolation of thymic Tregs (Chapter 5): Thymus tissue was processed as described above. Isolated thymocytes were transported to STEMCELL Technologies, where $CD25^{+}CD8^{-}$ thymic Tregs were isolated by CD25 positive selection using Releasable RapidSpheres, followed

by CD8 depletion using either a small-scale magnet capable of processing up to 4 mL of cell suspension or a large-scale capable of processing up to 100 mL of cell suspension.

Isolation of cells from peripheral blood: Peripheral blood mononuclear cells (PBMCs), naïve Tregs, and naïve Tconv were isolated from buffy coats of healthy adults by density gradient centrifugation using Lymphoprep (STEMCELL Technologies). For naïve peripheral blood Tregs, $CD4^+CD25^+$ cells were pre-enriched using RosetteSep Human $CD4^+$ T Cell Enrichment Cocktail (STEMCELL Technologies) and CD25 Microbeads II (Miltenyi Biotec), then sorted as $CD4^+CD25^+CD127^-CD45RA^{hi}$ Tregs (BD FACSAriaII). Naïve peripheral blood Tconv were sorted as $CD4^+CD25^-CD127^+CD45RA^{hi}$ from the $CD25^-$ fraction.

2.2 Cell expansion

Expansion using non-cell-based stimulation (Chapter 3): Thawed thymic Tregs were activated with ImmunoCult Human CD3/CD28 T Cell Activator, ImmunoCult Human CD3/CD28/CD2 T Cell Activator (both STEMCELL Technologies), CTS Dynabeads Treg Xpander (Treg Xpander) (Thermo Fisher Scientific) at a 4:1 bead to cell ratio, or T cell TransAct (Miltenyi Biotec). Tregs were cultured as indicated in ImmunoCult-XF with 1% P/S, with or without 5% CTS Immune Cell Serum Replacement, X-Vivo 15 (Lonza) with 5% CTS Immune Cell Serum Replacement (Thermo Fisher Scientific), 1% P/S and phenol red, TexMACS Medium (Miltenyi Biotec) with 5% human serum (Wisent Bioproducts) and 1% P/S, or OpTmizer T Cell Expansion Media (Thermo Fisher Scientific) with 5% CTS Immune Cell Serum Replacement, 1% GlutaMAX and 1% P/S. Thymic Tconv were activated with ImmunoCult Human CD3/CD28/CD2 T Cell Activator and cultured in ImmunoCult-XF with 1%

P/S. Naïve peripheral blood Tregs were activated with Treg Xpander at a 4:1 bead to cell ratio and cultured in ImmunoCult-XF with 1% P/S. Naïve peripheral blood Tconv were activated with Dynabeads Human T-Expander at a 3:1 bead to cell ratio and cultured in ImmunoCult-XF with 1% P/S. 100 ng/mL rapamycin (Sigma Aldrich) was added to Treg cultures from day 0-7. Recombinant human (rh) IL-2 (Proleukin) (Tregs: 1000 IU/mL, Tconv: 100 IU/mL) was added from day 0. Cells were seeded at $5x10^5$ cells/mL in 96-well or 24-well plates with the concentration maintained at $5x10^5$ cells/mL and media/additives refreshed every 2-3 days. Cells were restimulated as indicated. For cultures with Treg Xpander or Dynabeads Human T-Expander, a 1:1 bead to cell ratio was used for restimulation.

aAPC-based stimulation (Chapter 3): In some cases, cells were activated with irradiated (75 Gy) L cells preloaded with 100 ng/mL anti-CD3 mAb (OKT3, UBC AbLab) at a 1:1 ratio (aAPCs : Tregs) (14) and cultured as indicated in ImmunoCult-XF with 1% P/S. 100 ng/mL rapamycin was added from day 0-7 and 1000 IU/mL IL-2 was added from day 0. Cell concentration was maintained at $5x10^5$ cells/mL with media/additives refreshed every 2-3 days. Cells were restimulated as indicated. Alternatively, cells were activated with irradiated (100 Gy) K562 cells transduced to express CD64 and CD86 (KT64/86) that had been pre-loaded with 1 µg/mL anti-CD3 (OKT3, Miltenyi Biotec) at a 1:1 ratio. Tregs were cultured in X-Vivo 15 with 10% heat inactivated human AB serum (Valley Biomedical), L-glutamine (Invitrogen) and N-acetylcysteine (American Regent). 300 IU/mL recombinant human IL-2 (Proleukin) was added at day 2. Cell concentration was maintained at $2.5x10^5$ cells/mL from day 0-11, $5x10^5$ cells/mL from days 12-15 with media/additives refreshed every 2-3 days [195].

Expansion using non-cell-based stimulation (Chapter 4, 6): Thawed thymic Tregs were activated with CTS Dynabeads Treg Xpander at a 4:1 bead to cell ratio (unless otherwise indicated), and expanded in ImmunoCult-XF T cell Expansion Medium with 1% P/S. In chapter 4, cells were seeded in 96-well, 48-well, or 24-well plates at the indicated volumetric cell concentrations (cells/mL) and/or culture surface cell densities (cells/cm^2). In chapter 6, cells were seeded at $5x10^5$ cells/mL in 24-well plates. Cultures were fed every 2 days starting from day 3 by adding additional media to adjust the cell concentration and/or cell density to indicated levels. 1000 IU/mL recombinant human IL-2 was added at day 0 and each day the cells were fed. 100 ng/mL rapamycin was added on days 0, 3, and 5. Cultures were restimulated on day 11 by adjusting the cell concentration and/or cell density to the indicated levels and adding additional Dynabeads Treg Xpander at a 1:1 bead to cell ratio.

Treatment with cell surface protein inhibitors (Chapter 4): Tregs were restimulated by adjusting the cell surface density to the indicated levels and treated with 1 μg/mL of anti-PD1 (Nivolumab; Bristol Myers Squibb), anti-hCTLA-4 (InvivoGen), recombinant human CTLA-4 (R&D Systems), or TGFβR1 inhibitor SB 431542 (Cedarlane Laboratories).

Expansion under low oxygen (Chapter 4): Tissue culture plates were placed in a hypoxia incubator chamber, which was filled with gas containing 1.5% O_2, 5% CO_2, and 93.5% N_2. The chamber was sealed and placed in an 37ºC incubator for 2 days. Oxygen concentration in the chamber was measured using a Wireless Oxygen Gas Sensor (Pasco Scientific) and SPARKvue Data Analysis Software version 4.6.1 (Pasco Scientific).

Treatment with antioxidants (Chapter 4): Tregs were restimulated by adjusting the cell surface density to the indicated levels and treated with 10 mM N-acetylcysteine or 100 U/mL catalase starting on day 13. Additional N-acetylcysteine or catalase was added at each feed.

Large-scale expansion (Chapter 5): Tregs were activated with Dynabeads Treg Xpander at a 4:1 bead to cell ratio and cultured for 7 days in ImmunoCult-XF with 1% P/S. 100 ng/mL rapamycin was added from day 0-7 and 1000 IU/mL IL-2 was added from day 0. Cell concentration was maintained at $5x10^5$ cells/mL with media/additives refreshed every 2-3 days. On day 7, Tregs were split into tissue culture flasks, gas permeable cell expansion bags, the WAVE rocking motion bioreactor, or the G-Rex 100M and restimulated with Dynabeads Treg Xpander at a 1:1 bead to cell ratio. Each culture was handled and fed as indicated in Table B.1 and Table B.2.

2.3 Cryopreservation of expanded cells

Expanded cells were resuspended at $4x10^6$ cells/mL in CS10. Cells were aliquoted into cryotubes (0.5-1 mL per tube) which were transferred to a Mr. Frosty Freezing Container (Thermo Fisher Scientific) and placed at -80ºC overnight. Alternatively, cells were cryopreserved using the CryoMed Controlled-Rate Freezer (Thermo Fisher Scientific) or the ViaFreeze Controlled Rate Freezer (Cytiva) where indicated. Once frozen, cryopreserved cells were stored in liquid nitrogen for 1-4 weeks. Cells were thawed by placing cryovials in a 37ºC water bath for 1-2 minutes, until just melted. In chapters 3 and 5, RPMI medium with 10% heat inactivated FBS, 1% GlutaMAX and 1% P/S was used as thawing medium. In chapter 6, ImmunoCult-XF with 1% P/S was used as thawing medium. 1 mL of warmed thawing medium was added dropwise to each cryovial,

then the cell suspension was transferred to a Falcon tube containing an additional 9 mL of warmed thawing medium. Thawed cells were washed once with PBS, then resuspended in ImmunoCult-XF with 1% P/S. For overnight culture after thawing, cells were seeded at $1x10^6$ cells/mL and cultures were supplemented with IL-2 (Tregs: 1000 IU/mL, Tconv: 100 IU/mL).

2.4 Flow cytometry and cytokine analysis

Surface markers and fixable viability dye (FVD) (Thermo Fisher Scientific) were stained in PBS or Brilliant Stain Buffer (BD Biosciences). Cells were fixed and intracellular staining was done using the FOXP3/Transcription Factor Staining Buffer Set (Thermo Fisher Scientific). For intracellular cytokine staining, expanded Tregs were activated for 4 hours using phorbol myristate acetate (PMA, 10 or 2 ng/mL), Ionomycin (500 or 750 ng/mL) and 10 μg/mL brefeldin A prior to staining. Staining with Hypoxia Green Reagent for Flow Cytometry (Thermo Fisher Scientific) was performed by adding dye directly to cell culture medium to reach a final concentration of 0.5 μM and incubating cells at 37ºC for 3 hours. Data were acquired on a BD LSRII, BD LSRFortessa X-20, BD FACSymphony or Beckman Coulter CytoFLEX. Analysis was performed using FlowJo version 10. A full list of antibodies and labelling dyes used in this thesis can be found in Appendix A.

2.5 DNA isolation and Treg-specific demethylation region (TSDR) analysis

The EZ DNA Methylation-Direct Kit (Zymo Research) was used to isolate DNA from frozen cell pellets and to perform disulfite conversion according to manufacturer's instructions. The TSDR region was PCR amplified using AllTaq PCR core kit (QIAGEN). PCR products were

analyzed with the PyroMark Q96 MD pyrosequencing system (QIAGEN) and results were calculated with Pyro-CpG software (Biotage).

2.6 In vitro suppression assays.

PBMCs and Tregs were labelled with cell proliferation dye (CPD) (Thermo Fisher Scientific) or carboxyfluorescein succinimidyl ester (CFSE) (Thermo Fisher Scientific). Cells were mixed at indicated ratios, stimulated with Dynabeads Human T-Expander (Thermo Fisher Scientific) at a 1:8 or 1:16 bead to cell ratio or anti-CD3 beads (Invitrogen) at 1:1 ratio and cultured in X-Vivo 15 supplemented with 5 or 10% human serum, 1% GlutaMAX, 1% P/S, and/or L-glutamine and N-acetylcysteine at 37ºC for 4 days. Percentage of suppression was calculated using division index (DI) using the following equation:

$$\text{Suppression of proliferation (\%)} = 100 - \frac{\text{Division index}_{\text{sample}}}{\text{Division index}_{\text{positive control}}} \times 100$$

PBMCs stimulated with beads without Tregs served as positive controls.

2.7 Apoptosis assay

Cell viability was determined using Abcam's blue, green, red Apoptosis/Necrosis Assay Kit according to the manufacturer's instructions. Staining was performed in Assay Buffer for 30 min at room temperature. The volume was topped up using Assay Buffer after staining. Live apoptosis negative cells were defined as CytoCalcein Violet 450 positive, Apopxin Green negative. Cells in early stages of apoptosis were defined as Apopxin Green positive, 7-aminoactinomycin D (7AAD) negative. Cells in late stages of apoptosis were defined as Apopxin Green positive, 7AAD positive.

2.8 Media analysis

Analysis of nutrient and metabolite levels in conditioned medium: Samples of conditioned medium were taken prior to feeding on each day that cells were fed. Levels of glucose and lactate in cell culture medium were measured using a Stat Profile pHOx Ultra blood gas analyzer (Nova Biomedical). Samples were diluted with RO water prior to analysis if required. The concentration of ammonium was determined by measuring blood urea nitrogen levels and calculating the corresponding concentration of ammonium based on a standard curve. Concentrations of glucose and lactate after feeding were calculated based on concentrations measured in conditioned medium and in fresh medium using the following equation:

$$S_1 = \frac{S_0 V_0 + S_f V_f}{V_T}$$

Where S_1 refers to the new concentration of glucose or lactate in culture, S_0, and S_f refer to the concentrations of glucose or lactate in the conditioned and fresh medium respectively, V_0 and V_f refer to the volume of conditioned and fresh medium respectively, and V_T refers to the total volume of culture.

Concentrations of amino acids were determined by high performance liquid chromatography (HPLC). Nanosep centrifugal ultra-filters with a cut-off of 3 kDa were used to remove proteins in the supernatant. Samples were tagged using AccQFluor reagent (Waters) and run on the HPLC using 3.9 x 150 mm 4 μm silica base bonded with C18 HPLC columns (Waters). Amino acid concentrations were calculated based on the areas under resolved peaks compared to standards, which were prepared from a mixture of Amino Acid Standard H (Pierce Biotechnology), supplemented by glutamine, hydroxyproline, and tryptophan.

2.9 Calculation of specific growth rates, specific glucose uptake rates, and specific lactate production rates

Specific growth rate was determined using the following equation:

$$\mu = \frac{\ln\left(\frac{N_1}{N_0}\right)}{\Delta t}$$

Where μ is the specific growth rate, N_0 and N_1 refer to the number of cells in culture at the beginning and end of the feeding interval respectively, and Δt refers to the time between feeds.

The rates of specific glucose uptake and lactate production were determined per cell using the following equations:

$$q_g = \frac{S_0V_0 \ - S_1V_1}{\Delta t\left(\frac{N_1 - N_0}{\ln\left(\frac{N_1}{N_0}\right)}\right)}$$

Where S_0, V_0, and N_0 refer to the glucose concentration, volume, and cell number at the beginning of the feeding interval respectively, and S_1, V_1, and N_1 refer to the glucose concentration, volume, and cell number at the end of the feeding interval respectively. Δt refers to the time between feeds.

$$q_L = \frac{S_1V_1 \ - S_0V_0}{\Delta t\left(\frac{N_1 - N_0}{\ln\left(\frac{N_1}{N_0}\right)}\right)}$$

Where S_0, V_0, and N_0 refer to the lactate concentration, volume, and cell number at the beginning of the feeding interval respectively, and S_1, V_1, and N_1 refer to the lactate concentration, volume, and cell number at the end of the feeding interval respectively. Δt refers to the time between feeds.

2.10 Cell labelling with ^{19}F-perfluorocarbon

Labelling cells with ^{19}F-perfluorocarbon for *in vivo* experiments: Tregs were thawed and cultured at 5x10^6 cells/mL in ImmunoCult-XF T cell medium + 1% P/S. After 3 hours, 5 mg/mL ^{19}F-perfluorocarbon (^{19}F-PFC) (CS-1000; Celsense Inc) was added and cells were cultured for 20 hours at 37ºC for labelling. The ^{19}F-PFC labelled cells were collected, washed with PBS 3 times, then resuspended in PBS for injection into mice. Some cells were labelled with a red fluorescent ^{19}F-PFC (CS-ATM DM Red; Celsense Inc) for analysis by flow cytometry.

Labelling cells with ^{19}F-PFC during expansion: Tregs were expanded for 11 days as described above. The culture was split into two flasks for restimulation on day 11, one of which had 5 mg/mL ^{19}F-PFC added on day 12 to label cells during the final day of culture. On day 13, beads were removed and the cells were used for analysis or cryopreserved at 4x10^6 cells/mL in CS10.

Quantification of ^{19}F-PFC labelling and MRI signal: The mean ^{19}F-PFC content of labelled Tregs was determined by quantifying the number of ^{19}F spins of a known number of cells by NMR spectroscopy. The number of ^{19}F-PFC labelled Tregs within MRI images was quantified in comparison to reference tubes based on the number of ^{19}F spins/cell measured by NMR.

2.11 ^{19}F-PFC labelled cell injection into immunocompromised mice

10x10^6 ^{19}F-PFC labelled Tregs were injected intravenously with 10x10^6 PBMCs into the tail vein of nu/nu or CB17-SCID immunodeficient mice. 3T ^{1}H/^{19}F MRI images were taken 1, 2, and 4 days following cell injection. MRI images were taken and analyzed by the Dekaban and Foster Labs at Western University.

2.12 Statistical analyses

Statistical tests used are indicated in the Figure legends and were performed using Graphpad Prism 9. P values: *P < 0.05, **P < 0.01, ***P < 0.001, ****P < 0.0001.

Chapter 3: Cryopreservation timing is a critical process parameter in a thymic regulatory T-cell therapy manufacturing protocol

3.1 Introduction

Multiple protocols have been developed to manufacture Tregs for clinical trials, with variations in almost all key process parameters, including media, activation reagents, IL-2 concentration, restimulation timing and culture duration [129, 134, 136, 140, 141, 147, 150, 153, 157, 184-186, 191, 220]. Recently, a variety of new GMP-compatible reagents to activate T cells have been released but there are no reported comparisons of the performance of these now commercially available products. The lack of systematic studies to define critical process parameters and optimal reagents leads to uncertainty about the best methods to isolate and expand Tregs for clinical use [1].

Another uncertainty in the Treg manufacturing process is the feasibility of cryopreserving expanded cells. Some studies reported that cryopreservation reduces Treg quality, resulting in decreased FOXP3 expression and impaired suppressive capacity [213, 214]. Consequently, to date only a limited number of clinical trials have used cryopreserved Tregs [138, 157, 184]. Using fresh cells as a clinical treatment creates many logistical hurdles: release testing must be done in a shorter time and there is limited notice of manufacturing failure; there is less infusion time flexibility to accommodate changes in patient health status; and it is difficult to quickly produce cells for rapidly progressing diseases such as acute GVHD. Finding ways to cryopreserve clinical-grade Tregs to be used as an "off-the-shelf" product would overcome these hurdles, enable centralized manufacturing and allow a single product to be used to treat multiple

patients [174, 249]. Indeed, the concept of using “off-the-shelf” allogeneic cells is seen as the future of cell therapy products.

In order to develop a protocol to manufacture clinical-grade thymus-derived Tregs, we have comprehensively compared multiple process parameters using GMP-compatible reagents. We also report on a new protocol to cryopreserve expanded thymus-derived Tregs to enable their use as an "off-the-shelf" cell therapy product.

3.2 Results

3.2.1 Development of clinical-grade thymic Treg isolation protocol

We previously showed that $CD25^+CD8^-$ Tregs can be isolated from pediatric thymus tissue using manual dissociation with scissors, complement-mediated lysis to deplete CD8-expressing cells, and magnetic-bead-based positive selection of $CD25^+$ cells [158]. To develop a protocol that would be appropriate for GMP manufacturing, we first tested alternative methods for thymus tissue processing, seeking a method that minimized manual steps, ideally in a closed system. Thymuses were collected and processed either using manual dissociation (with scissors, razor blades or a tissue chopper), or with the gentleMACS dissociator. The number of live thymocytes per gram thymus released by each method was compared, revealing that manual dissociation resulted in a significantly higher thymocyte yield and viability **(Figure 3.1A-B)**. No differences in the frequency of Tregs (%$CD4^+CD8^-CD25^+$ cells) within the isolated thymocytes were observed **(Figure 3.1C)**.

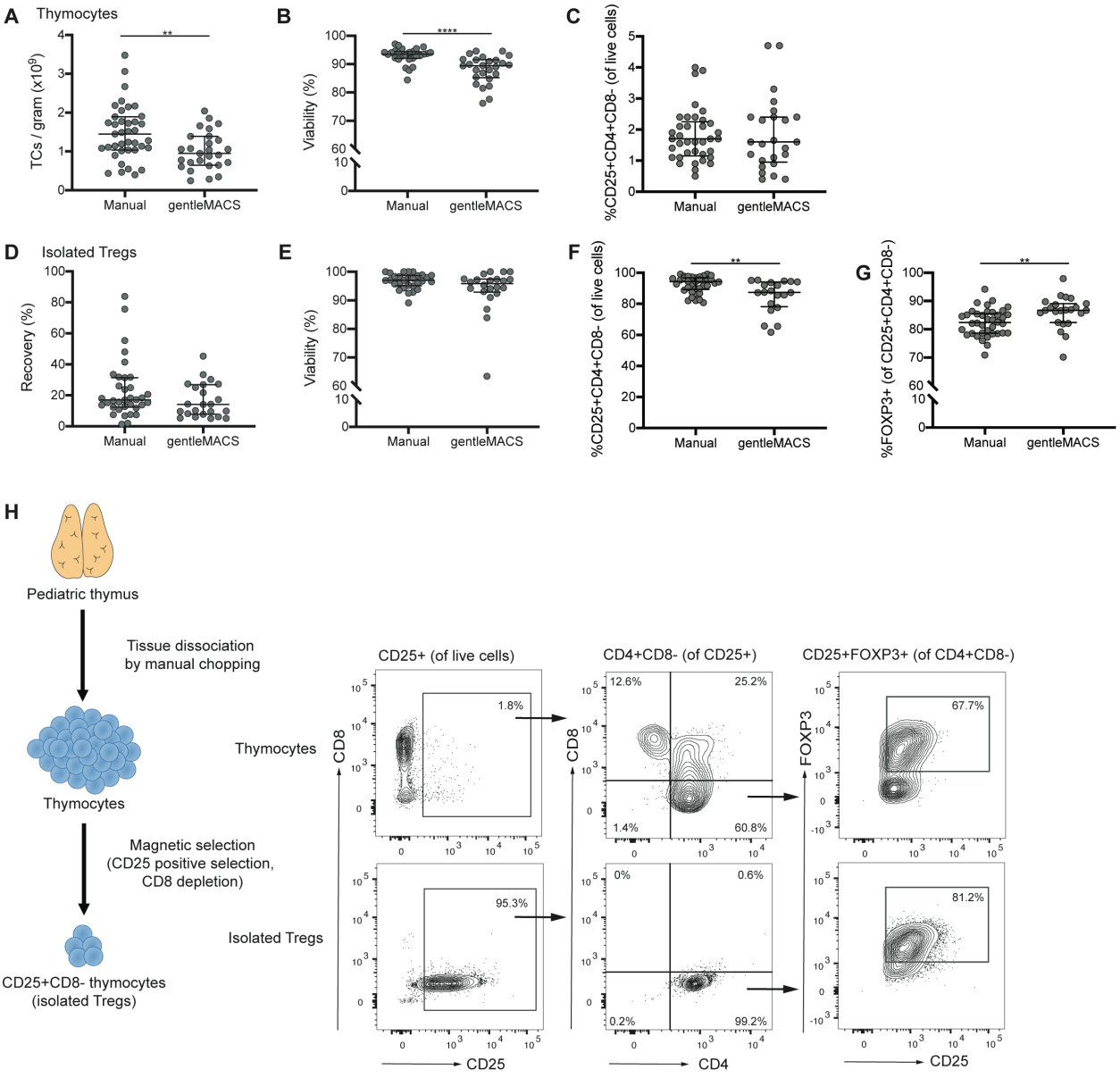

Figure 3.1: Isolation of thymic Treg using a two-step magnetic-bead-based selection process.
(A-H) Pediatric thymuses removed during cardiac surgery were collected and processed within 24 hours into a single cell suspension using either manual dissociation (n=27-39 donors) or the gentleMACS tissue dissociator (n=20-26 donors). A two-step magnetic cell selection process with positive selection for CD25 followed by negative selection for CD8 was used to isolate Tregs from thymocytes. **(A)** Yield of thymocytes (TCs) per gram of tissue, **(B)** viability of isolated thymocytes and **(C)** frequency of $CD25^{+}CD4^{+}CD8^{-}$ cells within total live thymocytes. **(D)** Recovery of Tregs, defined as the number of $CD25^{+}CD4^{+}CD8^{-}$ cells isolated relative to the number of $CD25^{+}CD4^{+}CD8^{-}$ cells within the starting population of thymocytes. **(E)** Viability and **(F)** purity, defined as $\%CD25^{+}CD4^{+}CD8^{-}$ cells, of isolated cells. **(G)** Proportion of $FOXP3^{+}$ cells within the $\%CD25^{+}CD4^{+}CD8^{-}$ population. **(H)** Schematic diagram of cell isolation process with representative flow cytometry data for thymocytes and isolated Tregs. Each symbol represents an individual subject, bars indicate median ± interquartile range. Significance was determined by Mann-Whitney test.

To eliminate the need for complement-mediated lysis of $CD8^+$ cells, we next tested a magnetic bead-based separation protocol with two steps: positive selection of $CD25^+$ cells using Releasable RapidSpheres (reagents not currently produced in a GMP format but which could be validated for use in a clinical setting), followed by negative selection of $CD8^+$ cells. With this method, the median Treg recovery from thymocytes using manual dissociation was 17.0% (range: 1.4-83.9%, n=35) and using the gentleMACS was 14.1% (range: 5.0-45.3%, n=23) **(Figure 3.1D)** with no significant difference in viability **(Figure 3.1E)** or yield (data not shown).

Flow cytometry was used to characterize the purity of the resulting cells, revealing that the Treg purity (defined as $CD25^+CD4^+CD8^-$ cells) was significantly higher when they were isolated from manually-dissociated (median: 94.4%, range: 80.8-99.1%, n=37) versus gentleMACS-dissociated thymocytes (median: 87.4%, range: 61.7-95.3% n=20) **(Figure 3.1F)**; however, within the $CD25^+CD4^+CD8^-$ cell population, FOXP3 expression was slightly higher in samples processed using the gentleMACS **(Figure 3.1G)**. These data show that a two-step, GMP-compatible process for thymic Treg isolation by magnetic selection is feasible **(Figure 3.1H)** and that the advantage of the gentleMACS closed system is outweighed by the higher yield and viability of thymocytes obtained with manual dissociation.

3.2.2 Comparison of activation reagents for thymic Treg expansion

We previously developed a method to expand thymic Tregs by activation with an artificial antigen-presenting cell (aAPC)-based system using L cells, a mouse fibroblast cell line expressing CD58, CD80 and CD32, and loaded with anti-CD3 monoclonal antibodies (mAbs) [77, 158]. Although aAPCs have been used to expand Tregs in a GMP-setting [136, 195], the increased cost and complexity for a manufacturing process with aAPCs led us to seek a cell-free

alternative. We compared our original aAPC-based protocol with four cell-free activation reagents (ImmunoCult CD3/CD28 T Cell Activator, ImmunoCult CD3/CD28/CD2 T Cell Activator, Dynabeads Treg Xpander or T Cell TransAct) to determine their ability to effectively expand thymic Tregs without loss of FOXP3 expression. We used ImmunoCult-XF medium for CD3/CD28 and CD3/CD28/CD2 T Cell Activators; X-Vivo 15 with 5% CTS Immune Cell Serum Replacement (SR) for Treg Xpander; and TexMACS with 5% human serum for T Cell TransAct. ImmunoCult-XF medium was used for the aAPC conditions. On the basis of protocols used in previous studies [158], thymic Tregs were activated on day 0, restimulated on day 7 then counted and analyzed on day 12 and 15 **(Figure 3.2A)**. Rapamycin was included in the culture medium from day 0-7 to prevent the outgrowth of effector T cells during Treg expansion [201, 202].

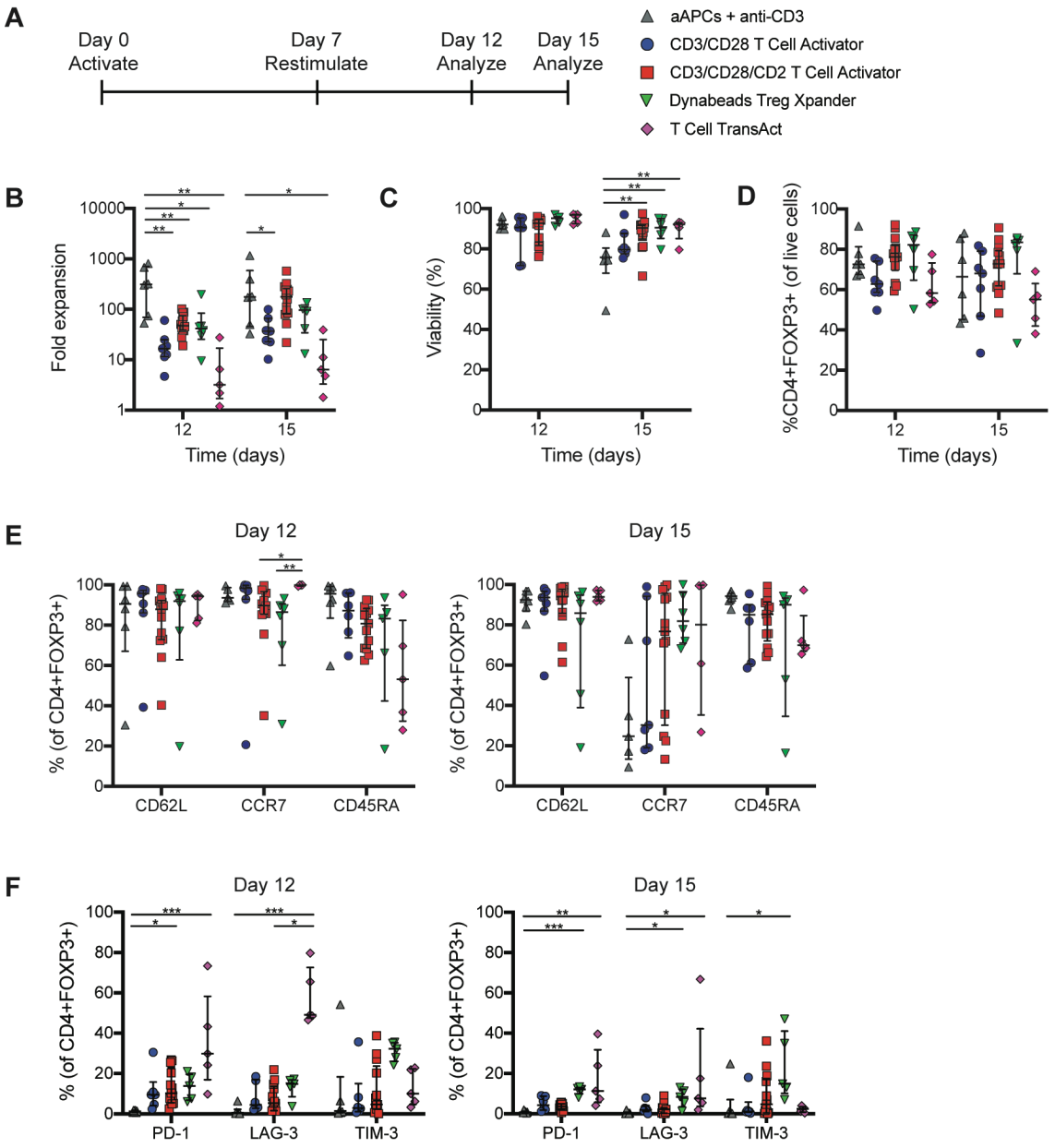

Figure 3.2: Comparison of cell-free activation reagents for thymic Treg expansion.
(A-F) Isolated thymic Tregs were expanded and restimulated with the indicated type of activation reagent (n=5-6 donors for L cell-based aAPCs + anti-CD3 mAbs, n=6-7 donors for CD3/CD28 T Cell Activator, n=13-14 donors for CD3/CD28/CD2 T Cell Activator, n=5-6 donors for Dynabeads Treg Xpander, and n=4-5 donors for T Cell TransAct, all tested in 9-10 experiments). **(A)** Schematic of thymic Treg expansion. **(B)** Fold expansion, **(C)** viability, and **(D)** FOXP3 expression, determined after 12 or 15 days in culture. Expression of markers of **(E)** T cell differentiation **(F)** or activation. Within each group, each symbol represents cells from a different subject and bars indicate median ± interquartile range. Significance was determined by **(B-C)** two-way ANOVA with Tukey's multiple comparisons test to compare expansion or viability between conditions on each day or **(E-F)** Kruskal-Wallis test with Dunn's multiple comparisons test to compare expression for each protein among conditions.

We found that at both day 12 and 15, the aAPC-based method stimulated the highest fold expansion, and that among the cell-free reagents, activation with T Cell TransAct resulted in the lowest expansion **(Figure 3.2B)**. Whereas thymic Treg viability remained high throughout culture with the cell-free activation reagents, by day 15 it declined in cultures activated with aAPCs **(Figure 3.2C)**. There was a trend towards higher FOXP3 expression in cultures expanded with Treg Xpander compared to those with the other activation reagents; however, this did not reach statistical significance **(Figure 3.2D)**.

We next compared the phenotypes of the expanded cells, focussing on markers of T cell differentiation and activation/exhaustion. After 12 days of culture, expression of markers associated with naïve T cells remained high, with the majority of cells expressing CD62L, CCR7, and CD45RA regardless of the activation condition **(Figure 3.2E)**. However, after 15 days the naïve phenotype became more variable, particularly for CCR7, suggesting that prolonged culture may affect lymph node homing capacity. In $CD8^+$ T cells, expression of PD-1, LAG-3 and TIM-3 is associated with exhaustion [250] whereas in Tregs this is associated with suppressive function [251-253]. We found that Tregs expanded with cell-free activation reagents had higher expression of PD-1 and LAG-3 than those expanded with aAPCs at day 12, with the highest expression on cells expanded with T Cell TransAct **(Figure 3.2F)**. Expression of these markers was generally reduced at day 15, suggesting that in Tregs these markers were likely associated with cell activation rather than exhaustion.

3.2.3 Effect of activation reagents on thymic Treg function

We next compared selected activation reagents for their ability to promote favourable cytokine production profiles and preserve thymic Treg suppressive function. Cultures stimulated with T

Cell TransAct were excluded due to their low expansion **(Figure 3.2B)**. Thymic Tregs expanded as in **Figure 3.2A** were stimulated with PMA and ionomycin and intracellular cytokine expression was analyzed by flow cytometry. As expected, a relatively low proportion of cells expressed inflammatory cytokines [77, 158], with those activated with Treg Xpander containing the lowest proportion of cells producing IL-2 **(Figure 3.3A)**. Consistent with previous observations, very few cells expressed IL-10 [77, 158].

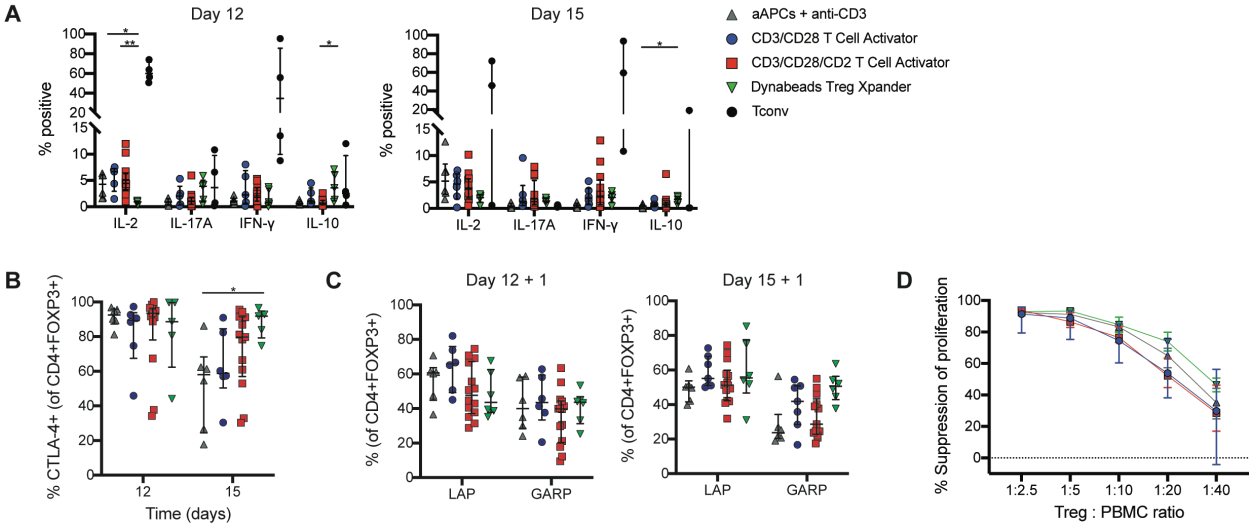

Figure 3.3: Function of thymic Tregs expanded with cell-free activation reagents.
(A-D) Isolated thymic Tregs were expanded with the indicated type of activation reagent and analyzed after 12 or 15 days (n=4-6 donors for L cell aAPCs + anti-CD3 mAbs, n=4-6 donors for CD3/CD28 T Cell Activator, n=4-14 donors for CD3/CD28/CD2 T Cell Activator, n=2-6 donors for Dynabeads Treg Xpander, and n=3-4 donors for Tconv all tested in 4-9 individual experiments). Expression of **(A)** intracellular cytokines in Treg ($CD4^+FOXP3^+$) and Tconv after 4 hours of activation with PMA, ionomycin and brefeldin A, **(B)** CTLA-4 or **(C)** LAP and GARP after 24 hours of activation with anti-CD3/CD28 beads at a 1:16 bead to cell ratio. **(D)** After 15 days of expansion, thymic Tregs were cocultured with cell proliferation dye (CPD)-labelled PBMC at the indicated ratios and stimulated with a 1:16 ratio of anti-CD3/CD28 beads for 4 days. Suppression of $CD8^+$ T cells within PBMC was determined by division index. **(A-C)** Within each group, each symbol represents cells from a different subject and bars indicate median ± interquartile range. **(D)** Median ± interquartile range is shown. Significance was determined by **(A)** Kruskal-Wallis test with Dunn's multiple comparisons test to compare expression for each cytokine among activation reagents or **(B)** two-way ANOVA with Tukey's multiple comparisons test to compare CTLA-4 expression between conditions on each day.

To assess the suppressive function of expanded thymic Tregs, we measured expression of proteins known to be major mediators of human Treg suppression, specifically CTLA-4 [254], LAP (the inactive form of TGF-β) and GARP [255]. Thymic Tregs expanded with Treg Xpander

had higher expression of CTLA-4 than those expanded with aAPCs **(Figure 3.3B)**, but expression of LAP and GARP **(Figure 3.3C)** and suppressive function **(Figure 3.3D)** were similar among all conditions tested.

3.2.4 Effect of cell culture media on thymic Treg expansion

In **Figures 3.2** and **3.3**, the activation reagents were tested in different cell culture media, raising the possibility that some of the observed differences could be due to the media. We selected the two best-performing cell-free activation reagents (as defined by the highest fold expansion and FOXP3 expression): Treg Xpander and CD3/CD28/CD2 T Cell Activator, and compared their effects in four different media. Specifically, cells were expanded in ImmunoCult-XF, X-Vivo 15 and OpTmizer with serum replacement and ImmunoCult-XF without serum replacement. As before, the cells were activated at day 0, restimulated on day 7, and then analyzed on days 12 and 15 **(Figure 3.4A)**. We found that cells cultured in ImmunoCult-XF had the highest fold expansion on day 15, and that this was not significantly affected by the presence or absence of serum replacement **(Figure 3.4B)**. All media conditions preserved high cell viability **(Figure 3.4C)**. Notably, expansion in OpTmizer resulted in significantly lower expression of FOXP3 with either activation reagent **(Figure 3.4D)**.

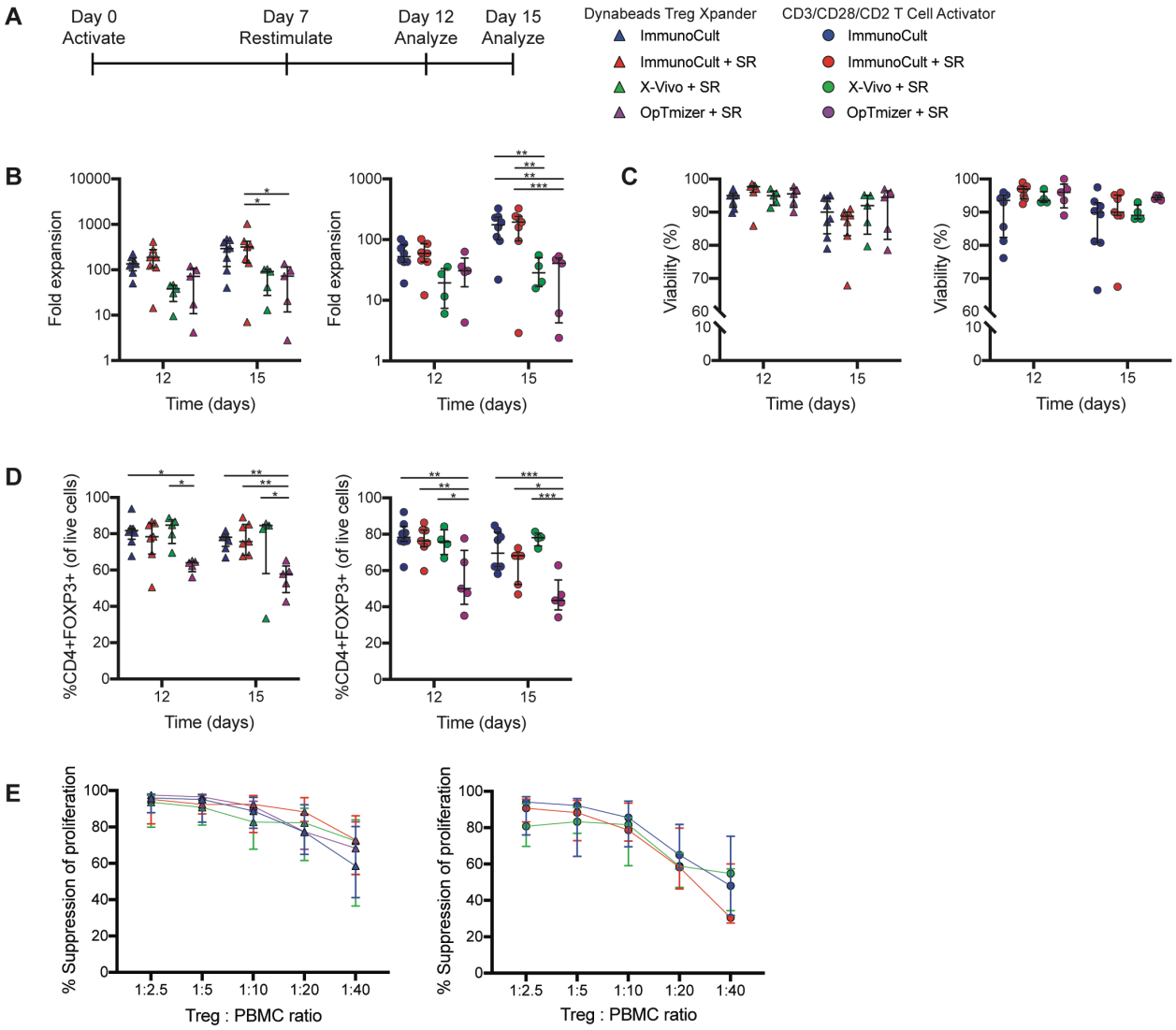

Figure 3.4: Effect of cell culture media on thymic Treg expansion.
(A-E) Isolated thymic Tregs were expanded and restimulated with Dynabeads Treg Xpander or CD3/CD28/CD2 T Cell Activator in different types of media as indicated (n=6-8 donors for ImmunoCult, n=4-7 donors for ImmunoCult + serum replacement (SR), n=4-5 donors for X-Vivo + SR, and n=2-5 donors for OpTmizer + SR tested in 4-5 experiments). **(A)** Schematic for thymic Treg expansion. **(B)** Fold expansion, **(C)** viability and **(D)** FOXP3 expression after 12 or 15 days of expansion. **(E)** After 15 days of expansion, thymic Tregs were cocultured with CPD-labelled PBMC at the indicated ratios and stimulated 1:16 beads to cells with anti-CD3/CD28 beads for 4 days. Suppression of $CD8^+$ T cells within PBMC was determined by division index. **(B-D)** Within each group, each symbol represents cells from a different subject and bars indicate median ± interquartile range. **(E)** Median ± interquartile range is shown. Significance was determined by two-way ANOVA with Tukey's multiple comparisons test to compare expansion or FOXP3 expression between conditions on each day.

Analysis of the effects of media on the thymic Treg phenotype revealed no significant differences in expression of naïve cell markers (CD62L, CCR7, CD45RA) at day 12 **(Figure**

3.5B) or 15 (data not shown), with the exception of cells expanded with CD3/CD28/CD2 T Cell Activator in ImmunoCult-XF which showed higher levels of CD45RA expression but no difference in CD62L or CCR7. The media conditions also had little effect on markers of activation on day 12 **(Figure 3.5C)** or 15 (data not shown), with the exception of a higher proportion of cells expressing TIM3 when cultured in X-Vivo 15 with serum replacement. Similarly, varying the type of medium had little effect on intracellular cytokine production **(Figure 3.5D)**, expression of CTLA-4, LAP and GARP **(Figure 3.5E-F)** or suppressive function. **(Figure 3.4E)**.

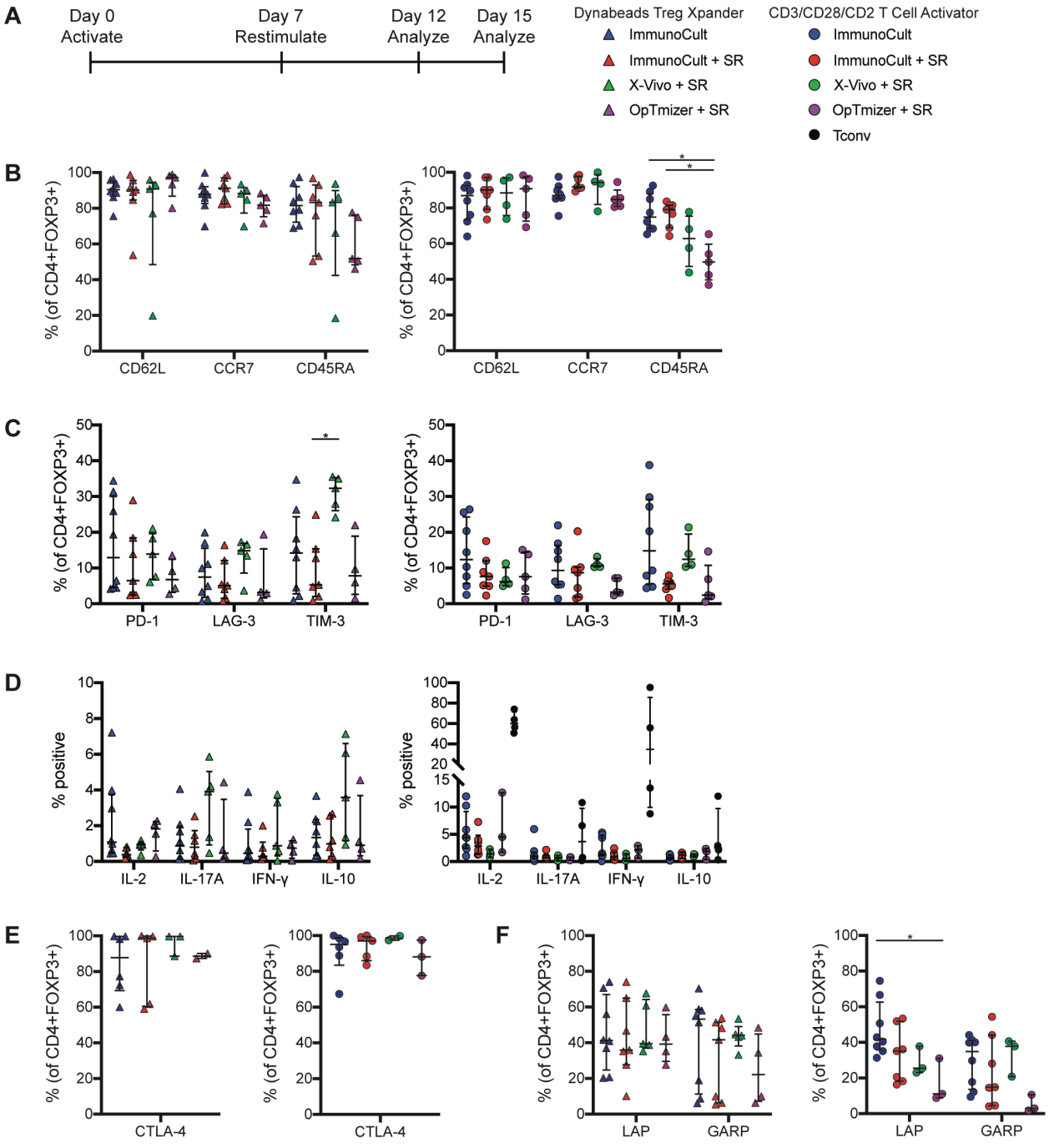

Figure 3.5: Effect of cell culture media on thymic Treg expansion with Dynabeads Treg Xpander or CD3/CD28/CD2 T Cell Activator.

(A-F) Isolated thymic Tregs were expanded and restimulated with Dynabeads Treg Xpander or CD3/CD28/CD2 T Cell Activator using different types of media as indicated (n=6-8 donors for ImmunoCult, n=4-7 donors for ImmunoCult + SR, n=3-5 donors for X-Vivo + SR, n=2-5 donors for OpTmizer + SR, and n=4 donors for Tconv tested in 4-5 experiments). **(A)** Schematic for thymic Treg expansion. Expression of markers of T cell **(B)** differentiation or **(C)** activation after 12 days of expansion. **(D)** Expression of intracellular cytokines in Tregs ($CD4^+FOXP3^+$) and Tconv was determined after 4 hours of activation with PMA, ionomycin and brefeldin A. **(E)**

Expression of CTLA-4, or **(F)** LAP and GARP after 24 hours of activation with anti-CD3/CD28 beads at a 1:16 bead to cell ratio. Within each group, each symbol represents cells from a different subject and bars indicate median ± interquartile range. Significance was determined by Kruskal-Wallis test with Dunn's multiple comparisons test to compare protein expression between conditions.

Table 3.1 summarizes the results of media comparisons using the Treg Xpander or CD3/CD28/CD2 T Cell Activator. Expanding thymic Tregs in ImmunoCult-XF using Treg Xpander gave the best combination of fold expansion, viability and FOXP3 expression.

Table 3.1: Effects of media on fold expansion, viability and phenotype of thymic Tregs.
Cells were activated with Dynabeads Treg Xpander or CD3/CD28/CD2 T Cell Activator in ImmunoCult-XF, ImmunoCult-XF with serum replacement (SR), X-Vivo + SR or OpTmizer + SR. After 7 days the cells were restimulated with the same activators and after a total of 15 days of expansion, fold expansion, viability and expression of FOXP3 were determined. All values are listed as median (range).

	Dynabeads Treg Xpander				**CD3/CD28/CD2 T Cell Activator**			
	ImmunoCult-XF (n=8)	**ImmunoCult-XF + SR (n=7)**	**X-Vivo + SR (n=5)**	**OpTmizer + SR (n=5)**	**ImmunoCult-XF (n=8)**	**ImmunoCult-XF + SR (n=7)**	**X-Vivo + SR (n=4)**	**OpTmizer + SR (n=5)**
Fold expansion (day 15)	295 (40-475)	317 (7-1024)	92 (13-103)	73 (3-135)	177 (22-326)	194 (3-326)	28 (16-55)	41 (2-53)
Viability	90% (79-95%)	89% (68-91%)	92% (80-95%)	95% (79-97%)	90% (67-98%)	90% (68-96%)	89% (88-93%)	94% (94-95%)
%FOXP3$^+$	78% (67-82%)	76% (68-89%)	85% (33-86%)	58% (43-65%)	70% (58-85%)	68% (47-72%)	78% (72-81%)	44% (34-63%)
% Suppression of proliferation (1:20 Treg to PBMC)	77% (43-95%)	89% (83-97%)	82% (46-96%)	78% (68-87%)	65% (51-92%)	58% (43-86%)	59% (45-67%)	---

3.2.5 Comparison of thymic Treg expansion with Treg Xpander versus GMP-compatible aAPCs

The selected combination of reagents tested above stimulated ~300 fold expansion of thymic Tregs over two weeks **(Table 3.1)**. This fold expansion is substantially lower than the reported fold expansion for cord blood-derived Tregs using a GMP-validated aAPC system involving activation with K562 cells expressing CD64 (loaded with anti-CD3 mAbs) and CD86 (these cells hereafter referred to as KT64/86 aAPCs) [136, 195]. We therefore tested if the fold expansion of thymic Tregs could be increased through activation with KT64/86 aAPCs. Replicate aliquots of $CD25^{+}CD8^{-}$ thymic Tregs were expanded and restimulated using the optimized Treg Xpander-based system in ImmunoCult-XF as described above, or expanded with KT64/86 aAPCs in a previously-selected medium (X-Vivo 15 with 10% human AB serum) [195] without restimulation **(Figure 3.6A)**.

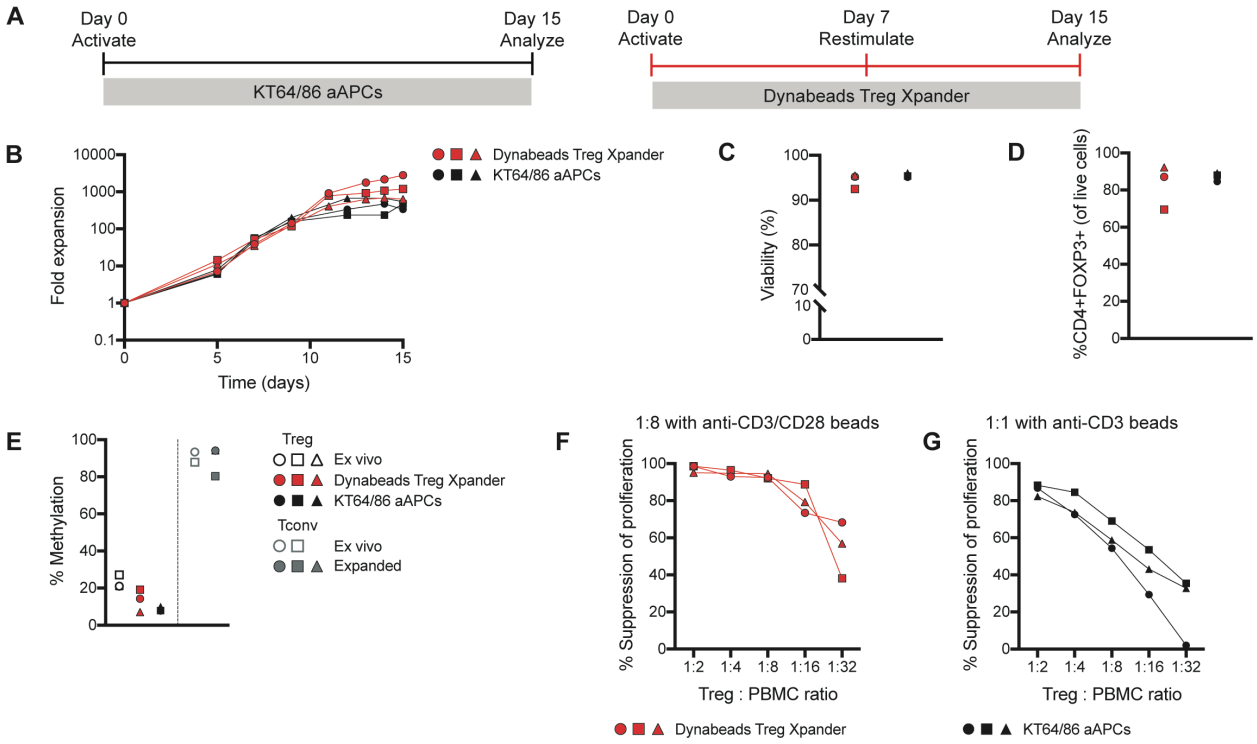

Figure 3.6: Thymic Treg expansion with KT64/86 aAPCs.
(A-G) Replicate aliquots of thymic Tregs were expanded using KT64/86 aAPCs or Treg Xpander (n=3 donors from 1-3 experiments). **(A)** Schematic for expansion. **(B)** Cells were counted to determine fold expansion. **(C)** Viability and **(D)** FOXP3 expression after 15 days of expansion. **(E)** TSDR analysis of ex vivo and expanded thymic Tregs and Tconv; all data are from males and the average methylation for 7 CpGs within the TSDR is shown. **(F-G)** Expanded thymic Tregs were cocultured with CPD-labelled **(F)** or CFSE-labelled **(G)** PBMC at the indicated ratios and stimulated at 1:8 beads to cells with anti-CD3/CD28 beads or **(F)** 1:1 with anti-CD3 beads **(G)** for 4 days. Suppression of $CD8^+$ T cells within PBMC was determined by division index. Within each group, each symbol represents cells from a different subject and matched subjects are shown with the same symbol.

We found that expansion of thymic Tregs after a single activation with KT64/86 aAPCs median 474-fold; range 338-557, n=3) resulted in a similar expansion as that previously reported for cord blood-derived Tregs [195]. The median expansion after two stimulations with the Treg Xpander-based protocol was 1199-fold (range: 637-2806, n=3) **(Figure 3.6B)**, and both protocols demonstrated similar viability **(Figure 3.6C).** Both protocols resulted in similar FOXP3 expression **(Figure 3.6D)**, methylation at the Treg-specific demethylation region (TSDR) **(Figure 3.6E)** and suppressive function **(Figure 3.6F-G)**. Comparison of Tregs expanded with KT64/86 aAPCs or Treg Xpander revealed similar patterns of differentiation and

homing marker expression, as well as cytokine production **(Figure 3.7A-C)**. As such, the remainder of the experiments were performed with Treg Xpander.

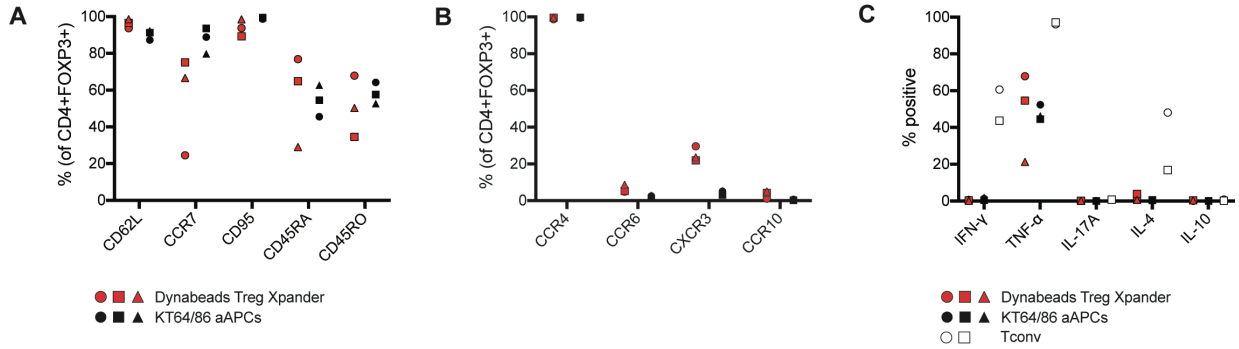

Figure 3.7: Phenotype of thymic Tregs expanded using KT64/86 aAPCs or Dynabeads Treg Xpander. **(A-C)** Isolated thymic Tregs were expanded using KT64/86 aAPCs or Dynabeads Treg Xpander activation reagents (n=3 donors for Dynabeads Treg Xpander, n=3 donors for KT64/86 aAPCs, and n=2 donors for Tconv from 1-3 experiments). After 15 days, cells were analyzed for expression of **(A)** markers of T cell differentiation, **(B)** chemokine receptors or **(C)** intracellular cytokines in Tregs ($CD4^+FOXP3^+$) and Tconv after 4 hours of activation with PMA, ionomycin and brefeldin A. Within each group, each symbol represents cells from a different subject and matched subjects are shown with the same symbol.

3.2.6 Cryopreservation 1-3 days post-restimulation preserves Treg viability, phenotype and function

In order to facilitate their use as an "off-the-shelf" product, we next sought to optimize the cryopreservation of thymic Tregs. As we hypothesized that activation state may affect recovery after cryopreservation, we examined the effect of cryopreserving Tregs at different time points following restimulation with Treg Xpander **(Figure 3.8A)**, with and without a second restimulation before harvest and cryopreservation. We found that after a second restimulation at day 14, the cells continued to expand and maintained high viability but FOXP3 expression began to decline after day 16 **(Figure 3.8B-D)**. Cell diameter increased after restimulation at day 14, reaching its peak at day 16 **(Figure 3.8E)**.

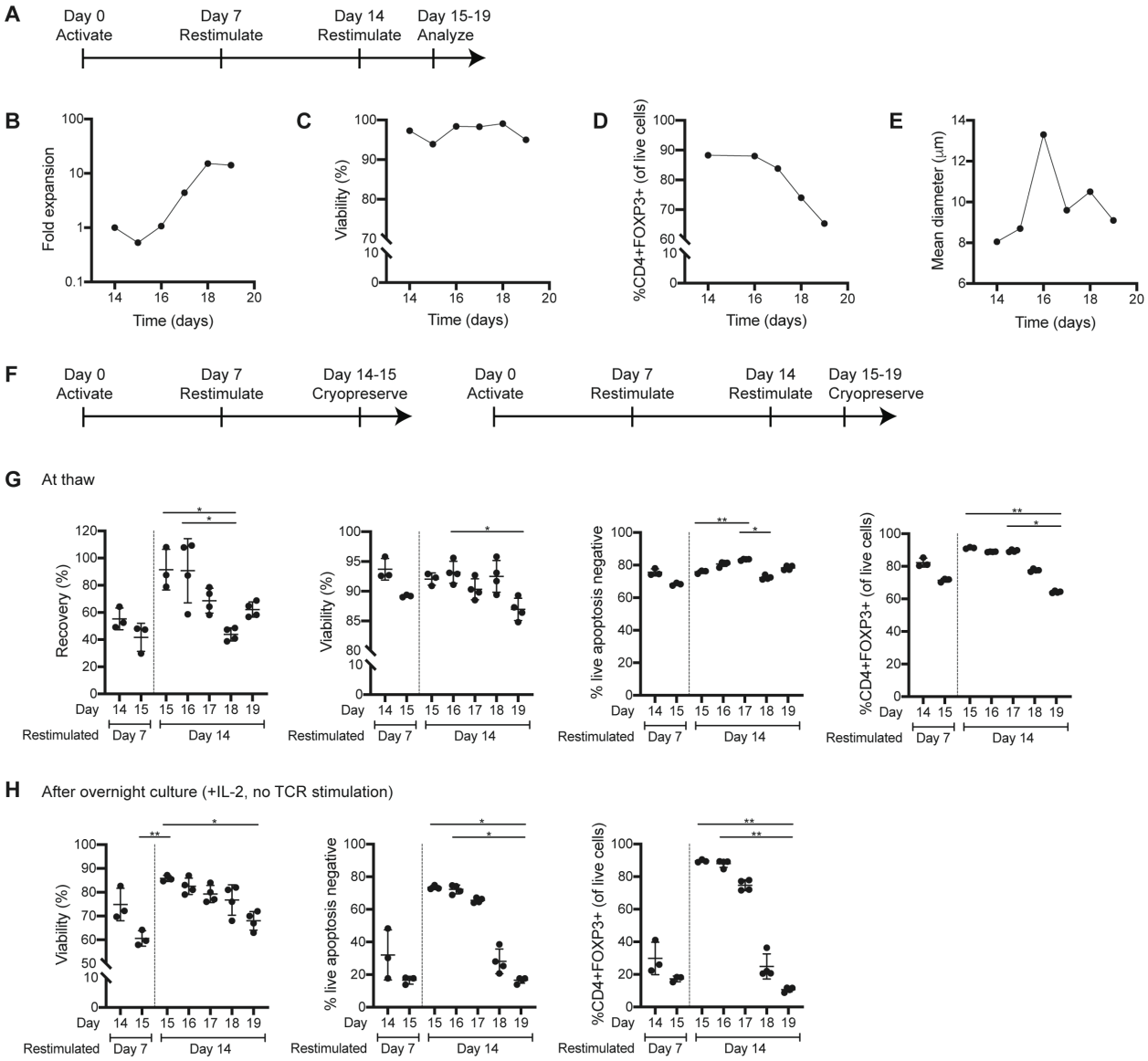

Figure 3.8: Cryopreservation of thymic Tregs following a second restimulation at day 14.
(A-E) Isolated thymic Tregs were activated at day 0, restimulated at days 7 and 14, and analyzed at day 15-19 (n=1 donor from 1 experiment). **(A)** Schematic for thymic Treg expansion. **(B)** Fold expansion, **(C)** viability, **(D)** FOXP3 expression, and **(E)** mean diameter of thymic Tregs following restimulation at day 14. **(F-H)** Isolated thymic Tregs were activated at day 0, restimulated at days 7 and 14, and cryopreserved at day 14 or 15 following the first restimulation, or day 15-19 following the second restimulation (n=1 donor from 1 experiment). **(F)** Schematic for thymic Treg expansion and cryopreservation. **(G)** Recovery (defined as the number of live apoptosis negative cells thawed relative to the number of live cells cryopreserved), viability (measured by acridine orange/propidium iodide staining or a flow cytometry-based apoptosis assay) and FOXP3 expression for cryopreserved thymic Tregs shown at thaw. **(H)** Viability (measured by acridine orange/propidium iodide staining and apoptosis assay) and FOXP3 expression for cryopreserved thymic Tregs after thaw and overnight culture with IL-2. **(G-H)** Within each group, each symbol represents a separate vial of cells cryopreserved from the same subject and bars indicate mean ± standard deviation. Significance was determined by Kruskal-Wallis test with Dunn's multiple comparisons test.

We next tested how the day of cryopreservation relative to the last restimulation affected Treg recovery post-thaw. Expanded Tregs were cryopreserved at day 14 or 15 (7 or 8 days post-day 7 restimulation), or restimulated a second time on day 14 and then cryopreserved on days 15-19 (1-5 days post-restimulation) **(Figure 3.8F)**. Upon thawing, cells were either immediately analyzed for recovery, viability and FOXP3 expression, or cultured overnight in ImmunoCult-XF with IL-2 (without additional TCR stimulation). We found that cell recovery was significantly higher for cells that were cryopreserved 1 or 2 days following their last stimulation than at 4 days (i.e. days 15-16 vs. day 18 in **Figure 3.8G**). Viability and FOXP3 expression had a similar trend, decreasing with longer times between restimulation and cryopreservation. After overnight culture, the effect of the day of cryopreservation was even more striking: if cells were cryopreserved > 3 days following restimulation there was a dramatic drop in viability, live apoptosis-negative cells and FOXP3 expression **(Figure 3.8H)**.

3.2.7 Increased expansion when Tregs are restimulated after returning to resting size

In light of the dramatic increase in post-thaw Treg health when cryopreserved shortly after restimulation, we altered our expansion protocol to allow cryopreservation within 1-3 days after restimulation. As a second restimulation increases the risk of Treg instability and/or outgrowth of contaminating non-Tregs [194, 256], and cryopreserving cells 2 days following restimulation at day 7 would curtail cell yields, we tested extending the length of the first activation period from 7 to 9 days. Cells restimulated at day 7 were analyzed after 2, 3 or 7 days and those restimulated at day 9 were analyzed after 2, 3 or 5 days **(Figure 3.9A)**. Cells restimulated at day 9 reached a significantly higher level of overall expansion **(Figure 3.9B-C)** and sustained a higher growth rate following restimulation **(Figure 3.9D)** compared to those restimulated at day 7. It has been

reported that allowing T cells to return to resting size (~8.5 μm) prior to restimulation maximizes their subsequent expansion [183, 194, 257], and that if cells are restimulated too early, they likely undergo activation-induced cell death [183, 258]. We found that thymic Tregs returned to resting size by day 9 **(Figure 3.9E)**, providing an explanation for the superior expansion of cells restimulated on day 9.

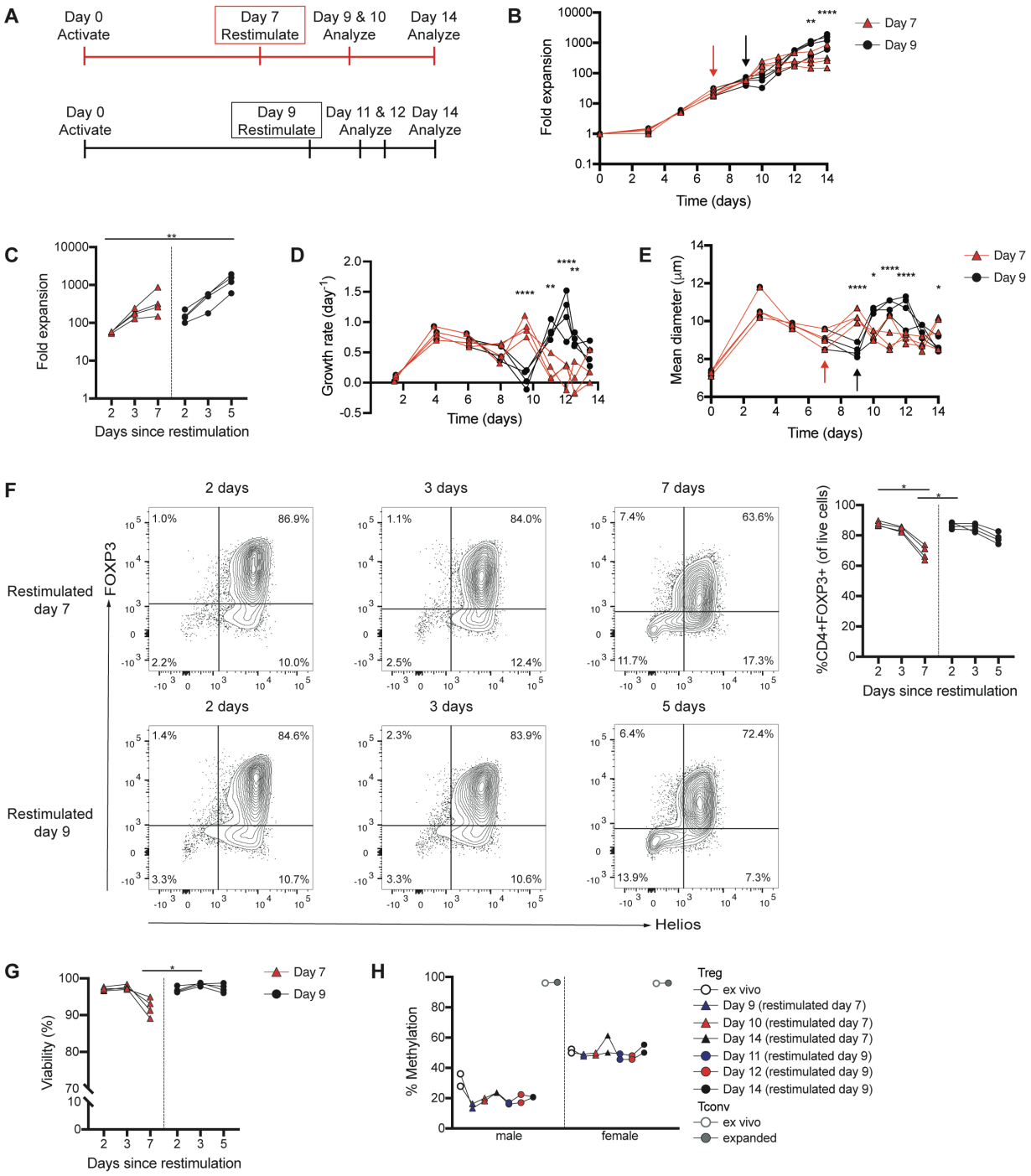

Figure 3.9: Effect of restimulation time on thymic Treg expansion.
(A-H) Thymic Tregs were activated and restimulated with Dynabeads Treg Xpander and restimulated on either day 7 or day 9 (n=4 donors from 2 experiments). **(A)** Schematic for Treg expansion. **(B)** Fold expansion of thymic Tregs restimulated on day 7 or day 9. Arrows indicate the day cells were restimulated. **(C)** Fold expansion was measured 2, 3 or 7 days following restimulation at day 7 (day 9, 10 or 14), or 2, 3 or 5 days following restimulation at day 9 (day 11, 12 or 14). **(D)** Growth rate of thymic Tregs restimulated on day 7 or day 9, calculated from cell concentration over the course of culture. **(E)** Mean diameter of thymic Tregs restimulated on day 7 or day 9 over the

course of culture. Arrows indicate the day cells were restimulated. **(F)** FOXP3 expression and **(G)** viability were measured 2, 3 or 7 days following restimulation at day 7, or 2, 3 or 5 days following restimulation at day 9. Flow cytometry plots are shown for a representative donor. **(H)** TSDR analysis of ex vivo and expanded thymic Tregs and Tconv. Average data from male and female donors shown is the average methylation for 7 CpGs within the TSDR. Each symbol represents cells from a different subject; data points from the same subject are linked. Significance was determined by **(B, D-E)** repeated measures two-way ANOVA with Sidak's multiple comparisons test to compare between cells restimulated on day 7 or day 9 on each day, or **(C, F-G)** Friedman test with Dunn's multiple comparison test.

Although cell viability and FOXP3 levels began to decrease 5 days after restimulation **(Figure 3.9F-G)**, TSDR methylation levels remained similar **(Figure 3.9H),** suggesting that lower FOXP3 expression is likely the consequence of a decreased activation state [259] rather than Treg instability.

3.2.8 Thymic Treg cryopreservation timing is a more critical process parameter than restimulation day

We next investigated the impact of cryopreservation timing on cells restimulated at day 9. Cells were restimulated at day 9, then cryopreserved after 2, 3 or 5 days. Consistent with **Figure 3.8**, we found that higher Treg viability and FOXP3 expression were obtained when cells were cryopreserved shortly after restimulation. If they were cryopreserved > 3 days after restimulation, there was a significant drop in recovery, viability and FOXP3 expression **(Figure 3.10A-B)**. These declines were even greater after the thawed cells were cultured overnight, with viability and FOXP3 expression dropping well below what would be acceptable for a therapeutic product **(Figure 3.10C-D)**. Consistent with their low viability and FOXP3 expression, thymic Tregs cryopreserved > 3 days post-restimulation were also significantly less potent at suppressing the proliferation of $CD8^+$ T cells **(Figure 3.10E)**. In summary, we observed that cells cryopreserved 2 days following restimulation had the highest viability and FOXP3 expression upon thawing.

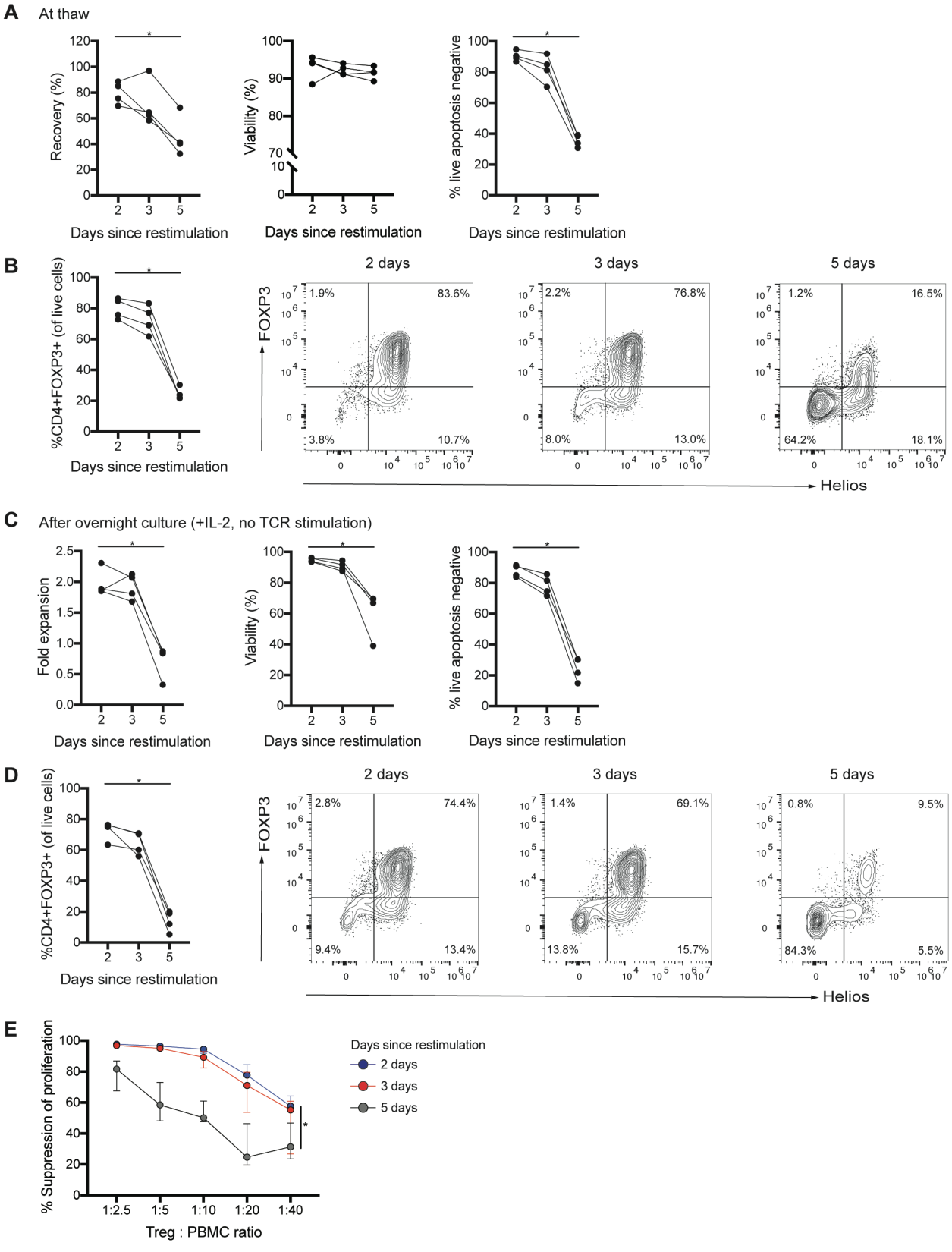
A
At thaw
Recovery (%)
Viability (%)
% live apoptosis negative
Days since restimulation
B
%CD4+FOXP3+ (of live cells)
2 days
3 days
5 days
FOXP3
1.9%
83.6%
3.8%
10.7%
2.2%
76.8%
8.0%
13.0%
1.2%
16.5%
64.2%
18.1%
Helios
C
After overnight culture (+IL-2, no TCR stimulation)
Fold expansion
D
2.8%
74.4%
9.4%
13.4%
1.4%
69.1%
13.8%
15.7%
0.8%
9.5%
84.3%
5.5%
E
% Suppression of proliferation
Treg : PBMC ratio
1:2.5
1:5
1:10
1:20
1:40
Days since restimulation
2 days
3 days
5 days

Figure 3.10: Cryopreservation of thymic Tregs following restimulation on day 9.
(A-E) Isolated thymic Tregs were expanded with Dynabeads Treg Xpander and cryopreserved 2, 3 or 5 days following restimulation on day 9 (n=4 donors from 2 experiments). **(A)** Recovery (defined as the number of live apoptosis negative cells thawed relative to the number of live cells cryopreserved), viability (measured by acridine orange/propidium iodide staining and apoptosis assay) and **(B)** FOXP3 expression for cells upon thawing. **(C)** Fold expansion, viability (measured by acridine orange/propidium iodide staining and apoptosis assay) and **(D)** FOXP3 expression for cryopreserved cells after thawing and overnight culture with IL-2. **(E)** After thawing and overnight culture, thymic Tregs were cocultured with CPD-labelled PBMC at the indicated ratios and stimulated 1:16 with anti-CD3/CD28 beads for 4 days. Suppression of $CD8^+$ T cells within PBMC was determined by division index. Each symbol represents the mean of 3 technical replicates of cryopreserved cells from a different subject; data points from the same subject are linked. For E, median ± interquartile range of subjects is shown. Significance was determined by **(A-D)** Friedman test with Dunn's multiple comparison test or **(E)** Friedman test with Dunn's multiple comparison test to compare total area under each curve (AUC). Statistics on graph are for AUC of 2 days since restimulation relative to 5 days since restimulation.

To investigate if the effect of cryopreservation timing was specific to thymic Tregs or more broadly applicable, the experiments were repeated with naïve peripheral blood-derived Tregs ($CD4^+CD25^+CD127^-CD45RA^+$) and Tconv ($CD4^+CD25^-CD127^+CD45RA^+$). Cells were activated and restimulated at day 9 with Treg Xpander (Tregs) or Dynabeads Human T-Expander (Tconv), then cryopreserved 2, 3 or 5 days following restimulation **(Figure 3.11A-D)**. Analysis of cells post thawing revealed results that were consistent with **Figure 3.10**. Specifically, naïve peripheral blood-derived Tregs cryopreserved 2 or 3 days after restimulation had higher viability and FOXP3 expression than those cryopreserved at day 5 **(Figure 3.11E)**. These findings were even more pronounced after culturing the thawed cells overnight **(Figure 3.11F)**. Notably, we did not observe a large increase in TSDR methylation post cryopreservation **(Figure 3.11G)**, suggesting that loss of FOXP3 expression was likely more related to cell viability than lineage instability. This conclusion is further supported by the finding that inflammatory cytokine production did not change significantly between cells cryopreserved at different days, although there was a slight increase in the production of IL-2 by $FOXP3^-$ cells in thymic Tregs cryopreserved 5 days following restimulation **(Figure 3.11H)**.

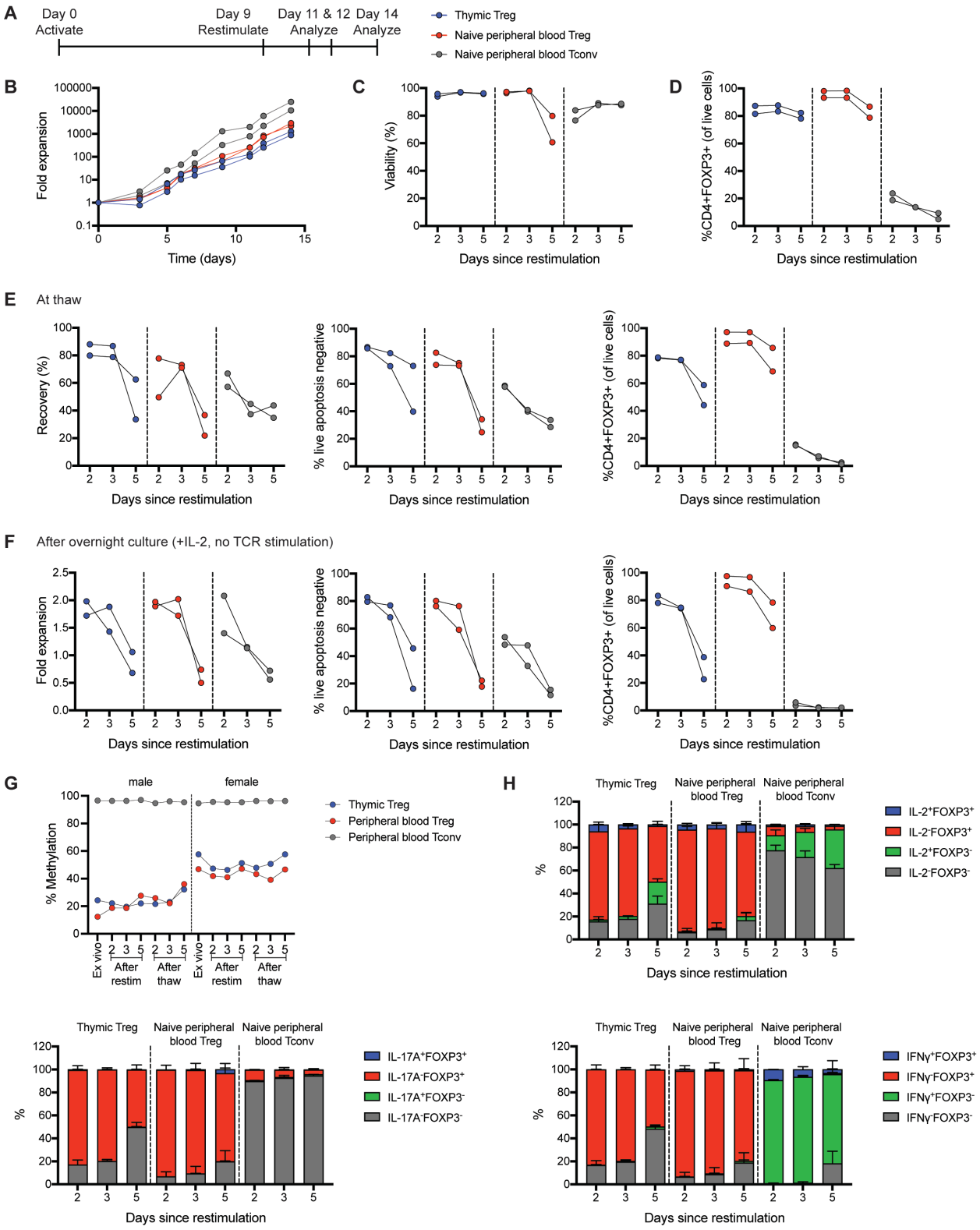

Figure 3.11: Cryopreservation of thymic Tregs, naïve peripheral blood Tregs and naïve peripheral blood Tconv following restimulation at day 9.

(A-H) Thymic Tregs, naïve peripheral blood Tregs and naïve peripheral blood Tconv were expanded with Dynabeads Treg Xpander (Treg) or Dynabeads Human T-Expander (Tconv), restimulated at day 9 and cryopreserved 2, 3 or 5 days following restimulation (n=2 donors from 1 experiment). **(A)** Schematic of expansion. **(B)** Fold expansion of cells over the course of culture. **(C)** Viability and **(D)** FOXP3 expression were measured 2, 3 or 5 days following restimulation. **(E)** Recovery (defined as the number of live apoptosis negative cells thawed relative to the number of live cells cryopreserved), viability (measured by apoptosis assay) and FOXP3 expression for cells upon thawing. Cryopreserved cells were cultured overnight with IL-2 and **(F)** fold expansion, viability (measured by apoptosis assay) and FOXP3 expression were determined. **(G)** TSDR analysis of ex vivo and expanded thymic Tregs and Tconv after restimulation and after thawing and overnight culture. Average data from male and female donors shown is the average methylation for 7 CpGs within the TSDR. **(H)** Expression of intracellular cytokines after 4 hours of activation with PMA, ionomycin and brefeldin A. **(B-D, G)** Each symbol represents cells from a different subject and matched subjects are linked. **(E-F)** Each symbol represents the mean of 3 technical replicates of cryopreserved cells from a different subject. **(H)** Each bar represents the median and range of data from 2 subjects, using the mean of 3 technical replicates of cryopreserved cells per subject.

To ask if the decrease in viability and FOXP3 expression was functionally relevant, the suppressive function of the thawed cells was tested, revealing that for both thymic and naïve peripheral blood Tregs, cells cryopreserved at day 5 were substantially less able to suppress the proliferation of $CD8^+$ T cells in comparison to those cryopreserved 2-3 days following restimulation **(Figure 3.12A)**. Consistent with their lower suppressive function, Tregs cryopreserved 5 days following restimulation also had a lower proportion of $FOXP3^+$ cells expressing CTLA-4, LAP and/or GARP **(Figure 3.12B)**.

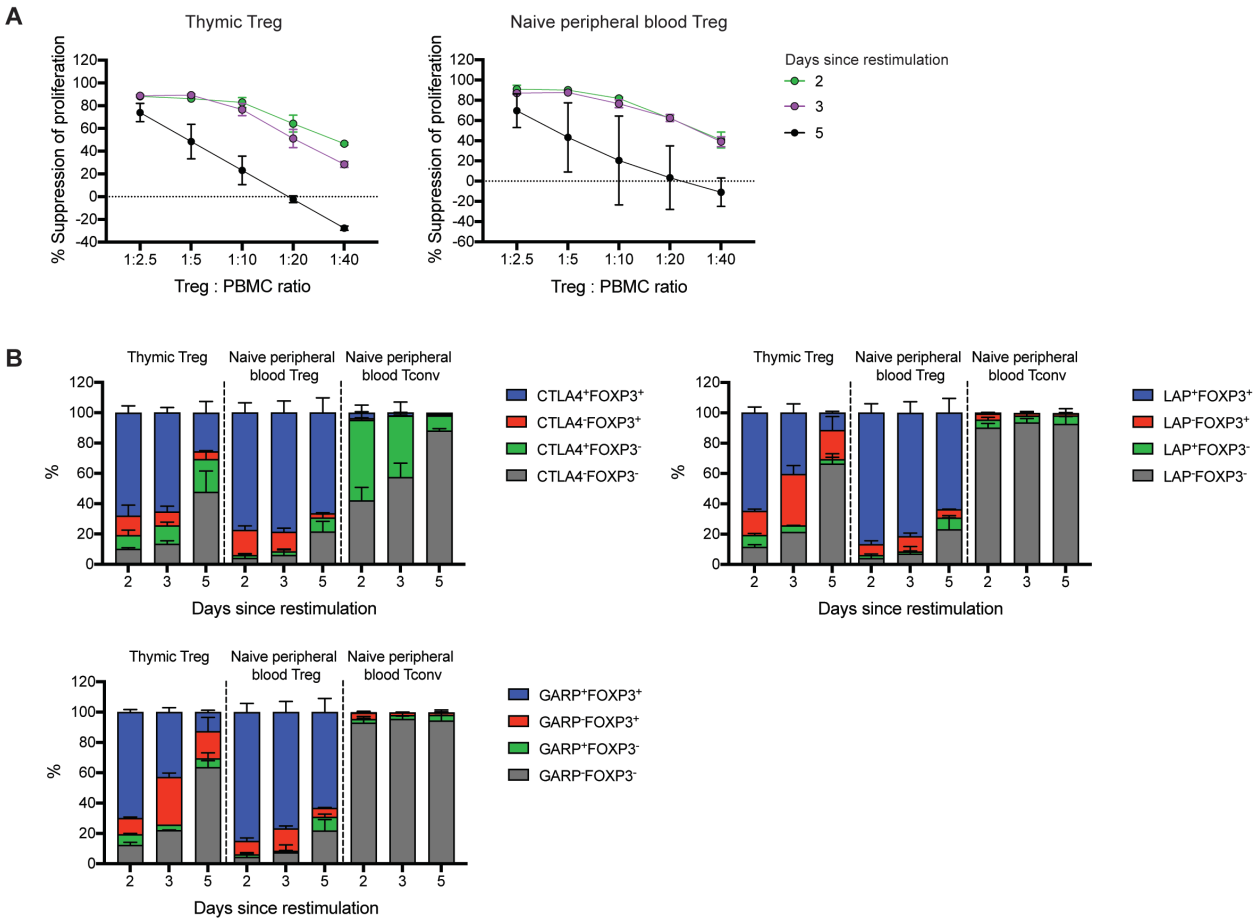

Figure 3.12: Function of cryopreserved thymic Tregs, naïve peripheral blood Tregs and naïve peripheral blood Tconv.
(A-B) Thymic Tregs, naïve peripheral blood Tregs and naïve peripheral blood Tconv were expanded with Dynabeads Treg Xpander (Treg) or Dynabeads Human T-Expander (Tconv), restimulated at day 9 and cryopreserved 2, 3 or 5 days following restimulation (n=2 donors from 1 experiment). Cells were thawed and cultured overnight prior to testing. **(A)** Tregs were cocultured with CPD-labelled PBMC at the indicated ratios and stimulated 1:16 with anti-CD3/CD28 beads for 4 days. Suppression of $CD8^+$ T cells within PBMC was determined by division index. **(B)** Tregs and Tconv were analyzed for expression of CTLA-4, LAP and GARP. **(A)** Median ± range of subjects is shown. **(B)** Each bar represents the median and range of data from 2 subjects, using the mean of 3 technical replicates of cryopreserved cells per subject.

Finally, we tested whether the length of the first activation period could be extended longer than 9 days by measuring the expansion, viability and phenotype of cells restimulated at days 9-14 **(Figure 3.13A)**. In each case, cells were analyzed 2 days following restimulation. For each restimulation day tested, thymic Treg numbers doubled 2 days following restimulation **(Figure 3.13B)**. Cells restimulated on days 11-14 reached higher levels of overall expansion than those

restimulated on day 9; however, this difference was only reached significance for the cultures restimulated on day 14 **(Figure 3.13C)**. Viability, FOXP3 expression and TSDR methylation were similar for the restimulation days tested **(Figures 3.13D-F)**. FOXP3 expression decreased from day 7 to the day of restimulation, but increased following restimulation on all days (shown in **Figure 3.14** for cells restimulated on day 11).

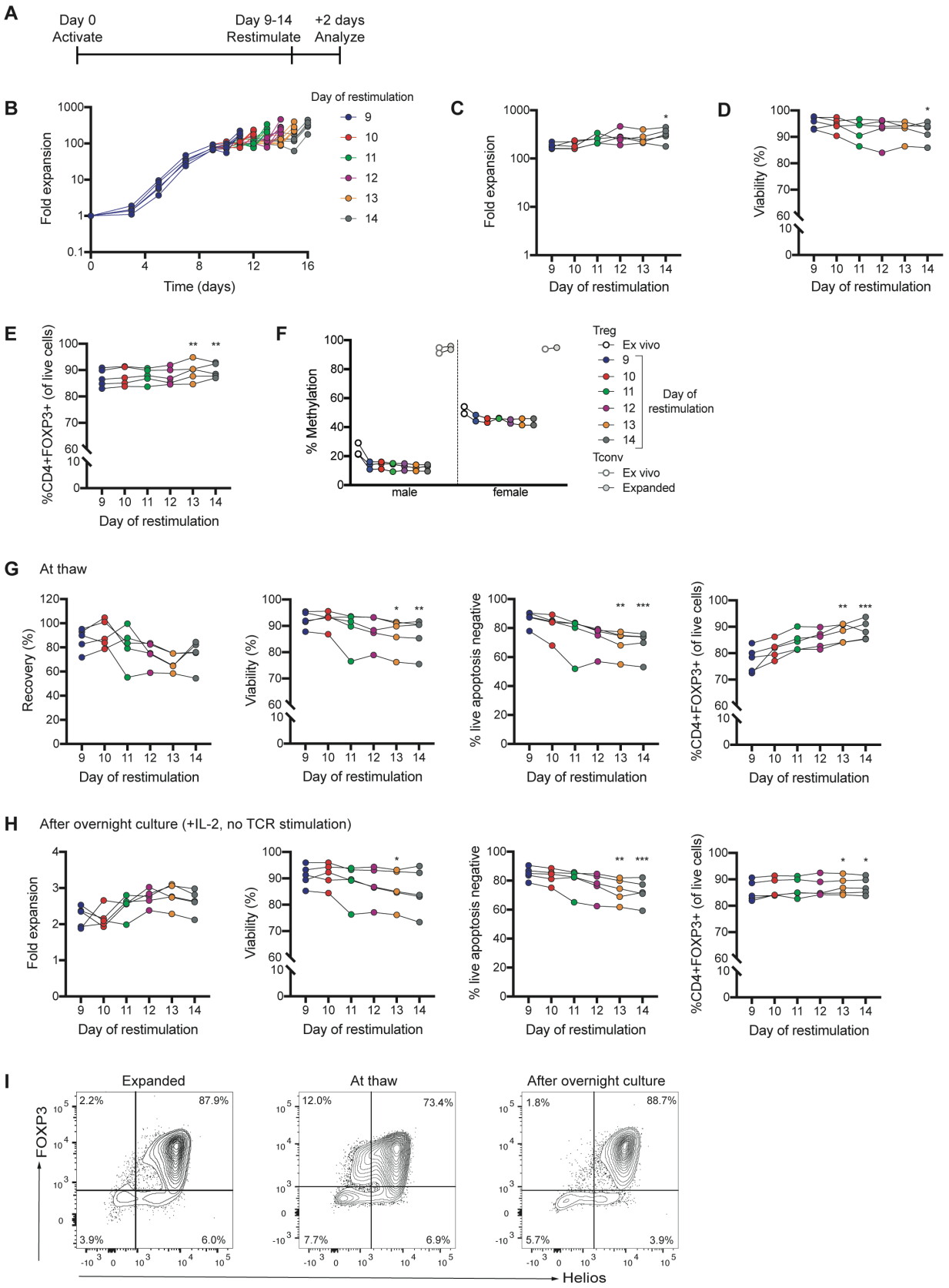
A
Day 0
Activate
Day 9-14
Restimulate
+2 days
Analyze
B
Fold expansion
Time (days)
Day of restimulation
9
10
11
12
13
14
C
Fold expansion
Day of restimulation
D
Viability (%)
Day of restimulation
E
%CD4+FOXP3+ (of live cells)
Day of restimulation
F
% Methylation
male
female
Treg
Ex vivo
9
10
11
12
13
14
Day of restimulation
Tconv
Ex vivo
Expanded
G
At thaw
Recovery (%)
Viability (%)
% live apoptosis negative
%CD4+FOXP3+ (of live cells)
Day of restimulation
H
After overnight culture (+IL-2, no TCR stimulation)
Fold expansion
Viability (%)
% live apoptosis negative
%CD4+FOXP3+ (of live cells)
Day of restimulation
I
Expanded
At thaw
After overnight culture
FOXP3
Helios
2.2%
87.9%
3.9%
6.0%
12.0%
73.4%
7.7%
6.9%
1.8%
88.7%
5.7%
3.9%

Figure 3.13: Effect of restimulation on day 9-14.
(A-I) Isolated thymic Tregs were expanded with Treg Xpander and restimulated on day 9-14 (n=5 donors from 3 experiments). **(A)** Schematic for Treg expansion. In each case, cells were analyzed and cryopreserved 2 days following restimulation. **(B)** Fold expansion of thymic Tregs restimulated on day 9-14. The day in the legend refers to the day cells were restimulated. **(C)** Fold expansion, **(D)** viability and **(E)** FOXP3 expression measured 2 days following restimulation. **(F)** TSDR analysis of ex vivo and expanded thymic Tregs and Tconv. Average data from male and female donors shown is the average methylation for 7 CpGs within the TSDR. **(G)** Recovery (defined as the number of live apoptosis negative cells thawed relative to the number of live cells cryopreserved), viability (measured by acridine orange/propidium iodide staining and apoptosis assay) and FOXP3 expression for cryopreserved thymic Tregs shown at thaw. **(H)** Fold expansion, viability (measured by acridine orange/propidium iodide staining and apoptosis assay) and FOXP3 expression for cryopreserved thymic Tregs after thawing and overnight culture with IL-2. **(I)** Flow cytometry plots are shown for a representative donor. **(B-F)** Each symbol represents cells from a different subject and matched subjects are linked. **(G-H)** Each symbol represents the mean of 3 technical replicates of cryopreserved cells from a different subject and matched subjects are linked. Significance was determined by a Friedman test with Dunn's multiple comparison test to compare each restimulation day to day 9.

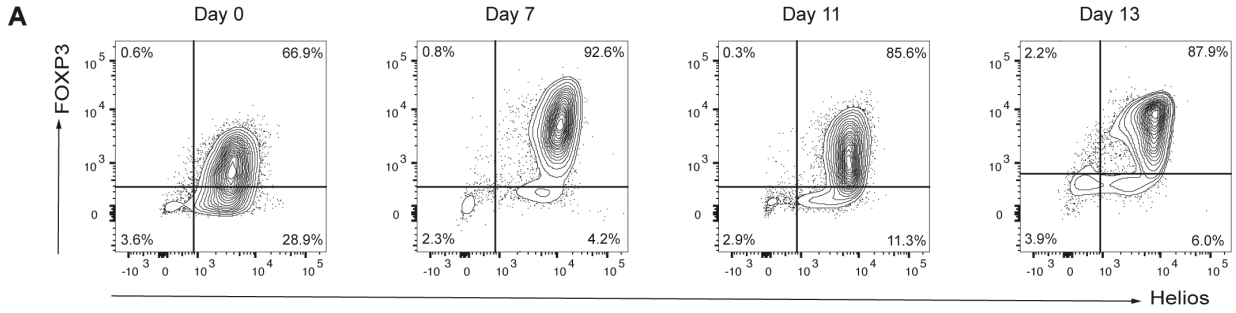

Figure 3.14: FOXP3 expression of thymic Tregs over the course of expansion.
Isolated thymic Tregs were expanded with Dynabeads Treg Xpander, restimulated on day 11 and analyzed 2 days following restimulation. Representative flow cytometry data for FOXP3 expression of expanded thymic Tregs, measured at day 0, 7, 11 (prior to restimulation) and 13.

In parallel, cells were cryopreserved 2 days following each day of restimulation. These cells were thawed and tested immediately or after overnight culture. There was a trend towards lower viability for cells restimulated on days 13-14 compared to day 9 **(Figures 3.13G-H)**. At thaw, there was a trend towards higher FOXP3 expression for cells restimulated on days 13-14 compared to day 9; however, FOXP3 expression was similar between conditions after overnight culture **(Figures 3.13H-I)**. Overall, the differences between cells restimulated on different days were far less than those seen in **Figure 3.10**. Thus, the cryopreservation timing relative to the restimulation day is a much more critical process parameter than the day of restimulation.

3.3 Discussion

Here we report the first comprehensive testing of activation reagents, media, restimulation timing and cryopreservation conditions to optimize a GMP-compatible manufacturing protocol for Tregs isolated from discarded pediatric thymuses. We found large differences between the types of activation reagents and media, with the combination of Dynabeads Treg Xpander and ImmunoCult-XF medium resulting in the most efficient expansion of cells which retained high FOXP3 expression and suppressive capacity. Allowing cells to return to resting size (~8.5 μm) prior to restimulation resulted in greater expansion following restimulation and the timing of cryopreservation had a major effect on cell viability, FOXP3 expression and suppressive function. Only cells cryopreserved 1-3 days following restimulation retained phenotypic and functional properties that would be acceptable for a clinical grade cell product upon thawing. These data have significant implications for the development of more feasible and cost-effective approaches to manufacture Tregs for clinical use.

Manual tissue dissociation and magnetic selection resulted in a Treg product with high (median of 94%) purity, as judged by CD25 and CD8 expression. Notably, as CD25 expression precedes that of FOXP3 in human Treg development [39], ~20% of the isolated $CD25^+$ cells did not express FOXP3 directly after isolation; however, its expression was strongly upregulated after TCR activation. An advantage of thymic Tregs is that magnetic-bead-based selection alone was sufficient to achieve a high purity cell product, without the additional need for GMP-grade flow cytometric sorting.

We found that the maximum fold expansion for thymic Tregs was less than that which has been previously reported for Tregs isolated from peripheral or cord blood [184, 194, 195]. In comparison to Tregs from peripheral blood, the difference in expansion likely relates to the

relative purity of the cultures and/or the state of T cell maturation. Unless peripheral blood Tregs are sorted as $CD45RA^+$ cells, they contain a significant proportion of activated, non-regulatory T cells [158, 187, 260], which have a higher expansion potential. Indeed, as mentioned above, some of the isolated $CD25^+$ cells were still undergoing differentiation and did not yet express FOXP3. This immaturity of the thymus-derived Tregs may underlie their lower expansion potential [77].

The type of activation reagent and media used had surprisingly large effects on Treg expansion potential and phenotype. Similar findings have been reported in other studies; for example, activation with KT64/86 aAPCs promotes higher expansion than antibody-conjugated beads [194, 195], and differences in expansion have been observed for beads from different suppliers [183]. These differences are likely related to the strength of stimulation/costimulation provided by each reagent and the format in which the signals are provided (soluble antibodies, beads, cells, etc.). Many commercially available activation reagents are designed for Tconv rather than Tregs, and since Tregs are thought to experience stronger TCR stimulation than Tconv during development [6], the two cell types may require a different strength of stimulation for optimal expansion *in vitro*. As both activation reagents and media composition are proprietary, it is difficult to know the exact mechanism driving the differences observed here. However, these data clearly show that testing of activation reagents and media from a variety of manufacturers is warranted.

Similar to other reports, we found that expression of FOXP3 waxed and waned over the course of cell expansion [194, 261]. These data raise the question of whether lower FOXP3 expression is the result of activation state, impending cell death and/or loss of Treg stability. FOXP3 expression in Tregs is known to vary with activation state, with higher expression

shortly following activation/restimulation [261]. FOXP3 expression is also known to decline in cell populations with low viability, such as after cryopreservation [213]. We have previously shown that thymus-derived Tregs are stable, even when exposed to inflammatory cytokines [77], consistent with the findings reported here that despite variation in FOXP3 expression during expansion, expanded thymic Tregs maintained a demethylated TSDR and did not produce IL-2. Although there was a trend to a higher proportion of IL-2^+ cells in Tregs cryopreserved 5 days following restimulation, the effect on viability was much more pronounced, suggesting that the low FOXP3 expression and suppressive function of these cells is likely mostly related to the high proportion of dead/dying cells.

We found that expanded Tregs cryopreserved 1-3 days following restimulation survived cryopreservation much better than those cryopreserved > 3 days following restimulation. Tregs are known to be sensitive to cryopreservation, with many cells in the early stages of apoptosis at the time of thaw [213], although their phenotype and suppressive function can be rescued by restimulation [213, 214]. The impact of cryopreservation on different cell types is influenced by many variables including metabolic state, membrane permeability, and sensitivity to stresses such as osmotic shock, toxicity and cold shock [262], all of which make cells susceptible to apoptosis and necrosis. Activation state has also been shown to affect the ability of T cells to recover from cryopreservation [263], but to the best of our knowledge, the critical effect of timing post-T cell stimulation on the success of cryopreservation has not been previously described. Further studies are required to determine the underlying mechanism for this effect which may be influenced by factors such as metabolism, speed of ice crystallization, cell composition and/or cell size. A limitation of our study is that cells were cryopreserved using Mr.

Frosty freezing containers for all cryopreservation experiments. While these containers provide a rate of cooling near 1ºC/min, the cooling rate is less controlled than with controlled rate freezers.

In summary, we comprehensively tested protocols to isolate, expand and cryopreserve thymus-derived Tregs. This work will enable large numbers of Tregs to be produced and cryopreserved for cell therapy applications. The ability to effectively cryopreserve expanded Tregs is step towards the development of these cells as an "off-the-shelf" cell therapy product.

Chapter 4: Consequences of adjusting cell density and feed frequency on serum-free expansion of thymic regulatory T cells

4.1 Introduction

Preclinical studies in mice required high ratios of regulatory to effector T cells for effective suppression [119, 120], likely because only a fraction of unmodified, polyclonal Tregs are antigen-specific and thus stimulated in a disease-relevant way [155]. Thus clinical testing of polyclonal Tregs has used doses up to $100x10^6$ cells/kg (7 billion cells for a 70 kg individual) [136]. Since Tregs comprise a small proportion of circulating $CD4^+$ T cells [155], it is challenging to consistently achieve such large cell doses. In the last chapter, we optimized a protocol to expand and cryopreserve thymic Tregs in serum-free medium, with preserved viability, FOXP3 expression, and suppressive function [3]. However, cell yields remained significantly lower than those of parallel cultures of Tconv, thus limiting the number of doses that could be produced per thymus and stored until needed as an "off-the-shelf" allogeneic Treg therapy.

The potential for Treg expansion up to 10^7-fold over ~55 days when stimulated 5 times was recently demonstrated using K562 cells transduced to express CD64 and CD86 in medium supplemented with serum. However, as therapies move to treat many patients, the use of artificial antigen presenting cells and serum should be reduced since they add greatly to the risk of inadvertent introduction of adventitious viral or prion agents [264, 265] as well as to improve cell manufacturing control by eliminating serum lot-to-lot variability [197, 198]. It is especially important for cell therapy production to develop processes with defined inputs since the final product cannot be effectively purified from these inputs after expansion (such as done for protein

therapeutics by including multiple order of magnitude viral removal steps). In addition, the elimination of both serum and artificial antigen presenting cells should reduce costs in the longer-term [215]. Thus, though challenging to do, it is important to develop manufacturing protocols using non-cell-based activation reagents and serum-free media.

Here, we investigated process parameters that affect the magnitude and variability of Treg expansion using non-cell-based activation reagents and serum-free media, seeking conditions that maximized cell division and increased consistency between donors. We compared expansion of Tregs at different cell densities, analyzing the effect on cell-cell interactions, nutrient and oxygen gradients, and the impact of these parameters on the yield and quality of the resulting Treg cell product.

4.2 Results

4.2.1 Cell density at restimulation correlates with subsequent variation in Treg expansion and viability

To extend our previously developed Treg expansion protocol [3], thymic Tregs were isolated as $CD25^{+}CD8^{-}$ T cells, stimulated with a 4:1 (bead:cell) ratio of anti-CD3/CD28 beads in ImmunoCult-XF medium (a serum-free, xeno-free medium) with 1000 IU/mL IL-2 and 100 ng/mL rapamycin at $5x10^5$ cells/mL. The cells were restimulated on day 11 with a 1:1 ratio of anti-CD3/CD28 beads and expanded for another 10 days for a total of 21 days of culture **(Figure 4.1A)**. Whereas some donors expanded >1,000-fold and maintained viability > 80% **(Figure 4.1B-C)**, for others, the expansion and viability declined on days 15 or 17, and by day 21 these cultures had unacceptable levels of both viability as well as FOXP3 and Helios co-expression, the latter being a surrogate measure of Tregs [24, 266] **(Figure 4.1D)**. While there was some

donor-to-donor variability, there appeared to be a source of variability between experiments with donors that were expanded in parallel having similar trends in viability and fold expansion.

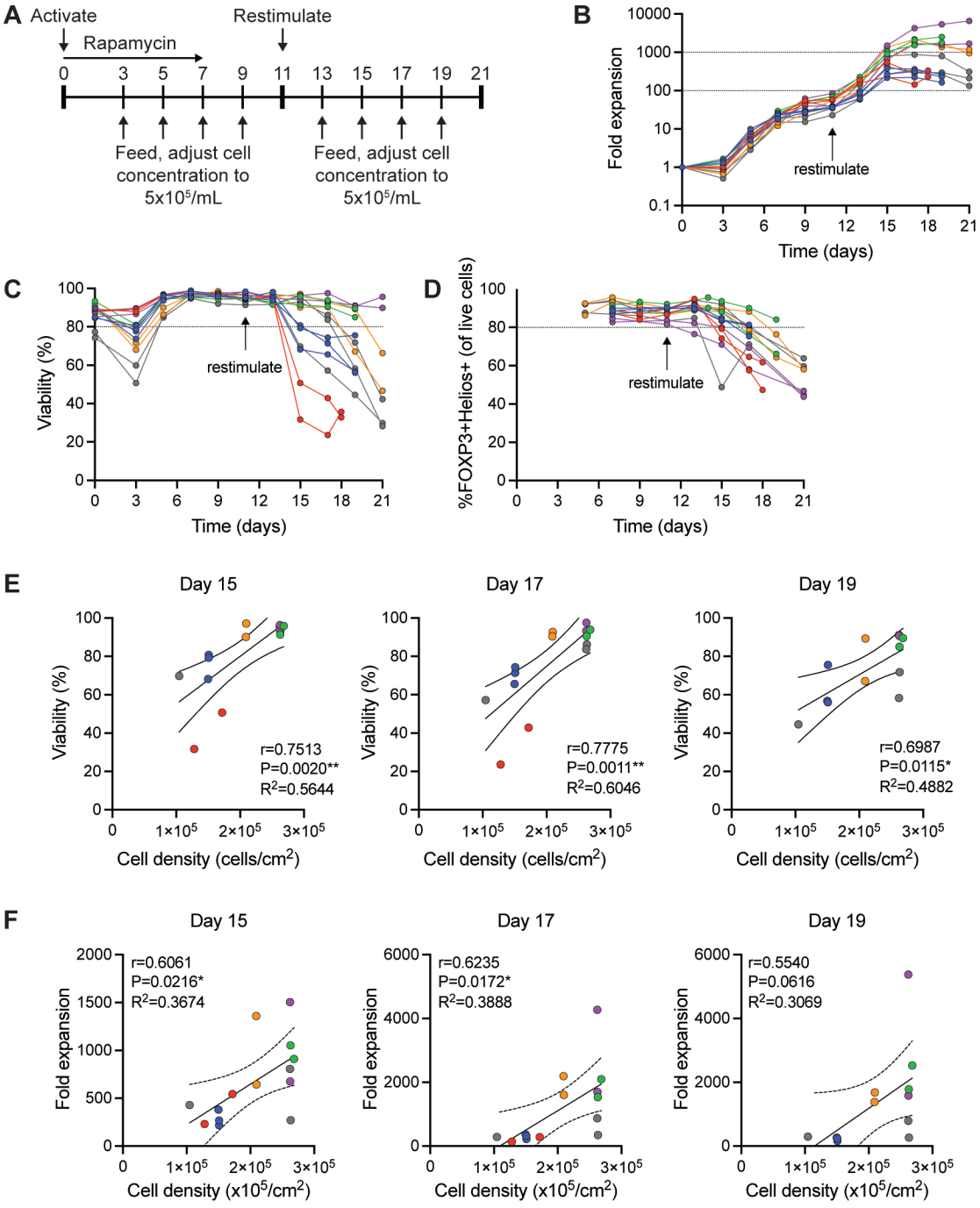

Figure 4.1: Variability in Treg viability and expansion correlated with cell density at restimulation.
(A-F) Tregs were activated with 4:1 bead:cell and expanded as indicated (n=11 donors from 6 experiments, each experiment represented by a different color). **(A)** Schematic overview of thymic Treg expansion protocol. **(B)** Fold expansion, calculated from cell counts. **(C)** Viability, measured by acridine orange and propidium iodide staining.

(D) Expression of FOXP3 and Helios, measured by flow cytometry. **(E)** Correlations of viability at day 15, 17, or 19 with cell density at restimulation on day 11. **(F)** Correlations of fold expansion at day 15, 17, or 19 with cell density at restimulation on day 11. **(B-F)** depict individual donors, 3 donors were repeated and with repeats shown as separate lines or points. Pearson correlation coefficient shown in **(E-F)**.

Given the observed variability between experiments, we tested if activating Tregs with lower bead ratios or adding rapamycin for different durations could reduce the variability. Reducing the bead ratio at activation from 4:1 to 1:1 (bead:cell) did not significantly affect fold expansion, viability, or co-expression of FOXP3 and Helios **(Figure 4.2B-D)**. We next tested the effect of rapamycin by comparing the effect of adding it only during the first stimulation or throughout the whole culture. Cultures with rapamycin present either from days 0-7 or throughout the whole culture tended to have higher viability and frequency of $FOXP3^{+}Helios^{+}$ cells from days 7-13 than those without rapamycin; however, there was not a significant difference in fold expansion and all cultures had low viability at day 21 **(Figure 4.2E-G)**.

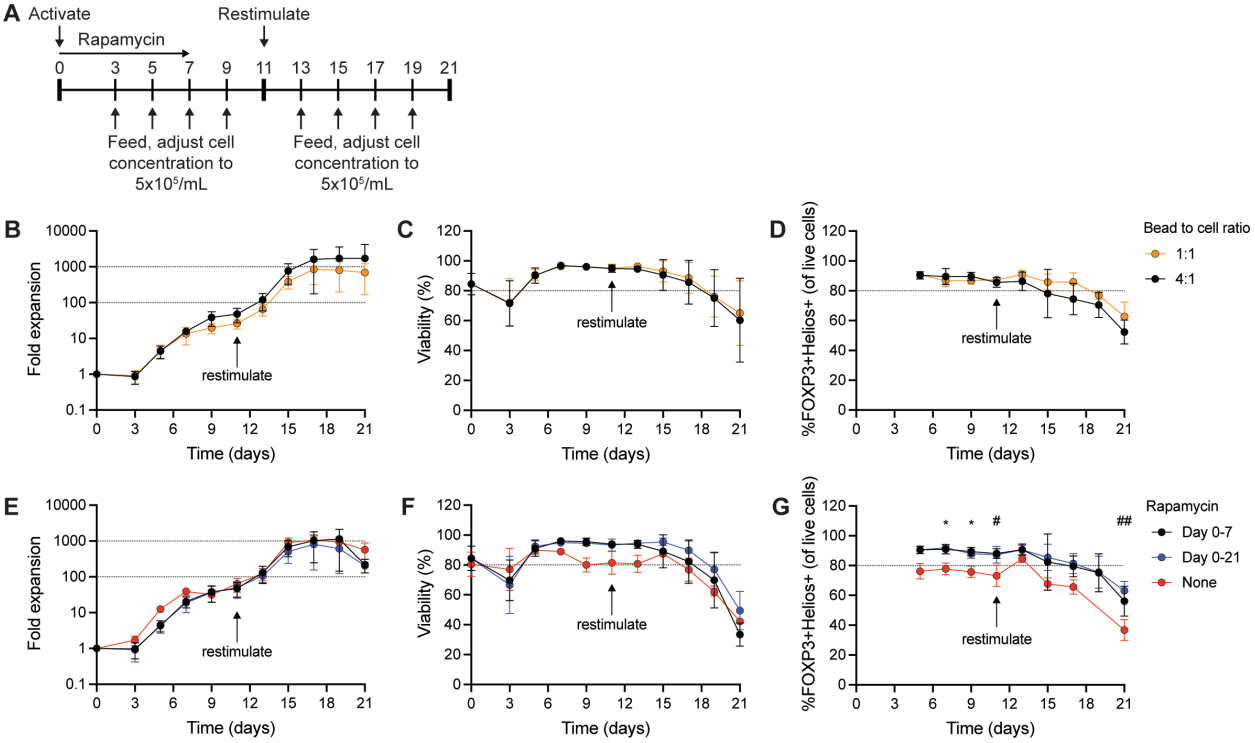

Figure 4.2: Changing the bead ratio or rapamycin did not improve Treg expansion or viability.

(A) Schematic overview of thymic Treg expansion protocol. **(B-D)** Tregs were activated with 4:1 or 1:1 bead per cell on day 0 and expanded as indicated in (A). Cells in both conditions were restimulated with 1:1 bead per cell on day 11 (n=6 donors from 3 experiments). **(B)** Fold expansion, **(C)** viability, and **(D)** expression of FOXP3 and Helios throughout expansion. **(E-G)** Tregs were activated with 4:1 bead per cell on day 0 and expanded as indicated in (A) without/with rapamycin from day 0-7, or 0-21 (n=3-5 donors from 2 experiments). **(E)** Fold expansion, **(F)** viability, and **(G)** expression of FOXP3 and Helios throughout expansion. Mean ± SD are shown. Arrows indicate restimulation on day 11. **(G)** Significance was determined by repeated measures two-way ANOVA with Tukey's multiple comparisons test. * indicate significant differences between rapamycin present from day 0-7 and not added, # indicate significant differences between rapamycin present throughout the whole expansion and not added.

The variability in expansion and viability between donors and experiments suggested there may be a critical process parameter that was not being controlled, leading us to identify that although cell concentration was controlled, cell density – the number of cells per unit area of the flask or well – was inconsistent. Specifically, the cell concentration was adjusted to $5x10^5$ cells/mL at each feed but, since the culture surface cell density was not fixed, cultures in larger culture vessels (e.g. 6-well plates or T-flasks) had lower cell densities than those in smaller culture vessels (e.g. 96-well or 24-well plates). We found a positive correlation between cell density at restimulation and subsequent viability **(Figure 4.1E)** and expansion **(Figure 4.1F)** at days 15, 17, and 19. These data suggested that culture surface cell density was a key process parameter that had not been previously investigated in Treg expansion protocols.

4.2.2 Cell density influences Treg viability and phenotype

To test the hypothesis that culture surface cell density was a critical process parameter in Treg expansion, we compared Treg expansion in cultures where cell density was fixed at $1x10^5$ cells/cm^2, $3x10^5$ cells/cm^2, or $5x10^5$ cells/cm^2 at each feed **(Figure 4.3A)**. Since the cell concentration was also adjusted to $5x10^5$ cells/mL, the medium height varied. The viability of cultures expanded at $1x10^5$ cells/cm^2 fell to ~40% by day 21, whereas cultures expanded at $5x10^5$ cells/cm^2 remained ~80% viable at day 21 **(Figure 4.3B)**. Cultures expanded at all cell densities reached similar maximum fold expansion on day 17 **(Figure 4.3C)**; however, the overall fold

expansion then declined for low density cultures due to declining viability, whereas higher cell density cultures sustained their viability and cell number. Cultures expanded at $1x10^5$ cells/cm^2 had higher growth rates from day 13-15 (2-4 days post restimulation) but their growth rate declined at days 15-17. In contrast, although cells restimulated at $5x10^5$ cells/cm^2 had lower growth rates from days 13-15, they were better able to sustain growth between days 15-17 **(Figure 4.3D)**.

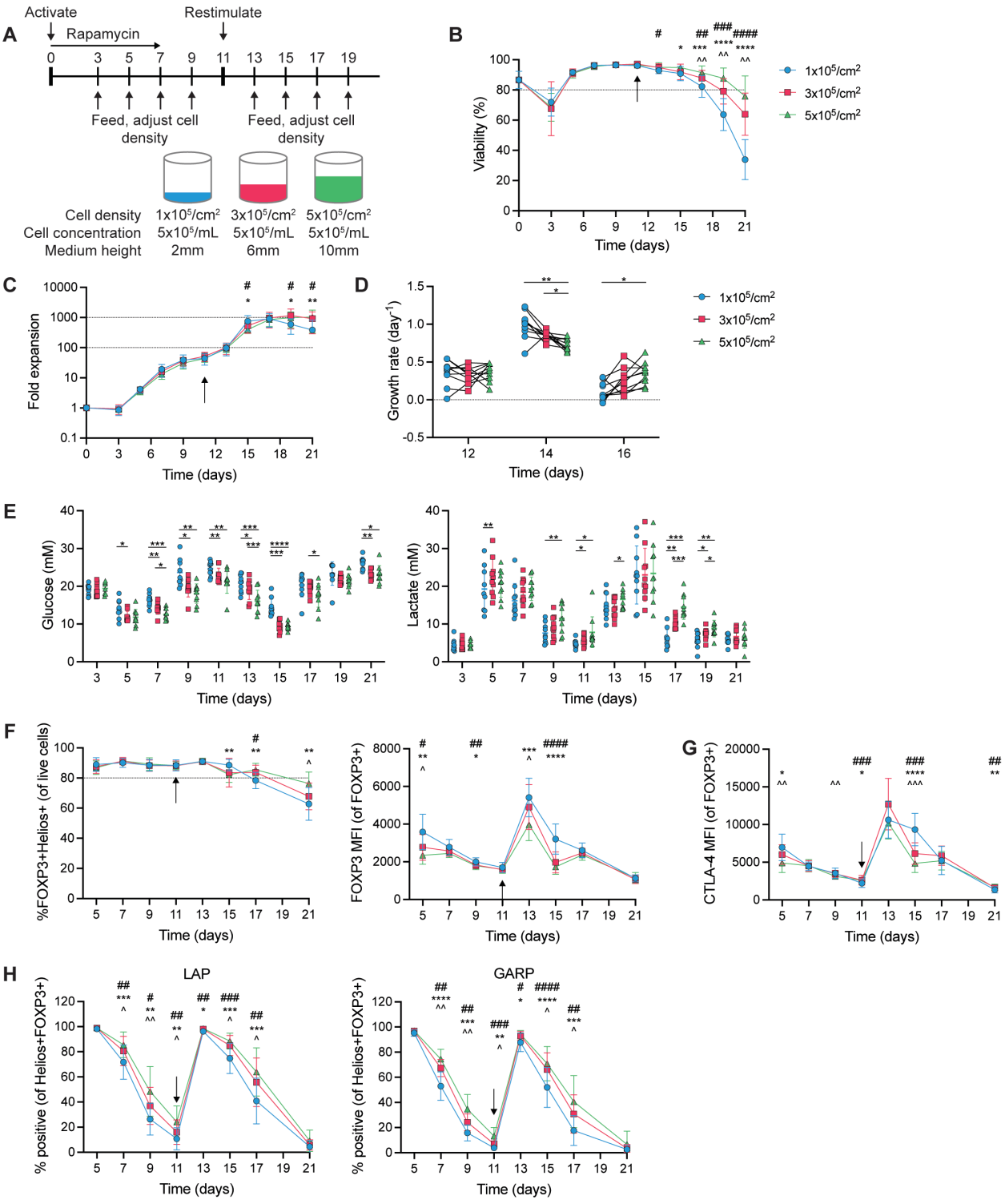

Figure 4.3: Varying cell density affects Treg viability and phenotype.
(A-I) Tregs were expanded at cell densities of $1x10^5$ cells/cm^2, $3x10^5$ cells/cm^2, or $5x10^5$ cells/cm^2 (n=10 donors from 6 experiments). **(A)** Schematic overview of Treg expansion protocol. At each feed, cell numbers and culture volumes were adjusted to maintain the cell densities and cell concentrations indicated. **(B)** Viability, measured by acridine orange and propidium iodide staining. **(C)** Fold expansion, calculated from cell counts. **(D)** Growth rate

calculated for each two-day interval between feeds and shown at the mid-point for the interval. **(E)** Glucose and lactate concentrations were measured in samples of culture medium taken before feeding. **(F)** Expression of FOXP3 and Helios, FOXP3 MFI, **(G)** CTLA-4 MFI, and **(H)** expression of LAP and GARP. **(B-C, F-H)** mean ± SD are shown. **(D)** depicts individual donors. **(E)** Individual points are shown with lines representing Mean ± SD. Arrows indicate restimulation on day 11. Significance was determined by repeated measures two-way ANOVA with Tukey's multiple comparisons test. **(B-C, F-H)** # indicate significant differences between $1x10^5$ cells/cm^2 and $3x10^5$ cells/cm^2, * indicate significant differences between $1x10^5$ cells/cm^2 and $5x10^5$ cells/cm^2, ^ indicate significant differences between $3x10^5$ cells/cm^2 and $5x10^5$ cells/cm^2.

We measured the concentration of glucose and lactate in samples of conditioned medium taken before the cells were fed to determine whether medium limitations may have been responsible for the reduced viability of cultures expanded at $1x10^5$ cells/cm^2. Cultures expanded at $3x10^5$ cells/cm^2 and $5x10^5$ cells/cm^2 had lower average concentrations of glucose and higher average concentrations of lactate than those expanded at $1x10^5$ cells/cm^2 on many days during the expansion **(Figure 4.3E)**, suggesting that the reduced viability of low density cultures was likely not related to limiting levels of nutrients or metabolites.

As the medium heights also varied with cell density, we tested expanding Tregs at $1x10^5$ cells/cm^2 and $5x10^5$ cells/cm^2 with either the height of medium that gave a cell concentration of $5x10^5$ cells/mL (2 mm or 10 mm respectively), or with the same height of medium for both conditions (6 mm) **(Figure 4.4A)**. The expansion, viability, and frequency of $FOXP3^+Helios^+$ cells were similar between cultures expanded at $1x10^5$ cells/cm^2 with either 2 mm or 6 mm medium heights, and between those expanded at $5x10^5$ cells/cm^2 with either 10 mm or 6 mm medium heights **(Figure 4.4B-D)**. These data suggest that the differences observed in Figure 4.3 were not simply due to differences in medium height, such as due to different oxygen concentrations.

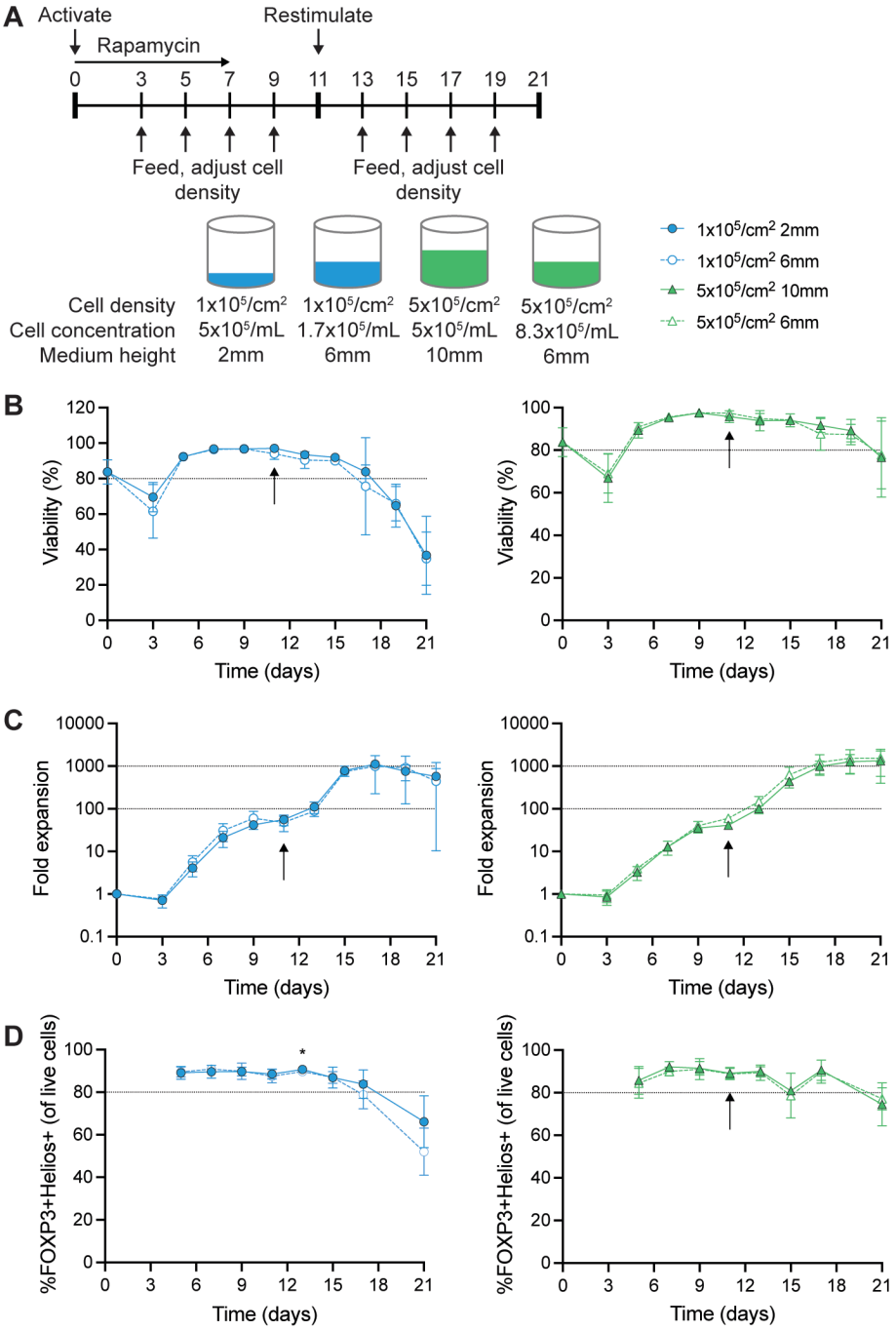

Figure 4.4: Expansion of Tregs at 1x10^5 cells/cm^2 or 5x10^5 cells/cm^2 with varying medium heights.
(A-D) Tregs were expanded at cell densities of 1x10^5 cells/cm^2 or 5x10^5 cells/cm^2 with the indicated medium heights (n=4 donors from 2 experiments). **(A)** Schematic overview of Treg expansion protocol. At each feed, cell numbers and culture volumes were adjusted to maintain the cell densities and cell concentrations indicated. **(B)** Viability, measured by acridine orange and propidium iodide staining. **(C)** Fold expansion, calculated from cell counts. **(D)** Expression of FOXP3 and Helios. Mean ± SD are shown. Arrows indicate restimulation on day 11. Significance was determined by repeated measures two-way ANOVA with Tukey's multiple comparison test.

There were also density-dependent differences in Treg phenotype. The frequency of $FOXP3^{+}Helios^{+}$ cells was high for all densities on day 13, but fell with time as viability declined **(Figure 4.3F)**. A similar trend was observed for FOXP3 and CTLA-4 MFI, with cultures expanded at $1x10^5$ cells/cm^2 having higher expression on day 13 and/or 15 but expression falling for all cultures with time **(Figure 4.3F-G)**. LAP and GARP, proteins expressed by activated Tregs and involved in their suppressive function [107, 267], were highly expressed by Tregs at all cell densities shortly after activation or restimulation but expression declined more rapidly in low versus high density cultures **(Figure 4.3H)**.

In summary, cell density impacted the viability and phenotype of Tregs over 3 weeks of expansion. While all cultures reached a similar maximum fold expansion, Tregs expanded at $5x10^5$ cells/cm^2 sustained higher viability and maintained high and consistent expression of FOXP3 and Treg suppressive proteins, resulting in a sustained level of high quality Tregs.

4.2.3 Comparing Treg cultures from $1x10^5$ to $20x10^5$ cells/cm^2

To test a wider range of cell densities, Tregs were expanded for 11 days, then restimulated at densities of $1x10^5$ cells/cm^2 – $20x10^5$ cells/cm^2 and maintained at these densities with adjustments at each feed. In contrast to the previous experiments, the cell concentration was not kept constant, because cell concentrations of $5x10^5$ cells/mL for densities > $5x10^5$ cells/cm^2 would require medium heights beyond the capacity of standard tissue culture plates. Thus, all conditions were grown with the same 6 mm medium height and varying cell concentrations **(Figure 4.5A, 4.6A)**. Despite the difference in cell concentrations, the previously observed density-dependent differences were maintained, with the viability of cultures at $1x10^5$ cells/cm^2 decreasing more rapidly than those at $5x10^5$ cells/cm^2 **(Figure 4.5B)**. The viability for cultures

expanded at higher densities ($10x10^5$ cells/cm^2 **(Figure 4.6B)** and $20x10^5$ cells/cm^2 **(Figure 4.5B)**) declined rapidly soon after restimulation (from days 13-17) but increased later in the culture (days 17-21). There was no difference in viability between conditions restimulated at varying cell densities if the cell density was adjusted a consistent value for all conditions at day 12, indicating that >24h of culture was required to observe density-driven differences in viability **(Figure 4.6C)**.

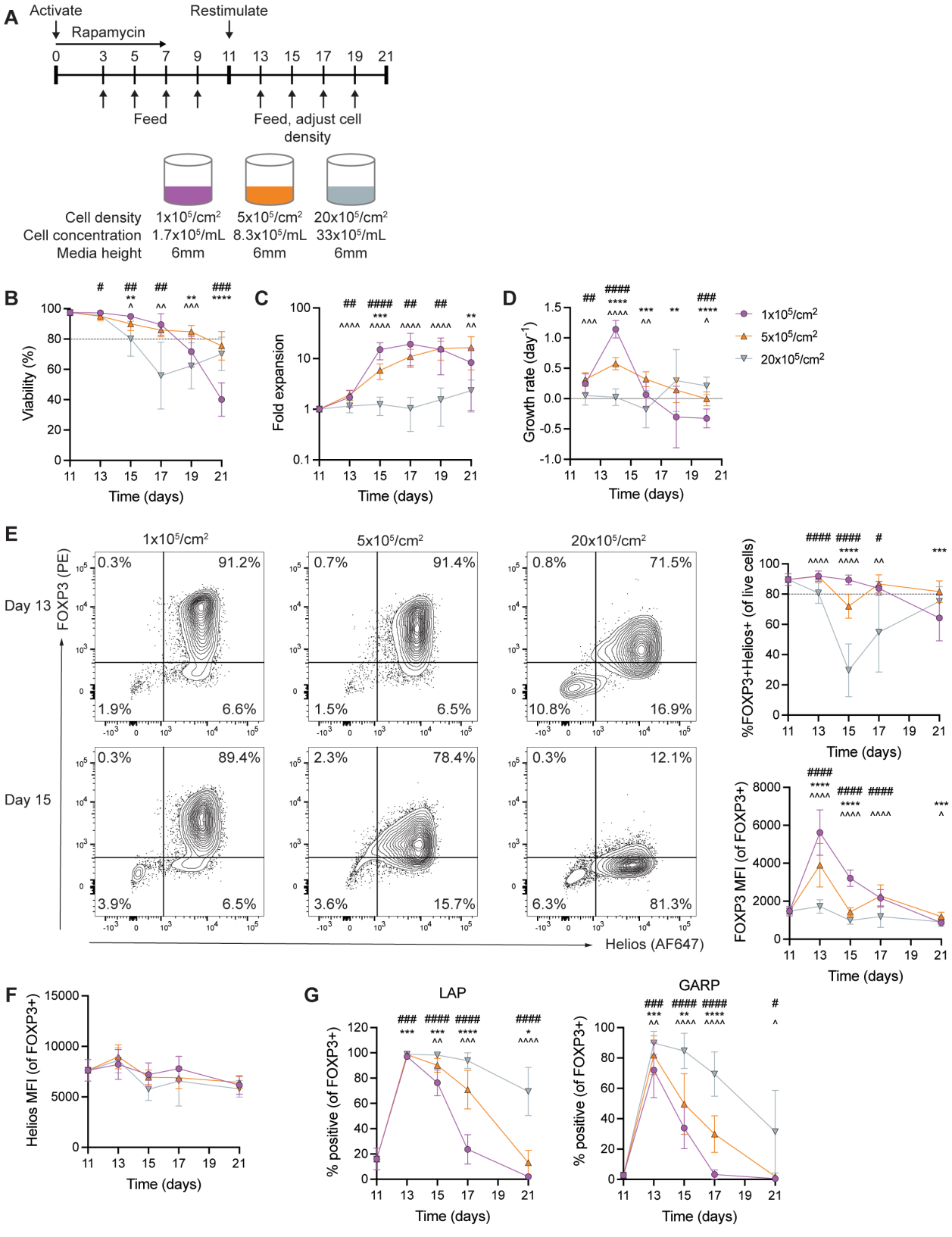

Figure 4.5: Comparing Treg expansion at 1x10^5 to 20x10^5 cells/cm^2.

(A-F) Tregs were restimulated at cell densities of $1x10^5$ cells/cm^2, $5x10^5$ cells/cm^2, or $20x10^5$ cells/cm^2 (n=10 donors from 5 experiments). **(A)** Schematic overview of Treg expansion protocol. At each feed, cell numbers and culture volumes were adjusted to maintain the cell densities and cell concentrations indicated. **(B)** Viability, measured by acridine orange and propidium iodide staining. **(C)** Fold expansion, calculated from cell counts. **(D)** Growth rate calculated for each two-day interval between feeds and shown at the mid-point for the interval. **(E)** Expression of FOXP3 and Helios, FOXP3 MFI, and **(F)** Helios MFI. **(G)** Expression of LAP and GARP. Mean ± SD are shown. Significance was determined by repeated measures two-way ANOVA with Tukey's multiple comparisons test. # indicate significant differences between $1x10^5$ cells/cm^2 and $20x10^5$ cells/cm^2, * indicate significant differences between $1x10^5$ cells/cm^2 and $5x10^5$ cells/cm^2, ^ indicate significant differences between $5x10^5$ cells/cm^2 and $20x10^5$ cells/cm^2.

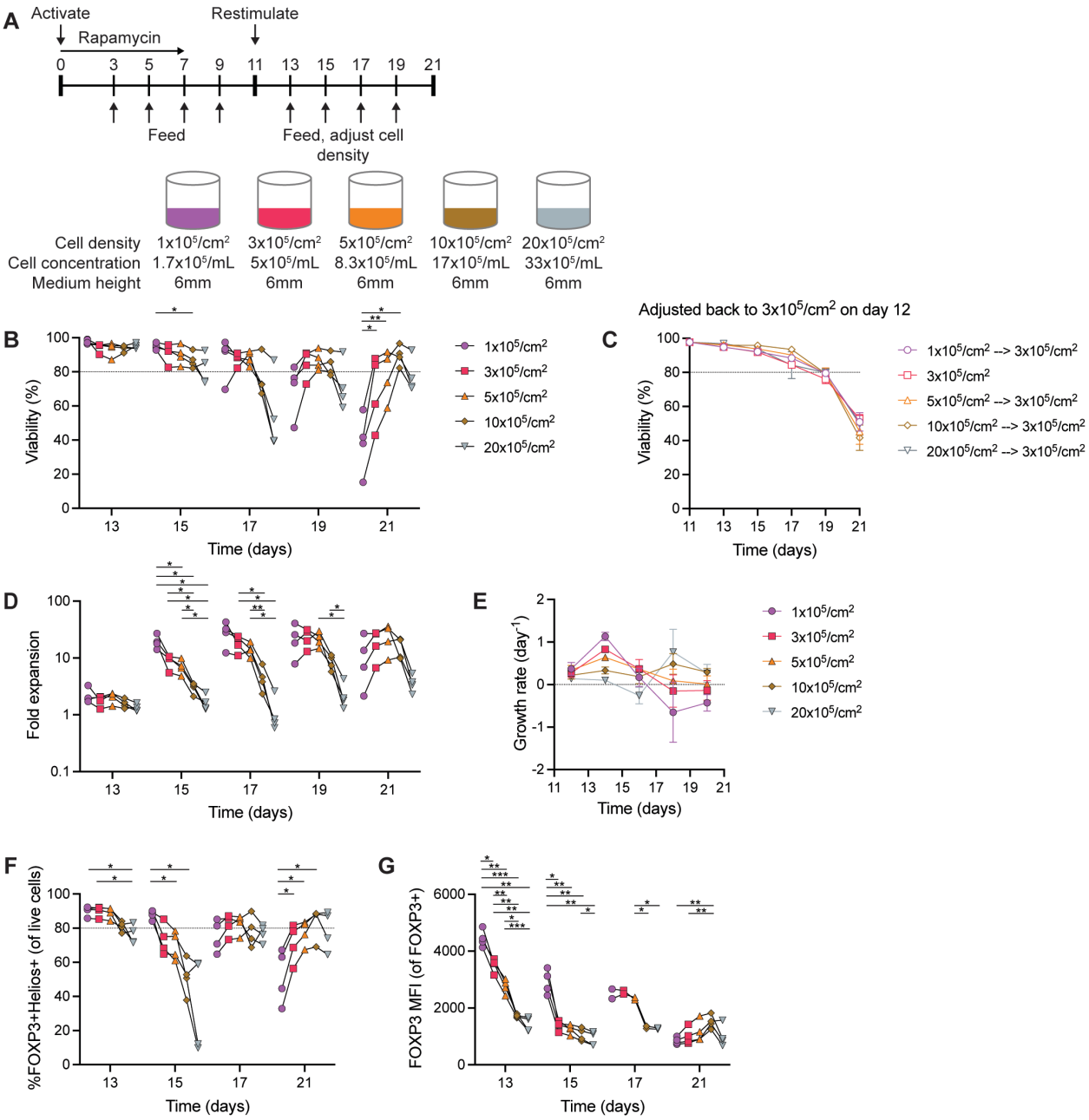

Figure 4.6: Expansion of Tregs adjusted to different cell densities at restimulation.
(A-H) Tregs were restimulated at cell densities of $1x10^5$ cells/cm^2, $3x10^5$ cells/cm^2, $5x10^5$ cells/cm^2, $10x10^5$ cells/cm^2, or $20x10^5$ cells/cm^2 (n=4 donors from 2 experiments for B, D-H; n=2 donors from 1 experiment for C). **(A)** Schematic overview of Treg expansion protocol. At each feed, cell numbers and culture volumes were adjusted to maintain the cell densities and cell concentrations indicated. **(B-C)** Viability, measured by acridine orange and propidium iodide staining for conditions **(B)** adjusted to the indicated cell density at each feed or **(C)** adjusted to $3x10^5$ cells/cm^2 on day 12. **(D)** Fold expansion, calculated from cell counts. **(E)** Growth rate calculated for each two-day interval between feeds and shown at the mid-point for the interval. **(F)** Expression of FOXP3 and Helios and **(G)** FOXP3 MFI. **(B, D, F-G)** mean ± SD or **(C, E)** individual donors are shown. Significance was determined by repeated measures two-way ANOVA with Tukey's multiple comparison test.

The previously observed density-dependent differences in growth kinetics were also maintained. Cultures restimulated at $1x10^5$ cells/cm^2 – $5x10^5$ cells/cm^2 reached similar maximum fold expansion at day 19 **(Figure 4.5C)**; however, there were differences in growth rates from days 13-17, with cultures restimulated at $1x10^5$ cells/cm^2 initially having high growth rates which then fell to 0, whereas those restimulated at $5x10^5$ cells/cm^2 had lower but more sustained growth rates **(Figure 4.5D).** Cultures restimulated at $10x10^5$ cells/cm^2 **(Figure 4.6D-E)** and $20x10^5$ cells/cm^2 **(Figure 4.5C-D)** had even lower growth rates from days 13-15, with limited expansion for cultures at $20x10^5$ cells/cm^2 even by day 21.

Tregs restimuated at different cell densities also had phenotypic differences following restimulation **(Figure 4.5E, 4.6F)**. The frequency of $FOXP3^+Helios^+$ cells was high on days 13 and 15 for cultures restimulated at $1x10^5$ cells/cm^2, then fell as the viability of these cultures declined. Cultures restimulated at $5x10^5$ cells/cm^2 had reduced frequencies of $FOXP3^+Helios^+$ cells at day 15, but this frequency increased to ~80% at days 17 and 21. Cultures restimulated at $20x10^5$ cells/cm^2 had low frequencies of $FOXP3^+Helios^+$ cells at days 13-17, but these increased to levels similar to those in cells cultured at $5x10^5$ cells/cm^2 at day 21. These differences were due to differences in FOXP3 rather than Helios expression. Cultures restimulated at low cell densities had higher FOXP3 MFI, particularly at days 13 and 15 **(Figure 4.5E, 4.6G)**. In contrast, there were no differences in the MFI of Helios on any day during culture **(Figure 4.5F)**. Finally, Tregs that were expanded at higher cell densities maintained higher expression of LAP and GARP than those at lower densities **(Figure 4.5G)**.

Similar to the results in Figure 4.3, adjusting the cell density at restimulation affected Treg expansion, viability, and phenotype, with suboptimal phenotypes observed at the cell densities > $5x10^5$ cells/cm^2. The trends for differences in viability, growth rates, and phenotype between

cultures restimulated at $1x10^5$ cells/cm^2 and $5x10^5$ cells/cm^2 were similar between conditions expanded here with varying cell concentrations and the same medium height and those expanded in **Figure 4.3** with the same cell concentration and varying medium heights. However, the magnitude of differences in growth rate and FOXP3 expression were larger here, possibly as these cultures had varying cell concentrations as well as densities. Interestingly, the $1x10^5$ cells/cm^2 cultures provided a similar expansion, higher FOXP3 expression and higher viability at day 15 than the $5x10^5$ cells/cm^2 cultures reached at their maximum expansion at day 21. Nonetheless, the viability and FOXP3 expression were again more stable in the $5x10^5$ cells/cm^2 cultures. Also, the low cell concentration of the $1x10^5$ cells/cm^2 cultures required 5-fold greater use of media, which would be undesirable for manufacturing processes as well as research lab expenditures. Thus, it remained important to better understand the high cell density performance.

4.2.4 Excessively dense culture conditions inhibit Treg proliferation and increase in cell size

To assess whether differences in expansion for Tregs restimulated at different cell densities were driven by uniform effects on all cells in culture, or a small subset of cells, Tregs were stained with a cell proliferation dye and proliferation was analyzed by flow cytometry at day 15. The data showed that, on average, cultures restimulated at $1x10^5$ cells/cm^2 underwent several cell divisions, those at $5x10^5$ cells/cm^2 underwent fewer cell divisions, and those at $20x10^5$ cells/cm^2 had limited proliferation **(Figure 4.7A, 4.8A)**.

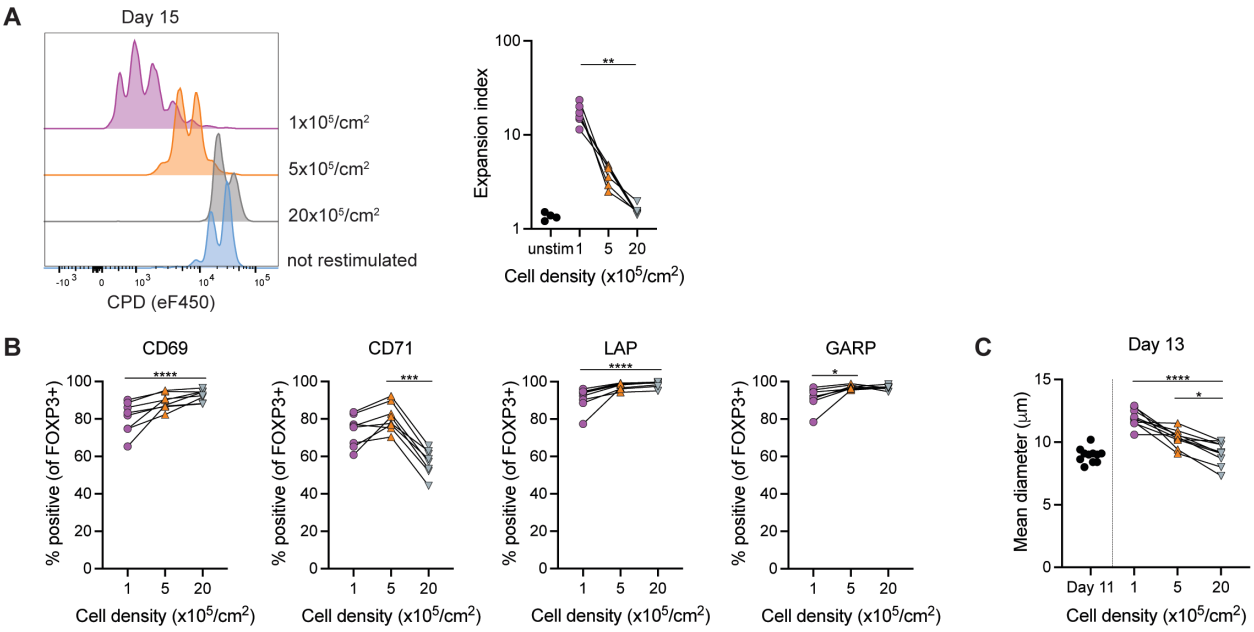

Figure 4.7: Restimulation at high densities inhibits cell proliferation and increase in cell size.
(A-C) Tregs were restimulated at cell densities of $1x10^5$ cells/cm^2, $5x10^5$ cells/cm^2, or $20x10^5$ cells/cm^2. **(A)** Proliferation was measured by dilution of cell proliferation dye on day 15, 4 days following restimulation (n=6 donors from 3 experiments). Expansion index was determined using FlowJo. **(B)** Expression of CD69, CD71, LAP, and GARP measured by flow cytometry 18-20 hours after cells were restimulated (n=8 donors from 4 experiments). **(C)** Mean diameter on day 11 (prior to restimulation) and 13, determined by automated cell counter (n=10 donors from 5 experiments). **(A-C)** depict individual donors. Significance was determined by Friedman test with Dunn's multiple correction test.

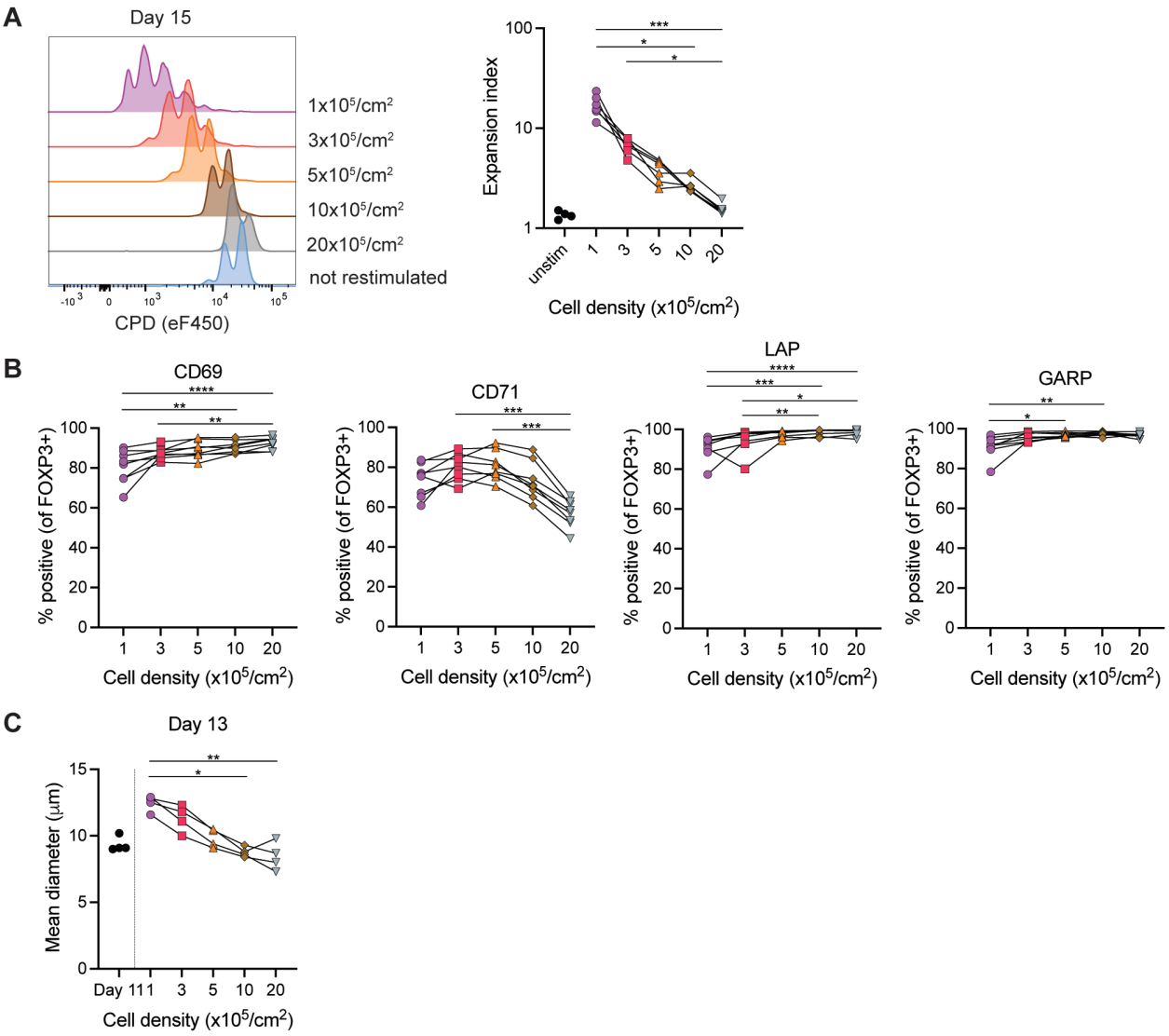

Figure 4.8: Restimulation at high cell densities inhibits proliferation and increase in cell size.
(A-C) Tregs were restimulated at cell densities of $1x10^5$ cells/cm^2, $3x10^5$ cells/cm^2, $5x10^5$ cells/cm^2, $10x10^5$ cells/cm^2, or $20x10^5$ cells/cm^2. **(A)** Proliferation of Tregs measured by dilution of cell proliferation dye 4 days following restimulation (n=6 donors from 3 experiments). Expansion index was determined using FlowJo. **(B)** Expression of CD69, CD71, LAP, and GARP measured by flow cytometry 18-20 hours after cells were restimulated (n=8 donors from 4 experiments). **(C)** Mean diameter on day 11 (prior to restimulation) and 13, determined by automated cell counter (n=4 donors from 2 experiments). **(A-C)** depict individual donors. Significance was determined by Friedman test with Dunn's multiple correction test.

To exclude the possibility that Tregs restimulated at high cell densities were insufficiently activated, we assessed expression of activation-associated proteins. Tregs restimulated at all cell densities expressed high levels of CD69, LAP, and GARP; however, cultures restimulated at $20x10^5$ cells/cm^2 expressed lower levels of CD71 than those restimulated at $5x10^5$ cells/cm^2

(Figure 4.7B, 4.8B). Tregs restimulated at $20x10^5$ cells/cm^2 also did not increase in average size following restimulation **(Figure 4.7C, 4.8C)**. Since increased cell size is characteristic of T cell activation [3, 268], this indicates that a higher number of cells in these cultures were less activated and that restimulation at this very high density impairs activation.

4.2.5 Density dependent effects on costimulatory and co-inhibitory proteins do not influence Treg expansion

Tregs restimulated at low cell densities ($1x10^5$ cells/cm^2) had high expression of CD28, CD86 and CTLA-4 at day 15 **(Figure 4.9A)**, whereas those at very high cell densities ($20x10^5$ cells/cm^2) had high expression of PD-1 **(Figure 4.9A)**. To investigate if expression of any of these proteins mediated density-dependent effects on expansion, Tregs were restimulated at different densities in the presence of anti-PD1 mAbs, anti-CTLA-4 mAbs, CTLA-4 Ig (to bind CD80 and CD86), or a TGFβR1 inhibitor. We found that these inhibitors did not impact Treg expansion and viability, and that even in their presence cell density strongly influenced Treg expansion **(Figure 4.9B-C)**.

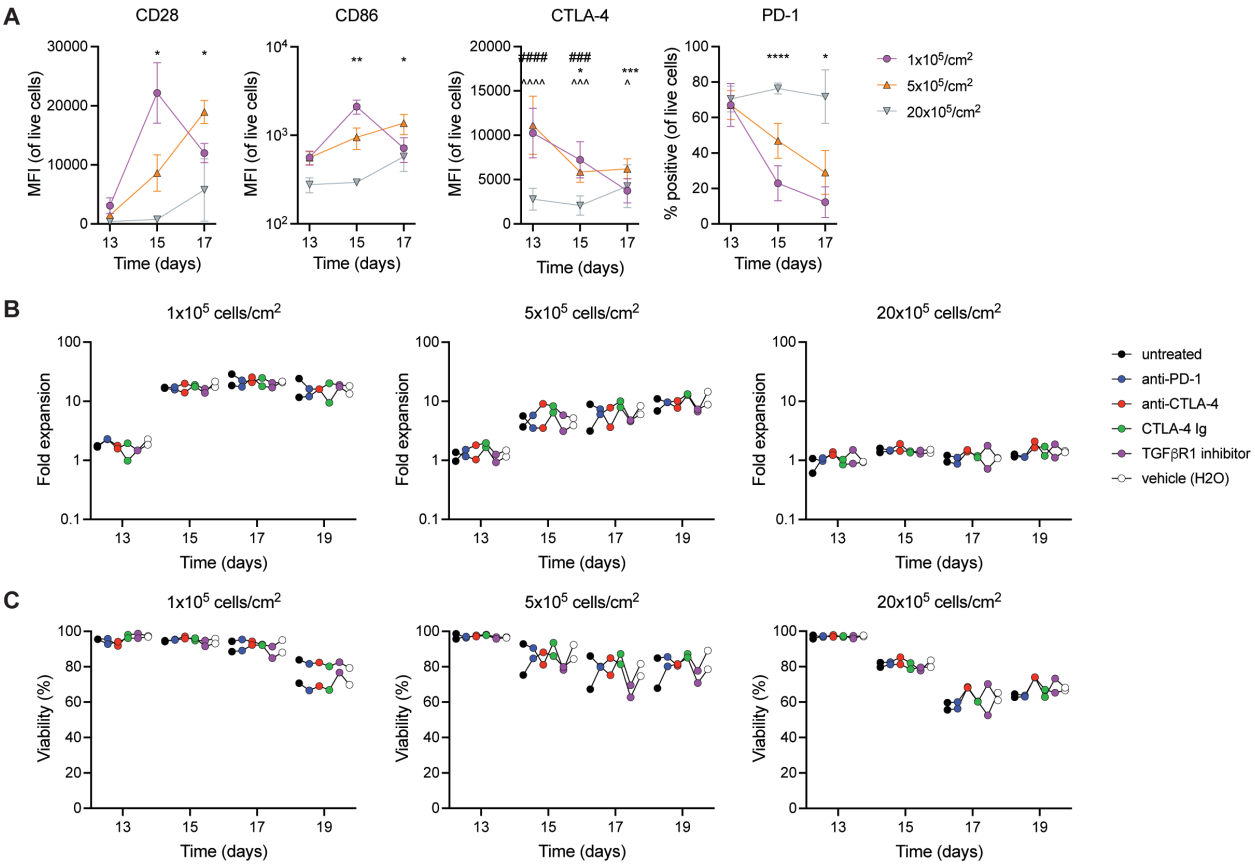

Figure 4.9: Tregs expanded at different cell densities differentially express costimulatory and co-inhibitory proteins.
(A) Tregs were restimulated at cell densities of $1x10^5$ cells/cm^2, $5x10^5$ cells/cm^2, or $20x10^5$ cells/cm^2 as in Figure 4.5. Expression of CD28, CD86, CTLA-4, and PD-1 were determined by flow cytometry (n=4-10 donors from 2-5 experiments). **(B-C)** Tregs were restimulated at cell densities of $1x10^5$ cells/cm^2, $5x10^5$ cells/cm^2, or $20x10^5$ cells/cm^2 and treated with anti-PD1, anti-CTLA-4, CTLA-4 Ig, or a TGFβR1 inhibitor (n=2 donors from 1 experiment). **(B)** Fold expansion, calculated from cell counts. **(C)** Viability, measured by acridine orange and propidium iodide staining. **(A)** mean ± SD are shown. **(B-C)** depict individual donors. Significance was determined by repeated measures two-way ANOVA with Tukey's multiple comparison test. **(A)** # indicate significant differences between $1x10^5$ cells/cm^2 and $20x10^5$ cells/cm^2, * indicate significant differences between $1x10^5$ cells/cm^2 and $5x10^5$ cells/cm^2, ^ indicate significant differences between $5x10^5$ cells/cm^2 and $20x10^5$ cells/cm^2.

4.2.6 Transient exposure to low oxygen concentration does not affect Treg expansion

We next sought to better understand to what extent the impact of expanding Tregs at high densities could be due to low oxygen concentrations. In standard cell culture using multi-well plates or flasks, oxygen is mainly exchanged at the air-medium interface then diffuses through the medium to reach cells at the bottom of the well [269], such that the cells are exposed to a

reduced oxygen concentration. If the rate of oxygen transfer is less than the cell capacity for oxygen uptake, then the cellular oxygen uptake rate will be limited by the mass transfer. The oxygen uptake rate is increased by increased cell density [270], so we sought to determine whether cells restimulated at high cell densities were impacted by low oxygen concentrations.

Tregs were stained with an oxygen sensitive dye, which releases rhodamine at when oxygen levels are < 5%, resulting in increased fluorescence. Tregs restimulated at $5x10^5$ cells/cm^2 or $20x10^5$ cells/cm^2 had increased fluorescence on day 13, indicating that these cells experienced lower oxygen concentrations than those restimulated at $1x10^5$ cells/cm^2 **(Figure 4.10A)**. As expected, the addition of sodium azide reduced fluorescence **(Figure 4.11A)**, as it inhibits oxygen utilization at complex IV of the electron transport chain. Cultures restimulated at $1x10^5$ cells/cm^2 had increased fluorescence on day 15 compared to day 13 **(Figure 4.10A)**, indicating that these cells were also experiencing lower oxygen concentrations. These cultures had increased in cell density by day 15, reaching a cell density closer to that of cultures restimulated at $5x10^5$ cells/cm^2 and $20x10^5$ cells/cm^2 **(Figure 4.10B)**. Nonetheless, cultures restimulated at $5x10^5$ cells/cm^2 still had higher fluorescence than those restimulated at $1x10^5$ cells/cm^2 at day 15.

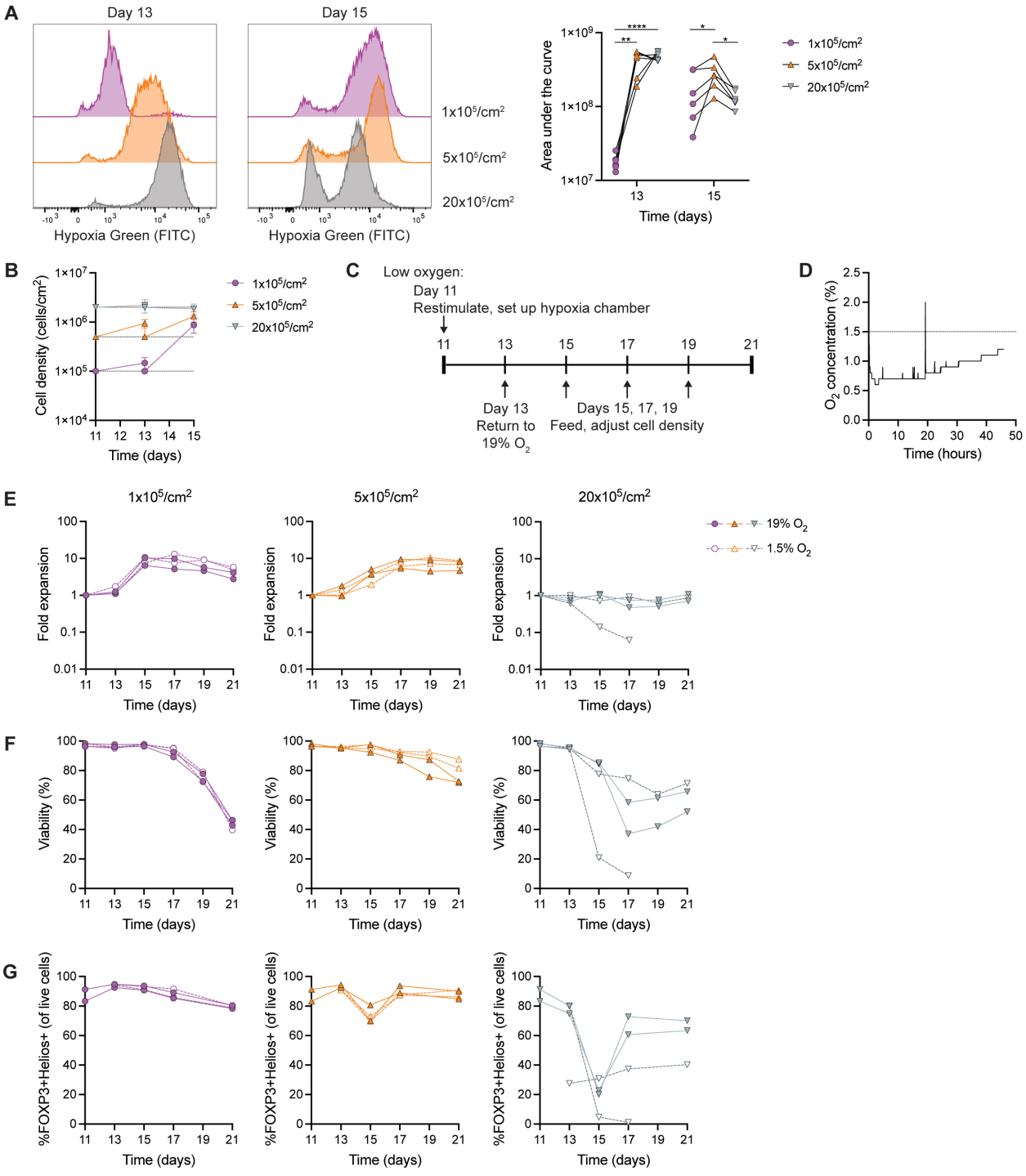

Figure 4.10: Low oxygen concentrations at high cell densities did not affect Treg expansion.
(A-B) Tregs were restimulated at cell densities of $1x10^5$ cells/cm^2, $5x10^5$ cells/cm^2, or $20x10^5$ cells/cm^2 (n=6 donors from 3 experiments). **(A)** Tregs were stained with Hypoxia Green Reagent for Flow Cytometry on the indicated days and the fluorescence was measured by flow cytometry. Increased fluorescence indicates reduced oxygen concentration. Sample flow plots are shown and the fluorescence was quantified by calculating the area under the curve. **(B)** Cell density of Tregs during expansion. The two points on day 13 indicate the cell densities before and after feeding. **(C-G)** Tregs were restimulated at cell densities of $1x10^5$ cells/cm^2, $5x10^5$ cells/cm^2, or $20x10^5$

cells/cm^2 and cultured under normoxic conditions (~19% O_2 in the gas phase; assuming 20.9% O_2 in air, corrected for 5% CO_2 and 6% H_2O [270])) or in a sealed chamber filled with 1.5% O_2 (5% CO_2, balance N_2) from day 11-13. The cells were re-exposed to oxygen on day 13 and all conditions were cultured under normoxic conditions until day 21 (n=2 donors from 1 experiment). **(C)** Schematic for expansion of cells exposed to low oxygen conditions. **(D)** Oxygen concentration in hypoxia chamber from day 11-13, measured using a wireless oxygen sensor. A dotted line is shown at 1.5% for reference. **(E)** Fold expansion, calculated from cell counts. **(F)** Viability, measured by acridine orange and propidium iodide staining. **(G)** Expression of FOXP3 and Helios. **(A, E-G)** depict individual donors. **(B)** Mean ± SD are shown. Significance was determined by repeated measures two-way ANOVA with Tukey's multiple comparisons test.

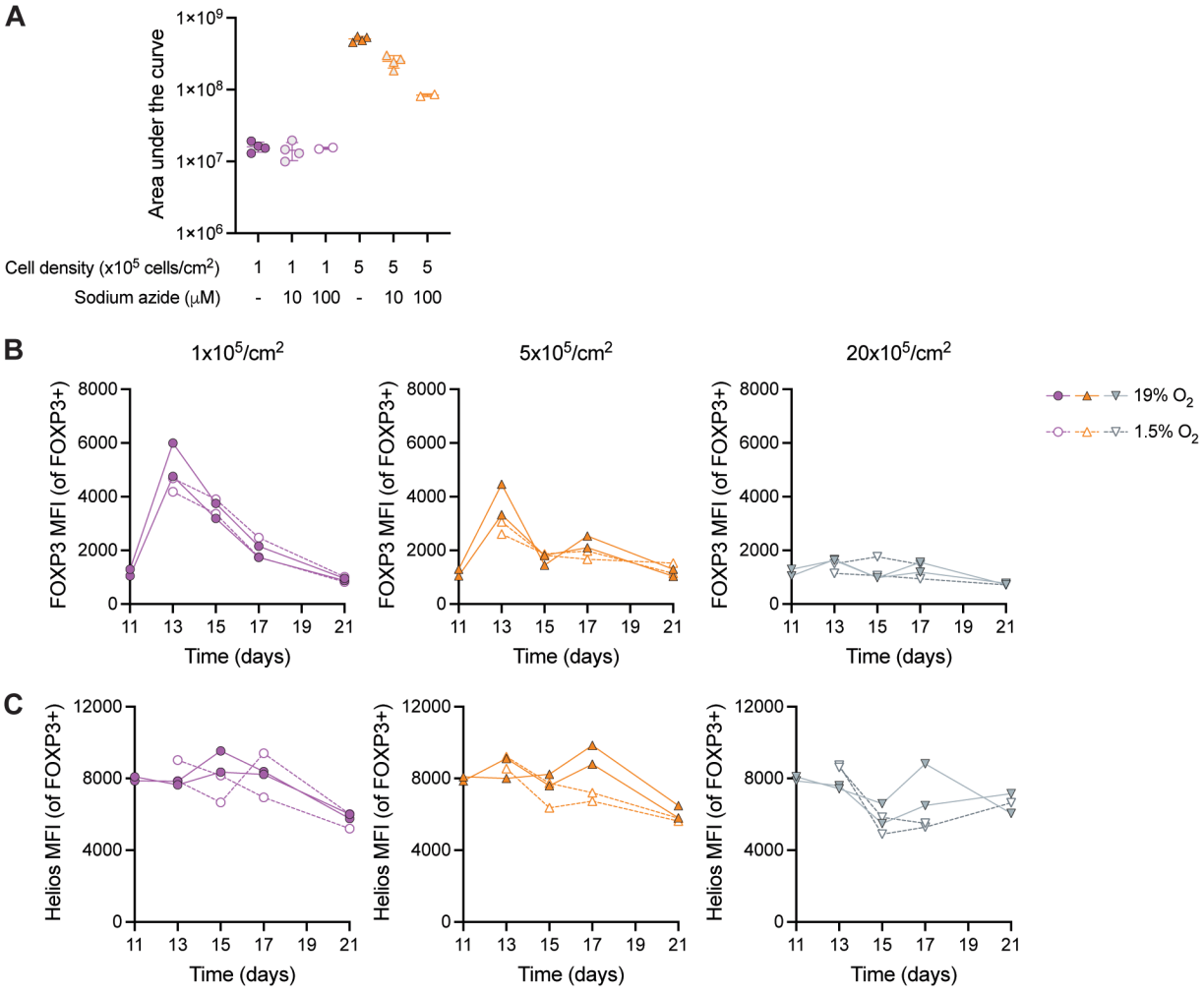

Figure 4.11: Oxygen staining of Tregs treated with sodium azide and phenotype of Tregs restimulated under low oxygen.

(A) Tregs were restimulated on day 11 at cell densities of 1x10^5 cells/cm^2, 5x10^5 cells/cm^2, or 20x10^5 cells/cm^2 with or without sodium azide (n=2-4 donors from 1-2 experiments). Tregs were stained with Hypoxia Green Reagent for Flow Cytometry on day 13 and the fluorescence was measured by flow cytometry. Fluorescence was quantified by calculating the area under the curve. Increased fluorescence indicates reduced oxygen concentration. **(B-C)** Tregs were restimulated at cell densities of 1x10^5 cells/cm^2, 5x10^5 cells/cm^2, or 20x10^5 cells/cm^2 and cultured under normoxic conditions (~19% O_2 in the gas phase) or in a sealed chamber filled with 1.5% O_2 (5% CO_2, balance N_2) from day 11-13. The cells were re-exposed to oxygen on day 13 and all conditions were cultured under normoxic conditions until day 21 (n=2 donors from 1 experiment). **(B)** FOXP3 MFI, and **(C)** Helios MFI. **(A)** Individual points are shown with bars representing mean ± SD. **(B-C)** Individual points are shown.

To directly test the effect of low oxygen concentrations during restimulation, we restimulated Tregs at $1x10^5$ cells/cm^2, $5x10^5$ cells/cm^2, or $20x10^5$ cells/cm^2 and cultured them in a sealed chamber filled with 1.5% O_2 from day 11-13 or under ~19% O_2 normoxic incubator conditions **(Figure 4.10C)**. After day 13, all of the cells were grown under normoxic conditions. A wireless oxygen sensor was used to confirm that the concentration of oxygen remained low during the culture in the hypoxia chamber **(Figure 4.10D)**. There was little difference in expansion, viability, or expression of FOXP3 and Helios between cells grown under low oxygen or normoxic conditions **(Figure 4.10E-G, 4.11B-C)**. Thus, although oxygen gradients did vary with cell density, this had little impact on expansion, viability, or phenotype.

4.2.7 Medium limitations affect Treg proliferation and FOXP3 expression

Activated conventional T cells mainly utilize glycolysis upon activation to produce energy and precursor molecules required for cell growth and proliferation [271]. While it is often cited that Tregs rely on oxidative metabolism [272, 273], they also increase aerobic glycolysis upon activation [274], producing metabolites such as lactate and ammonium. To investigate whether low concentrations of nutrients or accumulation of these metabolites could limit cell growth at high densities, concentrations of glucose, lactate, and ammonium were measured in the conditioned medium, sampled before the cells were fed on days 13 to 21. The **Figure 4.3E** results showed that medium limitations were likely not the cause of the day 15 to 21 declining viability for cultures expanded at $1x10^5$ cells/cm^2; however, low concentrations of nutrients or accumulation of metabolites could limit cell growth for cultures restimulated at higher densities and concentrations.

We confirmed that cultures restimulated at $1x10^5$ cells/cm^2 maintained relatively high (> 15 mM) glucose and low (< 15 mM) lactate concentrations from days 13 to 21 **(Figure 4.12A, 4.13A)**. In contrast, samples from $5x10^5$ cells/cm^2 or $20x10^5$ cells/cm^2 cultures had concentrations of glucose < 10 mM and lactate up to 30 mM. The concentration of ammonium was higher for cultures restimulated at $5x10^5$ cells/cm^2 than $1x10^5$ cells/cm^2 on day 17 but similar on other days. Cultures restimulated at $1x10^5$ cells/cm^2 had higher specific (per cell) glucose uptake and lactate production rates than those from higher cell densities **(Figure 4.13B)**, indicating that the lower glucose and higher lactate concentrations measured for higher cell density cultures were due to the increased cell concentration of these conditions.

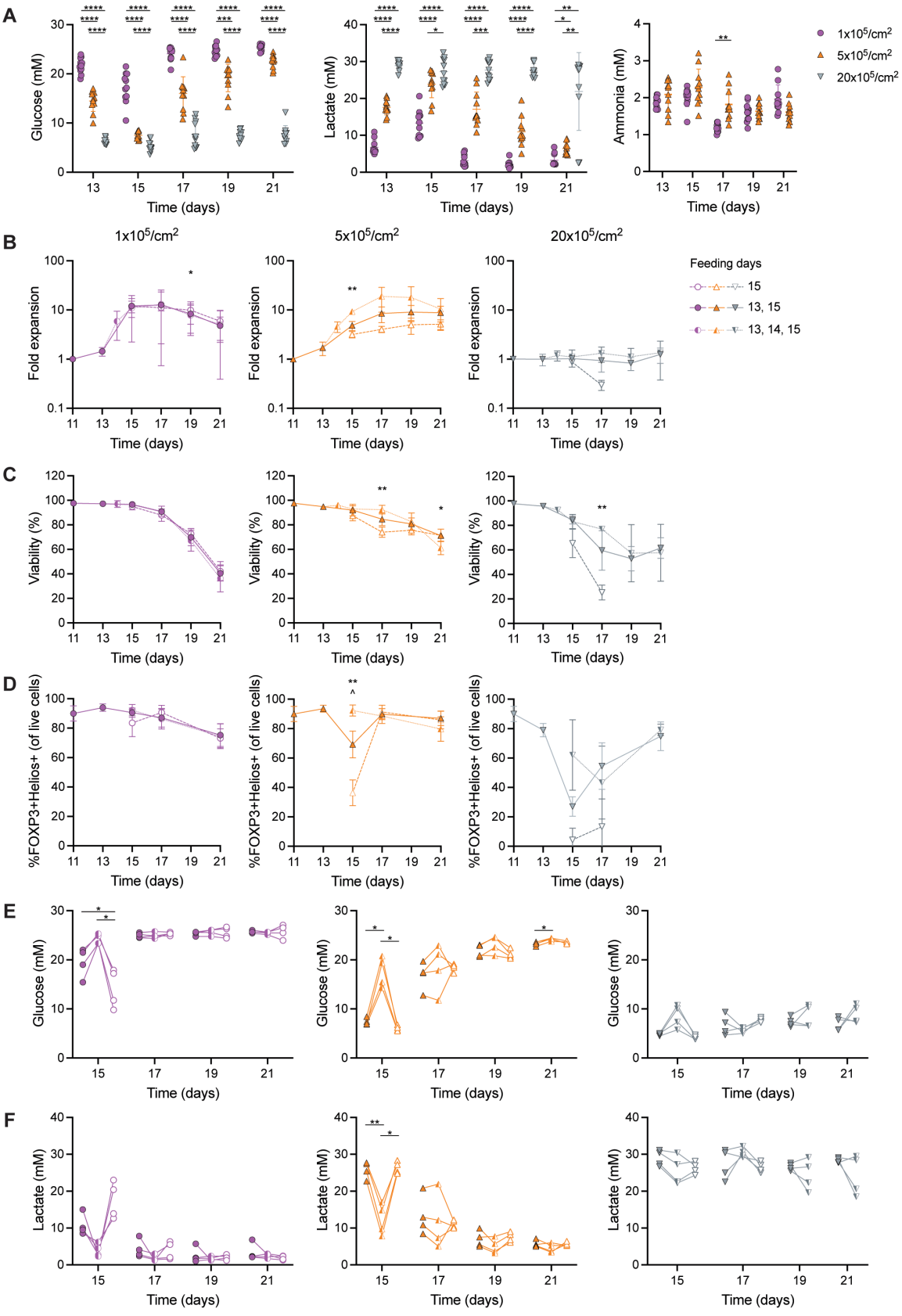
A
Glucose (mM)
Lactate (mM)
Ammonia (mM)
Time (days)
1x10^5/cm^2
5x10^5/cm^2
20x10^5/cm^2
B
1x10^5/cm^2
5x10^5/cm^2
20x10^5/cm^2
Fold expansion
Feeding days
15
13, 15
13, 14, 15
C
Viability (%)
D
%FOXP3+Helios+ (of live cells)
E
Glucose (mM)
F
Lactate (mM)

Figure 4.12: Additional feeding improved expansion, viability and phenotype for Tregs restimulated at $5x10^5$ cells/cm^2.
(A) Tregs were restimulated at cell densities of $1x10^5$ cells/cm^2, $5x10^5$ cells/cm^2, or $20x10^5$ cells/cm^2 (n=10 donors from 5 experiments). **(A)** Glucose, lactate, and ammonium concentrations were measured in samples of culture medium taken before feeding. **(B-F)** Tregs were restimulated at cell densities of $1x10^5$ cells/cm^2, $5x10^5$ cells/cm^2, or $20x10^5$ cells/cm^2 and expanded with feeding as indicated (n=4 donors from 2 experiments). **(B)** Fold expansion, calculated from cell counts. **(C)** Viability, measured by acridine orange and propidium iodide staining. **(D)** Expression of FOXP3 and Helios. **(E)** Glucose and **(F)** lactate concentrations were measured in samples of culture medium taken before feeding. **(A)** Individual points are shown with lines representing mean ± SD. **(B-D)** Mean ± SD are shown. **(E-F)** depict individual donors. Significance was determined by repeated measures two-way ANOVA with Tukey's multiple comparisons test. **(B-D)** * indicate significant differences between '15,' and '13, 14, 15', ^ indicate significant differences between '15' and '13, 15'.

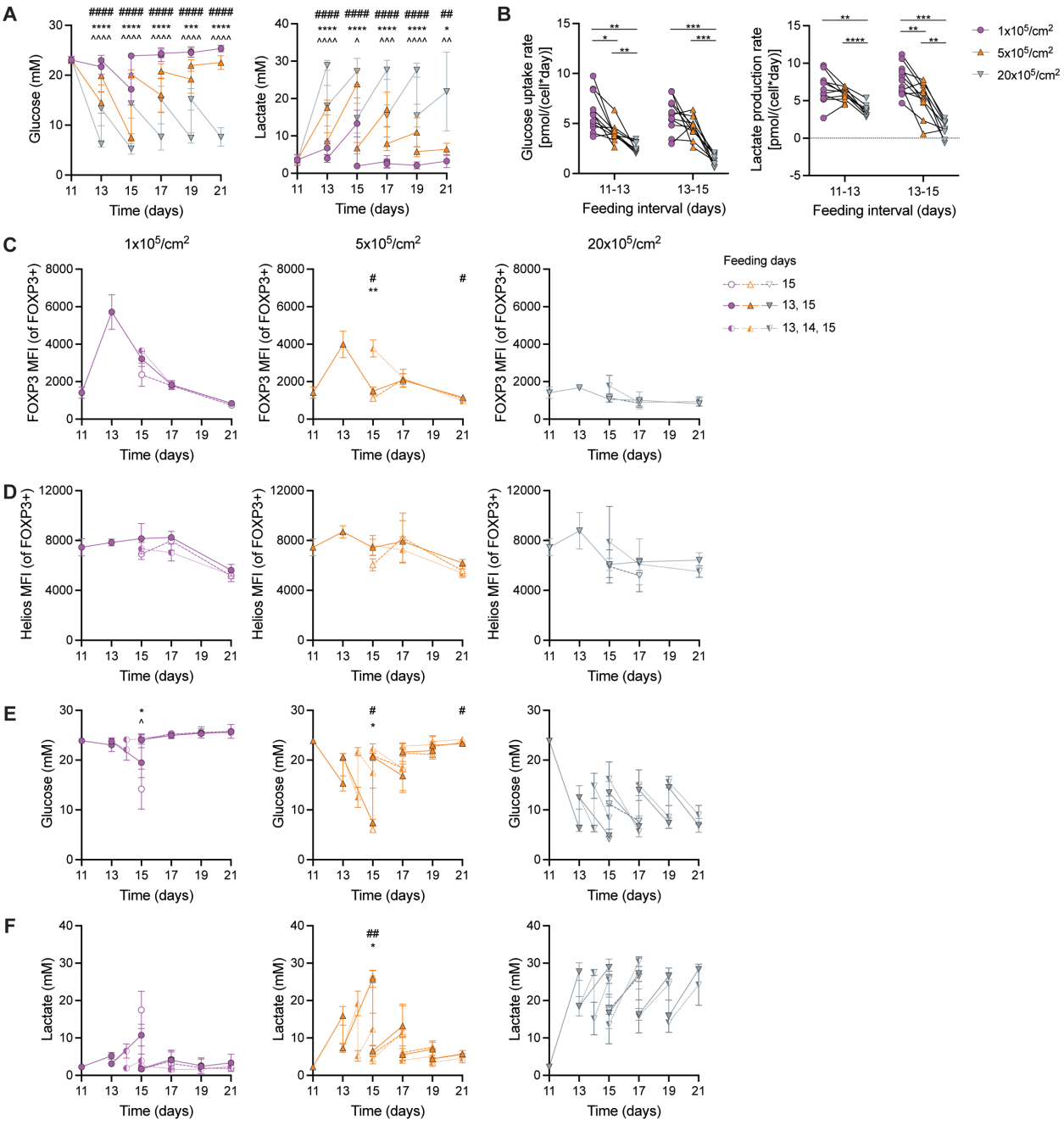

Figure 4.13: Nutrient/metabolite levels and phenotype of Tregs restimulated at different cell densities with different feeding strategies.

(A-B) Tregs were restimulated at cell densities of $1x10^5$ cells/cm^2, $5x10^5$ cells/cm^2, or $20x10^5$ cells/cm^2 (n=10 donors from 5 experiments). **(A)** Glucose and lactate concentrations were measured in samples of culture medium taken before feeding. The concentration of glucose and lactate after feeding were calculated based on concentrations measured in conditioned medium and the volumes of fresh medium added. **(B)** Glucose uptake rate and lactate production rate calculated for day 11-13 and day 13-15. **(C-F)** Tregs were restimulated at cell densities of $1x10^5$ cells/cm^2, $5x10^5$ cells/cm^2, or $20x10^5$ cells/cm^2 and expanded with feeding as indicated (n=4 donors from 2 experiments). **(C)** FOXP3 MFI, and **(D)** Helios MFI. **(E)** Glucose and **(F)** lactate concentrations were measured in samples of culture medium taken before feeding. The concentration of glucose and lactate after feeding were calculated based on concentrations measured in conditioned medium and the volumes of fresh medium added. **(A,**

C-F) Mean ± SD are shown. **(B)** depicts individual donors. Significance was determined by repeated measures two-way ANOVA with Tukey's multiple comparison test. **(A)** # indicate significant differences between $1x10^5$ cells/cm^2 and $20x10^5$ cells/cm^2, * indicate significant differences between $1x10^5$ cells/cm^2 and $5x10^5$ cells/cm^2, ^ indicate significant differences between $5x10^5$ cells/cm^2 and $20x10^5$ cells/cm^2. **(C-F)** # indicate significant differences between '13, 15' and '13, 14, 15', * indicate significant differences between '15' and '13, 14, 15', ^ indicate significant differences between '15' and '13, 15'.

At day 15 we noted that the glucose concentrations in the $5x10^5$ cells/cm^2 cultures were almost as low as in the $20x10^5$ cells/cm^2 cultures that did not expand and had a rapidly decreasing viability. To determine whether medium limitations could underlie differences in growth rate or viability, especially at $5x10^5$ cells/cm^2, we tested different feeding schedules from day 13 to 15. We either eliminated the feed on day 13 (i.e. feeding on days 11, 15, 17, and 19) or added an additional feed on day 14 (i.e. feeding on days 11, 13, 14, 15, 17, and 19). For cultures restimulated at $1x10^5$ cells/cm^2, there was minimal difference in expansion, viability, or FOXP3 expression. However, for cultures restimulated at $5x10^5$ cells/cm^2, eliminating the day 13 feed reduced expansion, viability, and co-expression of FOXP3 and Helios; adding a day 14 feed had the opposite effect **(Figure 4.12B-D)**. Effects on co-expression of FOXP3 and Helios were driven by changes in FOXP3 as Helios expression did not change **(Figure 4.13C-D)**. For cultures restimulated at $20x10^5$ cells/cm^2, removing the day 13 feed caused viability to decrease, such that by day 17 the cultures were discontinued. Adding an additional feed on day 14 increased the viability on day 17 but did not increase expansion.

Cultures restimulated at $1x10^5$ cells/cm^2 had lower glucose concentrations on day 15 if the feed on day 13 was eliminated **(Figure 4.12E, 4.13E)**. In contrast, there was no difference in glucose or lactate concentrations at day 15 between cultures restimulated at $5x10^5$ cells/cm^2 with or without a feed on day 13 **(Figure 4.12E-F, 4.13E-F),** suggesting that these cultures could be limited by the low concentration of glucose or another nutrient and/or accumulation of metabolites. With the additional feed on day 14, glucose concentrations remained > 10 mM and

lactate concentrations remained < 20 mM **(Figure 4.12E-F, 4.13E-F)** for cultures restimulated at both $1x10^5$ cells/cm^2 and $5x10^5$ cells/cm^2. These data suggest that, for cultures expanded at $1x10^5$ or $5x10^5$ cells/cm^2, low nutrient concentrations and/or metabolite accumulations contributed to the observed density-dependent differences in expansion, viability, and FOXP3 expression.

4.2.8 Supplementing antioxidants did not improve Treg expansion

As the physiological concentration of blood glucose is ~5 mM in non-diabetic humans [275], the culture glucose concentrations between 5-10 mM would not be expected to be limiting. However, the limited glucose uptake below those levels may be an indication that another nutrient was limiting expansion. We measured the concentration of amino acids in samples of conditioned medium on day 15, when the concentration of glucose was the lowest for cultures restimulated at $5x10^5$ cells/cm^2 (without the extra feed on day 14 that had been shown to alleviate a limitation, **Figure 4.12B**). While the concentration of most amino acids remained high in the conditioned medium, the concentrations of cysteine and serine were low, especially for the cultures restimulated at $5x10^5$ cells/cm^2 **(Figure 4.14A-B)**. Low serine levels would not be expected to be limiting as serine is considered to be a non-essential amino acid [276]; however, low cysteine levels could limit synthesis of glutathione, required for intracellular redox buffering [277]. To determine whether supplementing cultures with cysteine or antioxidants would improve cell quality, we restimulated Tregs at $1x10^5$ cells/cm^2, $5x10^5$ cells/cm^2, or $20x10^5$ cells/cm^2, supplemented with either N-acetylcysteine or catalase on day 13. These supplements did not improve the expansion, viability, or phenotype at any cell density **(Figure 4.14C-E)**. So, while cultures had low concentrations of cysteine on day 15, it is likely that low levels of a

different nutrient and/or accumulation of metabolites instead caused the limitations in expansion and FOXP3 expression at high densities.

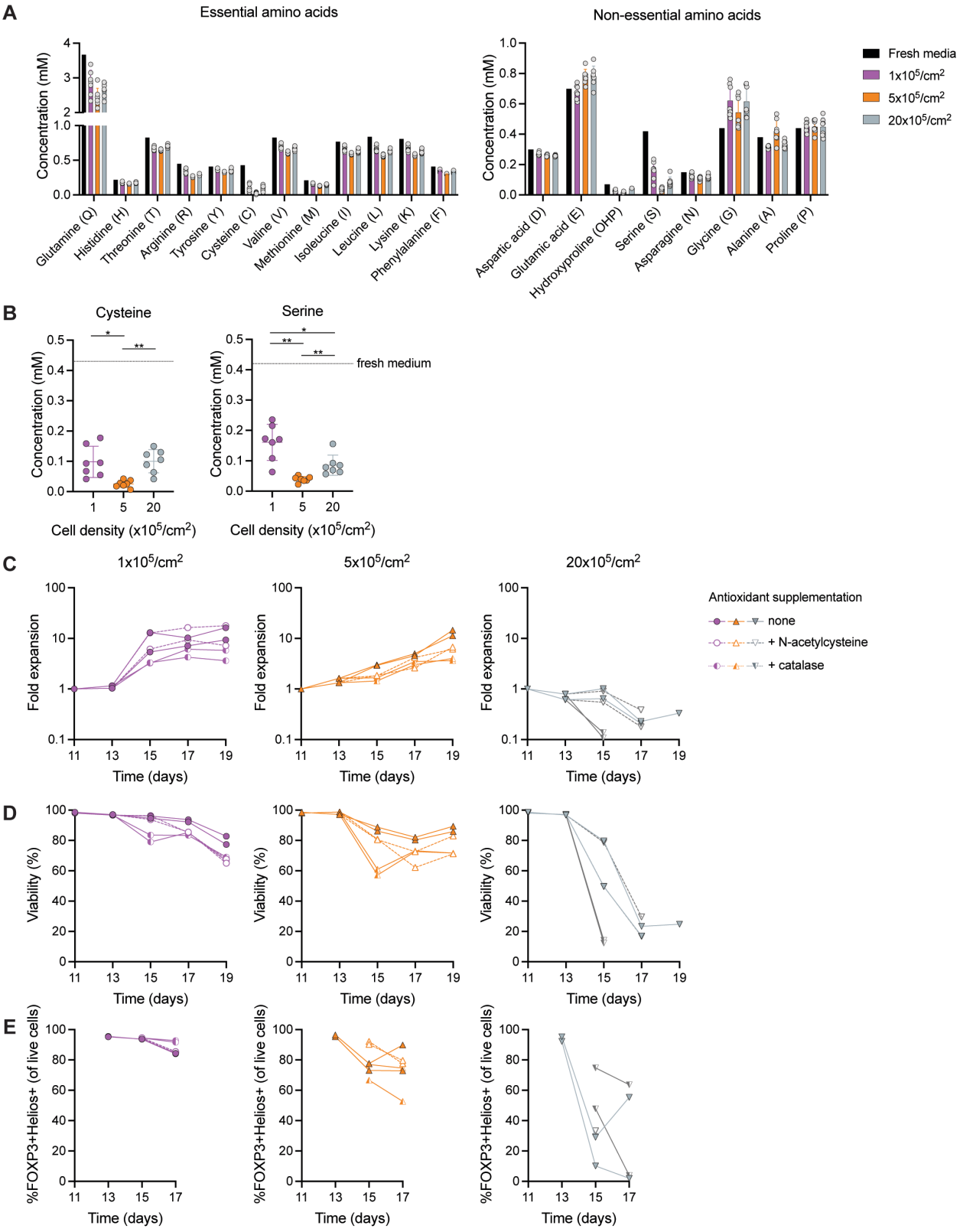

Figure 4.14: Supplementing antioxidants did not improve Treg expansion.

(A-B) Tregs were restimulated at cell densities of $1x10^5$ cells/cm^2, $5x10^5$ cells/cm^2, or $20x10^5$ cells/cm^2 (n=7 donors from 4 experiments). Amino acid concentrations were measured in samples of culture medium taken before feeding on day 15. **(C-E)** Tregs were restimulated at cell densities of $1x10^5$ cells/cm^2, $5x10^5$ cells/cm^2, or $20x10^5$ cells/cm^2. N-acetylcysteine or catalase was added to some conditions on day 13 and supplemented with each feed (n=2 donors from 1 experiment). **(C)** Fold expansion, calculated from cell counts. **(D)** Viability, measured by acridine orange and propidium iodide staining. **(E)** Expression of FOXP3 and Helios. **(A-B)** Individual points are shown with bars or lines representing Mean ± SD. **(C-E)** depict induvial donors. **(B)** Significance was determined by repeated measures two-way ANOVA with Tukey's multiple comparisons test.

4.3 Discussion

Stimulated by donor-to-donor and experiment-to-experiment variability in our previously published thymic Treg expansion protocol [3], we undertook a detailed analysis of process parameters that could underlie this observation. Unexpectedly, we found that adjusting cell density had significant effects on Treg expansion, viability, and phenotype. Restimulation at a low cell density ($1x10^5$ cells/cm^2) initially resulted in high rates of expansion, but viability in these cultures declined as or shortly after they reached their maximum expansion. Restimulation at densities > $5x10^5$ cells/cm^2 also resulted in low viability and limited expansion. In contrast, although cultures restimulated at $5x10^5$ cells/cm^2 had lower growth rates and reached their maximum expansion later than those at low cell densities, they maintained higher viability and FOXP3 expression upon reaching that maximum. Furthermore, their expansion could be improved by adjusting the feeding schedule. These data show that inconsistency in cell density, which is typically not reported in published Treg expansion protocols, could cause donor-to-donor variation and negatively affect the quality of Treg products.

The role of density in T cell biology is an emerging area of research. For example, it was recently shown that density affects mouse $CD8^+$ T cell expansion [278]. At low cell densities, activated $CD8^+$ T cells expressed CD80 and CD86, and interacted with CD28 on neighbouring T cells, resulting in enhanced IL-2 production and expansion. However, as cell density increased,

so did CTLA-4 expression, providing negative feedback to limit IL-2 production and expansion, and promote apoptosis [278]. We also found significant density dependent effects on expression of inhibitory molecules, such as LAP, CTLA-4 and PD-1. In contrast to higher inhibitory molecule expression, cells cultured at $20x10^5$ cells/cm^2 had decreased expression of CD71 and did not increase in cell size after restimulation. CD71, the transferrin receptor, is involved in iron uptake and its expression correlates with T cell proliferation [279, 280]. Furthermore, treating T cells with an anti-CD71 mAb or an iron chelator to block iron uptake has been shown to inhibit proliferation through cell cycle arrest [281, 282]. Thus, although addition of blocking antibodies to PD-1 or CTLA-4, or TGFβ inhibitors, did not significantly affect expansion, there could nevertheless be a role for density-induced activity of negative feedback pathways that limit Treg activation.

In studying the impact of expanding Tregs at higher densities, we found that the feeding strategy affected expansion, viability, and FOXP3 expression. For cells restimulated at $5x10^5$ cells/cm^2, removing the feed on day 13 resulted in relatively low glucose (<10 mM) and high lactate (>20 mM) concentrations at day 15 and reduced co-expression of FOXP3 and Helios. These limitations could be overcome if the cells received an extra feed on day 14. Recent studies have shown that mouse Tregs can survive in environments with low glucose and high lactate concentrations, such as tumor microenvironments [283], and even utilize lactic acid as a carbon source [284]. Thus, it is possible that the observed low concentrations of glucose and high concentrations of lactate may simply be an indicator of another medium limitation from a limiting nutrient, accumulation of an inhibitory metabolite, or pH change. Evidence that this limitation could be overcome by adjusting the feeding schedule points to the importance of

rigorously testing the feeding schedule to optimize cell expansion when operating at higher cell densities.

While low nutrient levels likely contributed to decreased viability and FOXP3 expression in cultures expanded at densities $\geq 5x10^5$ cells/cm^2, it is unlikely they caused the decreased viability observed at the end of expansion for cultures at $1x10^5$ cells/cm^2. Viability consistently fell in these low cell density cultures despite high availability of nutrients. We considered the possibility that prolonged exposure to the hyperoxic conditions of typical cell culture could increase mitochondrial oxidative stress [285], leading to DNA damage or lipid membrane damage, causing the observed cell death. Another possibility was that continuous stimulation and/or hypoxia could lead to T cell exhaustion or cell death, as has been shown for mouse Tregs or $CD8^+$ T cells, and could be mitigated by treating cells with antioxidants [286-288]. In testing the effect of oxygen concentration directly, we found little difference in viability for cultures restimulated under normoxic or low oxygen conditions. Furthermore, we found that treating the low cell density cultures with N-acetylcysteine or catalase did not prevent cell death. So overall, oxygen is unlikely to be a major factor driving the density-dependent effects.

We quantified Treg homogeneity on the basis of co-expression of FOXP3 and Helios, since $FOXP3^+Helios^+$ Tregs are more stable than $FOXP3^+Helios^-$ Tregs [24, 266]. Whereas FOXP3 expression varied over time and was affected by feeding strategy and density, Helios expression remained consistent throughout expansion. FOXP3 expression is known to vary with activation state, with recently activated or restimulated cells having higher FOXP3 expression than those in a resting state [3]. We found that FOXP3 expression decreased at day 15 for cells expanded at densities $\geq 5x10^5$ cells/cm^2, and that this effect was amplified if the cells were not fed on day 13. The fact that the decrease in FOXP3 expression could be mitigated if an

additional feed was added at day 14, suggests that these changes in FOXP3 could be related to nutrient limitations. Of note, these transient changes in FOXP3 expression in lineage-committed human Tregs may not result in large differences in cell phenotype or function as CRISPR-mediated deletion of FOXP3 in mature Tregs had minimal effects on Treg phenotype and function [289]. More substantial instability would be expected if Tregs lost both FOXP3 and Helios expression, but this was only observed when viability decreased at the end of expansion for low cell density cultures.

It is challenging to develop robust cell manufacturing processes with defined inputs. This work was performed using non-artificial antigen presenting cell-based activation and serum-free media, conditions which reduce the risk of introducing adventitious viral or prion agents and improve manufacturing control, but which also require additional optimization as process conditions developed in the presence of serum may not be directly transferrable. For example, it is common practice to maintain cells at low cell densities and concentrations to avoid medium limitations; however, we found that cultures maintained at these low densities did not maintain optimal viability or phenotype after reaching their maximum expansion. While this could potentially be overcome by harvesting cells at an earlier timepoint, the improved stability of cultures operated at $5x10^5$ cells/cm^2 would be preferred for manufacturing cells for clinical applications. Of note, adjusting the cell density also impacted several other variables, including cell concentration, medium height, oxygen concentration, nutrient and metabolite concentrations, pH, and cell-cell interactions.

This work highlights the importance of studying the impact of traditional bioprocess engineering variables such as cell density and feeding strategy on the yield and quality of Tregs when developing cell manufacturing protocols. The finding that Treg quantity and quality were

suboptimal at both low and high densities demonstrates the importance of controlling this parameter, particularly as protocols are scaled up and translated to new cell expansion platforms such as cell expansion bags or bioreactors to produce cells for clinical trials.

Chapter 5: Comparing platforms for large-scale thymic Treg manufacturing

5.1 Introduction

Large numbers of cells are required to treat patients with polyclonal Treg cell therapy products. Clinical trials to date have administered doses up to $100x10^6$ cells/kg [136], with doses in the range of $1\text{-}20x10^6$ cells/kg common in clinical trials [131, 133, 134, 136, 139, 143, 147, 151, 153, 173]. To reach these high cell doses, Treg cell manufacturing protocols such as those developed in Chapters 3 and 4 must be scaled-up.

Large-scale magnetic cell selection can be performed under GMP conditions with closed systems such as the CliniMACS (Miltenyi Biotech). This system has been used in several trials to isolate Tregs based on positive selection of $CD25^+$ cells with or without depletion of $CD8^+$ cells [131, 134, 136, 139, 141, 143-145, 153, 157, 184]. Alternatively, some trials have used fluorescence-activated cell sorting (FACS) to isolate Tregs [129, 140, 147, 150-152, 183, 186]. Flow sorting allows additional markers such as CD127, CD45RA or CD62L to be included to increase the purity of isolated Tregs or specifically isolate naïve Tregs [290]. Furthermore, precise gating allows for the isolation of $CD25^{high}$ cells rather than total $CD25^+$. However, flow sorting increases the complexity of the process and adds considerable processing time compared to magnetic isolation techniques [215, 291]. Additionally, there is a limited availability of GMP-compatible cell sorters and reagents.

Scaling up cell expansion protocols ideally also involves translating the process to closed cell expansion platforms to minimize the chances of microbial contamination. The standard tissue plates or flasks typically used in laboratory settings are open systems and require frequent medium changes by operators, so are not well suited to large-scale production under GMP conditions. As such, many T cell expansion protocols instead use platforms such as gas

permeable cell expansion bags, rocking motion bioreactors, or G-Rex flasks [215]. These systems have varied costs, availability of scale-down systems for process development, amount of handling required, potential for automation, and availability of online analytics. The most suitable cell expansion platform may differ depending on the cell type and scale of manufacturing.

Finally, scaling up cryopreservation protocols requires shifting from using Mr. Frosty or CoolCell freezing containers to rate controlled freezers. The Mr. Frosty and CoolCell freezing containers slow the rate of cooling of cryovials within closed containers in a -80°C freezer. Rate-controlled freezers such as the CryoMed (Thermo Fisher) or ViaFreeze (Cytiva) are stand-alone instruments that cool according to pre-set freezing rates to cryopreserve cells in cryovials or cryobags. These systems are more standardized than freezing containers and provide documentation of the temperature profile during freezing, making them better suited for use in GMP manufacturing.

We tested several platforms available for large-scale isolation, expansion, and cryopreservation of thymic Tregs. We compared isolating Tregs with our established two-step custom magnetic cell selection process using small-scale or large-scale magnets. We compared expanding Tregs using tissue culture flasks to gas permeable cell expansion bags, the WAVE rocking motion bioreactor, and the G-Rex flasks. Finally, we compared cryopreserving Tregs using a CoolCell freezing container to the CryoMed and ViaFreeze rate-controlled freezers.

5.2 Results

5.2.1 Isolating Tregs from an entire thymus

To isolate Tregs from an entire thymus, we first must process the full thymus to obtain a single cell suspension. We previously compared processing tissue using manual dissociation (scissors, razor blade or a tissue chopper) or with the gentleMACS dissociator with the goal of maximizing cell yield **(Figure 3.1)**. The yield and viability of thymocytes obtained by manual dissociation were higher than those obtained using the gentleMACS. However, when comparing techniques for large-scale processing, additional factors such as the processing time required, sterility, and whether the system is closed should also be considered. As such, we compared processing thymus tissue with the tissue chopper or gentleMACS to identify the platform that would be best suited for processing an entire thymus **(Figure 5.1A)**. We also tested using the gentleMACS with the recommended volume of 5 mL of medium to larger volumes of medium to reduce the amount of air in each tube during processing.

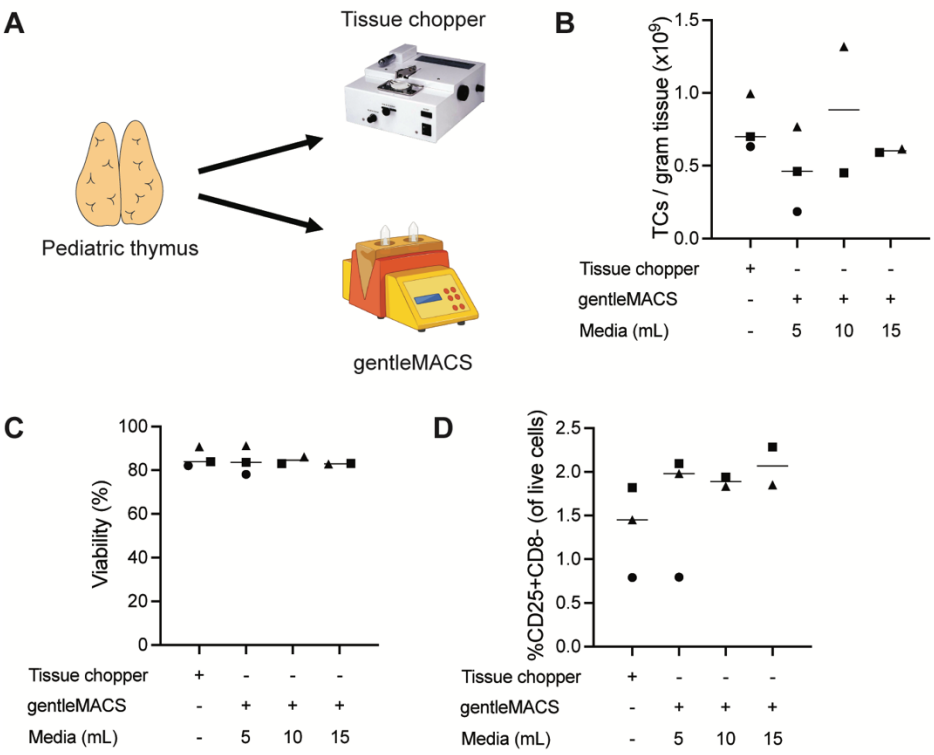

Figure 5.1: Comparison of thymus processing with tissue chopper or gentleMACS with varying media volumes.
(A-D) Pediatric thymuses were collected and processed within 24 hours into a single cell suspension using either a tissue chopper or the gentleMACS dissociator with 5 mL, 10 mL, or 15 mL of medium (n=2-3 donors). **(B)** Yield of thymocytes (TCs) per gram of tissue, **(C)** viability of isolated thymocytes, and **(D)** frequency of $CD25^{+}CD8^{-}$ thymocytes within total live thymocytes. Each symbol represents the mean of two replicates from an individual donor with bars showing the median. Each donor is represented with a different symbol.

We found that the yield of cells obtained using the gentleMACS with 5 mL of medium tended to be lower than that obtained using the tissue chopper **(Figure 5.1B)**. Filters tended to become clogged when filtering cell suspensions obtained from processing with the gentleMACS with 5 mL of medium, which hindered tissue processing and potentially reduced cell yields. This was less of an issue if 10 mL or 15 mL of medium was used. The viability of thymocytes obtained using the tissue chopper and gentleMACS was similar, regardless of the volume of medium used **(Figure 5.1C)**. The frequency of $CD25^{+}CD8^{-}$ thymocytes obtained using the gentleMACS was similar or higher than using the tissue chopper, and there was no difference among the different medium heights tested for the gentleMACS **(Figure 5.1D)**. We also

considered the time required for processing with each device. It took ~30 mins to process a single 3 g piece of tissue using the tissue chopper, whereas the same piece of tissue could be processed with two cycles on the gentleMACS in 2 mins. Scaling up to an entire thymus, ~4 hours of processing would be required to process an entire 25 g thymus using the tissue chopper, whereas the same tissue could be processed in ~1 hour with the gentleMACS. Overall, the closed nature and higher throughput of the gentleMACS made it better suited for processing an entire thymus.

We previously showed that Tregs can be isolated from the thymus by positive selection of $CD25^+$ cells and negative selection of $CD8^+$ cells **(Figure 3.1)**. We tested scaling-up this protocol, comparing isolation with a small-scale magnet capable of processing up to $8x10^8$ thymocytes (the scale typically used to isolate Tregs from a 3 g piece of tissue) and a large-scale magnet capable of processing up to $2x10^{10}$ thymocytes. The recovery, viability, and purity of Tregs isolated using the large-scale magnet were similar to those isolated using the small-scale magnet **(Figure 5.2A-D)**. This showed that Tregs can be isolated from an entire thymus using this custom magnetic cell selection protocol without sacrificing the purity of the final isolated product.

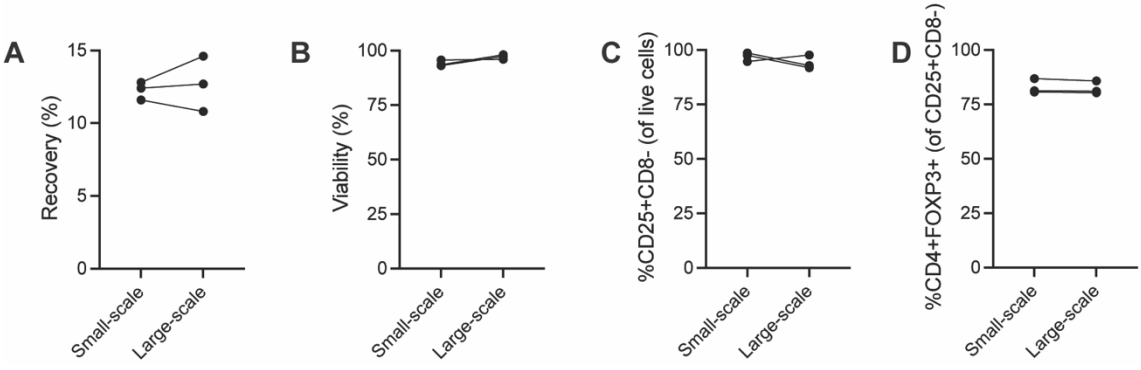

Figure 5.2: Isolation of thymic Tregs with either a small-scale or large-scale magnet.
(A-D) Pediatric thymuses were collected and processed within 24 hours into a single cell suspension, then $CD25^+CD8^-$ thymocytes were isolated by a two-step magnetic cell selection process consisting of positive selection

for CD25, then negative selection for CD8 (n=3 donors). **(A)** Recovery of Tregs, defined as the number of $CD25^+CD4^+CD8^-$ cells isolated relative to the number of $CD25^+CD4^+CD8^-$ cells within the starting population of thymocytes. **(B)** Viability, **(C)** purity, defined as $\%CD25^+CD8^-$, and **(D)** FOXP3 expression of isolated cells. Each point represents an individual donor and matched points are linked.

5.2.2 Comparing platforms for large-scale Treg expansion

Most Treg cell therapy products to date have been manufactured using tissue culture flasks or gas permeable cell expansion bags [139, 143, 145, 157, 184], with only one protocol reporting use of the G-Rex [141]. To determine the most suitable system for scale-up of our thymic Treg expansion protocol, we compared expansion using conventional tissue culture flasks, gas permeable cell expansion bags, the WAVE rocking motion bioreactor, and the G-Rex tissue culture flasks. We expanded cells from two donors in two separate experiments for this comparison using an expansion protocol in which cells were restimulated on day 7 and expanded for 14 days total. As large numbers of cells were required to compare these four systems in parallel, we first expanded Tregs for 7 days in tissue culture flasks. At day 7, we restimulated the cells and transferred them into the four different cell expansion platforms **(Figure 5.3A)**. Details of the cell handling in each platform, including the sampling and feeding steps are listed in **Table B.1** and **Table B.2**. The WAVE was operated with a low rocking rate and angle, on recommendation from the manufacturers.

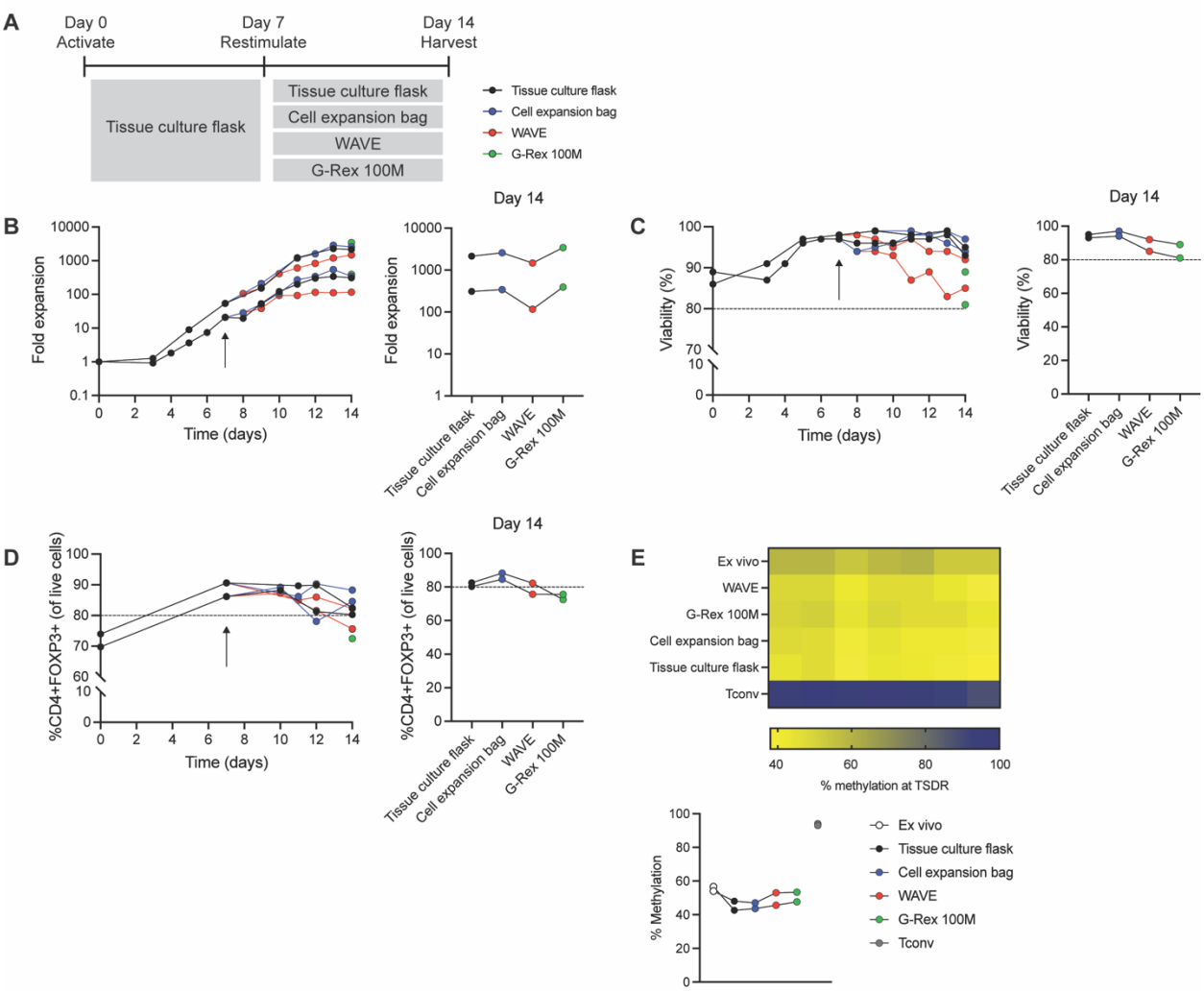

Figure 5.3: Expansion of thymic Tregs with large-scale expansion platforms.
(A-E) Thymic Tregs were expanded in tissue culture flasks for 7 days, then restimulated and expanded using the WAVE rocking motion bioreactor, G-Rex 100M tissue culture flask, gas permeable cell expansion bags, or conventional tissue culture flasks (n=2 donors from 2 experiments). **(B)** Fold expansion, calculated over the course of expansion or at day 14. **(C)** Viability and **(D)** FOXP3 expression over the course of expansion or at day 14. **(E)** Methylation of the TSDR for ex vivo or expanded cells on day 14 (both donors were female). Methylation of 7 CpGs is shown for a representative donor. Each point represents an individual donor and matched points are linked. Arrows indicate restimulation on day 7.

Tregs expanded in gas permeable cell expansion bags had similar expansion, viability, and FOXP3 expression to those expanded in conventional tissue culture flasks **(Figure 5.3B-D)**. Tregs expanded in the G-Rex had the highest level of expansion **(Figure 5.3B)** but lower viability and FOXP3 expression at day 14 than those expanded in the other devices **(Figure 5.3C-D)**. Finally, Tregs expanded in the WAVE had the lowest overall expansion, and had lower

viability and FOXP3 expression than those expanded in cell expansion bags **(Figure 5.3B-D)**. Tregs expanded in all devices maintained a demethylated TSDR **(Figure 5.3E)**.

We analyzed levels of glucose, lactate, and amino acids in samples of conditioned medium taken throughout the expansion to determine whether cells cultured in these different cell expansion systems were exposed to limiting levels of nutrients or waste products. The concentration of glucose remained high (>15 mM) in all systems for both donors tested **(Figure 5.4A)**. Lactate concentrations were ~20 mM on days 9 and 10 for one donor expanded in the WAVE, but were comparable to the levels in media from the cell expansion bag or tissue culture flask for the other donor. Based on literature that murine Tregs can withstand high lactate environments [283], these levels would not be expected to limit cell expansion. The concentration of most amino acids remained at levels similar to those in fresh medium throughout expansion **(Figure 5.5, Figure 5.6)**, with the exception of cysteine and serine that were low (<0.1 mM) on day 11 in media from tissue culture flasks but not in the cell expansion bag or WAVE **(Figure 5.5, Figure 5.6)**.

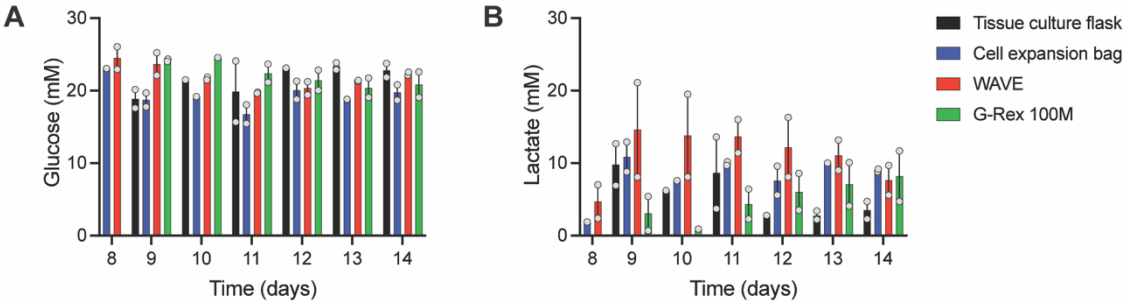

Figure 5.4: Analysis of conditioned medium from large-scale Treg expansions.
(A-B) Thymic Tregs were expanded in tissue culture flasks for 7 days, then restimulated and expanded using the WAVE rocking motion bioreactor, G-Rex 100M tissue culture flask, gas permeable cell expansion bags, or conventional tissue culture flasks (n=1-2 donors from 2 experiments). Concentration of **(A)** glucose and **(B)** lactate in samples of medium taken on the indicated days of expansion. Each point represents an individual donor with bars representing the mean ± range.

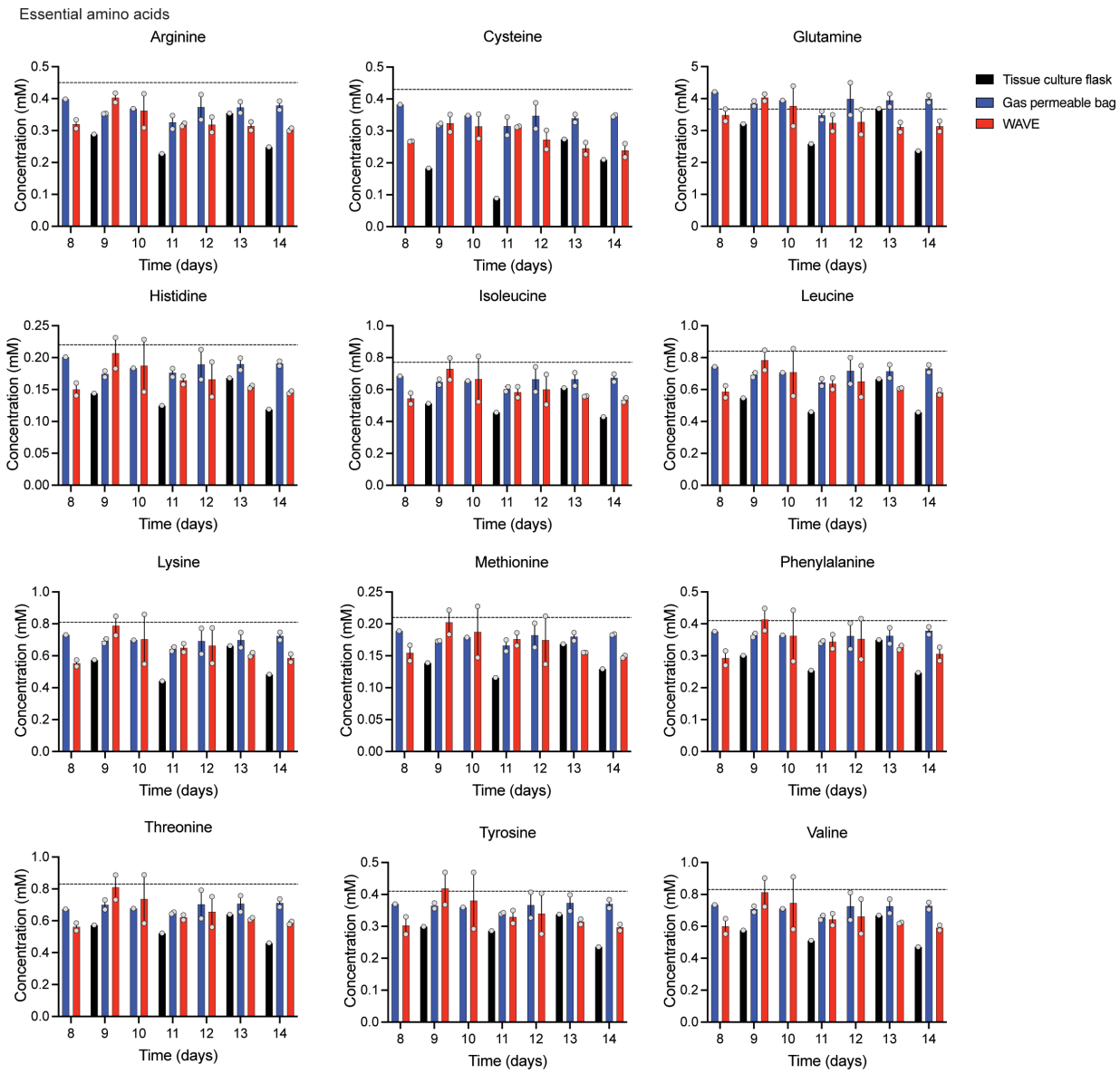

Figure 5.5: Concentration of essential amino acids in conditioned medium from large-scale Treg expansions. Thymic Tregs were expanded in tissue culture flasks for 7 days, then restimulated and expanded using the WAVE rocking motion bioreactor, G-Rex 100M tissue culture flask, gas permeable cell expansion bags, or conventional tissue culture flasks (n=1-2 donors from 2 experiments). Concentration of essential amino acids in samples of medium taken on the indicated days of expansion. Each point represents an individual donor with bars representing the mean ± range. The dashed lines indicate the concentration of each amino acid measured in fresh medium.

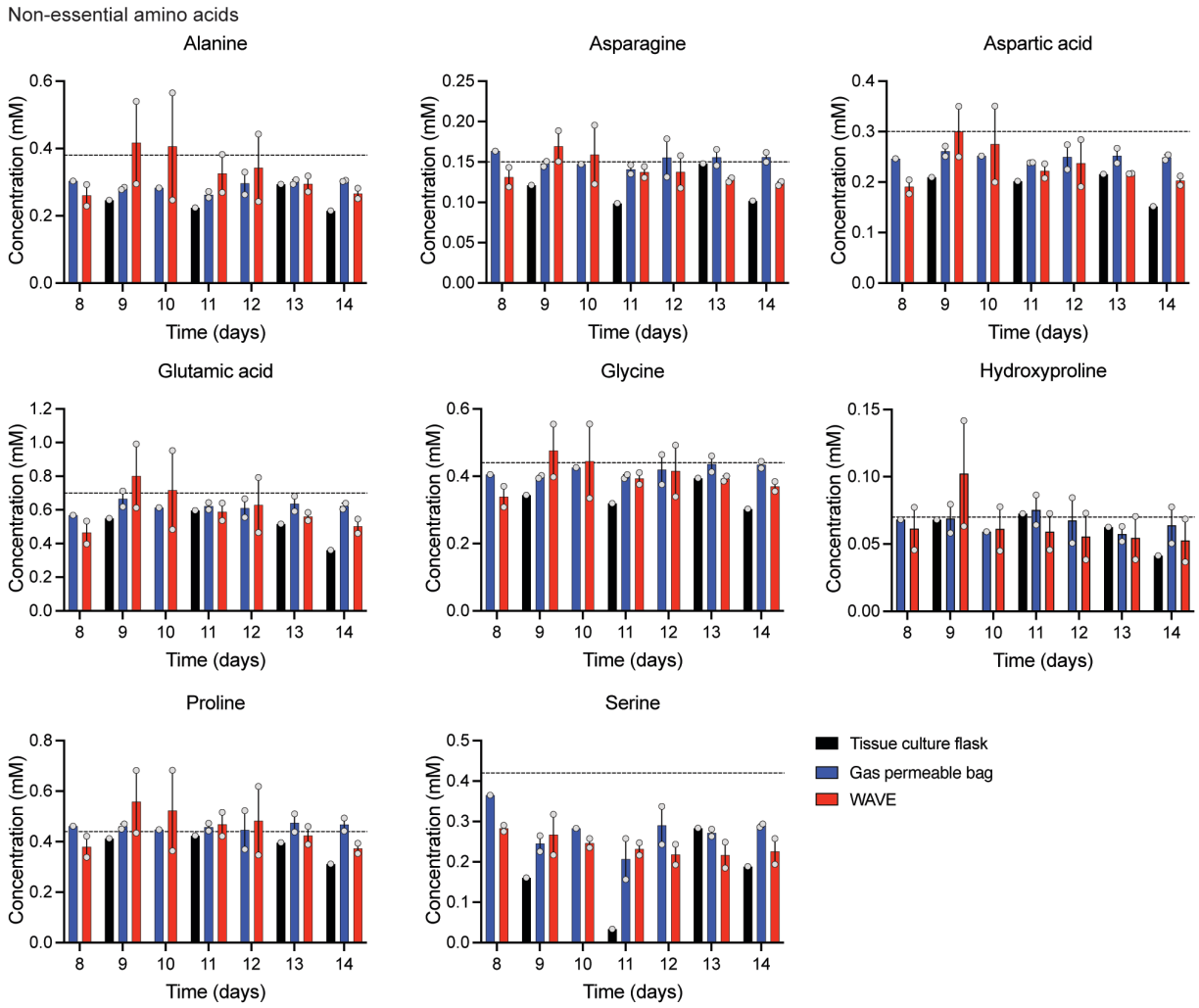

Figure 5.6: Amino acid concentrations in conditioned medium from large-scale Treg expansions. Thymic Tregs were expanded in tissue culture flasks for 7 days, then restimulated and expanded using the WAVE rocking motion bioreactor, G-Rex 100M tissue culture flask, gas permeable cell expansion bags, or conventional tissue culture flasks (n=1-2 donors from 2 experiments). Concentration of non-essential amino acids in samples of medium taken on the indicated days of expansion. Each point represents an individual donor with bars representing the mean ± range. The dashed lines indicate the concentration of each amino acid measured in fresh medium.

In summary, gas permeable cell expansion bags were determined to be the most appropriate for large-scale thymic Treg expansion **(Figure 5.3)**. The expansion, viability, and purity of expanded Tregs were similar or higher for those expanded in gas permeable cell expansion bags than those expanded using the WAVE or G-Rex, and analysis of conditioned medium showed that the cells likely did not encounter medium limitations during expansion. The similarity between the expansion characteristics of cells expanded in gas permeable cell

expansion bags and tissue culture flasks suggests that the process development work done in small-scale conventional tissue culture should translate to expansion in bags.

5.2.3 Cryopreserving Tregs using rate-controlled freezers

Finally, we compared cryopreserving Tregs in alternative rate-controlled freezers. The cryopreservation work in Chapter 3 was all performed using Mr. Frosty freezing containers, so we determined whether similar recovery, viability, and purity could be obtained if Tregs were cryopreserved with the rate-controlled freezers. We compared cryopreserving expanded Tregs at three different cell concentrations 2 days following restimulation in a CryoMed, ViaFreeze, and CoolCell freezing container (that controls the rate of cooling of cryovials placed into a -80°C freezer similar to a Mr. Frosty but does not require isopropanol). The ViaFreeze was tested with and without controlled nucleation. The cell number, viability, and purity of the cell product was assessed directly after thaw or after overnight culture with IL-2.

The recovery ranged from ~60-100% for the cell concentrations and freezers tested. The recovery was similar for cells cryopreserved with the CoolCell freezing container and CryoMed, with decreasing recovery for cells cryopreserved at higher cell concentrations **(Figure 5.7A)**. For cells cryopreserved with the ViaFreeze, the recovery was higher for cells cryopreserved at $10x10^6$ cells/mL than lower cell concentrations. The viability at thaw was similar for cells cryopreserved with all platforms when measured using an automated cell counter or apoptosis assay **(Figure 5.7B-C)**. The frequency of cells expressing FOXP3 and Helios at thaw ranged from ~70-80% for all cell concentrations and freezers tested, with higher co-expression of FOXP3 and Helios at higher cell concentrations for most freezers **(Figure 5.7D)**. Cells cryopreserved with all platforms expanded ~2-3 fold overnight **(Figure 5.7E)**, consistent with

previous observations for cells cryopreserved 2 days following restimulation **(Figure 3.8)**. The viability was similar for cells cryopreserved with all platforms after overnight culture **(Figure 5.7F-G)** and ~70-80% of cells expressed FOXP3 and Helios **(Figure 5.7H)**. Overall, Tregs cryopreserved 2 days following restimulation with the CryoMed or ViaFreeze (with or without controlled nucleation) had high viability and co-expression of FOXP3 and Helios after thaw, similar to those cryopreserved with a CoolCell freezing container and observations from previous experiments.

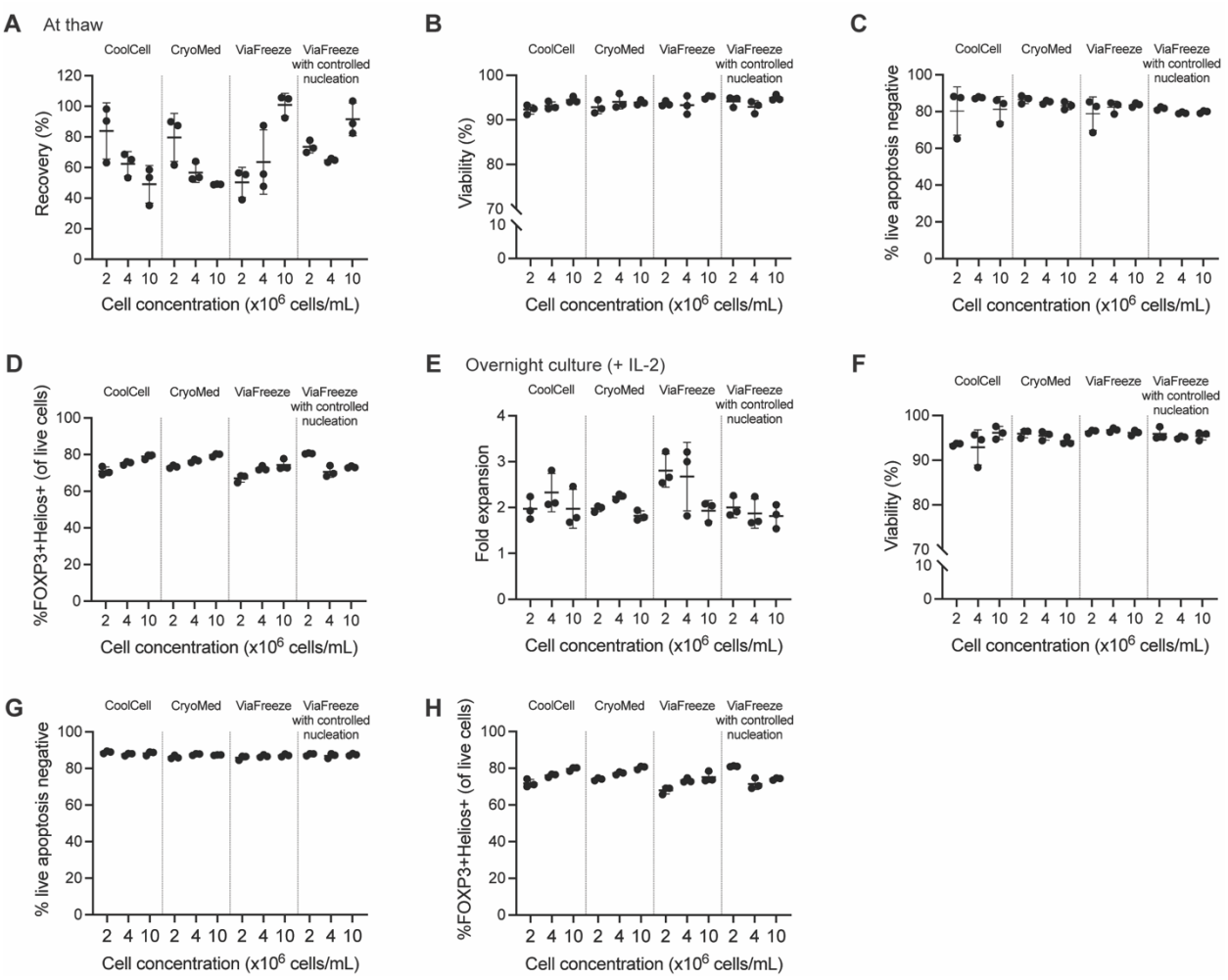

Figure 5.7: Cryopreservation of expanded Tregs using rate-controlled freezers.
(**A-H)** Thymic Tregs were expanded for 9 days, restimulated, then cryopreserved on day 11 at the indicated cell concentrations using a CoolCell freezing container, CryoMed rate-controlled freezer, or ViaFreeze rate-controlled freezer. Tregs were cryopreserved with the ViaFreeze rate-controlled freezer with or without controlled nucleation

(n=1 donor from 1 experiment). **(A)** Recovery, **(B)** viability measured by acridine orange/propidium iodide, **(C)** viability measured by apoptosis assay, and **(D)** expression of FOXP3 and Helios of Tregs at thaw. **(E)** Fold expansion, **(F)** viability measured by acridine orange/propidium iodide, **(G)** viability measured by apoptosis assay, and **(H)** expression of FOXP3 and Helios after thaw and overnight culture with IL-2. Each dot represents a replicate vial with lines showing the mean ± SD.

5.2.4 Estimate of Treg cell yield from large-scale manufacturing

Based on these experiments and data from small-scale process development, we calculated the number of Tregs that could be produced from an entire thymus. These numbers and the data that was used to perform these calculations are listed in **Table 5.1**. These calculations are based on fold expansion values from small-scale expansions in tissue culture flasks following a 13-day expansion protocol in which cells are restimulated on day 11 as following the large-scale experiments in **Figure 5.3**, we decided to delay restimulation until day 11 and harvest cells 2 days later based on the results of the experiments in **Figures 3.9-3.14**. These calculations include the recovery during isolation but do not include parameters such as cell loss during washing and bead removal steps as these steps have yet to be performed at the large-scale with closed bioprocessing instruments.

Table 5.1: Theoretical yield of Tregs from large-scale manufacturing.

	Median (range, n)
Age at time of sample collection (months)	6 (0.2-168, n=84)
Thymus mass (g)	25.2 (5.2-64.2, n=84)
Thymocytes per gram thymus tissue (x10^9 cells/g)	1.14 (0.22-3.11, n=75)
%$CD25^+CD8^-$ of live thymocytes	1.84% (0.50-5.48%, n=72)
Theoretical # of $CD25^+CD8^-$ Tregs per thymus (x10^6 cells)*	560 (43-1890, n=72)
Recovery (# of $CD25^+CD8^-$ cells isolated / # of $CD25^+CD8^-$ cells in thymus) (%)**	9.5% (7.6-10.5%, n=3)
Theoretical number of Tregs isolated (x10^6 cells)***	53
Fold expansion	140 (62-470, n=24)
Number of Tregs expanded (x10^9 cells)	7.5

*For each thymus, the theoretical # of Tregs was calculated as (thymus mass) × (thymocytes/g tissue) × (%$CD25^+CD8^-$)

**Recovery of Tregs in isolations using the large-scale magnet in Figure 5.2

***Calculated as (median theoretical # of Tregs per thymus) × (median recovery)

5.3 Discussion

Here we assessed platforms for large-scale isolation, expansion, and cryopreservation of thymic Tregs. The gentleMACS was better suited to processing an entire thymus than the tissue chopper. The recovery, viability, and purity of Tregs were similar between isolations performed with a small-scale or large-scale magnet. Tregs expanded in gas permeable cell expansion bags had higher viability and FOXP3 expression than those expanded in the WAVE or G-Rex. Finally, the recovery and quality of thawed cells were similar between those cryopreserved with rate-controlled freezers or freezing containers with which previous process development was performed.

We previously showed that mechanical chopping of thymus tissue resulted in a higher yield of thymocytes and higher viability than processing thymus tissue with the gentleMACS [3]. However, mechanical chopping using an instrument such as the tissue chopper is not well suited

for processing an entire thymus. The tissue chopper is an open system and only capable of processing a single 3 g piece of tissue at a time. The razor blade must be changed between tissue pieces as it dulls over the course of processing and it is difficult to change razor blades in a sterile manner. The gentleMACS is a closed system, reducing the potential for contamination during tissue processing. It uses single-use tubes with the rotor built into the lid of the tube, so a separate rotor is used for each tissue piece. Processing multiple pieces of tissue would be much faster with the gentleMACS since a single instrument can process 2-8 pieces of tissue at a time with ~1-2 minute cycles. Therefore, while processing tissue with the tissue chopper yields higher numbers of viable cells, the gentleMACS is better suited for processing a whole thymus.

In scaling up the isolation protocol, we tested multiple systems and configurations of magnet for magnetic cell selection. The first platform tested to scale up this protocol used a different configuration than the small-scale magnets – unlike small-scale magnets which vertically surround a tube, the bag was laid across a horizontal magnet in the large-scale system. The purity with this system was lower than parallel isolations with small scale-magnets (data not shown), so the large-scale system was adjusted to use vertical magnets surrounding a flask, resulting in comparable purities between the small- and large-scale systems.

The fold expansion, viability, and phenotype of expanded Tregs were similar in gas permeable cell expansion bags and tissue culture flasks. Tregs expanded in the WAVE rocking motion bioreactor had lower levels of expansion, and those expanded in the G-Rex had lower viability and FOXP3 expression. The availability of oxygen and nutrients may have differed between these large-scale culture platforms and conventional tissue culture. For oxygen, conventional tissue culture is normally limited by the solubility and diffusion of oxygen through the medium to reach cells. In the gas permeable bags and G-Rex, gas exchange occurred through

the sides of the bag or bottom of the flask, reducing the distance required for oxygen to diffuse to reach cells. In the WAVE, rocking likely reduced oxygen gradients through enhanced mixing. The G-Rex had greater availability of nutrients than conventional tissue culture given the increased medium volume; however, cells were handled every 1-2 days in the other platforms, so glucose and amino acids remained at high levels throughout the expansion in all systems.

It would be advantageous to translate the expansion to an automated expansion system in the future to reduce the amount of handling required and/or ease the handling of large culture volumes. However, translating the process to a system such as a rocking motion bioreactor requires further process development to determine the best feeding schedule, target cell concentrations, rocking speed and angle, sampling required, etc., and it is difficult to optimize these process parameters without a scale-down option available for process development. In contrast, gas permeable cell expansion bags are available in a variety of sizes and the similarity in expansion of cells in gas permeable bags and conventional tissue culture suggests that previous work done in conventional tissue culture may translate well to this system.

We tested different rate-controlled freezers to assess how the quality of cells after thaw would compare between these systems and freezing containers such as the CoolCell or Mr. Frosty with which previous cryopreservation testing was performed. Freezing containers such as the Mr. Frosty or CoolCell use isopropanol or polyethylate foam to reduce the rate of cooling in a -80°C freezer, but these systems are not well controlled and are subject to temperature variations in the freezer. Rate controlled freezers offer more control over the cryopreservation process and the ability to design programs where the cooling rate, target temperatures, and nucleation can be tailored for individual cell types. For this testing, we used default programs for the CryoMed and ViaFreeze, so further testing could be performed to tailor a freezing profile for

expanded thymic Tregs. As we move to large-scale manufacturing, cryopreservation protocols will also have to be adapted for cryopreserving cells in cryobags rather than cryovials. Cells in a cryobag will experience a different temperature profile than those in vials during cryopreservation given the larger volume and difference in surface area to volume ratio.

Based on data from small-scale process development, we estimate that ~$7.5x10^9$ Tregs can be produced from a single thymus. This would yield ~1 dose of $100x10^6$ Tregs/kg, the highest dose that has been tested in clinical trials to date, or ~3 doses of $30x10^6$ Tregs/kg for 70 kg patients. If the recovery of Tregs during isolation or fold expansion can be improved (such as by extending the expansion protocol based on the results from Chapter 4), then many doses could potentially be produced from a single thymus.

In conclusion, we tested platforms for large-scale isolation, expansion, and cryopreservation of thymic Tregs. We identified systems that are appropriate for scaling up our previously established protocols, a crucial step to translate these protocols to a GMP setting in order to perform engineering runs required for a clinical trial application.

Chapter 6: Tracking Tregs *in vivo* using ^{19}F-perfluorocarbon cell labelling and MRI

6.1 Introduction

Preclinical models suggest that adoptively transferred Tregs must be able to migrate to both lymph nodes and to the site of the graft or inflammation for Treg cell therapies to be effective [217, 219]. However, little is known about the migration patterns of Tregs in humans following infusion. To date, specific monitoring of infused Treg in clinical trials has been limited to analyzing cells in peripheral blood by unique HLA type using flow cytometry [134, 136] or deuterium labelling using mass spectrometry [140, 150, 151, 154]. These analyses offer a rough idea of the persistence of infused Tregs in the blood, but provide no information about migration to or persistence in tissues.

Many groups are developing methods to non-invasively monitor cells *in vivo* using imaging methods such as MRI, CT, or nuclear imaging methods including PET and SPECT (reviewed by [245, 246]). These methods utilize either direct cell labelling approaches where cells are labelled with contrast agents (e.g. iron oxide, gadolinium, [^{19}F]-fluorine) during manufacturing, or indirect cell labelling approaches where cells are genetically modified to express reporter genes that allow them to be imaged after administration of an appropriate labels or contrast agents [245]. While indirect cell labelling offers advantages for long-term cell tracking as the reporter gene will be passed on as cells divide and repeat imaging can be performed by re-administering contrast agents, direct cell labelling may be better suited for cell manufacturing settings that do not already include genetic engineering, as adding a genetic engineering step adds considerable regulatory burden and risk.

One such direct cell labelling method is to label cells with a ^{19}F perfluorocarbon (PFC) nanoemulsion. A perfluorocarbon has a similar structure to hydrocarbons, with all hydrogen atoms replaced with fluorine atoms. Cell Sense (CS-1000) is a ^{19}F-PFC nanoemulsion that has been approved by the US Food and Drug Administration (FDA) for use in clinical trials, with one trial completed where it was used to label autologous DCs in a vaccine trial in colorectal cancer [292], and another underway in which it is being used to monitor persistence of adipose-derived stem cells during breast reconstruction (NCT02035085). When cells are cultured with this ^{19}F-PFC, they can take it up by endocytosis and sequester it into vesicles within the cytoplasm. Carbon-fluorine bonds are very strong and cannot be easily broken by cells, rendering the PFC essentially chemically inert [293]. The ^{19}F-PFC can be detected using ^{19}F MRI with minimal interference as there is almost no endogenous ^{19}F present in the human body [294].

Cell Sense is potentially well-suited for monitoring polyclonal Tregs in an early phase clinical trial as it has a favourable safety profile, has a drug master file on record with both the FDA and Health Canada, and can be incorporated into established expansion protocols as it does not require genetic modification. Other studies have shown that human immune cells including PBMCs, DCs, NK cells, or CAR T cells can be labelled with Cell Sense during expansion with minimal impact on cell viability, phenotype, or function [292, 295-298], and that these cells can be detected in immunocompromised mice [295, 297-299]. As such, we tested labelling thymic Tregs with ^{19}F-PFC and tracking their migration in immunocompromised mice. We also investigated the effect of ^{19}F-PFC labelling during expansion on the viability, phenotype, and function of Tregs both before and after cryopreservation.

6.2 Results

6.2.1 Tregs can be efficiently labelled with ^{19}F-PFC

We first tested whether expanded Tregs could be labelled with ^{19}F-PFC. Previously expanded and cryopreserved thymic Tregs were thawed and cultured overnight with ^{19}F-PFC **(Figure 6.1A)**. After labelling overnight, cells were harvested, washed, and either prepared for injection into mice or analyzed directly. We labelled some cells with a red fluorescent version of the ^{19}F-PFC to analyze the extent of cell labelling and found that nearly 100% of cells were labelled with the ^{19}F-PFC **(Figure 6.1B)**. The extent of cell labelling was analyzed in more detail by NMR. The average ^{19}F-labelling of thymic Tregs was similar or higher than that of human T cells or human PBMCs reported by other studies using the same ^{19}F-PFC nanoemulsion [297, 299, 300] **(Figure 6.1C)**.

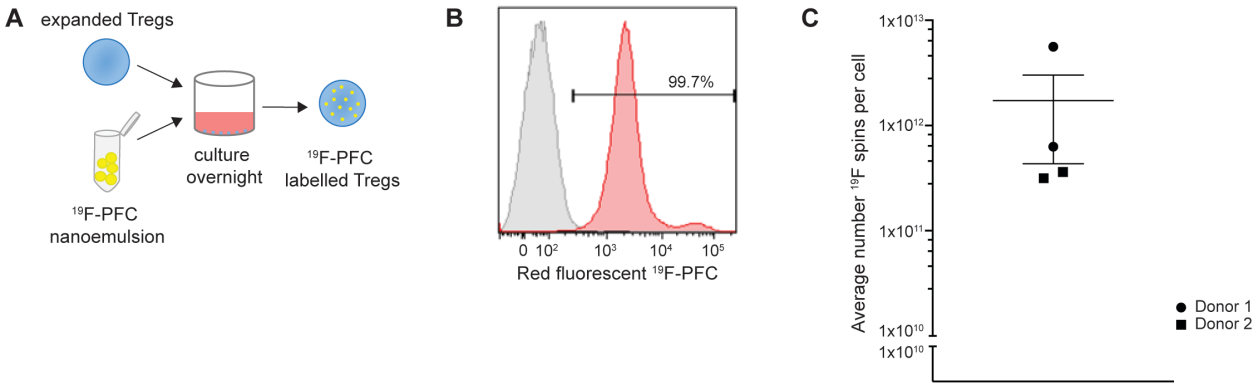

Figure 6.1: Tregs can be efficiently labelled with ^{19}F-PFC.
(A-C) Expanded thymic Tregs were thawed and cultured overnight with a ^{19}F-PFC labelling agent (n=2 donors from 2 experiments). **(A)** Schematic of protocol to label cells. **(B)** Tregs were labelled overnight with a red fluorescent version of the ^{19}F-PFC labelling agent and analyzed by flow cytometry. The percent of cells labelled with the ^{19}F-PFC (red) compared to an unlabelled control (grey). A flow plot is shown for a representative donor. **(C)** ^{19}F-PFC labelling was quantified by NMR.

6.2.2 Infused Tregs accumulate in lymph nodes and spleen

^{19}F-PFC labelled Tregs were intravenously injected into immunocompromised mice through the tail vein and mice were imaged using 3T ^{1}H/^{19}F MRI 1, 2, or 4 days following cell injection

(Figure 6.2A). ^{19}F-PFC labelled Tregs were detected in lymph nodes and the spleen of these mice **(Figure 6.2B)**. Tregs could still be detected 2 days and 4 days following cell infusion; however, the total number of cells detected decreased over time. While $8.52x10^5$ cells were detected on day 1, only $1.05x10^5$ cells were detected on day 4 **(Figure 6.2C)**. The decrease in ^{19}F signal could be due to cell proliferation (since the ^{19}F-PFC is divided between cells as they divide), dispersion of cells throughout the body (since a minimum threshold number of cells is required to detect a signal), or cell death. Of note, the $8.52x10^5$ cells detected on day 1 is still < 10% of the total number of cells injected into these mice. This indicates that many of the infused cells were dispersed throughout the body, proliferating, or had died already by day 1.

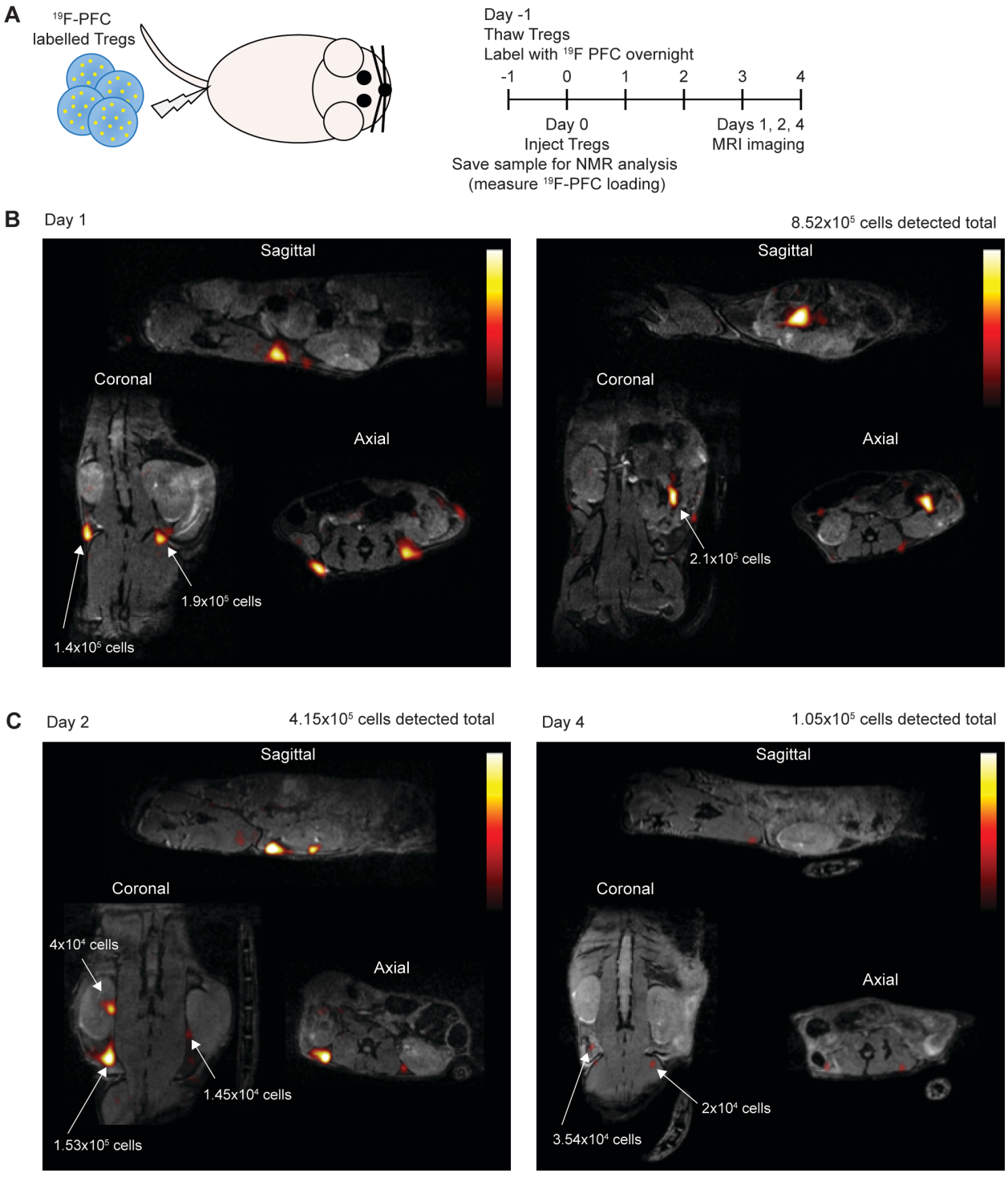

Figure 6.2: Tregs accumulate in lymph nodes and spleen of immunocompromised mice.
(A-C) $10x10^6$ ^{19}F-PFC labelled Tregs were injected intravenously with $10x10^6$ PBMCs into the tail vein of immunocompromised mice. 3T ^{1}H/^{19}F MRI images were taken 1, 2, and 4 days following cell injection. Tregs were quantified in comparison to reference tubes based on the number of ^{19}F spins/cell measured by NMR. Representative images are shown for 1 of 6 mice injected. **(A)** Schematic and timeline for cell labelling, injection, and MRI imaging. **(B-C)** ^{1}H/^{19}F MRI images from a single mouse taken **(B)** 1, **(C)** 2 or 4 days following cell injection.

Sagittal, coronal, and axial views are shown. Tregs were quantified in a few locations as shown and the total number of cells detected is indicated.

In summary, we found that the thymic Tregs could be labelled with ^{19}F-PFC and detected *in vivo* using 3T ^{1}H/^{19}F MRI. Tregs could be detected up to 4 days following injection with decreasing total numbers of Tregs detected over time.

6.2.3 Testing ^{19}F-PFC labelling during expansion

Having shown that Tregs could be labelled with ^{19}F-PFC and detected in vivo using 3T ^{1}H/^{19}F MRI, we investigated how ^{19}F-PFC cell labelling could be incorporated into our established Treg manufacturing protocol. If ^{19}F-PFC was used in a clinical setting, it would be advantageous to label cells prior to cryopreservation to avoid the need for additional processing to label cells prior to infusion. We therefore tested labelling cells during the last day of expansion **(Figure 6.3A)**. There was no difference in the expansion of ^{19}F-PFC labelled or unlabelled cells calculated either as total fold expansion from day 0 **(Figure 6.3B)** or fold expansion between days 11-13 **(Figure 6.3C)**. However, the ^{19}F-PFC labelled cultures had lower viability **(Figure 6.3D-E)** and an increased percentage of cells in late stages of apoptosis **(Figure 6.3E)**. There was also a decrease in the percentage of FOXP3^{+}Helios^{+} cells and the expression of Treg phenotypic markers after ^{19}F-PFC labelling **(Figure 6.3F-G)**.

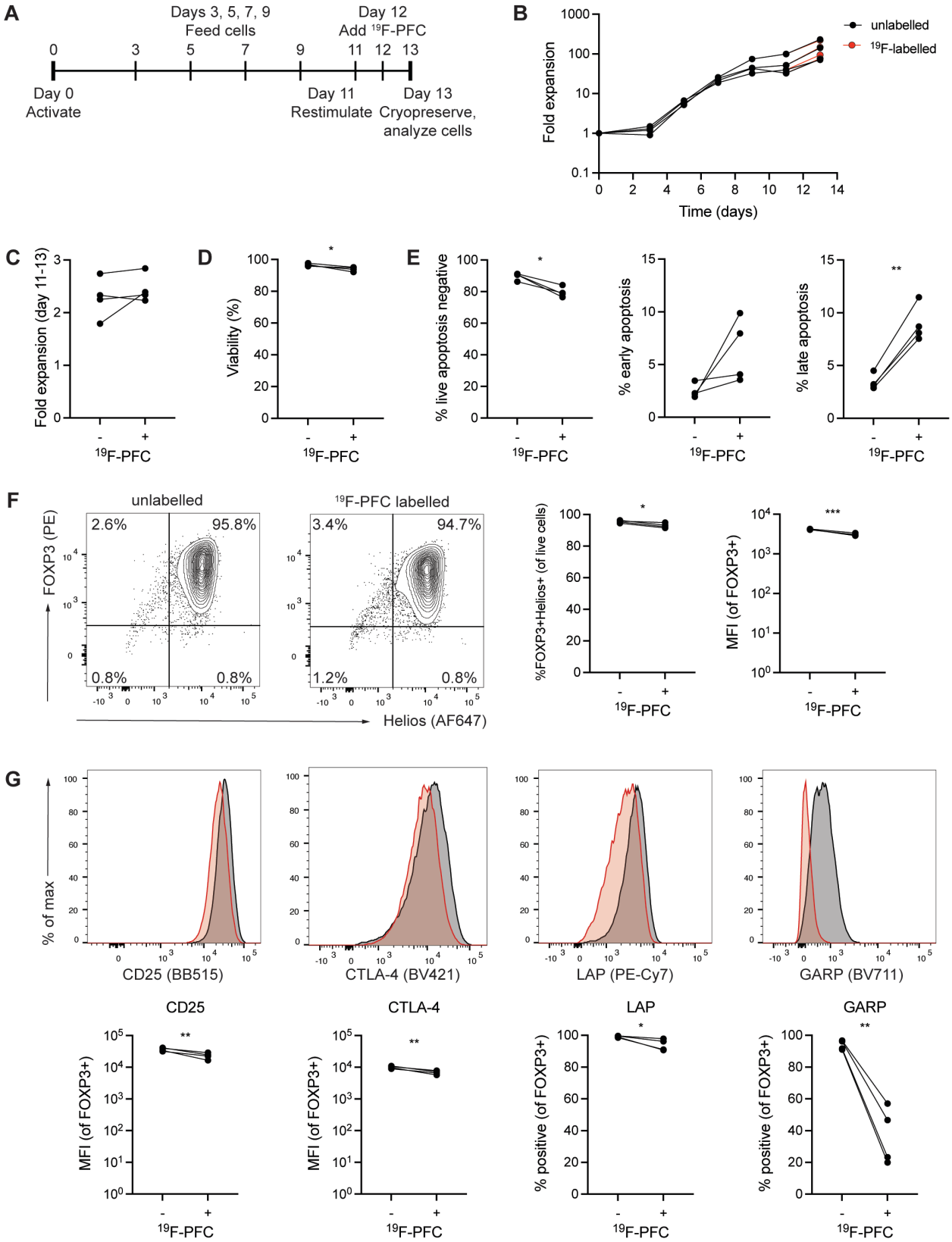
A
Days 3, 5, 7, 9
Feed cells
Day 12
Add 19F-PFC
0
3
5
7
9
11
12
13
Day 0
Activate
Day 11
Restimulate
Day 13
Cryopreserve,
analyze cells
B
Fold expansion
Time (days)
unlabelled
19F-labelled
C
Fold expansion (day 11-13)
19F-PFC
D
Viability (%)
19F-PFC
E
% live apoptosis negative
% early apoptosis
% late apoptosis
19F-PFC
F
unlabelled
19F-PFC labelled
FOXP3 (PE)
Helios (AF647)
2.6%
95.8%
0.8%
0.8%
3.4%
94.7%
1.2%
0.8%
%FOXP3+Helios+ (of live cells)
MFI (of FOXP3+)
19F-PFC
G
% of max
CD25 (BB515)
CTLA-4 (BV421)
LAP (PE-Cy7)
GARP (BV711)
CD25
CTLA-4
LAP
GARP
MFI (of FOXP3+)
% positive (of FOXP3+)
19F-PFC

Figure 6.3: ^{19}F-PFC labelling during expansion induced apoptosis, reduced expression of Treg phenotypic markers.
(A-G) Thymic Tregs were labelled with ^{19}F-PFC during expansion (n=4 donors from 2 experiments). **(A)** Timeline of thymic Treg expansion. On day 11, Tregs were split into two parallel cultures and restimulated. 5mg/mL ^{19}F-PFC was added to one of these cultures on day 12 to label cells. **(B-C)** Fold expansion of unlabelled or ^{19}F-PFC labelled cells **(B)** over the course of culture or **(C)** between day 11-13. **(D)** Viability of unlabelled or ^{19}F-PFC labelled cells, measured by acridine orange/propidium iodide. **(E)** Percentage of live non-apoptotic, early apoptotic (Apopxin Green^{+}, 7AAD^{-}), or late apoptotic cells (Apopxin Green^{+}, 7AAD^{+}), determined using an apoptosis assay. **(F)** Frequency of FOXP3^{+}Helios^{+} cells and FOXP3 MFI for unlabelled (black) or ^{19}F-PFC labelled cells (red). **(G)** Expression of CD25, CTLA-4, LAP, and GARP. **(B-D)** Each symbol represents an individual subject and data points from the same subject are linked. **(E-G)** Each symbol represents the mean of 3 technical replicates from an individual subject; data points from the same subject are linked. **(D-G)** Significance was determined by paired t test.

We also compared cytokine production by and suppressive function of the ^{19}F-PFC labelled or unlabelled Tregs. ^{19}F-PFC labelled and unlabelled Tregs maintained low expression of inflammatory cytokines including IL-2, IFNγ, IL-17A, and IL-4 **(Figure 6.4A)**. They also expressed low levels of IL-10, as has been observed previously for thymic Tregs [3, 77, 158]. Both ^{19}F-PFC and unlabelled Tregs suppressed the proliferation of CD8 and CD4 T cell responders within PBMCs; however, the unlabelled cells were more suppressive than the ^{19}F-PFC labelled cells **(Figure 6.4B)**.

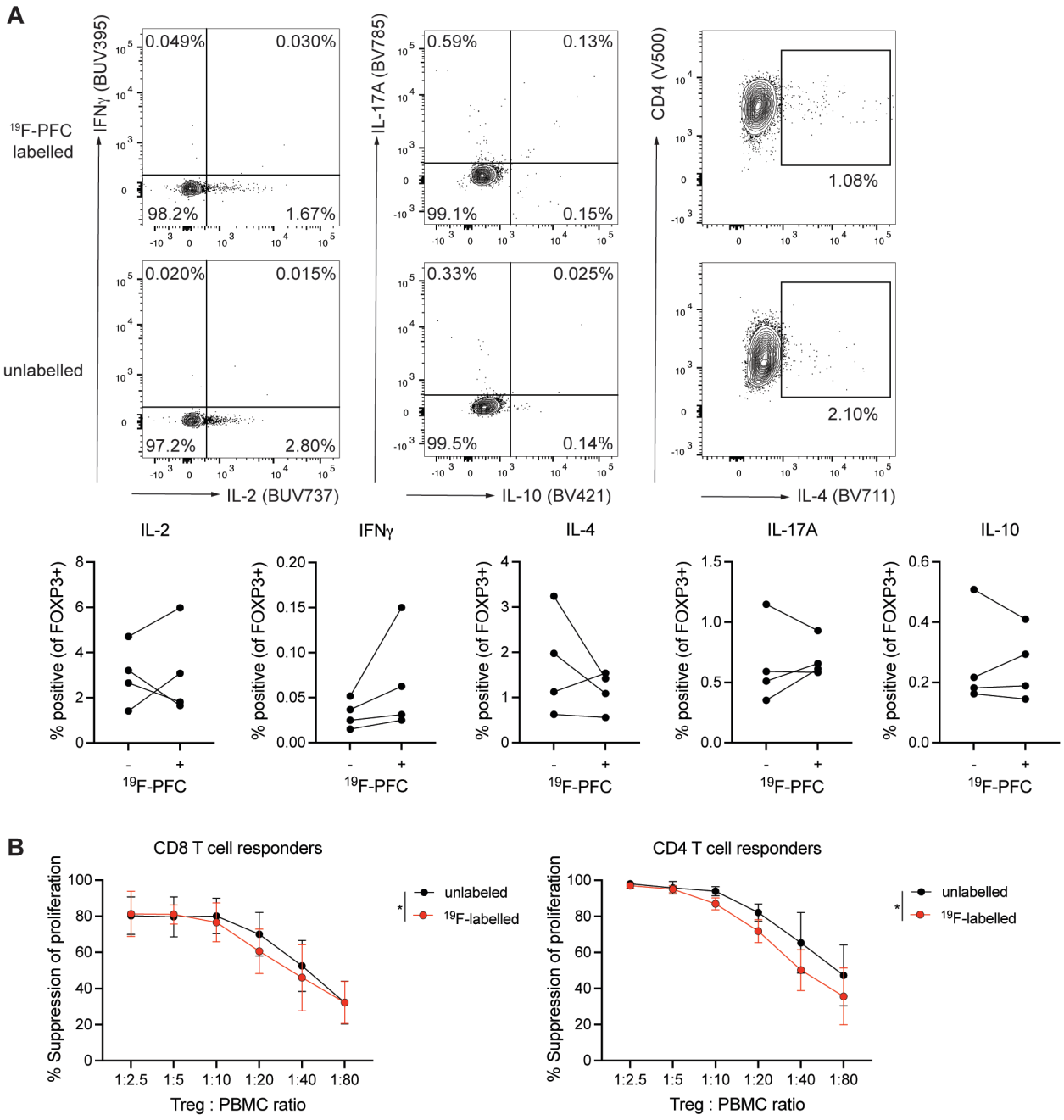

Figure 6.4: Function of Tregs labelled with ^{19}F-PFC during expansion.
(A-B) Thymic Tregs were labelled with ^{19}F-PFC during expansion (n=4 donors from 2 experiments). **(A)** Expression of cytokines by unlabelled or ^{19}F-PFC labelled cells after 4 hours of stimulation with PMA, ionomycin, and brefeldin A. **(B)** Expanded Tregs were co-cultured with CPD-labelled PBMC at the indicated ratios and stimulated 1:16 beads to cells with anti-CD3/CD28 beads for 4 days. Suppression of $CD8^+$ T cells or $CD4^+$ T cells within PBMC was determined by division index. **(A)** Each symbol represents the mean of 3 technical replicates from an individual subject; data points from the same subject are linked. **(B)** Mean ± SD are shown. Significance was determined by paired t test comparing the areas under the curve for labelled or unlabelled cells.

Overall, labelling Tregs with ^{19}F-PFC during expansion caused a decrease in viability, expression of Treg phenotypic markers, and suppressive function compared to unlabelled cells.

6.2.4 Recovery and viability of ^{19}F-PFC labelled Tregs after cryopreservation

Finally, we cryopreserved ^{19}F-PFC labelled and unlabelled Tregs and analyzed their recovery, viability, phenotype, and function at thaw. ^{19}F-PFC labelled Tregs had lower recovery and viability **(Figure 6.5A-B)** and an increased number of cells undergoing apoptosis **(Figure 6.5B)** at thaw compared to unlabelled Tregs. The percentage of FOXP3^{+}Helios^{+} cells at thaw was also lower for ^{19}F-PFC labelled Tregs than unlabelled Tregs **(Figure 6.5C)**. After these cells were cultured overnight, the viability of ^{19}F-PFC labelled Tregs remained lower than unlabelled cells **(Figure 6.5D-E)**; however, there was no difference in the co-expression of FOXP3 and Helios or suppressive function **(Figure 6.5F-G)**.

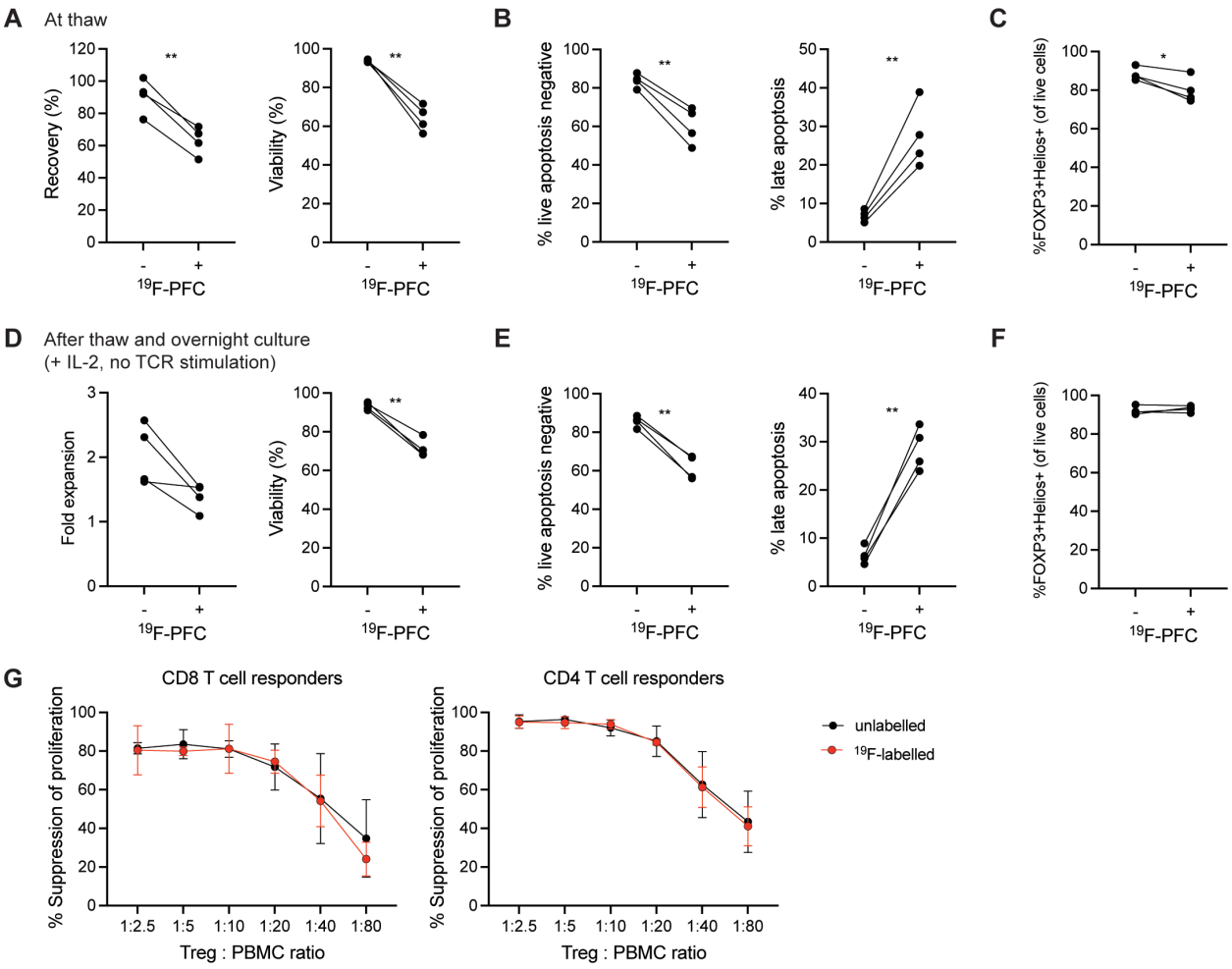

Figure 6.5: Recovery, viability, and phenotype of Tregs labelled with ^{19}F-PFC prior to cryopreservation. **(A-G)** Thymic Tregs were labelled with ^{19}F-PFC during expansion and cryopreserved after harvest on day 13 (n=4 donors from 2 experiments). **(A)** Recovery (defined as the number of live apoptosis negative cells thawed relative to the number of live cells cryopreserved) and viability (measured by acridine orange/propidium iodide) for unlabelled or ^{19}F-PFC labelled cells at thaw. **(B)** Percentage of live non-apoptotic, early apoptotic (Apopxin Green$^+$, 7AAD$^-$), or late apoptotic cells (Apopxin Green$^+$, 7AAD$^+$), determined using an apoptosis assay. **(C)** Expression of FOXP3 and Helios for unlabelled or ^{19}F-PFC labelled cells at thaw. **(D)** Fold expansion and viability (measured by acridine orange/propidium iodide) for unlabelled or ^{19}F-PFC labelled cells after thawing and overnight culture with IL-2. **(E)** Percentage of live non-apoptotic, early apoptotic, or late apoptotic cells after thaw and overnight culture, determined using an apoptosis assay. **(F)** Expression of FOXP3 and Helios for unlabelled or ^{19}F-PFC labelled cells after thaw and overnight culture. **(G)** Expanded Tregs were co-cultured with CPD-labelled PBMC at the indicated ratios and stimulated 1:16 beads to cells with anti-CD3/CD28 beads for 4 days. Suppression of CD8$^+$ T cells or CD4$^+$ T cells within PBMC was determined by division index. **(A-F)** Each symbol represents the mean of 3 technical replicates of cryopreserved cells from an individual subject; data points from the same subject are linked. **(G)** Mean ± SD are shown. Significance was determined by paired t test.

6.3 Discussion

In this study, we observed migration of ^{19}F-PFC labelled Tregs to the spleen and lymph nodes of immunocompromised mice. We could detect cells for up to 4 days following infusion; however, by day 4 the signal had already considerably decreased compared to the signal on day 1 of imaging. The deterioration of signal over time is a disadvantage of direct cell labelling methods such as ^{19}F-PFC labelling [245, 246]. The ^{19}F-PFC label is diluted as cells divide and the signal diminishes if the cells disperse throughout the body, so it is hard to know whether the loss of signal is due to cell proliferation, cell dispersion, or cell death. Given that the cells used in this study had been cryopreserved 2 days following restimulation, so were still in the log phase of growth, the cells may have continued to proliferate after infusion even without additional stimulation by antigen. There was no specific site of antigen for Tregs to accumulate in these mice, so the cells may have been dispersed throughout the body. Furthermore, there was no IL-2 present beyond that produced by the co-transferred PBMCs, so long-term Treg survival may have also been impaired. In summary, cell proliferation, cell dispersion, and cell death may all have contributed to the loss of signal in this study.

To apply ^{19}F-PFC labelling in a clinical setting, it would be optimal to incorporate the labelling step into the expansion process. As such, we tested adding the ^{19}F-PFC nanoemulsion during the last day of expansion, prior to cryopreservation. While labelling did not impact Treg expansion, ^{19}F-PFC labelled Tregs had lower viability, lower expression of FOXP3 and other Treg phenotypic markers, and lower suppressive capacity than unlabelled Tregs. We found that the reduced viability was amplified after cryopreservation, with ^{19}F-PFC labelled Tregs having lower viability both immediately after thaw and after overnight culture with IL-2. This is in contrast to other studies with human immune cells which showed that cell viability, phenotype,

and function was not altered by ^{19}F-PFC labelling [292, 295-298]. We have previously shown that Tregs are sensitive to stresses encountered during cell manufacturing with variables such as the timing of cryopreservation [3] and cell density at restimulation having critical effects on the quality of the final Treg cell product. It is possible that Tregs were more sensitive to this labelling than other cell types. Further work should be done to test different concentrations of ^{19}F-PFC or labelling times to determine whether this cell labelling process can be improved for Tregs.

In summary, cell labelling with ^{19}F-PFC has the potential to be used to non-invasively track Tregs in vivo using ^{19}F MRI. However, labelling Tregs with 5 mg/mL during the last day of expansion resulted in reduced viability and FOXP3 expression, so further optimization is required to determine how to best incorporate cell labelling into established manufacturing protocols. Developing methods to non-invasively monitor cells after infusion will allow us to determine their migration patterns and survival after infusion. This knowledge will aid in understanding how migration patterns correlate with clinical outcomes, and help in designing next generation Treg cell therapies in which cells or expansion conditions can be modified to enable proper migration or enhance cell survival [1, 2].

Chapter 7: Conclusion

7.1 Summary

Treg cell therapy holds great promise as a treatment to induce tolerance in transplantation and autoimmunity, but producing large numbers of high quality Tregs without the use of serum or cell-based activation reagents still poses a significant challenge. This research developed methods to produce thymic Tregs for clinical applications, investigating the impact of process parameters on the yield and quality of the final Treg cell product.

Previous work demonstrated that the thymus is an abundant source of naïve Tregs that better maintain their purity during expansion than blood Tregs isolated based on CD25 expression [158]. We showed that Tregs can be isolated with high purity using magnetic selection even when processing a full thymus. Furthermore, the Tregs isolated from the thymus are naïve Tregs, which are a more homogeneous population of Tregs than total $CD4^{+}CD25^{hi}CD127^{lo}$ isolated from the peripheral blood and have greater stability during *in vitro* expansion [186, 256]. A drawback to working with naïve Tregs isolated from peripheral blood is that a limited number can be isolated from a buffy coat or blood donation. The increased yields of thymic Tregs compared to naïve blood Tregs enable larger doses to be produced in cell manufacturing or enhance this type of process development work by allowing many conditions to be tested in parallel using cells from the same donor.

We identified non-cell-based activation reagents and serum-free media that enabled high levels of expansion while preserving FOXP3 expression and suppressive function. Transitioning to using these defined inputs required Treg-specific optimization of many aspects of the expansion protocol including restimulation timing, cell density, and feeding schedule. Through this, we identified Treg-specific responses to process parameters such as that variability in

viability and expansion for expansion > 2 weeks were correlated with the cell density at restimulation. In this case, simply restimulating Tregs at low densities ($1x10^5$ cells/cm^2) to avoid medium limitations was not optimal. These cells decreased in viability after reaching their maximal expansion whereas those restimulated at $5x10^5$ cells/cm^2 sustained higher viability, although they required additional feeding to avoid medium limitations. This was a new finding, as cell density during expansion has been poorly reported in Treg cell therapy manufacturing protocols to date and the effect of changing cell density on viability or feeding requirements had not been directly tested previously. In comparing large-scale expansion platforms, we showed Tregs expanded in gas permeable bags had higher viability and FOXP3 expression than those expanded in the WAVE or G-Rex, suggesting that Tregs behave differently than Tconv in suspension cultures, which are commonly used in CAR T cell manufacturing, again highlighting the need for Treg-specific process development. Through this process optimization, we also characterized Treg expansion kinetics over multiple stimulations and how attributes such as the expression of phenotypic markers changed over time.

Cryopreservation has been challenging to incorporate into Treg manufacturing protocols. While one centre has used cryopreserved products in their clinical trials [143, 145], many groups have reported that cryopreservation impairs Treg phenotype and function and one group actually switched from using cryopreserved to fresh cells during the clinical trial as they observed impaired suppressive function from cryopreserved cells [138]. We found that the timing of cryopreservation was a critical process parameter, and that only cells cryopreserved 2-3 days following restimulation maintained high viability and FOXP3 expression after thaw. This finding was surprising, as the effect of timing of restimulation on T cell survival had not previously been

shown, but will be critical in enabling the manufacturing of "off-the-shelf" Treg cell therapy products.

Finally, we investigated ^{19}F-PFC cell labelling and ^{19}F/^{1}H MRI as a method to track Tregs *in vivo*. Biodistribution and persistence of infused Tregs are still relatively unknown, but are important questions when putting together clinical trial applications and trying to understand how characteristics of the infused product correlate with clinical outcomes. Tregs could be labelled with ^{19}F-PFC and detected in the spleen and lymph nodes *in vivo*. However, the persistence of infused Tregs was limited and ^{19}F-PFC-labelled Tregs had impaired viability. This method will require further investigation including testing various concentrations of cell label and using more relevant models to determine whether there is utility in incorporating ^{19}F-PFC cell labelling in future clinical trials.

7.2 Limitations

In Chapters 3 and 5, we showed that Tregs can be isolated from the thymus using magnetic selection with high purity using both small-scale and large-scale magnets. However, the recovery of isolated Tregs was only ~10% at both scales. This recovery is sufficient to produce enough a therapeutic dose of Tregs, but is a major limitation as we think about scaling up these protocols with the goal of producing many doses per thymus.

In Chapter 4, we observed that Tregs cultured at low cell densities ($1x10^5$ cells/cm^2) consistently had low viability after 3 weeks of expansion. While the reduced expansion and FOXP3 expression for higher density cultures could be attributed to exposure to medium limitations, we were unable to explain the low viability observed at the end of expansion for the low cell density conditions. This was specific to Tregs, as Tconv cultured at the same density

maintained viability > 80% at the same time point in these experiments (data not shown). Furthermore, it was difficult to isolate the impact of individual process parameters in these experiments. Results from varying cell density were often confounded by other parameters such as cell concentration, medium height, oxygen concentration, nutrient and metabolite concentrations, and pH that varied with changing cell density.

When comparing expansion platforms in Chapter 5, Tregs were expanded for 7 days in T-flasks before splitting them into the different platforms at restimulation. This was necessary given the large minimum volumes of the WAVE and the G-Rex flask used; however, a question remains as to whether Tregs can be activated in these platforms on day 0, or whether initial activation in a T-flask is necessary for proper expansion. Initial expansion in T-flasks would likely be necessary with the WAVE, given the minimum volume requirement, and the G-Rex, as we have previously observed minimal expansion if Tregs are activated in the G-Rex on day 0 (unpublished data).

In comparing cryopreservation platforms, we observed that the quality of cells cryopreserved using freezing containers, the CryoMed, and the ViaFreeze were similar after thaw, but these experiments were conducted cryopreserving cells at low cell concentrations in cryovials. Further optimization will be required to ensure that high quality cells can also be obtained when cells are cryopreserved at higher concentrations in cryobags, as will be necessary to allow for delivery of large number of cells in clinical trials.

In Chapter 6, we investigated ^{19}F-PFC cell labelling and ^{19}F/^{1}H MRI as a method to track Tregs *in vivo*. For these experiments, polyclonal Tregs were infused into immunocompromised mice in the absence of ongoing inflammation, so it is hard to know whether the short persistence is inherent to the cell therapy or due to the absence of supporting signals such as antigen and

cytokines. In terms of the effect of labelling on cell quality, we tested labelling with a ^{19}F-PFC dose that had been used in previous studies, so it is possible that better results could be obtained if the dose was optimized.

Finally, polyclonal Treg products such as the ones generated using these manufacturing protocols are heterogenous cell populations. The resulting cells have a variety of antigen specificities and may be heterogenous in their expression of phenotypic markers (including homing receptors) and other functional characteristics. We characterized how changing process parameters including activation reagents, media, restimulation timing, and cell density affects Treg phenotype and, in some cases, function *in vitro*. However, further investigation should be done as to how changing these process parameters affects cell diversity (including TCR diversity) or cell function *in vivo*.

7.3 Future directions

In Chapter 3, we investigated the effect of a number of process parameters on thymic Treg expansion but many questions remain. It is not clear that antibody-coated beads are the optimal system to expand Tregs. They are used in many manufacturing protocols as they produce robust T cell expansion, have a history of use in producing both Treg and other T cell products for clinical trials, and have drug master files on record with regulatory agencies. However, these rigid beads do not fully recapitulate the more fluid-like immune synapse formed between Tregs and APCs during activation. Novel activation reagents that present anti-CD3 and anti-CD28 on fluid membranes have been developed to capture the fluid-like nature of Treg-APC interactions without the complexity of a cell-based system [301, 302]. These should be investigated for their utility in expanding Tregs. We also observed differences in the expansion and phenotype of

Tregs depending on the cell culture medium used, likely due to differences in medium composition. It should be noted that all of the media tested have supraphysiologic levels of medium components such as glucose or amino acids. Recent findings such as reduced suppression by mouse Tregs cultured under high glucose conditions [284] indicate that the effect of medium composition or exposure to high nutrient levels on Treg function should be investigated in more detail.

In Chapter 4, we observed that Tregs expanded at $5x10^5$ cells/cm^2 maintain viability and FOXP3 expression until at least day 19. Further restimulation and cryopreservation studies similar to those performed in chapter 3 should be undertaken to determine the best time points to restimulate and cryopreserve these cells to finalize this extended expansion protocol for use in generating cells for therapy. Finally, these findings should be replicated with peripheral-blood derived Tregs as peripheral blood is the most common source for manufacturing cell therapy products. We expect that thymic Tregs would behave similarly to peripheral blood-derived Tregs in these manufacturing protocols, but have only performed limited testing to verify the findings regarding the effect of adjusting cell density with peripheral blood-derived Tregs.

In Chapter 5, we compared platforms for large-scale isolation, expansion, and cryopreservation of thymic Tregs. These experiments were the first step in scaling up the thymic Treg manufacturing protocols; however, significant work remains before these protocols can be performed at full-scale under GMP conditions. The expansion experiments were performed using a previous version of the protocol in which cells were restimulated on day 7, and cells were first expanded for 7 days in tissue culture flasks. Additional experiments must be performed in which Tregs are activated from day 0 in gas permeable cell expansion bags and expanded using the optimized protocol with restimulation on day 11 to verify that the results using this protocol in

tissue culture flasks can be translated to expansion with gas permeable bags. Furthermore, recommendations for minimum and maximum volumes for each bag size must be determined and protocols for processing steps such as media exchanges, cell concentration steps, and bead removal must be established. Finally, protocols to cryopreserve expanded Tregs must still be optimized. We identified that the timing of cryopreservation was a critical process parameter, but the effect of variables such as cell concentration, the volume of cells cryopreserved, and the temperature profile during cryopreservation must still be investigated. In comparing cryopreservation platforms, we observed that the quality of cells cryopreserved using freezing containers, the CryoMed, and the ViaFreeze were similar after thaw, but these experiments were conducted freezing cells at low cell concentrations in cryovials. Further optimization will be required to verify that high quality cells can be obtained using these rate-controlled freezers when cells are cryopreserved at higher concentrations in cryobags.

In Chapter 6, we investigated whether ^{19}F-PFC direct cell labelling could be incorporated into our manufacturing protocols. Future work should focus on optimizing Treg cell labeling with ^{19}F-PFC by testing different labelling times or PFC concentrations, or establishing methods for indirect cell labelling for products that will already include genetic modification. Once these are established, these methods should be used to track Treg migration in preclinical models of transplantation or autoimmunity to observe how modifications to manufacturing protocols influence cell migration and persistence, and how differences in migration and persistence influence outcomes in these models.

Another question is how the *in vivo* function of thymic Tregs produced using these optimized protocols compares to cells used in previous studies. Because Tregs must be cryopreserved shortly following restimulation, the resulting Treg cell product will be more

activated than those that have been used in other studies, where Tregs have been infused after coming back to a "resting" state. These cells must be tested in a preclinical model such as a model of xenoGVHD, in which PBMCs are injected into irradiated NOD/SCID IL-2Rγ^{null} (NSG) mice with or without Tregs. The injected PBMCs rapidly cause xenoGVHD, which should be delayed by co-injection of Tregs. Thymic Tregs generated with these optimized protocols should be tested in this model to ensure that their persistence or suppressive function is not impaired by infusion in a highly activated state.

Finally, there is a need to identify measures of Treg phenotype or function that correlate with clinical outcomes. For example, in CAR T cell therapy, groups are undertaking studies in which the transcriptome, phenotype, and function of the cell product are evaluated and linked to clinical outcomes to identify quality attributes that correlate with improved clinical outcomes. These studies have identified that *in vivo* expansion and persistence of infused cells are correlated with improved clinical outcomes, and that these appear to be linked to the differentiation status of the cells [243]. As further trials of Treg cell therapy are completed, particularly phase II trials with increased numbers of patients and more emphasis on measuring efficacy, similar mechanistic studies should be undertaken in parallel. Once these quality attributes are identified, manufacturing processes should be modified to favour these attributes.

7.4 Overall significance

The overall aim of this research was to develop methods to manufacture thymus-derived Tregs for use as a cell therapy product. In this work, we developed standardized methods to isolate naïve Tregs using magnetic selection of $CD25^{+}CD8^{-}$ cells, expand Tregs using non-cell-based activation reagents and serum-free media and cryopreserve cells shortly after restimulation to

preserve cell quality after thaw. In contrast to the protocols currently being used to generate cells for clinical trials, our protocols will allow large doses of cells to be produced without the use of serum or cell-based activation reagents, and with a single restimulation. The ability to effectively cryopreserve expanded cells will also allow them to be manufactured and stored for use as an "off-the-shelf" product.

We are now scaling-up these protocols to transfer them to the Alberta Cell Therapy Manufacturing facility to complete engineering runs required for a clinical trial application for thymic Treg cell therapy. In the proposed clinical trial, patients at high risk of chronic GVHD will receive infusion of thymic Tregs around 100 days after HSCT, when immunosuppressive drugs are being tapered and immune reconstitution has begun, to prevent the development of chronic GVHD. This will be the first clinical trial of Treg cell therapy using cells manufactured in Canada and the first clinical trial of thymic Treg cell therapy in adults. These optimized protocols can also be applied to blood Tregs and genetically modified Tregs in future trials. The work in Chapters 4 and 6 forms the foundation for the next stage of manufacturing protocols, in which the length of Treg expansion will be extended to generate many doses from a single thymus and direct cell labelling can be incorporated into the expansion to allow for monitoring of the infused cell product.

Addressing these bioprocessing challenges is critical to enabling large numbers of cells to be generated for use an "off-the-shelf" allogeneic therapy. Cell therapy with thymic Tregs has the potential to improve the safety of HSCT and solid organ transplantation by reducing the risk of GVHD or organ rejection, increasing their utility as treatments for hematological malignancies and late stage diseases.

Bibliography

1 **MacDonald, K. N., Piret, J. M. and Levings, M. K.,** Methods to manufacture regulatory T cells for cell therapy. *Clinical & Experimental Immunology* 2019. **197**: 52-63.

2 **Wardell, C. M., MacDonald, K. N., Levings, M. K. and Cook, L.,** Cross talk between human regulatory T cells and antigen presenting cells: Lessons for clinical applications. *European Journal of Immunology* 2020.

3 **MacDonald, K. N., Ivison, S., Hippen, K. L., Hoeppli, R. E., Hall, M., Zheng, G., Dijke, I. E., Aklabi, M. A., Freed, D. H., Rebeyka, I., Gandhi, S., West, L. J., Piret, J. M., Blazar, B. R. and Levings, M. K.,** Cryopreservation timing is a critical process parameter in a thymic regulatory T-cell therapy manufacturing protocol. *Cytotherapy* 2019. **21**: 1216-1233.

4 **Germain, R. N.,** T-cell development and the CD4–CD8 lineage decision. *Nature reviews immunology* 2002. **2**: 309.

5 **Neefjes, J., Jongsma, M. L., Paul, P. and Bakke, O.,** Towards a systems understanding of MHC class I and MHC class II antigen presentation. *Nature Reviews Immunology* 2011. **11**: 823.

6 **Li, M. O. and Rudensky, A. Y.,** T cell receptor signalling in the control of regulatory T cell differentiation and function. *Nature Reviews Immunology* 2016. **16**: 220.

7 **Bour-Jordan, H., Esensten, J. H., Martinez-Llordella, M., Penaranda, C., Stumpf, M. and Bluestone, J. A.,** Intrinsic and extrinsic control of peripheral T-cell tolerance by costimulatory molecules of the CD28/B7 family. *Immunological reviews* 2011. **241**: 180-205.

8 **Geginat, J., Paroni, M., Facciotti, F., Gruarin, P., Kastirr, I., Caprioli, F., Pagani, M. and Abrignani, S.,** The CD4-centered universe of human T cell subsets *Seminars in immunology*. Elsevier 2013, pp 252-262.

9 **Zhu, J.,** T Helper Cell Differentiation, Heterogeneity, and Plasticity. *Cold Spring Harb Perspect Biol* 2018. **10**.

10 **Wing, J. B., Tanaka, A. and Sakaguchi, S.,** Human FOXP3+ Regulatory T Cell Heterogeneity and Function in Autoimmunity and Cancer. *Immunity* 2019. **50**: 302-316.

11 **Caramalho, Í., Nunes-Cabaço, H., Foxall, R. B. and Sousa, A. E.,** Regulatory T-Cell Development in the Human Thymus. *Frontiers in Immunology* 2015. **6**.

12 **Sakaguchi, S., Yamaguchi, T., Nomura, T. and Ono, M.,** Regulatory T cells and immune tolerance. *Cell* 2008. **133**: 775-787.

13 **Cook, L., Stahl, M., Han, X., Nazli, A., MacDonald, K. N., Wong, M. Q., Tsai, K., Dizzell, S., Jacobson, K., Bressler, B., Kaushic, C., Vallance, B. A., Steiner, T. S. and Levings, M. K.,** Suppressive and Gut-Reparative Functions of Human Type 1 T Regulatory Cells. *Gastroenterology* 2019. **157**: 1584-1598.

14 **Roncarolo, M. G., Gregori, S., Bacchetta, R., Battaglia, M. and Gagliani, N.,** The Biology of T Regulatory Type 1 Cells and Their Therapeutic Application in Immune-Mediated Diseases. *Immunity* 2018. **49**: 1004-1019.

15 **Flippe, L., Bézie, S., Anegon, I. and Guillonneau, C.,** Future prospects for CD8(+) regulatory T cells in immune tolerance. *Immunol Rev* 2019. **292**: 209-224.

16 **Baron, U., Floess, S., Wieczorek, G., Baumann, K., Grützkau, A., Dong, J., Thiel, A., Boeld, T. J., Hoffmann, P. and Edinger, M.,** DNA demethylation in the human FOXP3 locus discriminates regulatory T cells from activated FOXP3+ conventional T cells. *European journal of immunology* 2007. **37**: 2378-2389.

17 **Floess, S., Freyer, J., Siewert, C., Baron, U., Olek, S., Polansky, J., Schlawe, K., Chang, H.-D., Bopp, T., Schmitt, E., Klein-Hessling, S., Serfling, E., Hamann, A. and Huehn, J.,** Epigenetic Control of the foxp3 Locus in Regulatory T Cells. *PLOS Biology* 2007. **5**: e38.

18 **Kim , H.-P. and Leonard , W. J.,** CREB/ATF-dependent T cell receptor–induced FoxP3 gene expression: a role for DNA methylation. *Journal of Experimental Medicine* 2007. **204**: 1543-1551.

19 **Williams, L. M. and Rudensky, A. Y.,** Maintenance of the Foxp3-dependent developmental program in mature regulatory T cells requires continued expression of Foxp3. *Nature Immunology* 2007. **8**: 277-284.

20 **Polansky, J. K., Kretschmer, K., Freyer, J., Floess, S., Garbe, A., Baron, U., Olek, S., Hamann, A., von Boehmer, H. and Huehn, J.,** DNA methylation controls Foxp3 gene expression. *European journal of immunology* 2008. **38**: 1654-1663.

21 **Lu, L., Barbi, J. and Pan, F.,** The regulation of immune tolerance by FOXP3. *Nature Reviews Immunology* 2017. **17**: 703-717.

22 **Seddiki , N., Santner-Nanan , B., Martinson , J., Zaunders , J., Sasson , S., Landay , A., Solomon , M., Selby , W., Alexander , S. I., Nanan , R., Kelleher , A. and de St. Groth , B. F.,** Expression of interleukin (IL)-2 and IL-7 receptors discriminates between human regulatory and activated T cells. *Journal of Experimental Medicine* 2006. **203**: 1693-1700.

23 **Dawson, N. A., Lamarche, C., Hoeppli, R. E., Bergqvist, P., Fung, V. C., McIver, E., Huang, Q., Gillies, J., Speck, M., Orban, P. C., Bush, J. W., Mojibian, M. and Levings, M. K.,** Systematic testing and specificity mapping of alloantigen-specific chimeric antigen receptors in regulatory T cells. *JCI Insight* 2019. **4**.

24 **Lam, A. J., Uday, P., Gillies, J. K. and Levings, M. K.,** Helios is a marker, not a driver, of human Treg stability. *Eur J Immunol* 2021.

25 **Lind, E. F., Prockop, S. E., Porritt, H. E. and Petrie, H. T.,** Mapping precursor movement through the postnatal thymus reveals specific microenvironments supporting defined stages of early lymphoid development. *The Journal of experimental medicine* 2001. **194**: 127-134.

26 **Spits, H.,** Development of αβ T cells in the human thymus. *Nature Reviews Immunology* 2002. **2**: 760-772.

27 **Radtke, F., Wilson, A., Stark, G., Bauer, M., van Meerwijk, J., MacDonald, H. R. and Aguet, M.,** Deficient T Cell Fate Specification in Mice with an Induced Inactivation of Notch1. *Immunity* 1999. **10**: 547-558.

28 **De Smedt, M., Reynvoet, K., Kerre, T., Taghon, T., Verhasselt, B., Vandekerckhove, B., Leclercq, G. and Plum, J.,** Active Form of Notch Imposes T Cell Fate in Human Progenitor Cells. *The Journal of Immunology* 2002. **169**: 3021-3029.

29 **Dik, W. A., Pike-Overzet, K., Weerkamp, F., de Ridder, D., de Haas, E. F. E., Baert, M. R. M., van der Spek, P., Koster, E. E. L., Reinders, M. J. T., van Dongen, J. J. M., Langerak, A. W. and Staal, F. J. T.,** New insights on human T cell development by

quantitative T cell receptor gene rearrangement studies and gene expression profiling. *The Journal of experimental medicine* 2005. **201**: 1715-1723.

30 **Staal, F. J., Weerkamp, F., Langerak, A. W., Hendriks, R. W. and Clevers, H. C.,** Transcriptional control of t lymphocyte differentiation. *Stem Cells* 2001. **19**: 165-179.

31 **Famili, F., Wiekmeijer, A.-S. and Staal, F. J.,** The development of T cells from stem cells in mice and humans. *Future science OA* 2017. **3**: FSO186-FSO186.

32 **Park, J.-E., Botting, R. A., Conde, C. D., Popescu, D.-M., Lavaert, M., Kunz, D. J., Goh, I., Stephenson, E., Ragazzini, R., Tuck, E., Wilbrey-Clark, A., Roberts, K., Kedlian, V. R., Ferdinand, J. R., He, X., Webb, S., Maunder, D., Vandamme, N., Mahbubani, K. T., Polanski, K., Mamanova, L., Bolt, L., Crossland, D., Rita, F. d., Fuller, A., Filby, A., Reynolds, G., Dixon, D., Saeb-Parsy, K., Lisgo, S., Henderson, D., Vento-Tormo, R., Bayraktar, O. A., Barker, R. A., Meyer, K. B., Saeys, Y., Bonfanti, P., Behjati, S., Clatworthy, M. R., Taghon, T., Haniffa, M. and Teichmann, S. A.,** A cell atlas of human thymic development defines T cell repertoire formation. *Science* 2020. **367**: eaay3224.

33 **Abbey, J. L. and O'Neill, H. C.,** Expression of T-cell receptor genes during early T-cell development. *Immunology & Cell Biology* 2008. **86**: 166-174.

34 **Klein, L., Kyewski, B., Allen, P. M. and Hogquist, K. A.,** Positive and negative selection of the T cell repertoire: what thymocytes see (and don't see). *Nature Reviews Immunology* 2014. **14**: 377-391.

35 **Derbinski, J., Schulte, A., Kyewski, B. and Klein, L.,** Promiscuous gene expression in medullary thymic epithelial cells mirrors the peripheral self. *Nature Immunology* 2001. **2**: 1032-1039.

36 **Zachariah, M. A. and Cyster, J. G.,** Neural crest-derived pericytes promote egress of mature thymocytes at the corticomedullary junction. *Science (New York, N.Y.)* 2010. **328**: 1129-1135.

37 **Hsieh, C.-S., Lee, H.-M. and Lio, C.-W. J.,** Selection of regulatory T cells in the thymus. *Nature Reviews Immunology* 2012. **12**: 157-167.

38 **Caton, A. J., Kropf, E., Simons, D. M., Aitken, M., Weissler, K. A. and Jordan, M. S.,** Strength of TCR signal from self-peptide modulates autoreactive thymocyte deletion and Foxp3(+) Treg-cell formation. *Eur J Immunol* 2014. **44**: 785-793.

39 **Caramalho, I., Nunes-Silva, V., Pires, A. R., Mota, C., Pinto, A. I., Nunes-Cabaço, H., Foxall, R. B. and Sousa, A. E.,** Human regulatory T-cell development is dictated by Interleukin-2 and -15 expressed in a non-overlapping pattern in the thymus. *Journal of Autoimmunity* 2015. **56**: 98-110.

40 **Lio, C.-W. J. and Hsieh, C.-S.,** A Two-Step Process for Thymic Regulatory T Cell Development. *Immunity* 2008. **28**: 100-111.

41 **Burchill, M. A., Yang, J., Vang, K. B., Moon, J. J., Chu, H. H., Lio, C.-W. J., Vegoe, A. L., Hsieh, C.-S., Jenkins, M. K. and Farrar, M. A.,** Linked T Cell Receptor and Cytokine Signaling Govern the Development of the Regulatory T Cell Repertoire. *Immunity* 2008. **28**: 112-121.

42 **Owen, D. L., Mahmud, S. A., Sjaastad, L. E., Williams, J. B., Spanier, J. A., Simeonov, D. R., Ruscher, R., Huang, W., Proekt, I., Miller, C. N., Hekim, C., Jeschke, J. C., Aggarwal, P., Broeckel, U., LaRue, R. S., Henzler, C. M., Alegre, M.-L., Anderson, M. S., August, A., Marson, A., Zheng, Y., Williams, C. B. and Farrar,**

M. A., Thymic regulatory T cells arise via two distinct developmental programs. *Nature Immunology* 2019. **20**: 195-205.

43 **Tai, X., Erman, B., Alag, A., Mu, J., Kimura, M., Katz, G., Guinter, T., McCaughtry, T., Etzensperger, R., Feigenbaum, L., Singer, Dinah S. and Singer, A.,** Foxp3 Transcription Factor Is Proapoptotic and Lethal to Developing Regulatory T Cells unless Counterbalanced by Cytokine Survival Signals. *Immunity* 2013. **38**: 1116-1128.

44 **Tuovinen, H., Pekkarinen, P. T., Rossi, L. H., Mattila, I. and Arstila, T. P.,** The FOXP3+ subset of human CD4+CD8+ thymocytes is immature and subject to intrathymic selection. *Immunology & Cell Biology* 2008. **86**: 523-529.

45 **Nunes-Cabaço, H., Ribot, J. C., Caramalho, I., Serra-Caetano, A., Silva-Santos, B. and Sousa, A. E.,** Foxp3 induction in human and murine thymus precedes the CD4+ CD8+ stage but requires early T-cell receptor expression. *Immunol Cell Biol* 2010. **88**: 523-528.

46 **Nunes-Cabaço, H., Caramalho, Í., Sepúlveda, N. and Sousa, A. E.,** Differentiation of human thymic regulatory T cells at the double positive stage. *European Journal of Immunology* 2011. **41**: 3604-3614.

47 **Vanhanen, R., Leskinen, K., Mattila, I. P., Saavalainen, P. and Arstila, T. P.,** Epigenetic and transcriptional analysis supports human regulatory T cell commitment at the CD4+CD8+ thymocyte stage. *Cellular Immunology* 2020. **347**: 104026.

48 **Vanhanen, R., Tuulasvaara, A., Mattila, J., Pätilä, T. and Arstila, T. P.,** Common gamma chain cytokines promote regulatory T cell development and survival at the CD4+ CD8+ stage in the human thymus. *Scandinavian Journal of Immunology* 2018. **88**: e12681.

49 **Kanamori, M., Nakatsukasa, H., Okada, M., Lu, Q. and Yoshimura, A.,** Induced Regulatory T Cells: Their Development, Stability, and Applications. *Trends Immunol* 2016. **37**: 803-811.

50 **Maruyama, T., Konkel, J. E., Zamarron, B. F. and Chen, W.,** The molecular mechanisms of Foxp3 gene regulation. *Seminars in Immunology* 2011. **23**: 418-423.

51 **Tone, Y., Furuuchi, K., Kojima, Y., Tykocinski, M. L., Greene, M. I. and Tone, M.,** Smad3 and NFAT cooperate to induce Foxp3 expression through its enhancer. *Nat Immunol* 2008. **9**: 194-202.

52 **Belkaid, Y. and Oldenhove, G.,** Tuning microenvironments: induction of regulatory T cells by dendritic cells. *Immunity* 2008. **29**: 362-371.

53 **Kang, S. G., Lim, H. W., Andrisani, O. M., Broxmeyer, H. E. and Kim, C. H.,** Vitamin A Metabolites Induce Gut-Homing FoxP3+ Regulatory T Cells. *The Journal of Immunology* 2007. **179**: 3724-3733.

54 **Hoeppli, R. E., Wu, D., Cook, L. and Levings, M. K.,** The environment of regulatory T cell biology: cytokines, metabolites, and the microbiome. *Frontiers in immunology* 2015. **6**: 61-61.

55 **Samstein, Robert M., Josefowicz, Steven Z., Arvey, A., Treuting, Piper M. and Rudensky, Alexander Y.,** Extrathymic Generation of Regulatory T Cells in Placental Mammals Mitigates Maternal-Fetal Conflict. *Cell* 2012. **150**: 29-38.

56 **Goldstein, J. D., Pérol, L., Zaragoza, B., Baeyens, A., Marodon, G. and Piaggio, E.,** Role of cytokines in thymus- versus peripherally derived-regulatory T cell differentiation and function. *Frontiers in immunology* 2013. **4**: 155-155.

57 **Vahl, J. C., Drees, C., Heger, K., Heink, S., Fischer, Julius C., Nedjic, J., Ohkura, N., Morikawa, H., Poeck, H., Schallenberg, S., Rieß, D., Hein, Marco Y., Buch, T., Polic, B., Schönle, A., Zeiser, R., Schmitt-Gräff, A., Kretschmer, K., Klein, L., Korn, T., Sakaguchi, S. and Schmidt-Supprian, M.,** Continuous T Cell Receptor Signals Maintain a Functional Regulatory T Cell Pool. *Immunity* 2014. **41**: 722-736.

58 **Levine, A. G., Arvey, A., Jin, W. and Rudensky, A. Y.,** Continuous requirement for the TCR in regulatory T cell function. *Nature Immunology* 2014. **15**: 1070-1078.

59 **Zorn, E., Nelson, E. A., Mohseni, M., Porcheray, F., Kim, H., Litsa, D., Bellucci, R., Raderschall, E., Canning, C., Soiffer, R. J., Frank, D. A. and Ritz, J.,** IL-2 regulates FOXP3 expression in human CD4+CD25+ regulatory T cells through a STAT-dependent mechanism and induces the expansion of these cells in vivo. *Blood* 2006. **108**: 1571-1579.

60 **Yao, Z., Kanno, Y., Kerenyi, M., Stephens, G., Durant, L., Watford, W. T., Laurence, A., Robinson, G. W., Shevach, E. M., Moriggl, R., Hennighausen, L., Wu, C. and O'Shea, J. J.,** Nonredundant roles for Stat5a/b in directly regulating Foxp3. *Blood* 2007. **109**: 4368-4375.

61 **Ogawa, C., Tone, Y., Tsuda, M., Peter, C., Waldmann, H. and Tone, M.,** TGF-β–Mediated Foxp3 Gene Expression Is Cooperatively Regulated by Stat5, Creb, and AP-1 through CNS2. *The Journal of Immunology* 2014. **192**: 475-483.

62 **Nair, V. S., Song, M. H., Ko, M. and Oh, K. I.,** DNA Demethylation of the Foxp3 Enhancer Is Maintained through Modulation of Ten-Eleven-Translocation and DNA Methyltransferases. *Molecules and cells* 2016. **39**: 888-897.

63 **Almeida, A. R. M., Zaragoza, B. and Freitas, A. A.,** Indexation as a Novel Mechanism of Lymphocyte Homeostasis: The Number of CD4+CD25+ Regulatory T Cells Is Indexed to the Number of IL-2-Producing Cells. *The Journal of Immunology* 2006. **177**: 192-200.

64 **Amado, I. F., Berges, J., Luther, R. J., Mailhé, M.-P., Garcia, S., Bandeira, A., Weaver, C., Liston, A. and Freitas, A. A.,** IL-2 coordinates IL-2–producing and regulatory T cell interplay. *Journal of Experimental Medicine* 2013. **210**: 2707-2720.

65 **Pierson, W., Cauwe, B., Policheni, A., Schlenner, S. M., Franckaert, D., Berges, J., Humblet-Baron, S., Schönefeldt, S., Herold, M. J., Hildeman, D., Strasser, A., Bouillet, P., Lu, L.-F., Matthys, P., Freitas, A. A., Luther, R. J., Weaver, C. T., Dooley, J., Gray, D. H. D. and Liston, A.,** Antiapoptotic Mcl-1 is critical for the survival and niche-filling capacity of Foxp3+ regulatory T cells. *Nature Immunology* 2013. **14**: 959-965.

66 **Hilligan, K. L. and Ronchese, F.,** Antigen presentation by dendritic cells and their instruction of CD4+ T helper cell responses. *Cellular & Molecular Immunology* 2020. **17**: 587-599.

67 **Tran, G. T., Hodgkinson, S. J., Carter, N. M., Verma, N. D., Plain, K. M., Boyd, R., Robinson, C. M., Nomura, M., Killingsworth, M. and Hall, B. M.,** IL-5 promotes induction of antigen-specific CD4+CD25+ T regulatory cells that suppress autoimmunity. *Blood* 2012. **119**: 4441-4450.

68 **Cretney, E., Kallies, A. and Nutt, S. L.,** Differentiation and function of Foxp3(+) effector regulatory T cells. *Trends Immunol* 2013. **34**: 74-80.

69 **Duhen, T., Duhen, R., Lanzavecchia, A., Sallusto, F. and Campbell, D. J.,** Functionally distinct subsets of human FOXP3+ Treg cells that phenotypically mirror effector Th cells. *Blood* 2012. **119**: 4430-4440.
70 **Wing, J. B., Lim, E. L. and Sakaguchi, S.,** Control of foreign Ag-specific Ab responses by Treg and Tfr. *Immunol Rev* 2020.
71 **Koch, M. A., Tucker-Heard, G. s., Perdue, N. R., Killebrew, J. R., Urdahl, K. B. and Campbell, D. J.,** The transcription factor T-bet controls regulatory T cell homeostasis and function during type 1 inflammation. *Nature immunology* 2009. **10**: 595-602.
72 **Levine, A. G., Mendoza, A., Hemmers, S., Moltedo, B., Niec, R. E., Schizas, M., Hoyos, B. E., Putintseva, E. V., Chaudhry, A., Dikiy, S., Fujisawa, S., Chudakov, D. M., Treuting, P. M. and Rudensky, A. Y.,** Stability and function of regulatory T cells expressing the transcription factor T-bet. *Nature* 2017. **546**: 421-425.
73 **Chaudhry, A., Rudra, D., Treuting, P., Samstein, R. M., Liang, Y., Kas, A. and Rudensky, A. Y.,** CD4+ regulatory T cells control TH17 responses in a Stat3-dependent manner. *Science* 2009. **326**: 986-991.
74 **Zheng, Y., Chaudhry, A., Kas, A., deRoos, P., Kim, J. M., Chu, T. T., Corcoran, L., Treuting, P., Klein, U. and Rudensky, A. Y.,** Regulatory T-cell suppressor program co-opts transcription factor IRF4 to control T(H)2 responses. *Nature* 2009. **458**: 351-356.
75 **Linterman, M. A., Pierson, W., Lee, S. K., Kallies, A., Kawamoto, S., Rayner, T. F., Srivastava, M., Divekar, D. P., Beaton, L., Hogan, J. J., Fagarasan, S., Liston, A., Smith, K. G. and Vinuesa, C. G.,** Foxp3+ follicular regulatory T cells control the germinal center response. *Nat Med* 2011. **17**: 975-982.
76 **Chung, Y., Tanaka, S., Chu, F., Nurieva, R. I., Martinez, G. J., Rawal, S., Wang, Y. H., Lim, H., Reynolds, J. M., Zhou, X. H., Fan, H. M., Liu, Z. M., Neelapu, S. S. and Dong, C.,** Follicular regulatory T cells expressing Foxp3 and Bcl-6 suppress germinal center reactions. *Nat Med* 2011. **17**: 983-988.
77 **Hoeppli, R. E., MacDonald, K. N., Leclair, P., Fung, V. C. W., Mojibian, M., Gillies, J., Rahavi, S. M. R., Campbell, A. I. M., Gandhi, S. K., Pesenacker, A. M., Reid, G., Lim, C. J. and Levings, M. K.,** Tailoring the homing capacity of human Tregs for directed migration to sites of Th1-inflammation or intestinal regions. *American Journal of Transplantation* 2019. **19**: 62-76.
78 **Halim, L., Romano, M., McGregor, R., Correa, I., Pavlidis, P., Grageda, N., Hoong, S.-J., Yuksel, M., Jassem, W., Hannen, R. F., Ong, M., McKinney, O., Hayee, B. H., Karagiannis, S. N., Powell, N., Lechler, R. I., Nova-Lamperti, E. and Lombardi, G.,** An Atlas of Human Regulatory T Helper-like Cells Reveals Features of Th2-like Tregs that Support a Tumorigenic Environment. *Cell reports* 2017. **20**: 757-770.
79 **Sakaguchi, S., Mikami, N., Wing, J. B., Tanaka, A., Ichiyama, K. and Ohkura, N.,** Regulatory T Cells and Human Disease. *Annu Rev Immunol* 2020. **38**: 541-566.
80 **Romano, M., Fanelli, G., Albany, C. J., Giganti, G. and Lombardi, G.,** Past, Present, and Future of Regulatory T Cell Therapy in Transplantation and Autoimmunity. *Front Immunol* 2019. **10**: 43.
81 **Schmidt, A., Oberle, N. and Krammer, P. H.,** Molecular mechanisms of treg-mediated T cell suppression. *Frontiers in immunology* 2012. **3**: 51.
82 **Tang, Q., Adams, J. Y., Tooley, A. J., Bi, M., Fife, B. T., Serra, P., Santamaria, P., Locksley, R. M., Krummel, M. F. and Bluestone, J. A.,** Visualizing regulatory T cell

control of autoimmune responses in nonobese diabetic mice. *Nature Immunology* 2006. **7**: 83-92.

83 **Tadokoro , C. E., Shakhar , G., Shen , S., Ding , Y., Lino , A. C., Maraver , A., Lafaille , J. J. and Dustin , M. L.,** Regulatory T cells inhibit stable contacts between CD4+ T cells and dendritic cells in vivo. *Journal of Experimental Medicine* 2006. **203**: 505-511.

84 **Yan, J., Liu, B., Shi, Y. and Qi, H.,** Class II MHC–independent suppressive adhesion of dendritic cells by regulatory T cells in vivo. *Journal of Experimental Medicine* 2017. **214**: 319-326.

85 **Chen, J., Ganguly, A., Mucsi, A. D., Meng, J., Yan, J., Detampel, P., Munro, F., Zhang, Z., Wu, M., Hari, A., Stenner, M. D., Zheng, W., Kubes, P., Xia, T., Amrein, M. W., Qi, H. and Shi, Y.,** Strong adhesion by regulatory T cells induces dendritic cell cytoskeletal polarization and contact-dependent lethargy. *Journal of Experimental Medicine* 2017. **214**: 327-338.

86 **Akkaya, B., Oya, Y., Akkaya, M., Al Souz, J., Holstein, A. H., Kamenyeva, O., Kabat, J., Matsumura, R., Dorward, D. W., Glass, D. D. and Shevach, E. M.,** Regulatory T cells mediate specific suppression by depleting peptide–MHC class II from dendritic cells. *Nature Immunology* 2019. **20**: 218-231.

87 **Tran, D. Q., Glass, D. D., Uzel, G., Darnell, D. A., Spalding, C., Holland, S. M. and Shevach, E. M.,** Analysis of Adhesion Molecules, Target Cells, and Role of IL-2 in Human FOXP3+ Regulatory T Cell Suppressor Function. *The Journal of Immunology* 2009. **182**: 2929-2938.

88 **Collins, A. V., Brodie, D. W., Gilbert, R. J. C., Iaboni, A., Manso-Sancho, R., Walse, B., Stuart, D. I., van der Merwe, P. A. and Davis, S. J.,** The Interaction Properties of Costimulatory Molecules Revisited. *Immunity* 2002. **17**: 201-210.

89 **Oderup, C., Cederbom, L., Makowska, A., Cilio, C. M. and Ivars, F.,** Cytotoxic T lymphocyte antigen-4-dependent down-modulation of costimulatory molecules on dendritic cells in CD4+ CD25+ regulatory T-cell-mediated suppression. *Immunology* 2006. **118**: 240-249.

90 **Ovcinnikovs, V., Ross, E. M., Petersone, L., Edner, N. M., Heuts, F., Ntavli, E., Kogimtzis, A., Kennedy, A., Wang, C. J., Bennett, C. L., Sansom, D. M. and Walker, L. S. K.,** CTLA-4-mediated transendocytosis of costimulatory molecules primarily targets migratory dendritic cells. *Sci Immunol* 2019. **4**.

91 **Qureshi, O. S., Zheng, Y., Nakamura, K., Attridge, K., Manzotti, C., Schmidt, E. M., Baker, J., Jeffery, L. E., Kaur, S., Briggs, Z., Hou, T. Z., Futter, C. E., Anderson, G., Walker, L. S. K. and Sansom, D. M.,** Trans-endocytosis of CD80 and CD86: a molecular basis for the cell-extrinsic function of CTLA-4. *Science (New York, N.Y.)* 2011. **332**: 600-603.

92 **Fallarino, F., Grohmann, U., Hwang, K. W., Orabona, C., Vacca, C., Bianchi, R., Belladonna, M. L., Fioretti, M. C., Alegre, M.-L. and Puccetti, P.,** Modulation of tryptophan catabolism by regulatory T cells. *Nature Immunology* 2003. **4**: 1206-1212.

93 **Frumento , G., Rotondo , R., Tonetti , M., Damonte , G., Benatti , U. and Ferrara , G. B.,** Tryptophan-derived Catabolites Are Responsible for Inhibition of T and Natural Killer Cell Proliferation Induced by Indoleamine 2,3-Dioxygenase. *Journal of Experimental Medicine* 2002. **196**: 459-468.

94 **Terness , P., Bauer , T. M., Röse , L., Dufter , C., Watzlik , A., Simon , H. and Opelz , G.,** Inhibition of Allogeneic T Cell Proliferation by Indoleamine 2,3-Dioxygenase–expressing Dendritic Cells : Mediation of Suppression by Tryptophan Metabolites. *Journal of Experimental Medicine* 2002. **196**: 447-457.

95 **Fallarino, F., Grohmann, U., Vacca, C., Bianchi, R., Orabona, C., Spreca, A., Fioretti, M. C. and Puccetti, P.,** T cell apoptosis by tryptophan catabolism. *Cell Death & Differentiation* 2002. **9**: 1069-1077.

96 **Pandiyan, P., Zheng, L., Ishihara, S., Reed, J. and Lenardo, M. J.,** CD4+ CD25+ Foxp3+ regulatory T cells induce cytokine deprivation–mediated apoptosis of effector CD4+ T cells. *Nature immunology* 2007. **8**: 1353.

97 **Sitrin, J., Ring, A., Garcia, K. C., Benoist, C. and Mathis, D.,** Regulatory T cells control NK cells in an insulitic lesion by depriving them of IL-2. *The Journal of experimental medicine* 2013. **210**: 1153-1165.

98 **Whiteside, T. L., Mandapathil, M. and Schuler, P.,** The role of the adenosinergic pathway in immunosuppression mediated by human regulatory T cells (Treg). *Curr Med Chem* 2011. **18**: 5217-5223.

99 **Kobie, J. J., Shah, P. R., Yang, L., Rebhahn, J. A., Fowell, D. J. and Mosmann, T. R.,** T Regulatory and Primed Uncommitted CD4 T Cells Express CD73, Which Suppresses Effector CD4 T Cells by Converting 5′-Adenosine Monophosphate to Adenosine. *The Journal of Immunology* 2006. **177**: 6780-6786.

100 **Mandapathil, M., Hilldorfer, B., Szczepanski, M. J., Czystowska, M., Szajnik, M., Ren, J., Lang, S., Jackson, E. K., Gorelik, E. and Whiteside, T. L.,** Generation and accumulation of immunosuppressive adenosine by human CD4+CD25highFOXP3+ regulatory T cells. *The Journal of biological chemistry* 2010. **285**: 7176-7186.

101 **Borsellino, G., Kleinewietfeld, M., Di Mitri, D., Sternjak, A., Diamantini, A., Giometto, R., Höpner, S., Centonze, D., Bernardi, G., Dell'Acqua, M. L., Rossini, P. M., Battistini, L., Rötzschke, O. and Falk, K.,** Expression of ectonucleotidase CD39 by Foxp3+ Treg cells: hydrolysis of extracellular ATP and immune suppression. *Blood* 2007. **110**: 1225-1232.

102 **Deaglio, S., Dwyer, K. M., Gao, W., Friedman, D., Usheva, A., Erat, A., Chen, J. F., Enjyoji, K., Linden, J., Oukka, M., Kuchroo, V. K., Strom, T. B. and Robson, S. C.,** Adenosine generation catalyzed by CD39 and CD73 expressed on regulatory T cells mediates immune suppression. *J Exp Med* 2007. **204**: 1257-1265.

103 **Jarvis, L. B., Rainbow, D. B., Coppard, V., Howlett, S. K., Georgieva, Z., Davies, J. L., Mullay, H. K., Hester, J., Ashmore, T., Van Den Bosch, A., Grist, J. T., Coles, A. J., Mousa, H. S., Pluchino, S., Mahbubani, K. T., Griffin, J. L., Saeb-Parsy, K., Issa, F., Peruzzotti-Jametti, L., Wicker, L. S. and Jones, J. L.,** Therapeutically expanded human regulatory T-cells are super-suppressive due to HIF1A induced expression of CD73. *Communications Biology* 2021. **4**: 1186.

104 **Yan, Z., Garg, S. K., Kipnis, J. and Banerjee, R.,** Extracellular redox modulation by regulatory T cells. *Nature Chemical Biology* 2009. **5**: 721-723.

105 **Yan, Z., Garg, S. K. and Banerjee, R.,** Regulatory T cells interfere with glutathione metabolism in dendritic cells and T cells. *The Journal of biological chemistry* 2010. **285**: 41525-41532.

106 **Gondek, D. C., DeVries, V., Nowak, E. C., Lu, L.-F., Bennett, K. A., Scott, Z. A. and Noelle, R. J.,** Transplantation survival is maintained by granzyme B+ regulatory cells and adaptive regulatory T cells. *The Journal of Immunology* 2008. **181**: 4752-4760.
107 **Tran, D. Q., Andersson, J., Wang, R., Ramsey, H., Unutmaz, D. and Shevach, E. M.,** GARP (LRRC32) is essential for the surface expression of latent TGF-β on platelets and activated FOXP3+ regulatory T cells. *Proceedings of the National Academy of Sciences* 2009. **106**: 13445-13450.
108 **Stockis, J., Colau, D., Coulie, P. G. and Lucas, S.,** Membrane protein GARP is a receptor for latent TGF-beta on the surface of activated human Treg. *Eur J Immunol* 2009. **39**: 3315-3322.
109 **Andersson , J., Tran , D. Q., Pesu , M., Davidson , T. S., Ramsey , H., O'Shea , J. J. and Shevach , E. M.,** CD4+FoxP3+ regulatory T cells confer infectious tolerance in a TGF-β–dependent manner. *Journal of Experimental Medicine* 2008. **205**: 1975-1981.
110 **Rubtsov, Y. P., Rasmussen, J. P., Chi, E. Y., Fontenot, J., Castelli, L., Ye, X., Treuting, P., Siewe, L., Roers, A., Henderson, W. R., Muller, W. and Rudensky, A. Y.,** Regulatory T Cell-Derived Interleukin-10 Limits Inflammation at Environmental Interfaces. *Immunity* 2008. **28**: 546-558.
111 **Vignali, D. A. A., Collison, L. W. and Workman, C. J.,** How regulatory T cells work. *Nature Reviews Immunology* 2008. **8**: 523-532.
112 **Sawant, D. V., Yano, H., Chikina, M., Zhang, Q., Liao, M., Liu, C., Callahan, D. J., Sun, Z., Sun, T., Tabib, T., Pennathur, A., Corry, D. B., Luketich, J. D., Lafyatis, R., Chen, W., Poholek, A. C., Bruno, T. C., Workman, C. J. and Vignali, D. A. A.,** Adaptive plasticity of IL-10+ and IL-35+ Treg cells cooperatively promotes tumor T cell exhaustion. *Nature Immunology* 2019. **20**: 724-735.
113 **Collison, L. W., Workman, C. J., Kuo, T. T., Boyd, K., Wang, Y., Vignali, K. M., Cross, R., Sehy, D., Blumberg, R. S. and Vignali, D. A. A.,** The inhibitory cytokine IL-35 contributes to regulatory T-cell function. *Nature* 2007. **450**: 566-569.
114 **Zhang, J., Zhang, Y., Wang, Q., Li, C., Deng, H., Si, C. and Xiong, H.,** Interleukin-35 in immune-related diseases: protection or destruction. *Immunology* 2019. **157**: 13-20.
115 **Gravano, D. M. and Vignali, D. A. A.,** The battle against immunopathology: infectious tolerance mediated by regulatory T cells. *Cellular and molecular life sciences : CMLS* 2012. **69**: 1997-2008.
116 **Romano, M., Fanelli, G., Tan, N., Nova-Lamperti, E., McGregor, R., Lechler, R. I., Lombardi, G. and Scottà, C.,** Expanded Regulatory T Cells Induce Alternatively Activated Monocytes With a Reduced Capacity to Expand T Helper-17 Cells. *Frontiers in Immunology* 2018. **9**.
117 **Esensten, J. H., Muller, Y. D., Bluestone, J. A. and Tang, Q.,** Regulatory T-cell therapy for autoimmune and autoinflammatory diseases: The next frontier. *Journal of Allergy and Clinical Immunology* 2018. **142**: 1710-1718.
118 **Cohen , J. L., Trenado , A. l., Vasey , D., Klatzmann , D. and Salomon , B. t. L.,** CD4+CD25+ Immunoregulatory T Cells : New Therapeutics for Graft-Versus-Host Disease. *Journal of Experimental Medicine* 2002. **196**: 401-406.
119 **Taylor, P. A., Lees, C. J. and Blazar, B. R.,** The infusion of ex vivo activated and expanded CD4(+)CD25(+) immune regulatory cells inhibits graft-versus-host disease lethality. *Blood* 2002. **99**: 3493-3499.

120 **Hoffmann, P., Ermann, J., Edinger, M., Fathman, C. G. and Strober, S.,** Donor-type CD4(+)CD25(+) regulatory T cells suppress lethal acute graft-versus-host disease after allogeneic bone marrow transplantation. *J Exp Med* 2002. **196**: 389-399.

121 **Edinger, M., Hoffmann, P., Ermann, J., Drago, K., Fathman, C. G., Strober, S. and Negrin, R. S.,** CD4+CD25+ regulatory T cells preserve graft-versus-tumor activity while inhibiting graft-versus-host disease after bone marrow transplantation. *Nat Med* 2003. **9**: 1144-1150.

122 **Joffre, O., Santolaria, T., Calise, D., Al Saati, T., Hudrisier, D., Romagnoli, P. and van Meerwijk, J. P. M.,** Prevention of acute and chronic allograft rejection with CD4+CD25+Foxp3+ regulatory T lymphocytes. *Nature medicine* 2008. **14**: 88-92.

123 **Boardman, D. A., Jacob, J., Smyth, L. A., Lombardi, G. and Lechler, R. I.,** What Is Direct Allorecognition? *Current transplantation reports* 2016. **3**: 275-283.

124 **Tang , Q., Henriksen , K. J., Bi , M., Finger , E. B., Szot , G., Ye , J., Masteller , E. L., McDevitt , H., Bonyhadi , M. and Bluestone , J. A.,** In Vitro–expanded Antigen-specific Regulatory T Cells Suppress Autoimmune Diabetes. *Journal of Experimental Medicine* 2004. **199**: 1455-1465.

125 **Scalapino, K. J., Tang, Q., Bluestone, J. A., Bonyhadi, M. L. and Daikh, D. I.,** Suppression of Disease in New Zealand Black/New Zealand White Lupus-Prone Mice by Adoptive Transfer of Ex Vivo Expanded Regulatory T Cells. *The Journal of Immunology* 2006. **177**: 1451-1459.

126 **Kohm, A. P., Carpentier, P. A., Anger, H. A. and Miller, S. D.,** Cutting Edge: CD4+CD25+ Regulatory T Cells Suppress Antigen-Specific Autoreactive Immune Responses and Central Nervous System Inflammation During Active Experimental Autoimmune Encephalomyelitis. *The Journal of Immunology* 2002. **169**: 4712-4716.

127 **Thomson, A. W., Sasaki, K. and Ezzelarab, M. B.,** Non-human Primate Regulatory T Cells and Their Assessment as Cellular Therapeutics in Preclinical Transplantation Models. *Frontiers in Cell and Developmental Biology* 2021. **9**.

128 **Ma, A., Qi, S., Song, L., Hu, Y., Dun, H., Massicotte, E., Dupuis, M., Daloze, P. and Chen, H.,** Adoptive transfer of CD4+CD25+ regulatory cells combined with low-dose sirolimus and anti-thymocyte globulin delays acute rejection of renal allografts in Cynomolgus monkeys. *International Immunopharmacology* 2011. **11**: 618-629.

129 **Trzonkowski, P., Bieniaszewska, M., Juścińska, J., Dobyszuk, A., Krzystyniak, A., Marek, N., Myśliwska, J. and Hellmann, A.,** First-in-man clinical results of the treatment of patients with graft versus host disease with human ex vivo expanded CD4+ CD25+ CD127− T regulatory cells. *Clinical immunology* 2009. **133**: 22-26.

130 **Martelli, M. F., Di Ianni, M., Ruggeri, L., Falzetti, F., Carotti, A., Terenzi, A., Pierini, A., Massei, M. S., Amico, L., Urbani, E., Del Papa, B., Zei, T., Iacucci Ostini, R., Cecchini, D., Tognellini, R., Reisner, Y., Aversa, F., Falini, B. and Velardi, A.,** HLA-haploidentical transplantation with regulatory and conventional T-cell adoptive immunotherapy prevents acute leukemia relapse. *Blood* 2014. **124**: 638-644.

131 **Di Ianni, M., Falzetti, F., Carotti, A., Terenzi, A., Castellino, F., Bonifacio, E., Del Papa, B., Zei, T., Ostini, R. I. and Cecchini, D.,** Tregs prevent GVHD and promote immune reconstitution in HLA-haploidentical transplantation. *Blood* 2011. **117**: 3921-3928.

132 **Ruggeri, L., Carotti, A., Pierini, A., Falzetti, F., Terenzi, A., Urbani, E., Lucia, A., Tricarico, S., Piccinelli, S., Massei, M. S., Ciardelli, S., Di Ianni, M., Zei, T., Iacucci Ostini, R., Lancellotta, V., Saldi, S., Minelli, O., Tognellini, R., Merluzzi, M., Marchesi, M., Caniglia, M., Aristei, C., Falini, B., Martelli, M. F. and Velardi, A.,** How Adoptive Immunotherapy with Conventional T and Regulatory T Cells Exerts a Gvl Effect without GvHD, after Haploidentical Hematopoietic Transplantation. *Blood* 2018. **132**: 3333-3333.

133 **Pierini, A., Ruggeri, L., Carotti, A., Falzetti, F., Saldi, S., Terenzi, A., Zucchetti, C., Ingrosso, G., Zei, T., Iacucci Ostini, R., Piccinelli, S., Bonato, S., Tricarico, S., Mancusi, A., Ciardelli, S., Limongello, R., Merluzzi, M., Di Ianni, M., Tognellini, R., Minelli, O., Mecucci, C., Martelli, M. P., Falini, B., Martelli, M. F., Aristei, C. and Velardi, A.,** Haploidentical age-adapted myeloablative transplant and regulatory and effector T cells for acute myeloid leukemia. *Blood Adv* 2021. **5**: 1199-1208.

134 **Brunstein, C. G., Miller, J. S., Cao, Q., McKenna, D. H., Hippen, K. L., Curtsinger, J., DeFor, T., Levine, B. L., June, C. H. and Rubinstein, P.,** Infusion of ex vivo expanded T regulatory cells in adults transplanted with umbilical cord blood: safety profile and detection kinetics. *Blood* 2011. **117**: 1061-1070.

135 **Brunstein, C. G., Blazar, B. R., Miller, J. S., Cao, Q., Hippen, K. L., McKenna, D. H., Curtsinger, J., McGlave, P. B. and Wagner, J. E.,** Adoptive transfer of umbilical cord blood-derived regulatory T cells and early viral reactivation. *Biol Blood Marrow Transplant* 2013. **19**: 1271-1273.

136 **Brunstein, C. G., Miller, J. S., McKenna, D. H., Hippen, K. L., DeFor, T. E., Sumstad, D., Curtsinger, J., Verneris, M. R., MacMillan, M. L., Levine, B. L., Riley, J. L., June, C. H., Le, C., Weisdorf, D. J., McGlave, P. B., Blazar, B. R. and Wagner, J. E.,** Umbilical cord blood-derived T regulatory cells to prevent GVHD: kinetics, toxicity profile, and clinical effect. *Blood* 2016. **127**: 1044-1051.

137 **MacMillan, M. L., Hippen, K. L., McKenna, D. H., Kadidlo, D., Sumstad, D., DeFor, T. E., Brunstein, C. G., Holtan, S. G., Miller, J. S., Warlick, E. D., Weisdorf, D. J., Wagner, J. E. and Blazar, B. R.,** First-in-human phase 1 trial of induced regulatory T cells for graft-versus-host disease prophylaxis in HLA-matched siblings. *Blood Advances* 2021. **5**: 1425-1436.

138 **Meyer, E. H., Laport, G., Xie, B. J., MacDonald, K., Heydari, K., Sahaf, B., Tang, S.-W., Baker, J., Armstrong, R., Tate, K., Tadisco, C., Arai, S., Johnston, L., Lowsky, R., Muffly, L., Rezvani, A. R., Shizuru, J., Weng, W.-K., Sheehan, K., Miklos, D. and Negrin, R. S.,** Transplantation of donor grafts with defined ratio of conventional and regulatory T cells in HLA-matched recipients. *JCI Insight* 2019. **4**.

139 **Theil, A., Tuve, S., Oelschlägel, U., Maiwald, A., Döhler, D., Oßmann, D., Zenkel, A., Wilhelm, C., Middeke, J. M., Shayegi, N., Trautmann-Grill, K., von Bonin, M., Platzbecker, U., Ehninger, G., Bonifacio, E. and Bornhäuser, M.,** Adoptive transfer of allogeneic regulatory T cells into patients with chronic graft-versus-host disease. *Cytotherapy* 2015. **17**: 473-486.

140 **Chandran, S., Tang, Q., Sarwal, M., Laszik, Z. G., Putnam, A. L., Lee, K., Leung, J., Nguyen, V., Sigdel, T., Tavares, E. C., Yang, J. Y. C., Hellerstein, M., Fitch, M., Bluestone, J. A. and Vincenti, F.,** Polyclonal Regulatory T Cell Therapy for Control of Inflammation in Kidney Transplants. *Am J Transplant* 2017. **17**: 2945-2954.

141 **Mathew, J. M., H.-Voss, J., LeFever, A., Konieczna, I., Stratton, C., He, J., Huang, X., Gallon, L., Skaro, A., Ansari, M. J. and Leventhal, J. R.,** A Phase I Clinical Trial with Ex Vivo Expanded Recipient Regulatory T cells in Living Donor Kidney Transplants. *Scientific Reports* 2018. **8**: 7428.

142 **Sawitzki, B., Harden, P. N., Reinke, P., Moreau, A., Hutchinson, J. A., Game, D. S., Tang, Q., Guinan, E. C., Battaglia, M., Burlingham, W. J., Roberts, I. S. D., Streitz, M., Josien, R., Böger, C. A., Scottà, C., Markmann, J. F., Hester, J. L., Juerchott, K., Braudeau, C., James, B., Contreras-Ruiz, L., van der Net, J. B., Bergler, T., Caldara, R., Petchey, W., Edinger, M., Dupas, N., Kapinsky, M., Mutzbauer, I., Otto, N. M., Öllinger, R., Hernandez-Fuentes, M. P., Issa, F., Ahrens, N., Meyenberg, C., Karitzky, S., Kunzendorf, U., Knechtle, S. J., Grinyó, J., Morris, P. J., Brent, L., Bushell, A., Turka, L. A., Bluestone, J. A., Lechler, R. I., Schlitt, H. J., Cuturi, M. C., Schlickeiser, S., Friend, P. J., Miloud, T., Scheffold, A., Secchi, A., Crisalli, K., Kang, S. M., Hilton, R., Banas, B., Blancho, G., Volk, H. D., Lombardi, G., Wood, K. J. and Geissler, E. K.,** Regulatory cell therapy in kidney transplantation (The ONE Study): a harmonised design and analysis of seven non-randomised, single-arm, phase 1/2A trials. *Lancet* 2020. **395**: 1627-1639.

143 **Harden, P. N., Game, D. S., Sawitzki, B., Van der Net, J. B., Hester, J., Bushell, A., Issa, F., Brook, M. O., Alzhrani, A., Schlickeiser, S., Scotta, C., Petchey, W., Streitz, M., Blancho, G., Tang, Q., Markmann, J., Lechler, R. I., Roberts, I. S. D., Friend, P. J., Hilton, R., Geissler, E. K., Wood, K. J. and Lombardi, G.,** Feasibility, long-term safety, and immune monitoring of regulatory T cell therapy in living donor kidney transplant recipients. *American Journal of Transplantation* 2021. **21**: 1603-1611.

144 **Roemhild, A., Otto, N. M., Moll, G., Abou-El-Enein, M., Kaiser, D., Bold, G., Schachtner, T., Choi, M., Oellinger, R., Landwehr-Kenzel, S., Juerchott, K., Sawitzki, B., Giesler, C., Sefrin, A., Beier, C., Wagner, D. L., Schlickeiser, S., Streitz, M., Schmueck-Henneresse, M., Amini, L., Stervbo, U., Babel, N., Volk, H. D. and Reinke, P.,** Regulatory T cells for minimising immune suppression in kidney transplantation: phase I/IIa clinical trial. *Bmj* 2020. **371**: m3734.

145 **Sánchez-Fueyo, A., Whitehouse, G., Grageda, N., Cramp, M. E., Lim, T. Y., Romano, M., Thirkell, S., Lowe, K., Fry, L., Heward, J., Kerr, A., Ali, J., Fisher, C., Lewis, G., Hope, A., Kodela, E., Lyne, M., Farzaneh, F., Kordasti, S., Rebollo-Mesa, I., Jose Lozano, J., Safinia, N., Heaton, N., Lechler, R., Martínez-Llordella, M. and Lombardi, G.,** Applicability, safety, and biological activity of regulatory T cell therapy in liver transplantation. *Am J Transplant* 2020. **20**: 1125-1136.

146 **Oberbauer, R., Edinger, M., Berlakovich, G., Kalhs, P., Worel, N., Heinze, G., Wolzt, M., Lion, T. and Wekerle, T.,** A Prospective Controlled Trial to Evaluate Safety and Efficacy of in vitro Expanded Recipient Regulatory T Cell Therapy and Tocilizumab Together With Donor Bone Marrow Infusion in HLA-Mismatched Living Donor Kidney Transplant Recipients (Trex001). *Front Med (Lausanne)* 2020. **7**: 634260.

147 **Marek-Trzonkowska, N., Myśliwiec, M., Dobyszuk, A., Grabowska, M., Techmańska, I., Juścińska, J., Wujtewicz, M. A., Witkowski, P., Młynarski, W. and Balcerska, A.,** Administration of CD4+ CD25highCD127− regulatory T cells preserves β-cell function in type 1 diabetes in children. *Diabetes care* 2012. **35**: 1817-1820.

148 **Marek-Trzonkowska, N., Myśliwiec, M., Dobyszuk, A., Grabowska, M., Derkowska, I., Juścińska, J., Owczuk, R., Szadkowska, A., Witkowski, P., Młynarski, W., Jarosz-Chobot, P., Bossowski, A., Siebert, J. and Trzonkowski, P.,** Therapy of type 1 diabetes with CD4(+)CD25(high)CD127-regulatory T cells prolongs survival of pancreatic islets - results of one year follow-up. *Clin Immunol* 2014. **153**: 23-30.

149 **Marek-Trzonkowska, N., Myśliwiec, M., Iwaszkiewicz-Grześ, D., Gliwiński, M., Derkowska, I., Żalińska, M., Zieliński, M., Grabowska, M., Zielińska, H., Piekarska, K., Jaźwińska-Curyłło, A., Owczuk, R., Szadkowska, A., Wyka, K., Witkowski, P., Młynarski, W., Jarosz-Chobot, P., Bossowski, A., Siebert, J. and Trzonkowski, P.,** Factors affecting long-term efficacy of T regulatory cell-based therapy in type 1 diabetes. *J Transl Med* 2016. **14**: 332.

150 **Bluestone, J. A., Buckner, J. H., Fitch, M., Gitelman, S. E., Gupta, S., Hellerstein, M. K., Herold, K. C., Lares, A., Lee, M. R. and Li, K.,** Type 1 diabetes immunotherapy using polyclonal regulatory T cells. *Science translational medicine* 2015. **7**: 315ra189-315ra189.

151 **Dong, S., Hiam-Galvez, K. J., Mowery, C. T., Herold, K. C., Gitelman, S. E., Esensten, J. H., Liu, W., Lares, A. P., Leinbach, A. S., Lee, M., Nguyen, V., Tamaki, S. J., Tamaki, W., Tamaki, C. M., Mehdizadeh, M., Putnam, A. L., Spitzer, M. H., Ye, C. J., Tang, Q. and Bluestone, J. A.,** The effects of low-dose IL-2 on Treg adoptive cell therapy in patients with Type 1 diabetes. *JCI Insight* 2021.

152 **Chwojnicki, K., Iwaszkiewicz-Grześ, D., Jankowska, A., Zieliński, M., Łowiec, P., Gliwiński, M., Grzywińska, M., Kowalczyk, K., Konarzewska, A., Glasner, P., Sakowska, J., Kulczycka, J., Jaźwińska-Curyłło, A., Kubach, M., Karaszewski, B., Nyka, W., Szurowska, E. and Trzonkowski, P.,** Administration of CD4+CD25highCD127−FoxP3+ Regulatory T Cells for Relapsing-Remitting Multiple Sclerosis: A Phase 1 Study. *BioDrugs* 2021. **35**: 47-60.

153 **Thonhoff, J. R., Beers, D. R., Zhao, W., Pleitez, M., Simpson, E. P., Berry, J. D., Cudkowicz, M. E. and Appel, S. H.,** Expanded autologous regulatory T-lymphocyte infusions in ALS: A phase I, first-in-human study. *Neurol Neuroimmunol Neuroinflamm* 2018. **5**: e465.

154 **Dall'Era, M., Pauli, M. L., Remedios, K., Taravati, K., Sandova, P. M., Putnam, A. L., Lares, A., Haemel, A., Tang, Q., Hellerstein, M., Fitch, M., McNamara, J., Welch, B., Bluestone, J. A., Wofsy, D. and Rosenblum, M. D.,** Adoptive Treg Cell Therapy in a Patient With Systemic Lupus Erythematosus. *Arthritis Rheumatol* 2019. **71**: 431-440.

155 **Tang, Q. and Lee, K.,** Regulatory T-cell therapy for transplantation: how many cells do we need? *Curr Opin Organ Transplant* 2012. **17**: 349-354.

156 **Baecher-Allan, C., Brown, J. A., Freeman, G. J. and Hafler, D. A.,** CD4+ CD25high regulatory cells in human peripheral blood. *The Journal of Immunology* 2001. **167**: 1245-1253.

157 **Safinia, N., Vaikunthanathan, T., Fraser, H., Thirkell, S., Lowe, K., Blackmore, L., Whitehouse, G., Martinez-Llordella, M., Jassem, W. and Sanchez-Fueyo, A.,** Successful expansion of functional and stable regulatory T cells for immunotherapy in liver transplantation. *Oncotarget* 2016. **7**: 7563.

158 **Dijke, I., Hoeppli, R., Ellis, T., Pearcey, J., Huang, Q., McMurchy, A., Boer, K., Peeters, A., Aubert, G. and Larsen, I.,** Discarded Human Thymus Is a Novel Source of Stable and Long-Lived Therapeutic Regulatory T Cells. *American Journal of Transplantation* 2016. **16**: 58-71.

159 **Seay, H. R., Putnam, A. L., Cserny, J., Posgai, A. L., Rosenau, E. H., Wingard, J. R., Girard, K. F., Kraus, M., Lares, A. P., Brown, H. L., Brown, K. S., Balavage, K. T., Peters, L. D., Bushdorf, A. N., Atkinson, M. A., Bluestone, J. A., Haller, M. J. and Brusko, T. M.,** Expansion of Human Tregs from Cryopreserved Umbilical Cord Blood for GMP-Compliant Autologous Adoptive Cell Transfer Therapy. *Molecular Therapy. Methods & Clinical Development* 2017. **4**: 178-191.

160 **Wing, K., Ekmark, A., Karlsson, H., Rudin, A. and Suri-Payer, E.,** Characterization of human $CD25^+$ $CD4^+$ T cells in thymus, cord and adult blood. *Immunology* 2002. **106**: 190-199.

161 **Takahata, Y., Nomura, A., Takada, H., Ohga, S., Furuno, K., Hikino, S., Nakayama, H., Sakaguchi, S. and Hara, T.,** CD25+ CD4+ T cells in human cord blood: an immunoregulatory subset with naive phenotype and specific expression of forkhead box p3 (Foxp3) gene. *Experimental hematology* 2004. **32**: 622-629.

162 **Fujimaki, W., Takahashi, N., Ohnuma, K., Nagatsu, M., Kurosawa, H., Yoshida, S., Dang, N. H., Uchiyama, T. and Morimoto, C.,** Comparative Study of Regulatory T Cell Function of Human $CD25^+CD4^+$ T Cells from Thymocytes, Cord Blood, and Adult Peripheral Blood. *Clinical and Developmental Immunology* 2008. **2008**: 305859.

163 **Riley, J. L., June, C. H. and Blazar, B. R.,** Human T Regulatory Cells as Therapeutic Agents: Take a Billion or So of These and Call Me in the Morning. *Immunity* 2009. **30**: 656-665.

164 **Pesenacker, A. M., Broady, R. and Levings, M. K.,** Control of tissue-localized immune responses by human regulatory T cells. *European Journal of Immunology* 2015. **45**: 333-343.

165 **Haque, R., Lei, F., Xiong, X., Bian, Y., Zhao, B., Wu, Y. and Song, J.,** Programming of Regulatory T Cells from Pluripotent Stem Cells and Prevention of Autoimmunity. *The Journal of Immunology* 2012. **189**: 1228-1236.

166 **Haque, M., Song, J., Fino, K., Sandhu, P., Song, X., Lei, F., Zheng, S., Ni, B., Fang, D. and Song, J.,** Stem cell-derived tissue-associated regulatory T cells ameliorate the development of autoimmunity. *Scientific reports* 2016. **6**: 20588-20588.

167 **Singh, J. and Zúñiga-Pflücker, J. C.,** Producing proT cells to promote immunotherapies. *International Immunology* 2018. **30**: 541-550.

168 **MacMillan, M. L., Hippen, K. L., McKenna, D. H., DeFor, T. E., Warlick, E. D., Brunstein, C. G., Miller, J. S., Weisdorf, D. J., Blazar, B. R. and Wagner, J. E.,** First-in-Human Clinical Trial to Determine the Safety and Potency of Inducible T Regulatory Cells after Allogeneic Hematopoietic Cell Transplantation. *Blood* 2018. **132**: 2112-2112.

169 **Allan, S. E., Song-Zhao, G. X., Abraham, T., McMurchy, A. N. and Levings, M. K.,** Inducible reprogramming of human T cells into Treg cells by a conditionally active form of FOXP3. *European Journal of Immunology* 2008. **38**: 3282-3289.

170 **Allan, S. E., Alstad, A. N., Merindol, N., Crellin, N. K., Amendola, M., Bacchetta, R., Naldini, L., Roncarolo, M. G., Soudeyns, H. and Levings, M. K.,** Generation of

potent and stable human CD4+ T regulatory cells by activation-independent expression of FOXP3. *Molecular Therapy* 2008. **16**: 194-202.

171 **Passerini, L. and Bacchetta, R.,** Forkhead-Box-P3 Gene Transfer in Human CD4(+) T Conventional Cells for the Generation of Stable and Efficient Regulatory T Cells, Suitable for Immune Modulatory Therapy. *Frontiers in immunology* 2017. **8**: 1282-1282.

172 **Honaker, Y., Xiang, Y., Fisher, L., Sommer, K., Torgerson, T. R., Scharenberg, A. M. and Rawlings, D. J.,** Conversion of T-Effector Cells to Immunosuppressive T-Regulatory-like Cells By CRISPR/Cas9-Mediated Integration of a FOXP3 Transgene *American Society of Hematology Annual Meeting*, San Diego, California, USA 2018.

173 **Kellner, J. N., Delemarre, E. M., Yvon, E., Nierkens, S., Boelens, J. J., McNiece, I., Olson, A., Nieto, Y., Ciurea, S., Popat, U., Ahmed, S., Champlin, R., Ramos, J., Nishimoto, M., Ma, H., Ke, Z., Thall, P., Khoury, J. D., Negrin, R., Andersson, B. and Parmar, S.,** Third party, umbilical cord blood derived regulatory T-cells for prevention of graft versus host disease in allogeneic hematopoietic stem cell transplantation: feasibility, safety and immune reconstitution. *Oncotarget* 2018. **9**: 35611-35622.

174 **Torikai, H. and Cooper, L. J. N.,** Translational Implications for Off-the-shelf Immune Cells Expressing Chimeric Antigen Receptors. *Molecular Therapy* 2016. **24**: 1178-1186.

175 **Poirot, L., Philip, B., Schiffer-Mannioui, C., Le Clerre, D., Chion-Sotinel, I., Derniame, S., Potrel, P., Bas, C., Lemaire, L., Galetto, R., Lebuhotel, C., Eyquem, J., Cheung, G. W.-K., Duclert, A., Gouble, A., Arnould, S., Peggs, K., Pule, M., Scharenberg, A. M. and Smith, J.,** Multiplex Genome-Edited T-cell Manufacturing Platform for "Off-the-Shelf" Adoptive T-cell Immunotherapies. *Cancer Research* 2015. **75**: 3853-3864.

176 **Steiner, D., Brunicki, N., Blazar, B. R., Bachar-Lustig, E. and Reisner, Y.,** Tolerance induction by third-party "off-the-shelf" CD4+CD25+ Treg cells. *Experimental Hematology* 2006. **34**: 66-71.

177 **Zhang, H., Guo, H., Lu, L., Zahorchak, A. F., Wiseman, R. W., Raimondi, G., Cooper, D. K. C., Ezzelarab, M. B. and Thomson, A. W.,** Sequential monitoring and stability of ex vivo-expanded autologous and non-autologous regulatory T cells following infusion in non-human primates. *American Journal of Transplantation* 2015. **15**: 1253-1266.

178 **Tzannou, I., Papadopoulou, A., Naik, S., Leung, K., Martinez, C. A., Ramos, C. A., Carrum, G., Sasa, G., Lulla, P., Watanabe, A., Kuvalekar, M., Gee, A. P., Wu, M.-F., Liu, H., Grilley, B. J., Krance, R. A., Gottschalk, S., Brenner, M. K., Rooney, C. M., Heslop, H. E., Leen, A. M. and Omer, B.,** Off-the-Shelf Virus-Specific T Cells to Treat BK Virus, Human Herpesvirus 6, Cytomegalovirus, Epstein-Barr Virus, and Adenovirus Infections After Allogeneic Hematopoietic Stem-Cell Transplantation. *Journal of clinical oncology : official journal of the American Society of Clinical Oncology* 2017. **35**: 3547-3557.

179 **Pierini, A., Colonna, L., Alvarez, M., Schneidawind, D., Nishikii, H., Baker, J., Pan, Y., Florek, M., Kim, B.-S. and Negrin, R. S.,** Donor Requirements for Regulatory T Cell Suppression of Murine Graft-versus-Host Disease. *The Journal of Immunology* 2015. **195**: 347-355.

180 **Jaimes, Y., Seltsam, A., Eiz-Vesper, B., Blasczyk, R. and Figueiredo, C.,** Regulation of HLA class II expression prevents allogeneic T-cell responses. *Tissue Antigens* 2011. **77**: 36-44.

181 **Torikai, H., Reik, A., Soldner, F., Warren, E. H., Yuen, C., Zhou, Y., Crossland, D. L., Huls, H., Littman, N., Zhang, Z., Tykodi, S. S., Kebriaei, P., Lee, D. A., Miller, J. C., Rebar, E. J., Holmes, M. C., Jaenisch, R., Champlin, R. E., Gregory, P. D. and Cooper, L. J. N.,** Toward eliminating HLA class I expression to generate universal cells from allogeneic donors. *Blood* 2013. **122**: 1341-1349.

182 **Gornalusse, G. G., Hirata, R. K., Funk, S. E., Riolobos, L., Lopes, V. S., Manske, G., Prunkard, D., Colunga, A. G., Hanafi, L.-A., Clegg, D. O., Turtle, C. and Russell, D. W.,** HLA-E-expressing pluripotent stem cells escape allogeneic responses and lysis by NK cells. *Nature Biotechnology* 2017. **35**: 765.

183 **Putnam, A. L., Safinia, N., Medvec, A., Laszkowska, M., Wray, M., Mintz, M. A., Trotta, E., Szot, G. L., Liu, W., Lares, A., Lee, K., Laing, A., Lechler, R. I., Riley, J. L., Bluestone, J. A., Lombardi, G. and Tang, Q.,** Clinical Grade Manufacturing of Human Alloantigen-Reactive Regulatory T Cells for Use in Transplantation. *American journal of transplantation : official journal of the American Society of Transplantation and the American Society of Transplant Surgeons* 2013. **13**: 3010-3020.

184 **Fraser, H., Safinia, N., Grageda, N., Thirkell, S., Lowe, K., Fry, L. J., Scottá, C., Hope, A., Fisher, C., Hilton, R., Game, D., Harden, P., Bushell, A., Wood, K., Lechler, R. I. and Lombardi, G.,** A Rapamycin-Based GMP-Compatible Process for the Isolation and Expansion of Regulatory T Cells for Clinical Trials. *Mol Ther Methods Clin Dev* 2018. **8**: 198-209.

185 **Parmar, S., Liu, X., Tung, S. S., Robinson, S. N., Rodriguez, G., Cooper, L. J. N., Yang, H., Shah, N., Yang, H., Konopleva, M., Molldrem, J. J., Garcia-Manero, G., Najjar, A., Yvon, E., McNiece, I., Rezvani, K., Savoldo, B., Bollard, C. M. and Shpall, E. J.,** Third-party umbilical cord blood–derived regulatory T cells prevent xenogenic graft-versus-host disease. *Cytotherapy* 2014. **16**: 90-100.

186 **Canavan, J. B., Scottà, C., Vossenkämper, A., Goldberg, R., Elder, M. J., Shoval, I., Marks, E., Stolarczyk, E., Lo, J. W., Powell, N., Fazekasova, H., Irving, P. M., Sanderson, J. D., Howard, J. K., Yagel, S., Afzali, B., MacDonald, T. T., Hernandez-Fuentes, M. P., Shpigel, N. Y., Lombardi, G. and Lord, G. M.,** Developing in vitro expanded CD45RA(+) regulatory T cells as an adoptive cell therapy for Crohn's disease. *Gut* 2016. **65**: 584-594.

187 **Hoffmann, P., Eder, R., Boeld, T. J., Doser, K., Piseshka, B., Andreesen, R. and Edinger, M.,** Only the CD45RA+ subpopulation of CD4+ CD25high T cells gives rise to homogeneous regulatory T-cell lines upon in vitro expansion. *Blood* 2006. **108**: 4260-4267.

188 **Liu, W., Putnam, A. L., Xu-yu, Z., Szot, G. L., Lee, M. R., Zhu, S., Gottlieb, P. A., Kapranov, P., Gingeras, T. R., de St. Groth, B. F., Clayberger, C., Soper, D. M., Ziegler, S. F. and Bluestone, J. A.,** CD127 expression inversely correlates with FoxP3 and suppressive function of human CD4(+) T reg cells. *The Journal of Experimental Medicine* 2006. **203**: 1701-1711.

189 **Johnston, L., Armstrong, R., Baker, J., Sahaf, B., Otani, J., Tate, K., Tudisco, C., Sheehan, K., Meyer, E., Miklos, D. and Negrin, R. S.,** A Phase I Study of Donor

Regulatory T Cells As Treatment for Steroid Dependent/Refractory Chronic Graft Versus Host Disease. *Blood* 2016. **128**: 385-385.

190 **Balcerek, J., Shy, B. R., Putnam, A. L., Masiello, L. M., Lares, A., Dekovic, F., Acevedo, L., Lee, M. R., Nguyen, V., Liu, W., Paruthiyil, S., Xu, J., Leinbach, A. S., Bluestone, J. A., Tang, Q. and Esensten, J. H.,** Polyclonal Regulatory T Cell Manufacturing Under cGMP: A Decade of Experience. *Frontiers in Immunology* 2021. **12**.

191 **Alsuliman, A., Appel, S. H., Beers, D. R., Basar, R., Shaim, H., Kaur, I., Zulovich, J., Yvon, E., Muftuoglu, M., Imahashi, N., Kondo, K., Liu, E., Shpall, E. J. and Rezvani, K.,** A robust, good manufacturing practice–compliant, clinical-scale procedure to generate regulatory T cells from patients with amyotrophic lateral sclerosis for adoptive cell therapy. *Cytotherapy* 2016. **18**: 1312-1324.

192 **Landwehr-Kenzel, S., Zobel, A., Hoffmann, H., Landwehr, N., Schmueck-Henneresse, M., Schachtner, T., Roemhild, A. and Reinke, P.,** Ex vivo expanded natural regulatory T cells from patients with end-stage renal disease or kidney transplantation are useful for autologous cell therapy. *Kidney International* 2018. **93**: 1452-1464.

193 **Landwehr-Kenzel, S., Issa, F., Luu, S.-H., Schmück, M., Lei, H., Zobel, A., Thiel, A., Babel, N., Wood, K., Volk, H.-D. and Reinke, P.,** Novel GMP-Compatible Protocol Employing an Allogeneic B Cell Bank for Clonal Expansion of Allospecific Natural Regulatory T Cells. *American Journal of Transplantation* 2014. **14**: 594-606.

194 **Hippen, K. L., Merkel, S. C., Schirm, D. K., Sieben, C. M., Sumstad, D., Kadidlo, D. M., McKenna, D. H., Bromberg, J. S., Levine, B. L., Riley, J. L., June, C. H., Scheinberg, P., Douek, D. C., Miller, J. S., Wagner, J. E. and Blazar, B. R.,** Massive ex vivo expansion of human natural regulatory T cells (T(regs)) with minimal loss of in vivo functional activity. *Sci Transl Med* 2011. **3**: 83ra41.

195 **McKenna, D. H., Jr., Sumstad, D., Kadidlo, D. M., Batdorf, B., Lord, C. J., Merkel, S. C., Koellner, C. M., Curtsinger, J. M., June, C. H., Riley, J. L., Levine, B. L., Miller, J. S., Brunstein, C. G., Wagner, J. E., Blazar, B. R. and Hippen, K. L.,** Optimization of cGMP purification and expansion of umbilical cord blood-derived T-regulatory cells in support of first-in-human clinical trials. *Cytotherapy* 2017. **19**: 250-262.

196 **Hippen, K. L., Furlan, S. N., Roychoudhuri, R., Wang, E., Zhang, Y., Osborn, M. J., Merkel, S. C., Hani, S., MacMillan, M. L., Cichocki, F., Miller, J. S., Wagner, J. E., Restifo, N. P., Kean, L. S. and Blazar, B. R.,** Multiply restimulated human thymic regulatory T cells express distinct signature regulatory T-cell transcription factors without evidence of exhaustion. *Cytotherapy* 2021. **23**: 704-714.

197 **Xu, J., Melenhorst, J. J. and Fraietta, J. A.,** Toward precision manufacturing of immunogene T-cell therapies. *Cytotherapy* 2018. **20**: 623-638.

198 **Brindley, D. A., Davie, N. L., Culme-Seymour, E. J., Mason, C., Smith, D. W. and Rowley, J. A.,** Peak serum: implications of serum supply for cell therapy manufacturing. *Regen Med* 2012. **7**: 7-13.

199 **Smith, C., Økern, G., Rehan, S., Beagley, L., Lee, S. K., Aarvak, T., Schjetne, K. W. and Khanna, R.,** Ex vivo expansion of human T cells for adoptive immunotherapy using

the novel Xeno-free CTS Immune Cell Serum Replacement. *Clinical & Translational Immunology* 2015. **4**: e31.

200 **Levings, M. K., Sangregorio, R. and Roncarolo, M.-G.,** Human Cd25+Cd4+ T Regulatory Cells Suppress Naive and Memory T Cell Proliferation and Can Be Expanded in Vitro without Loss of Function. *The Journal of Experimental Medicine* 2001. **193**: 1295-1302.

201 **Zeiser, R., Leveson-Gower, D. B., Zambricki, E. A., Kambham, N., Beilhack, A., Loh, J., Hou, J.-Z. and Negrin, R. S.,** Differential impact of mammalian target of rapamycin inhibition on $CD4^+CD25^+Foxp3^+$ regulatory T cells compared with conventional $CD4^+$ T cells. *Blood* 2008. **111**: 453-462.

202 **Strauss, L., Czystowska, M., Szajnik, M., Mandapathil, M. and Whiteside, T. L.,** Differential Responses of Human Regulatory T Cells (Treg) and Effector T Cells to Rapamycin. *PLOS ONE* 2009. **4**: e5994.

203 **Gedaly, R., De Stefano, F., Turcios, L., Hill, M., Hidalgo, G., Mitov, M. I., Alstott, M. C., Butterfield, D. A., Mitchell, H. C., Hart, J., Al-Attar, A., Jennings, C. D. and Marti, F.,** mTOR Inhibitor Everolimus in Regulatory T Cell Expansion for Clinical Application in Transplantation. *Transplantation* 2019. **103**: 705-715.

204 **Fekete, N., Béland, A. V., Campbell, K., Clark, S. L. and Hoesli, C. A.,** Bags versus flasks: a comparison of cell culture systems for the production of dendritic cell-based immunotherapies. *Transfusion* 2018. **58**: 1800-1813.

205 **Kalos, M., Levine, B. L., Porter, D. L., Katz, S., Grupp, S. A., Bagg, A. and June, C. H.,** T Cells with Chimeric Antigen Receptors Have Potent Antitumor Effects and Can Establish Memory in Patients with Advanced Leukemia. *Science Translational Medicine* 2011. **3**: 95ra73-95ra73.

206 **Hollyman, D., Stefanski, J., Przybylowski, M., Bartido, S., Borquez-Ojeda, O., Taylor, C., Yeh, R., Capacio, V., Olszewska, M., Hosey, J., Sadelain, M., Brentjens, R. J. and Rivière, I.,** Manufacturing Validation of Biologically Functional T Cells Targeted to CD19 Antigen for Autologous Adoptive Cell Therapy. *Journal of Immunotherapy* 2009. **32**: 169-180.

207 **Vera, J. F., Brenner, L. J., Gerdemann, U., Ngo, M. C., Sili, U., Liu, H., Wilson, J., Dotti, G., Heslop, H. E., Leen, A. M. and Rooney, C. M.,** Accelerated production of antigen-specific T cells for preclinical and clinical applications using gas-permeable rapid expansion cultureware (G-Rex). *Journal of immunotherapy (Hagerstown, Md. : 1997)* 2010. **33**: 305-315.

208 **Elkord, E.,** Frequency of human T regulatory cells in peripheral blood is significantly reduced by cryopreservation. *Journal of Immunological Methods* 2009. **347**: 87-90.

209 **Sattui, S., de la Flor, C., Sanchez, C., Lewis, D., Lopez, G., Rizo-Patrón, E., White, A. C. and Montes, M.,** Cryopreservation modulates the detection of regulatory T cell markers. *Cytometry Part B: Clinical Cytometry* 2012. **82B**: 54-58.

210 **Seale, A. C., de Jong, B. C., Zaidi, I., Duvall, M., Whittle, H., Rowland-Jones, S. and Jaye, A.,** Effects of cryopreservation on CD4+ CD25+ T cells of HIV-1 infected individuals. *Journal of Clinical Laboratory Analysis* 2008. **22**: 153-158.

211 **Van Hemelen, D., Oude Elberink, J. N. G., Heimweg, J., van Oosterhout, A. J. M. and Nawijn, M. C.,** Cryopreservation does not alter the frequency of regulatory T cells

in peripheral blood mononuclear cells. *Journal of Immunological Methods* 2010. **353**: 138-140.

212 **Dawson, N. A. J., Lam, A. J., Cook, L., Hoeppli, R. E., Broady, R., Pesenacker, A. M. and Levings, M. K.,** An optimized method to measure human FOXP3+ regulatory T cells from multiple tissue types using mass cytometry. *European Journal of Immunology* 2018. **48**: 1415-1419.

213 **Gołąb, K., Grose, R., Placencia, V., Wickrema, A., Solomina, J., Tibudan, M., Konsur, E., Ciepły, K., Marek-Trzonkowska, N., Trzonkowski, P., Millis, J. M., Fung, J. and Witkowski, P.,** Cell banking for regulatory T cell-based therapy: strategies to overcome the impact of cryopreservation on the Treg viability and phenotype. *Oncotarget* 2018. **9**: 9728-9740.

214 **Peters, J. H., Preijers, F. W., Woestenenk, R., Hilbrands, L. B., Koenen, H. J. P. M. and Joosten, I.,** Clinical Grade Treg: GMP Isolation, Improvement of Purity by CD127pos Depletion, Treg Expansion, and Treg Cryopreservation. *PLOS ONE* 2008. **3**: e3161.

215 **Iyer, R. K., Bowles, P. A., Kim, H. and Dulgar-Tulloch, A.,** Industrializing Autologous Adoptive Immunotherapies: Manufacturing Advances and Challenges. *Front Med (Lausanne)* 2018. **5**: 150.

216 **Lam, A. J., Hoeppli, R. E. and Levings, M. K.,** Harnessing advances in T regulatory cell biology for cellular therapy in transplantation. *Transplantation* 2017. **101**: 2277-2287.

217 **Issa, F., Hester, J., Milward, K. and Wood, K. J.,** Homing of Regulatory T Cells to Human Skin Is Important for the Prevention of Alloimmune-Mediated Pathology in an In Vivo Cellular Therapy Model. *PLOS ONE* 2013. **7**: e53331.

218 **Taylor, P. A., Panoskaltsis-Mortari, A., Swedin, J. M., Lucas, P. J., Gress, R. E., Levine, B. L., June, C. H., Serody, J. S. and Blazar, B. R.,** L-Selectin^{hi} but not the L-selectin^{lo} CD4^{+}25^{+} T-regulatory cells are potent inhibitors of GVHD and BM graft rejection. *Blood* 2004. **104**: 3804-3812.

219 **Zhang, N., Schröppel, B., Lal, G., Jakubzick, C., Mao, X., Chen, D., Yin, N., Jessberger, R., Ochando, J. C., Ding, Y. and Bromberg, J. S.,** Regulatory T cells sequentially migrate from the site of tissue inflammation to the draining LN to suppress the alloimmune response. *Immunity* 2009. **30**: 458-469.

220 **Parmar, S., Liu, X., Najjar, A., Shah, N., Yang, H., Yvon, E., Rezvani, K., McNiece, I., Zweidler-McKay, P., Miller, L., Wolpe, S., Blazar, B. R. and Shpall, E. J.,** Ex vivo fucosylation of third-party human regulatory T cells enhances anti–graft-versus-host disease potency in vivo. *Blood* 2015. **125**: 1502-1506.

221 **Marek-Trzonkowska, N., Piekarska, K., Filipowicz, N., Piotrowski, A., Gucwa, M., Vogt, K., Sawitzki, B., Siebert, J. and Trzonkowski, P.,** Mild hypothermia provides Treg stability. *Scientific Reports* 2017. **7**: 11915.

222 **Neildez-Nguyen, T. M. A., Bigot, J., Da Rocha, S., Corre, G., Boisgerault, F., Paldi, A. and Galy, A.,** Hypoxic culture conditions enhance the generation of regulatory T cells. *Immunology* 2015. **144**: 431-443.

223 **Ben-Shoshan, J., Maysel-Auslender, S., Mor, A., Keren, G. and George, J.,** Hypoxia controls CD4+CD25+ regulatory T-cell homeostasis via hypoxia-inducible factor-1α. *European Journal of Immunology* 2008. **38**: 2412-2418.

224 **Dang, Eric V., Barbi, J., Yang, H.-Y., Jinasena, D., Yu, H., Zheng, Y., Bordman, Z., Fu, J., Kim, Y., Yen, H.-R., Luo, W., Zeller, K., Shimoda, L., Topalian, Suzanne L., Semenza, Gregg L., Dang, Chi V., Pardoll, Drew M. and Pan, F.,** Control of TH17/Treg Balance by Hypoxia-Inducible Factor 1. *Cell* 2011. **146**: 772-784.

225 **Klysz, D., Tai, X., Robert, P. A., Craveiro, M., Cretenet, G., Oburoglu, L., Mongellaz, C., Floess, S., Fritz, V., Matias, M. I., Yong, C., Surh, N., Marie, J. C., Huehn, J., Zimmermann, V., Kinet, S., Dardalhon, V. and Taylor, N.,** Glutamine-dependent α-ketoglutarate production regulates the balance between T helper 1 cell and regulatory T cell generation. *Science Signaling* 2015. **8**: ra97-ra97.

226 **Hippen, K. L., O'Connor, R. S., Lemire, A. M., Saha, A., Hanse, E. A., Tennis, N. C., Merkel, S. C., Kelekar, A., Riley, J. L., Levine, B. L., June, C. H., Turka, L. A., Kean, L. S., MacMillan, M. L., Miller, J. S., Wagner, J. E., Munn, D. H. and Blazar, B. R.,** In Vitro Induction of Human Regulatory T Cells Using Conditions of Low Tryptophan Plus Kynurenines. *American Journal of Transplantation* 2017. **17**: 3098-3113.

227 **Furusawa, Y., Obata, Y., Fukuda, S., Endo, T. A., Nakato, G., Takahashi, D., Nakanishi, Y., Uetake, C., Kato, K., Kato, T., Takahashi, M., Fukuda, N. N., Murakami, S., Miyauchi, E., Hino, S., Atarashi, K., Onawa, S., Fujimura, Y., Lockett, T., Clarke, J. M., Topping, D. L., Tomita, M., Hori, S., Ohara, O., Morita, T., Koseki, H., Kikuchi, J., Honda, K., Hase, K. and Ohno, H.,** Commensal microbe-derived butyrate induces the differentiation of colonic regulatory T cells. *Nature* 2013. **504**: 446.

228 **Smith, P. M., Howitt, M. R., Panikov, N., Michaud, M., Gallini, C. A., Bohlooly-Y, M., Glickman, J. N. and Garrett, W. S.,** The microbial metabolites, short chain fatty acids, regulate colonic Treg cell homeostasis. *Science* 2013. **341**: 569-573.

229 **Arpaia, N., Campbell, C., Fan, X., Dikiy, S., van der Veeken, J., deRoos, P., Liu, H., Cross, J. R., Pfeffer, K., Coffer, P. J. and Rudensky, A. Y.,** Metabolites produced by commensal bacteria promote peripheral regulatory T-cell generation. *Nature* 2013. **504**: 451.

230 **Tsang, J. Y., Tanriver, Y., Jiang, S., Xue, S. A., Ratnasothy, K., Chen, D., Stauss, H. J., Bucy, R. P., Lombardi, G. and Lechler, R.,** Conferring indirect allospecificity on CD4+CD25+ Tregs by TCR gene transfer favors transplantation tolerance in mice. *J Clin Invest* 2008. **118**: 3619-3628.

231 **Sicard, A., Levings, M. K. and Scott, D. W.,** Engineering therapeutic T cells to suppress alloimmune responses using TCRs, CARs, or BARs. *Am J Transplant* 2018. **18**: 1305-1311.

232 **Dawson, N. A. J., Vent-Schmidt, J. and Levings, M. K.,** Engineered Tolerance: Tailoring Development, Function, and Antigen-Specificity of Regulatory T Cells. *Frontiers in Immunology* 2017. **8**.

233 **Fesnak, A. D., June, C. H. and Levine, B. L.,** Engineered T cells: the promise and challenges of cancer immunotherapy. *Nature Reviews Cancer* 2016. **16**: 566-581.

234 **Dawson, N. A. J. and Levings, M. K.,** Antigen-specific regulatory T cells: are police CARs the answer? *Transl Res* 2017. **187**: 53-58.

235 **Fransson, M., Piras, E., Burman, J., Nilsson, B., Essand, M., Lu, B., Harris, R. A., Magnusson, P. U., Brittebo, E. and Loskog, A. S. I.,** CAR/FoxP3-engineered T

regulatory cells target the CNS and suppress EAE upon intranasal delivery. *Journal of Neuroinflammation* 2012. **9**: 112.

236 **Blat, D., Zigmond, E., Alteber, Z., Waks, T. and Eshhar, Z.,** Suppression of murine colitis and its associated cancer by carcinoembryonic antigen-specific regulatory T cells. *Mol Ther* 2014. **22**: 1018-1028.

237 **MacDonald, K. G., Hoeppli, R. E., Huang, Q., Gillies, J., Luciani, D. S., Orban, P. C., Broady, R. and Levings, M. K.,** Alloantigen-specific regulatory T cells generated with a chimeric antigen receptor. *J Clin Invest* 2016. **126**: 1413-1424.

238 **Boardman, D. A., Philippeos, C., Fruhwirth, G. O., Ibrahim, M. A., Hannen, R. F., Cooper, D., Marelli-Berg, F. M., Watt, F. M., Lechler, R. I., Maher, J., Smyth, L. A. and Lombardi, G.,** Expression of a Chimeric Antigen Receptor Specific for Donor HLA Class I Enhances the Potency of Human Regulatory T Cells in Preventing Human Skin Transplant Rejection. *Am J Transplant* 2017. **17**: 931-943.

239 **Noyan, F., Zimmermann, K., Hardtke-Wolenski, M., Knoefel, A., Schulde, E., Geffers, R., Hust, M., Huehn, J., Galla, M., Morgan, M., Jokuszies, A., Manns, M. P. and Jaeckel, E.,** Prevention of Allograft Rejection by Use of Regulatory T Cells With an MHC-Specific Chimeric Antigen Receptor. *Am J Transplant* 2017. **17**: 917-930.

240 **Chen, X., Kozhaya, L., Tastan, C., Placek, L., Dogan, M., Horne, M., Abblett, R., Karhan, E., Vaeth, M., Feske, S. and Unutmaz, D.,** Functional Interrogation of Primary Human T Cells via CRISPR Genetic Editing. *J Immunol* 2018. **201**: 1586-1598.

241 **Eyquem, J., Mansilla-Soto, J., Giavridis, T., van der Stegen, S. J. C., Hamieh, M., Cunanan, K. M., Odak, A., Gönen, M. and Sadelain, M.,** Targeting a CAR to the TRAC locus with CRISPR/Cas9 enhances tumour rejection. *Nature* 2017. **543**: 113-117.

242 **Rupp, L. J., Schumann, K., Roybal, K. T., Gate, R. E., Ye, C. J., Lim, W. A. and Marson, A.,** CRISPR/Cas9-mediated PD-1 disruption enhances anti-tumor efficacy of human chimeric antigen receptor T cells. *Scientific Reports* 2017. **7**: 737.

243 **Fraietta, J. A., Lacey, S. F., Orlando, E. J., Pruteanu-Malinici, I., Gohil, M., Lundh, S., Boesteanu, A. C., Wang, Y., O'Connor, R. S., Hwang, W.-T., Pequignot, E., Ambrose, D. E., Zhang, C., Wilcox, N., Bedoya, F., Dorfmeier, C., Chen, F., Tian, L., Parakandi, H., Gupta, M., Young, R. M., Johnson, F. B., Kulikovskaya, I., Liu, L., Xu, J., Kassim, S. H., Davis, M. M., Levine, B. L., Frey, N. V., Siegel, D. L., Huang, A. C., Wherry, E. J., Bitter, H., Brogdon, J. L., Porter, D. L., June, C. H. and Melenhorst, J. J.,** Determinants of response and resistance to CD19 chimeric antigen receptor (CAR) T cell therapy of chronic lymphocytic leukemia. *Nature Medicine* 2018. **24**: 563-571.

244 **Oo, Y. H., Ackrill, S., Cole, R., Jenkins, L., Anderson, P., Jeffery, H. C., Jones, N., Jeffery, L. E., Lutz, P., Wawman, R. E., Athwal, A. K., Thompson, J., Gray, J., Guo, K., Barton, D., Hirschfield, G. M., Wong, T., Guest, P. and Adams, D. H.,** Liver homing of clinical grade Tregs after therapeutic infusion in patients with autoimmune hepatitis. *JHEP Reports* 2019. **1**: 286-296.

245 **Ashmore-Harris, C., Iafrate, M., Saleem, A. and Fruhwirth, G. O.,** Non-invasive Reporter Gene Imaging of Cell Therapies, including T Cells and Stem Cells. *Mol Ther* 2020. **28**: 1392-1416.

246 **Volpe, A., Kurtys, E. and Fruhwirth, G. O.,** Cousins at work: How combining medical with optical imaging enhances in vivo cell tracking. *Int J Biochem Cell Biol* 2018. **102**: 40-50.

247 **Sharif-Paghaleh, E., Sunassee, K., Tavaré, R., Ratnasothy, K., Koers, A., Ali, N., Alhabbab, R., Blower, P. J., Lechler, R. I., Smyth, L. A., Mullen, G. E. and Lombardi, G.,** In Vivo SPECT Reporter Gene Imaging of Regulatory T Cells. *PLOS ONE* 2011. **6**: e25857.

248 **Jacob, J., Nadkarni, S., Volpe, A., Peng, Q., Tung, S. L., Hannen, R. F., Mohseni, Y. R., Scotta, C., Marelli-Berg, F. M., Lechler, R. I., Smyth, L. A., Fruhwirth, G. O. and Lombardi, G.,** Spatiotemporal in vivo tracking of polyclonal human regulatory T cells (Tregs) reveals a role for innate immune cells in Treg transplant recruitment. *Molecular Therapy - Methods & Clinical Development* 2021. **20**: 324-336.

249 **Aijaz, A., Li, M., Smith, D., Khong, D., LeBlon, C., Fenton, O. S., Olabisi, R. M., Libutti, S., Tischfield, J., Maus, M. V., Deans, R., Barcia, R. N., Anderson, D. G., Ritz, J., Preti, R. and Parekkadan, B.,** Biomanufacturing for clinically advanced cell therapies. *Nature Biomedical Engineering* 2018. **2**: 362-376.

250 **Wherry, E. J. and Kurachi, M.,** Molecular and cellular insights into T cell exhaustion. *Nature Reviews Immunology* 2015. **15**: 486.

251 **Sakuishi, K., Ngiow, S. F., Sullivan, J. M., Teng, M. W. L., Kuchroo, V. K., Smyth, M. J. and Anderson, A. C.,** TIM3(+)FOXP3(+) regulatory T cells are tissue-specific promoters of T-cell dysfunction in cancer. *Oncoimmunology* 2013. **2**: e23849-e23849.

252 **Huang, C.-T., Workman, C. J., Flies, D., Pan, X., Marson, A. L., Zhou, G., Hipkiss, E. L., Ravi, S., Kowalski, J., Levitsky, H. I., Powell, J. D., Pardoll, D. M., Drake, C. G. and Vignali, D. A. A.,** Role of LAG-3 in Regulatory T Cells. *Immunity* 2004. **21**: 503-513.

253 **Ha, S.-J., Park, H. J., Park, J. S., Jeong, Y. H., Son, J., Ban, Y. H., Chang, J. and Chung, D. H.,** Role of PD-1 in regulatory T cells during chronic virus infection. *The Journal of Immunology* 2016. **196**: 79.71-79.71.

254 **Hou, T. Z., Qureshi, O. S. and Sansom, D. M.,** Measuring CTLA-4-Dependent Suppressive Function in Regulatory T Cells. In **Boyd, A. S.** (Ed.) *Immunological Tolerance: Methods and Protocols*. Springer New York, New York, NY 2019, pp 87-101.

255 **Liénart, S., Merceron, R., Vanderaa, C., Lambert, F., Colau, D., Stockis, J., van der Woning, B., De Haard, H., Saunders, M., Coulie, P. G., Savvides, S. N. and Lucas, S.,** Structural basis of latent TGF-β1 presentation and activation by GARP on human regulatory T cells. *Science* 2018. **362**: 952-956.

256 **Hoffmann, P., Boeld, T. J., Eder, R., Huehn, J., Floess, S., Wieczorek, G., Olek, S., Dietmaier, W., Andreesen, R. and Edinger, M.,** Loss of FOXP3 expression in natural human CD4+CD25+ regulatory T cells upon repetitive in vitro stimulation. *European Journal of Immunology* 2009. **39**: 1088-1097.

257 **Levine, B. L., Bernstein, W. B., Connors, M., Craighead, N., Lindsten, T., Thompson, C. B. and June, C. H.,** Effects of CD28 costimulation on long-term proliferation of CD4+ T cells in the absence of exogenous feeder cells. *The Journal of Immunology* 1997. **159**: 5921-5930.

258 **Golovina, T. N., Mikheeva, T., Suhoski, M. M., Aqui, N. A., Tai, V. C., Shan, X., Liu, R., Balcarcel, R. R., Fisher, N., Levine, B. L., Carroll, R. G., Warner, N., Blazar, B. R., June, C. H. and Riley, J. L.,** CD28 costimulation is essential for human T regulatory expansion and function. *Journal of immunology (Baltimore, Md. : 1950)* 2008. **181**: 2855-2868.

259 **Allan, S. E., Crome, S. Q., Crellin, N. K., Passerini, L., Steiner, T. S., Bacchetta, R., Roncarolo, M. G. and Levings, M. K.,** Activation-induced FOXP3 in human T effector cells does not suppress proliferation or cytokine production. *International Immunology* 2007. **19**: 345-354.

260 **Miyara, M., Yoshioka, Y., Kitoh, A., Shima, T., Wing, K., Niwa, A., Parizot, C., Taflin, C., Heike, T., Valeyre, D., Mathian, A., Nakahata, T., Yamaguchi, T., Nomura, T., Ono, M., Amoura, Z., Gorochov, G. and Sakaguchi, S.,** Functional Delineation and Differentiation Dynamics of Human CD4+ T Cells Expressing the FoxP3 Transcription Factor. *Immunity* 2009. **30**: 899-911.

261 **Putnam, A. L., Brusko, T. M., Lee, M. R., Liu, W., Szot, G. L., Ghosh, T., Atkinson, M. A. and Bluestone, J. A.,** Expansion of human regulatory T-cells from patients with type 1 diabetes. *Diabetes* 2009. **58**: 652-662.

262 **Woods, E. J., Thirumala, S., Badhe-Buchanan, S. S., Clarke, D. and Mathew, A. J.,** Off the shelf cellular therapeutics: Factors to consider during cryopreservation and storage of human cells for clinical use. *Cytotherapy* 2016. **18**: 697-711.

263 **Luo, Y., Wang, P., Liu, H., Zhu, Z., Li, C. and Gao, Y.,** The state of T cells before cryopreservation: Effects on post-thaw proliferation and function. *Cryobiology* 2017. **79**: 65-70.

264 **Jayme, D. W. and Smith, S. R.,** Media formulation options and manufacturing process controls to safeguard against introduction of animal origin contaminants in animal cell culture. *Cytotechnology* 2000. **33**: 27-36.

265 **Dwarshuis, N. J., Parratt, K., Santiago-Miranda, A. and Roy, K.,** Cells as advanced therapeutics: State-of-the-art, challenges, and opportunities in large scale biomanufacturing of high-quality cells for adoptive immunotherapies. *Adv Drug Deliv Rev* 2017. **114**: 222-239.

266 **Dawson, N. A. J., Rosado-Sánchez, I., Novakovsky, G. E., Fung, V. C. W., Huang, Q., McIver, E., Sun, G., Gillies, J., Speck, M., Orban, P. C., Mojibian, M. and Levings, M. K.,** Functional effects of chimeric antigen receptor co-receptor signaling domains in human regulatory T cells. *Science Translational Medicine* 2020. **12**: eaaz3866.

267 **Tran, D. Q., Andersson, J., Hardwick, D., Bebris, L., Illei, G. G. and Shevach, E. M.,** Selective expression of latency-associated peptide (LAP) and IL-1 receptor type I/II (CD121a/CD121b) on activated human FOXP3+ regulatory T cells allows for their purification from expansion cultures. *Blood* 2009. **113**: 5125-5133.

268 **Chapman, N. M. and Chi, H.,** Hallmarks of T-cell Exit from Quiescence. *Cancer Immunology Research* 2018. **6**: 502-508.

269 **Place, T. L., Domann, F. E. and Case, A. J.,** Limitations of oxygen delivery to cells in culture: An underappreciated problem in basic and translational research. *Free Radical Biology and Medicine* 2017. **113**: 311-322.

270 **Al-Ani, A., Toms, D., Kondro, D., Thundathil, J., Yu, Y. and Ungrin, M.,** Oxygenation in cell culture: Critical parameters for reproducibility are routinely not reported. *PLOS ONE* 2018. **13**: e0204269.
271 **Geltink, R. I. K., Kyle, R. L. and Pearce, E. L.,** Unraveling the Complex Interplay Between T Cell Metabolism and Function. *Annu Rev Immunol* 2018. **36**: 461-488.
272 **DePeaux, K. and Delgoffe, G. M.,** Metabolic barriers to cancer immunotherapy. *Nature Reviews Immunology* 2021.
273 **Kempkes, R. W. M., Joosten, I., Koenen, H. J. P. M. and He, X.,** Metabolic Pathways Involved in Regulatory T Cell Functionality. *Frontiers in Immunology* 2019. **10**.
274 **Procaccini, C., Carbone, F., Di Silvestre, D., Brambilla, F., De Rosa, V., Galgani, M., Faicchia, D., Marone, G., Tramontano, D., Corona, M., Alviggi, C., Porcellini, A., La Cava, A., Mauri, P. and Matarese, G.,** The Proteomic Landscape of Human Ex Vivo Regulatory and Conventional T Cells Reveals Specific Metabolic Requirements. *Immunity* 2016. **44**: 406-421.
275 **Psychogios, N., Hau, D. D., Peng, J., Guo, A. C., Mandal, R., Bouatra, S., Sinelnikov, I., Krishnamurthy, R., Eisner, R., Gautam, B., Young, N., Xia, J., Knox, C., Dong, E., Huang, P., Hollander, Z., Pedersen, T. L., Smith, S. R., Bamforth, F., Greiner, R., McManus, B., Newman, J. W., Goodfriend, T. and Wishart, D. S.,** The human serum metabolome. *PLoS One* 2011. **6**: e16957.
276 **Salazar, A., Keusgen, M. and von Hagen, J.,** Amino acids in the cultivation of mammalian cells. *Amino Acids* 2016. **48**: 1161-1171.
277 **Muri, J. and Kopf, M.,** Redox regulation of immunometabolism. *Nature Reviews Immunology* 2021. **21**: 363-381.
278 **Zenke, S., Palm, M. M., Braun, J., Gavrilov, A., Meiser, P., Böttcher, J. P., Beyersdorf, N., Ehl, S., Gerard, A., Lämmermann, T., Schumacher, T. N., Beltman, J. B. and Rohr, J. C.,** Quorum Regulation via Nested Antagonistic Feedback Circuits Mediated by the Receptors CD28 and CTLA-4 Confers Robustness to T Cell Population Dynamics. *Immunity* 2020. **52**: 313-327.e317.
279 **Motamedi, M., Xu, L. and Elahi, S.,** Correlation of transferrin receptor (CD71) with Ki67 expression on stimulated human and mouse T cells: The kinetics of expression of T cell activation markers. *Journal of Immunological Methods* 2016. **437**: 43-52.
280 **Schwab, L., Michel, G., Bein, G. and Hackstein, H.,** CD71 surface analysis of T cells: a simple alternative for extracorporeal photopheresis quality control. *Vox Sang* 2020. **115**: 81-93.
281 **Berg, V., Modak, M., Brell, J., Puck, A., Künig, S., Jutz, S., Steinberger, P., Zlabinger, G. J. and Stöckl, J.,** Iron Deprivation in Human T Cells Induces Nonproliferating Accessory Helper Cells. *Immunohorizons* 2020. **4**: 165-177.
282 **Yarosz, E. L., Ye, C., Kumar, A., Black, C., Choi, E.-K., Seo, Y.-A. and Chang, C.-H.,** Cutting Edge: Activation-Induced Iron Flux Controls CD4 T Cell Proliferation by Promoting Proper IL-2R Signaling and Mitochondrial Function. *The Journal of Immunology* 2020. **204**: 1708-1713.
283 **Angelin, A., Gil-de-Gómez, L., Dahiya, S., Jiao, J., Guo, L., Levine, M. H., Wang, Z., Quinn, W. J., 3rd, Kopinski, P. K., Wang, L., Akimova, T., Liu, Y., Bhatti, T. R., Han, R., Laskin, B. L., Baur, J. A., Blair, I. A., Wallace, D. C., Hancock, W. W. and**

Beier, U. H., Foxp3 Reprograms T Cell Metabolism to Function in Low-Glucose, High-Lactate Environments. *Cell metabolism* 2017. **25**: 1282-1293.e1287.

284 **Watson, M. J., Vignali, P. D. A., Mullett, S. J., Overacre-Delgoffe, A. E., Peralta, R. M., Grebinoski, S., Menk, A. V., Rittenhouse, N. L., DePeaux, K., Whetstone, R. D., Vignali, D. A. A., Hand, T. W., Poholek, A. C., Morrison, B. M., Rothstein, J. D., Wendell, S. G. and Delgoffe, G. M.,** Metabolic support of tumour-infiltrating regulatory T cells by lactic acid. *Nature* 2021. **591**: 645-651.

285 **Jagannathan, L., Cuddapah, S. and Costa, M.,** Oxidative stress under ambient and physiological oxygen tension in tissue culture. *Curr Pharmacol Rep* 2016. **2**: 64-72.

286 **Vardhana, S. A., Hwee, M. A., Berisa, M., Wells, D. K., Yost, K. E., King, B., Smith, M., Herrera, P. S., Chang, H. Y., Satpathy, A. T., van den Brink, M. R. M., Cross, J. R. and Thompson, C. B.,** Impaired mitochondrial oxidative phosphorylation limits the self-renewal of T cells exposed to persistent antigen. *Nat Immunol* 2020. **21**: 1022-1033.

287 **Scharping, N. E., Rivadeneira, D. B., Menk, A. V., Vignali, P. D. A., Ford, B. R., Rittenhouse, N. L., Peralta, R., Wang, Y., Wang, Y., DePeaux, K., Poholek, A. C. and Delgoffe, G. M.,** Mitochondrial stress induced by continuous stimulation under hypoxia rapidly drives T cell exhaustion. *Nature Immunology* 2021. **22**: 205-215.

288 **Alissafi, T., Kalafati, L., Lazari, M., Filia, A., Kloukina, I., Manifava, M., Lim, J. H., Alexaki, V. I., Ktistakis, N. T., Doskas, T., Garinis, G. A., Chavakis, T., Boumpas, D. T. and Verginis, P.,** Mitochondrial Oxidative Damage Underlies Regulatory T Cell Defects in Autoimmunity. *Cell Metab* 2020. **32**: 591-604.e597.

289 **Lam, A. J., Lin, D. T. S., Gillies, J. K., Uday, P., Pesenacker, A. M., Kobor, M. S. and Levings, M. K.,** Optimized CRISPR-mediated gene knockin reveals FOXP3-independent maintenance of human Treg identity. *Cell Reports* 2021. **36**: 109494.

290 **Trzonkowski, P., Bacchetta, R., Battaglia, M., Berglund, D., Bohnenkamp, H. R., ten Brinke, A., Bushell, A., Cools, N., Geissler, E. K., Gregori, S., Marieke van Ham, S., Hilkens, C., Hutchinson, J. A., Lombardi, G., Madrigal, J. A., Marek-Trzonkowska, N., Martinez-Caceres, E. M., Roncarolo, M. G., Sanchez-Ramon, S., Saudemont, A. and Sawitzki, B.,** Hurdles in therapy with regulatory T cells. *Sci Transl Med* 2015. **7**: 304ps318.

291 **Golab, K., Leveson-Gower, D., Wang, X. J., Grzanka, J., Marek-Trzonkowska, N., Krzystyniak, A., Millis, J. M., Trzonkowski, P. and Witkowski, P.,** Challenges in cryopreservation of regulatory T cells (Tregs) for clinical therapeutic applications. *Int Immunopharmacol* 2013. **16**: 371-375.

292 **Ahrens, E. T., Helfer, B. M., O'Hanlon, C. F. and Schirda, C.,** Clinical cell therapy imaging using a perfluorocarbon tracer and fluorine-19 MRI. *Magn Reson Med* 2014. **72**: 1696-1701.

293 **Krafft, M. P.,** Fluorocarbons and fluorinated amphiphiles in drug delivery and biomedical research. *Advanced Drug Delivery Reviews* 2001. **47**: 209-228.

294 **Ruiz-Cabello, J., Barnett, B. P., Bottomley, P. A. and Bulte, J. W. M.,** Fluorine (19F) MRS and MRI in biomedicine. *NMR in Biomedicine* 2011. **24**: 114-129.

295 **Helfer, B. M., Balducci, A., Nelson, A. D., Janjic, J. M., Gil, R. R., Kalinski, P., de Vries, I. J. M., Ahrens, E. T. and Mailliard, R. B.,** Functional assessment of human dendritic cells labeled for in vivo 19F magnetic resonance imaging cell tracking. *Cytotherapy* 2010. **12**: 238-250.

296 **O'Hanlon, C. F., Fedczyna, T., Eaker, S., Shingleton, W. D. and Helfer, B. M.,** Integrating a 19F MRI Tracer Agent into the Clinical Scale Manufacturing of a T-Cell Immunotherapy. *Contrast Media & Molecular Imaging* 2017. **2017**: 9548478.

297 **Fink, C., Gaudet, J. M., Fox, M. S., Bhatt, S., Viswanathan, S., Smith, M., Chin, J., Foster, P. J. and Dekaban, G. A.,** 19F-perfluorocarbon-labeled human peripheral blood mononuclear cells can be detected in vivo using clinical MRI parameters in a therapeutic cell setting. *Scientific Reports* 2018. **8**: 590.

298 **Bouchlaka, M. N., Ludwig, K. D., Gordon, J. W., Kutz, M. P., Bednarz, B. P., Fain, S. B. and Capitini, C. M.,** 19F-MRI for monitoring human NK cells in vivo. *OncoImmunology* 2016. **5**: e1143996.

299 **Fink, C., Smith, M., Sehl, O. C., Gaudet, J. M., Meagher, T. C., Sheikh, N. A., Dikeakos, J. D., Rieder, M. J., Foster, P. J. and Dekaban, G. A.,** Quantification and characterization of granulocyte macrophage colony-stimulating factor activated human peripheral blood mononuclear cells by fluorine-19 cellular MRI in an immunocompromised mouse model. *Diagnostic and Interventional Imaging* 2020. **101**: 577-588.

300 **Chapelin, F., Gao, S., Okada, H., Weber, T. G., Messer, K. and Ahrens, E. T.,** Fluorine-19 nuclear magnetic resonance of chimeric antigen receptor T cell biodistribution in murine cancer model. *Scientific Reports* 2017. **7**: 17748.

301 **Cheung, A. S., Zhang, D. K. Y., Koshy, S. T. and Mooney, D. J.,** Scaffolds that mimic antigen-presenting cells enable ex vivo expansion of primary T cells. *Nature Biotechnology* 2018. **36**: 160-169.

302 **Zhang, D. K. Y., Cheung, A. S. and Mooney, D. J.,** Activation and expansion of human T cells using artificial antigen-presenting cell scaffolds. *Nature Protocols* 2020. **15**: 773-798.

Appendices

Appendix A Antibodies and labelling dyes

Table A.1: Antibodies and labelling dyes used in this thesis.

Antigen	Fluorochrome	Clone	Company	Catalog #
CCR4	APC	L291H4	Biolegend	359408
CCR6	BV785	G034E3	Biolegend	353422
CCR7	PECy7	3D12	BD Biosciences	557648
CCR7	BV711	G043H7	Biolegend	353228
CCR10	PE	6588-5	Biolegend	341504
CD25	BB515	2A3	BD Biosciences	564467
CD25	BV421	BC96	Biolegend	302630
CD25	PE	2A3	STEMCELL	10512
CD28	APC	CD28.2	Biolegend	302912
CD3	BV786	UCHT1	BD Biosciences	565491
CD3	BV785	SK7	BD Biosciences	563800
CD4	BUV395	SK3	BD Biosciences	563550
CD4	BV510	OKT4	Biolegend	317444
CD4	FITC	RPA-T4	Thermo Fisher Scientific	11-0049-42
CD4	V500	RPA-T4	BD Biosciences	560768
CD45RA	BV711	HI100	Biolegend	304138
CD45RA	PECy7	HI100	Thermo Fisher Scientific	25-0458-42
CD45RO	BV421	UCHL1	Biolegend	304224
CD62L	FITC	SK11	BD Biosciences	11-0625-42
CD62L	BV605	DREG-56	BD Biosciences	562719
CD8	eF450	SK1	Thermo Fisher Scientific	48-0087-42
CD8	FITC	HIT8a	Thermo Fisher Scientific	11-0089-42
CD8	PE	HIT8a	BD Biosciences	555635
CD86	PECy7	IT2.2	Thermo Fisher Scientific	25-0869-42
CD95	FITC	DX2	BD Biosciences	556640
CTLA-4	BV421	BNI3	Biolegend	369606
CXCR3	BV421	G025H7	Biolegend	353716
FOXP3	APC	236A/E7	Thermo Fisher Scientific	17-4777-73
FOXP3	PE	236A/E7	Thermo Fisher Scientific	12-4777-42
FOXP3	PECy7	236A/E7	Thermo Fisher Scientific	25-4777-42
GARP	BV711	7B11	BD Biosciences	563958
Helios	AF647	22F6	Biolegend	137218
IFNγ	BUV395	B27	BD Biosciences	563563
IFNγ	BV785	4S.B3	Biolegend	502542
IFNγ	PECy7	4S.B3	Thermo Fisher Scientific	25-7319-82
IL-2	BUV737	MQ1-17H12	BD Biosciences	612836
IL-2	BV421	MQ1-17H12	BD Biosciences	564164
IL-4	BV711	MP4-25D2	BD Biosciences	564112
IL-10	PE	JES3-19F1	BD Biosciences	559330
IL-17A	APC	eBio64DEC17	Thermo Fisher Scientific	17-7179-42
IL-17A	BV711	BL168	Biolegend	512328
LAG3	PECy7	3DS223H	Invitrogen	25-2239-42
LAP	PECy7	FNLAP	Thermo Fisher Scientific	25-9829-42
PD1	BV421	EH12.2H7	Biolegend	329920

Antigen	Fluorochrome	Clone	Company	Catalog #
PD1	BV737	EH12.1	BD Biosciences	612791
TIM3	APC	F38-2E2	Thermo Fisher Scientific	17-3109-41
TNFα	AF488	Mab11	Thermo Fisher Scientific	53-7349-41
Fixable viability dye (FVD)	eF780	N/A	Thermo Fisher Scientific	65-0865-18
Cell proliferation dye (CPD)	eF450	N/A	Thermo Fisher Scientific	65-0842-90
Cell proliferation dye (CPD)	eF670	N/A	Thermo Fisher Scientific	65-0840-90
Hypoxia green	FITC	N/A	Thermo Fisher Scientific	H20035

Appendix B Cell Handling in large-scale Treg expansions

Table B.1: Cell handling in first large-scale Treg expansion.

	Tissue culture flask	Cell expansion bag	WAVE	G-Rex
Day 7	Restimulated cells and transferred into different cell expansion platforms			
Day 8			Took sample	
Day 9	Adjusted cell concentration to $5x10^5$ cells/mL	Moved cells from 7 mL bag to 30 mL bag (adjusted cell concentration to $5x10^5$ cells/mL)	Increased volume to ~500 mL (adjusted cell concentration to $1x10^6$ cells/mL)	
Day 10			Increased volume to 1 L (adjusted cell concentration to $1.2x10^6$ cells/mL – maximum capacity of bag)	
Day 11	Adjusted cell concentration to $5x10^5$ cells/mL	Moved cells from 30 mL bag to 100 mL bag (adjusted cell concentration to $7.5x10^5$ cells/mL – maximum capacity of bag)		
Day 12		Took sample	Removed 500 mL of media, replaced with fresh media	
Day 13	Adjusted cell concentration to $5x10^5$ cells/mL	Removed 50 mL of media, replaced with fresh media	Removed 500 mL of media, replaced with fresh media	
Day 14	Harvested cells			

Table B.2: Cell handling in second large-scale Treg expansion.

	Tissue culture flask	Cell expansion bag	WAVE	G-Rex
Day 7	Restimulated cells and transferred into different cell expansion platforms			
Day 8	Took sample	Took sample	Took sample	
Day 9	Adjusted cell concentration to $5x10^5$ cells/mL	Increased volume from 300 mL to 740 mL (adjusted cell concentration to $5x10^5$ cells/mL)	Increased volume to ~550 mL (adjusted cell concentration to $5x10^5$ cells/mL)	
Day 10	Adjusted cell concentration to $5x10^5$ cells/mL	Increased volume to 1 L (adjusted cell concentration to $7.8x10^5$ cells/mL)	Took sample	
Day 11	Adjusted cell concentration to $5x10^5$ cells/mL	Removed 500 mL of media, replaced with fresh media	Increased volume to 1 L (adjusted cell concentration to $6.7x10^5$ cells/mL)	Added IL-2 (1000 U/mL for whole volume)
Day 12	Adjusted cell concentration to $5x10^5$ cells/mL	Removed 500 mL of media, replaced with fresh media	Took sample	
Day 13	Took sample	Removed 500 mL of media, replaced with fresh media	Turned on perfusion to exchange 500 mL of media over last 21 hours	
Day 14	Harvested cells			